Fe(II) oxidation by metabolically flexible phototrophs

Dissertation

der Mathematisch-Naturwissenschaftlichen Fakultät

der Eberhard Karls Universität Tübingen

zur Erlangung des Grades eines

Doktors der Naturwissenschaften

(Dr. rer. nat.)

vorgelegt von

M.Sc. Verena Nikeleit

aus Stühlingen

Tübingen

2024

Gedruckt mit Genehmigung der Mathematisch-Naturwissenschaftlichen Fakultät der Eberhard Karls Universität Tübingen

Tag der mündlichen Qualifikation:	17.05.2024
Dekan:	Prof. Dr. Thilo Stehle
1. Berichterstatterin:	Dr. Casey Bryce
2. Berichterstatter:	Jun. Prof. Dr. Marie Mühe

List of contents

Summary

Iron (Fe) is ubiquitous and an important redox element. It is linked to many relevant element cycles and important for the fate and bioavailability of heavy metals, toxins and nutrients.

Fe redox processes can be mediated through abiotic and biotic processes. One bacteria that can use Fe are anoxygenic phototrophic Fe(II)-oxidizer. These bacteria, photoferrotrophs, gain energy via photosynthesis, fix CO_2 as carbon source and use Fe(II) as an electron donor. Photoferrotrophs are metabolically flexible and can use other substrates like H_2, $S_2O_3^-$ and organics as electron donors and carbon sources. This arises the question which substrate photoferrotrophs would use if multiple are present, the impact of co-substrate utilization on Fe(II) oxidation, particularly on Fe(II) oxidation rates and mineral formation at environmentally relevant substrate concentrations. We further addressed the impact of light exposure, through a day/night cycle, and optimal buffer concentration.

In **Chapter 2 and 3** we could show that Fe(II) was used simultaneously (with lactate and glucose) and sequential with preferring the organics (acetate, pyruvate and glucose) for *Rhodopseudomonas palustris* TIE-1. Fe(II) oxidation rates were significantly enhanced with lactate, pyruvate and glucose. Organic consumption rates were also enhanced for lactate, butyrate and glucose when Fe(II) was present. We found that in the absence of CO_2, only the organic co-substrates acetate, lactate and pyruvate, but not Fe(II), were consumed. All Fe(III) minerals were short-range ordered Fe(III) oxyhydroxides, likely Ferrihydrite. In additional experiments with 5 other photoferrotrophs we could observe that they utilized organics and Fe(II) simultaneous and prefer Fe(II) over H_2 for two strains. Fe(II) oxidation rates were significantly increased with acetate, lactate and glucose whereas H_2 slowed Fe(II) oxidation down for some photoferrotrophs. We could conclude that substrate preference, consumption scenario and impact on Fe(II) oxidation rates are strain and substrate specific.

In the next chapter **(chapter 4)** we wanted to investigate the role of phototrophic Fe(II) oxidation, iron cycling and the impact of organics in Großes Heiliges Meer, a dimictic lake. We successfully could demonstrate that iron cycling is happening during summer stratification and were able to enrich a phototrophic Fe(II)-oxidizer *Thiodictyon*. We further could show that iron cycling is impacted by organics.

Afterwards, we looked into the effect of day/night cycles and different buffer concentrations and compositions on Fe(II) oxidation and organic consumption in **chapter 5 and 6**. We found that day/night cycles increase maximum Fe(II) oxidation rates significantly but no change in Fe(III) minerals was observed. Regarding optimal buffer composition Fe(II) oxidation and organic consumption are favoured in a well buffered system. While for organic consumption low HCO_3^- are beneficial, the opposite was observed for Fe(II) oxidation.

In **chapter 7** we investigated if anoxygenic Fe(II)-oxidizer could produce methane (CH_4) while oxidizing Fe(II), H_2 and acetate. CH_4 was produced by *Rhodopseudomonas palustris* TIE-1, *Chlorobium ferrooxidans* KoFox and *Chlorobium phaeoferrooxidans* KB01 and ranged from 0.03±0.01 to 0.4±0.2 amol CH_4/(cell*d).

At the end we tried to enrich and isolate microaerophilic and phototrophic Fe(II)-oxidizer **(chapter 8)**. We were able to have 3 microaerophilic enrichments from iron-rich springs near Starzach and Rablönch. For phototrophic Fe(II)-oxidizer 6 different enrichments were successful and all were dominated by a purple sulfur bacteria Thiodictyon. This is the first time phototrophic Fe(II)-oxidizer were enriched from soils.

In this study we could show that phototrophic Fe(II)-oxidizer generally use substrates simultaneously and enhances the Fe(II) oxidation. Their flexible metabolism and simultaneous consumption of substrates enhances their competitiveness and survival. They are widespread and found in environments like dimictic stratified lakes and soils and probably many more. Growth conditions like availability of CO_2, day/night cycles, buffer composition and concentration have huge influence on growth and Fe(II) oxidation rates and should be considered in laboratory studies.

Zusammenfassung

Eisen (Fe) ist allgegenwärtig und ein wichtiges redox aktives Element. Es ist mit vielen relevanten Elementkreisläufen verknüpft und wichtig für die Bioverfügbarkeit von Schwermetallen, Toxinen und Nährstoffen. Redoxreaktionen mit Eisen können durch abiotische und biotische Prozesse durchgeführt werden. Bakterien, die Fe(II) oxidieren können, sind anoxygene phototrophe Fe(II)-oxidierer. Diese photoferrotrophen Bakterien gewinnen Energie durch die Photosynthese, fixieren CO_2 als Kohlenstoffquelle und verwenden Fe(II) als Elektronendonator. Photoferrotrophe Bakterien sind metabolisch flexibel und können weitere Substrate wie H_2, $S_2O_3^-$ und organische Stoffe als Elektronendonatoren und Kohlenstoffquellen nutzen. Dies wirft die Frage auf, welches Substrat photoferrotrophe Bakterien verwenden würden, wenn mehrere vorhanden sind, den Einfluss der Ko-Substratnutzung auf die Fe(II)-Oxidation, insbesondere auf die Fe(II)-Oxidationsraten und die Mineralbildung bei umweltrelevanten Substratkonzentrationen. Weiterhin haben wir den Einfluss der Lichtexposition durch einen Tag-/Nachtzyklus und die optimale Pufferkonzentration untersucht.

In **Kapitel 2 und 3** konnten wir zeigen, dass *Rhodopseudomonas palustris* TIE-1 Fe(II) gleichzeitig (mit Laktat und Glukose) und sequenziell unter Bevorzugung der organischen Stoffe (Acetat, Pyruvat und Glukose) verwendet wurde. Die Fe(II)-Oxidationsraten wurden mit Laktat, Pyruvat und Glukose signifikant erhöht. Auch die Verbrauchsraten der organischen Stoffe wurden für Laktat, Butyrat und Glukose erhöht, wenn Fe(II) vorhanden war. Wir fanden zusätzlich heraus, dass in Abwesenheit von CO_2 nur die organischen Ko-Substrate Acetat, Laktat und Pyruvat, aber nicht Fe(II), verbraucht wurden. Alle Fe(III)-Minerale waren Fe(III)-Oxyhydroxide. In zusätzlichen Experimenten mit 5 anderen photoferrotrophen Bakterien konnten wir beobachten, dass sie organische Stoffe und Fe(II) gleichzeitig nutzten und Fe(II) bevorzugt wurde bei zwei Stämmen. Die Fe(II)-Oxidationsraten wurden mit Acetat, Laktat und Glukose signifikant erhöht, während H_2 die Fe(II)-Oxidation für einige photoferrotrophe Bakterien verlangsamte. Wir konnten

schlussfolgern, dass Substratpräferenz, Bevorzugung bestimmter Stoffe und Einfluss auf die Fe(II)-Oxidationsraten bakterien- und substratspezifisch sind.

Im nächsten Kapitel **(Kapitel 4)** wollten wir die Bedeutung von photoferrotrophen Bakterien, des Eisenkreislaufs und den Einfluss von organisch Stoffen im Großen Heiligen Meer, einem dimiktischen See, untersuchen. Wir konnten erfolgreich demonstrieren, dass während der Sommerstratifikation ein Eisenkreislauf stattfindet und es gelang uns, einen phototrophen Fe(II)-Oxidierer *Thiodictyon* anzureichern. Weiterhin konnten wir zeigen, dass der Eisenkreislauf vdurch organische Stoffe beeinflusst wird.

Anschließend untersuchten wir in den **Kapiteln 5 und 6** den Effekt von Tag-/Nachtzyklen und verschiedenen Pufferkonzentrationen und -zusammensetzungen auf die Fe(II)-Oxidation und die Nutzung organischer Stoffe. Wir fanden heraus, dass Tag-/Nachtzyklen die maximalen Fe(II)-Oxidationsraten signifikant erhöhen, aber keine Veränderung bei den Fe(III)-Mineralien beobachtet wurde. Hinsichtlich der optimalen Pufferzusammensetzung werden Fe(II)-Oxidation und die Nutzung von organischen Stoffen durch ein gut gepuffertes System begünstigt. Während für den Verbrauch von organischen Stoffen niedrige HCO_3^- Konzentrationen vorteilhaft sind, wurde für die Fe(II)-Oxidation das Gegenteil beobachtet.

Im **Kapitel 7** untersuchten wir, ob anoxygene Fe(II)-Oxidierer Methan (CH4) produzieren können, während sie Fe(II), H_2 und Acetat oxidieren. CH_4 wurde von *Rhodopseudomonas palustris* TIE-1, *Chlorobium ferrooxidans* KoFox und *Chlorobium phaeoferrooxidans* KB01 produziert und ereichte Produktionsmengen von 0,03±0,01 bis 0,4±0,2 amol CH_4/(Zelle*d).

Am Ende versuchten wir, mikroaerophile und phototrophe Fe(II)-Oxidierer anzureichern und zu isolieren **(Kapitel 8)**. Wir konnten 3 mikroaerophile Anreicherungen aus eisenreichen Quellen in der Nähe von Starzach und Rablönch erhalten. Für phototrophe Fe(II)-Oxidierer waren 6 verschiedene Anreicherungen erfolgreich, die alle von einem pinken Schwefelbakterium, *Thiodictyon*, dominiert wurden. Das ist das erste Mal, dass phototrophe Fe(II)-Oxidierer aus Böden angereichert wurden.

In dieser Studie konnten wir zeigen, dass phototrophe Fe(II)-Oxidierer viele Substrate gleichzeitig nutzen können und dies die Fe(II)-Oxidationrate erhöht. Ihr flexibler Stoffwechsel und Fähigkeit Substrate gleichzeitig zu benutzen steigert ihre Wettbewerbsfähigkeit. Deshalb sind sie verbreitet zu finden, z.B. dimiktischen Seen und Böden und wahrscheinlich vielen anderen Orten. Wachstumsbedingungen wie die Verfügbarkeit von CO_2, Tag-/Nachtzyklen, Pufferzusammensetzung und -konzentration haben einen erheblichen Einfluss auf das Wachstum und die Fe(II)-Oxidationsraten von phototrophen Fe(II)-Oxidierer und sollten in Laborstudien berücksichtigt werden.

1 Chapter: Introduction

Iron and it's environmental importance

Iron (Fe) is ubiquitous and widespread throughout the earth's crust, soil, sediments and water bodies. It is an important redox-active element and occurs in two environmentally relevant redox states: Fe(II) and Fe(III). Iron can act as an electron donor or electron acceptor for abiotically and biotically mediated reactions. Fe(II), ferrous iron, can be soluble under anoxic conditions at neutral pH but can also occur as Fe(II) minerals such as siderite and vivianite. Contrary to Fe(III), ferric iron, which is poorly soluble at neutral pH and therefore forms Fe(III) minerals (Fe(III)-oxyhydroxides) like ferrihydrite, lepidocrocite and goethite. Decreasing the pH increases the solubility of Fe(II) and Fe(III) and below pH 4 Fe(II) exists primarily as aqueous species and is stable even in the presence of oxygen (Stumm & Morgan, 2012).

During the formation of iron minerals, nutrients, pollutants, and toxic metals can be sorbed, co-precipitated or complexed within the mineral or at the mineral surface and are, therefore, not bioavailable (Eickhoff et al., 2014; Kappler et al., 2021). When these minerals are dissolved again these compounds can be released back into the environment and become bioavailable. Additionally, iron interacts with major nutrient cycles including carbon, nitrogen and sulfur (Kappler et al., 2021; Mu et al., 2016; Tipping, 1981). Studies have found that organic carbon degradation can be affected by Fe(III) minerals. For example, organic carbon can be stabilised with Fe(III) minerals making them less reactive and less bioavailable (Lalonde et al., 2012; Wagai & Mayer, 2007; Zhao et al., 2016). Alternatively, through the dissolution of Fe(III) minerals, organic carbon can become more labile and bioavailable (Zhao et al., 2017). Studies found that Fe(II) oxidation is enhanced when certain organics are bound to it (Kopf et al., 2013; Peng et al., 2019). As iron and organics are often found simultaneously in the environment these interactions are of relevance (Laufer et al., 2016; Patzner et al., 2020).

Fe redox processes can happen through abiotically and biotically mediated processes. Fe(II) can be oxidized abiotically by O_2, reactive oxygen species (ROS), MnO_2, NO and NO_2^-. Fe(III) reduction can also happen abiotically via photoreduction or sulfide. (Kappler et al., 2021). Microbial processes, through the activity of microaerophilic, nitrate-reducing and phototrophic Fe(II)-oxidizers, play an important role in facilitating Fe(II) oxidation under microoxic and anoxic conditions (Bryce et al., 2018; Croal et al., 2004a; Heising et al., 1999; Kappler et al., 2021; Kucera & Wolfe, 1957; Laufer et al., 2017). On the other side of the microbial redox cycle Fe(III) reduction can be coupled to the oxidation of organics, CH_4, H_2 and NH_4^+. Abiotic

and biotic processes involved in Fe(II) oxidation and Fe(III) reduction can happen simultaneously. Indeed, Fe(II)-oxidizers and Fe(III)-reducers have been found in the same environment (Berg et al., 2016; Otte et al., 2018). This could lead to an active cryptic iron cycle where iron concentration changes are not measurable or observed although an active community exists. Such a cryptic iron cycle of microaerophilic and phototrophic Fe(II)-oxidizers and heterotrophic Fe(III)-reducers has been previously observed e.g. in Lake Cadagno (Berg et al., 2016). As systems with anoxic niches are ubiquitous in the environment it can be assumed that iron cycling could also be happening in other anoxic environment like stratified lakes with anoxic bottom waters (Akam et al., 2024; Crowe et al., 2008; Llirós et al., 2015a).

Phototrophic Fe(II)-oxidizers

Phototrophic Fe(II)-oxidizers (photoferrotrophs) use anoxygenic photosynthesis to obtain energy and produce biomass. Fe(II) is used as an electron donor to produce reducing equivalents (NAD(P)H) to fix CO_2 to build their biomass according to equation 1 (Widdel et al., 1993):

$$HCO_3^- + 4\ Fe^{2+} + 10\ H_2O + h\nu \rightarrow CH_2O + 4\ Fe(OH)_3 + 7\ H^+ \quad (1)$$

Photoferrotrophs need four main conditions to thrive: sufficient light, microoxic to anoxic conditions, an electron donor, and a carbon source (inorganic and/or organic). Phototrophic Fe(II)-oxidizers belong to a collection of microorganisms termed anoxygenic phototrophs and have been historically categorised in green sulfur, purple sulfur, and purple non-sulfur bacteria based on studies by Winogradsky in 1888. His work described the difference between these categories as being due to differences in bacteriochlorophyll composition and the ability or lack thereof to use and store sulfur (Winogradsky, 1888). Purple and green sulfur bacteria have distinctive bacteriochlorophylls that absorb light at specific wavelengths. Purple bacteria, like *Rhodopseudomonas* or *Rhodobacter*, have bacteriochlorophyll a (Bchl a) which has an absorption peak at 805 nm and between 830-890 nm or Bchl b (835-850 nm and 1020-1040 nm). Whereas green sulfur bacteria, like *Chlorobium*, can have Bchl c (745-755 nm), d (705-740 nm) or e (719-726 nm). Besides bacteriochlorophylls, anoxygenic phototrophs have other accessory pigments like carotenoids and phycobilins to harvest photons at specific wavelengths. Therefore, purple bacteria can look orange, red or pink and green sulfur bacteria's colour can range from green to brown. Besides contributing to additional light harvesting, carotenoids can also protect the cells from too much solar radiation (Blankenship et al., 1993; Blankenship & Matsuura, 2003; Renger & Wolff, 1977). Light energy is captured by an antenna complex and transferred to the reaction centre. The photons then transform a bacteriochlorophyll pair – P870 (in purple bacteria) or P840 (in green sulfur bacteria) – to an

exited state allowing an electron to be transferred to an electron acceptor between membrane-bound proteins. Thereby, a proton gradient is produced promoting ATP production through ATPase. When electrons are transferred back to the bacteriochlorophyll pair, it can be exited again. This process is also called cyclic electron flow where the electron stays in a cycle and can constantly produce ATP using photons. Non-cyclic electron flow takes place when the electrons are used to reduce $NAD(P)^+$ to NAD(P)H to fix CO_2 and build biomass (Canfield et al., 2005).

Phototrophic bacteria are adapted to differing light conditions, i.e. different light intensities or wavelengths. Some green sulfur bacteria are adapted to very low light intensities whereas purple sulfur bacteria can tolerate and thrive with higher light intensities (Llirós et al., 2015b; Schmidt et al., 2021). Additionally, based on their different pigments these bacteria are affected by and grow best at specific wavelengths (Schmidt et al., 2021). Furthermore, a huge impact on the growth of these bacteria is the length of time they are exposed to light. In the environment the activity of photoferrotrophs is greatly dependent on the day/night cycle as during the night no ATP can be produced. Indeed it has been shown that a day/night cycle can have beneficial effects on biomass, protein and enzymes production (Hauruseu & Koblízek, 2012; Zhi et al., 2019). However, no study to date has investigated the effect of day/night cycles on photoferrotrophs and the subsequent implications on Fe(II) oxidation and mineral formation.

Suitable habitats and representative model strains of photoferrotrophs

The availability of light is essential for photoferrotrophs and one of their key conditions for growth. Another important aspect for dictating photoferrotrophic growth, is oxygen. Most photoferrotrophs are facultative or strict anaerobes and prefer environments with micro- to anoxic conditions because, if oxygen levels are too high, abiotic oxidation of Fe(II) by O_2 is faster than biotic Fe(II) oxidation. Those conditions existed, for example, during the Archean eon from 4 to 2.5 Ga (“early Earth” period). The surface of the oceans and coastlands, during this time, provided an ideal habitat for these bacteria due to elevated concentrations of dissolved Fe(II) (up to 0.5 mM), the presence of light, and anoxic conditions (Poulton & Canfield, 2011). During this time vast formations of Fe(III)-rich deposits were formed and consisted of alternating Fe(III)-rich and silica-rich layers. It has been hypothesised that photoferrotrophs could have played a role in creating these so-called banded iron formations (BIF) (Kappler et al., 2005; Konhauser et al., 2002; Thompson et al., 2019). Thompson (2019) also linked photoferrotrophy and the formation of BIFs to methanogenesis and production of methane.

Methane (CH_4) is proposed to have played an important role in heating up the planet as at that time the radiance of the sun was less intense (Pavlov et al., 2000).

Although modern Earth is less favourable for photoferrotrophs, mainly due to the ubiquity of O_2 in the atmosphere, there are still environments where these bacteria can thrive. These are "sweet spots" where anoxic conditions, light, and dissolved Fe(II) or Fe(II) minerals coexist. Some of these habitats include iron-rich mats, ditches and ponds where key model strains such as *Rhodopseudomonas palustris* TIE-1, *Rhodobacter ferrooxidans* SW2 and *Thiodycton* F4 (Croal et al., 2004b; Ehrenreich & Widdel, 1994; Jiao et al., 2005) were isolated from. A representative list of model strains is found in Table 1. Another important habitat are marine and freshwater coastal sediments. In those environments O_2 only penetrates the sediment a few mm, which enables the photoferrotrophs to be present at depths where sunlight can still penetrate the sediment. At depths where O_2 is depleted an increase of Fe(II) of up to 100 µM was observed (Laufer et al., 2016; Melton et al., 2014; Otte et al., 2018). These sediments are rich in diverse substrates like carbon sources including volatile fatty acids, dissolved organic carbon (DOC) and inorganic carbon (IC) which can also act as a buffer in the system. For inorganic substrates sulphide, nitrite, and nitrate were found over a few mm to a few cm scale (Laufer et al., 2016; Melton et al., 2012) These marine and freshwater systems are highly diverse and show the presence and activity of other iron metabolising bacteria (Otte et al., 2018). From marine sediments *Rhodovulum iodosum, Rhodovulum robiginosum* and *Chlorobium* sp. N1 have been isolated and, so far, are the only strains originating from marine environments (Laufer et al., 2017; Straub et al., 1999). From freshwater sediments *Chlorobium ferrooxidans* KoFox and a co-culture with *Chlorobium* sp. were enriched (Heising et al., 1999; Schmidt et al., 2021). An additional habitat for photoferrotrophs are stratified lakes. Here geochemical gradients of O_2, Fe(II), Fe(III), light, IC, sulphide, nitrite, nitrate and methane can stretch over meter distances and often influence the whole water column (Akam et al., 2024; Berg et al., 2016; Crowe et al., 2008; Llirós et al., 2015b). *Chlorobium phaeoferrooxidans* KB01 is the only true isolate of green sulfur bacteria and the only model strain from a stratified lake. These environments are of particular interest as they have been associated with iron cycling and used as a model for Archean oceans (Berg et al., 2016; Thompson et al., 2019).

Table 1: Representative phototrophic Fe(II)-oxidizer model strains.

Isolate	Origin	Bacteria group	Reference
Rhodopseudomonas palustris TIE-1	Freshwater,iIron rich mat	Purple non-sulfur	(Jiao et al., 2005)
Rhodobacter ferrooxidans SW2	Freshwater ditch	Purple non-sulfur	(Ehrenreich & Widdel, 1994)
Rhodovulum iodosum	Marine sediment	Purple non-sulfur	(Straub et al., 1999)
Rhodovulum rubiginosum	Marine sediment	Purple non-sulfur	(Straub et al., 1999)
Thiodyction sp. strain F4	Freshwater, iron rich ditch	Purple sulfur	(Croal et al., 2004a)
Chlorobium ferrooxidans KoFox*	Freshwater sediment	Green sulfur	(Heising et al., 1999)
Chlorobium sp. strain N1*	Marine sediment	Green sulfur	(Laufer et al., 2017)
Chlorobium phaeoferrooxidans KB01	Stratified lake	Green sulfur	(Crowe et al., 2017)

* defined co-culture

Even though several additional isolates have been characterized and studied, there are many more environments where no successful isolation or enrichment has been possible so far, e.g. from soils. Therefore, the collection of isolated photoferrotrophs is small and more successful isolations and characterizations will enhance our understanding of phototrophic Fe(II)-oxidizers and their implications for modern and ancient environments.

Metabolic versatility and flexibility of photoferrotrophs

Phototrophic Fe(II)-oxidizers are able to obtain Fe(II) electrons from many sources, e.g. dissolved Fe(II), poorly crystalline Fe(II) minerals like siderite, FeS and Fe(II)/Fe(III) mixed minerals like green rust and magnetite. (Byrne et al., 2015; Han et al., 2020; Kappler & Newman, 2004). In addition to their flexibility when it comes to their use of Fe(II) sources, they are metabolically versatile and can grow photoautotrophically and/or photoheterotrophically with substrates other than Fe(II) as electron donors (Jiao et al., 2005; Laufer et al., 2017) (Figure 1). Other possible electron donors for photoautotrophic growth include H_2, H_2S and $S_2O_3^{2-}$. Alternatively, they can grow photoheterotrophically by utilizing a wide range of organics such as acetate, lactate, pyruvate, and larger molecules like glucose (Bryce et al., 2018). In this case carbon from the organics is used as carbon source to build biomass and/or used an as electron donor. Indeed, McKinlay and Harwood (2010) observed that *R. palustris* oxidized 22% of the provided acetate to CO_2, contributing to cofactor recycling crucial for biomass formation (McKinlay & Harwood, 2010). However, organics that are more redox negative than biomass need another substrate to serve as an electron sink. This could be CO_2, DMSO or protons (resulting from H_2 production) (McKinlay & Harwood, 2010).

With the ability to use both inorganic and organic substrates the question arises as to which substrates photoferrotrophs will preferentially use if multiple substrates are present. Indeed, early studies investigated this fundamental question. Following the discovery of photoferrotrophs, Ehrenreich and Widdel (1994) observed that *R. ferrooxidans* SW2 utilized organics (glucose and acetate) before Fe(II) was oxidized while *Chromatium* L7 used them simultaneously. In a later study, Melton et al. (2014) examined whether *R. palustris TIE-1* could oxidize Fe(II) in the presence of acetate and lactate. Acetate was consumed first followed by Fe(II) oxidation, whereas with lactate and Fe(II), both substrates were used simultaneously. This suggests that different photoferrotrophs prefer different substrates and potentially prefer different organics.

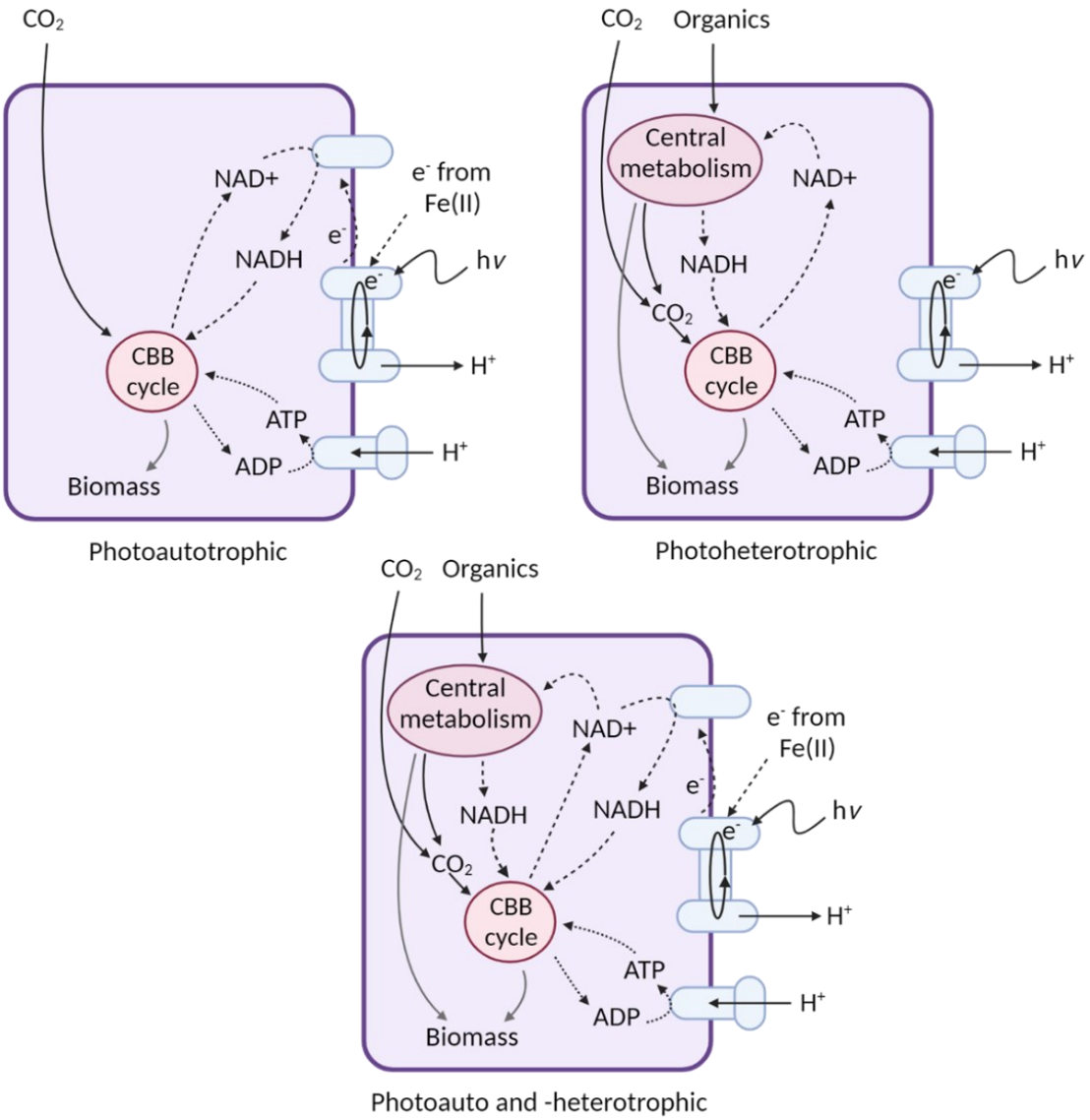

Figure 1: Schematics of photoautotrophic (left), photoheterotrophic (right) and mix of photoauto- and heterotrophic growth (middle) of purple bacteria R. palustris TIE-1. Created with Biorender.

Given the ubiquity of organic compounds and iron in the environment and their significant role for photoferrotrophic growth, more studies should address the question of substrate preference as this could have an impact on their contribution to the iron cycling. To date, no study has explicitly delved into the impact of co-substrate utilization on Fe(II) oxidation, particularly the effect of organic co-substrates on Fe(II) oxidation rates and mineral formation at environmentally relevant substrate concentrations.

Therefore, in this PhD thesis we investigated substrate preference on photoferrotrophic growth in detail and the impact of light exposure, through a day/night cycle, and buffer concentration.

We further investigated the environmental relevance of these altered conditions both in the lab and through *in-situ* field experiments. Each of these aspects is outlined in detail in the open questions below.

Open research questions

Main research questions (Chapter 2-4)

Substrate preference. In summary, Fe(II)-oxidizers have been studied in the past to ascertain their Fe(II) oxidation mechanism, Fe(II) oxidation rates, and Fe(II) mineral formation, whereas the influence of other substrates remains understudied. Therefore, the focus of this study is on the substrate preference of phototrophic Fe(II)-oxidizers and the implications this has for the environment:

In chapter 2 and 3 we performed batch experiments to:

a) Determine substrate preference of different photoferrotrophs (green sulfur and purple non-sulfur bacteria) between Fe(II) and acetate, lactate, pyruvate, butyrate, glucose or H_2 under environmentally relevant conditions.
b) Quantify the impact on Fe(II) oxidation rates, Fe(II) mineral formation, and mineral surface morphology

In chapter 4 we performed an *in situ* experiment in a stratified lake combined with batch experiments in the lab to investigate:

a) The influence of different substrate spikes of Fe(II) and organics on photoferrotrophs and bacterial community
b) How important is phototrophic Fe(II) oxidation in this system?
c) How important is iron cycling and what are the driving factors?

Additional research questions (Chapter 5-8)

Environmental conditions. During literature research it became apparent that laboratory conditions are often not comparable to those found in the environment due to parameters like high concentrations of buffers, buffer composition, and different light illumination. In this part of the study the influence of light exposure and buffer concentration on the growth photoferrotrophs and the impact on Fe(II) oxidation rates was investigated:

1. Day/night cycle (Chapter 5)**:** In recent studies the effect of different light intensities and wavelengths have been intensely studied. However, the fundamental condition of illumination duration has not been addressed so far, for example, in nature, where phototrophic Fe(II)-oxidizers would experience day/night cycles. To this end, we determined:

a) How does a light/dark cycle influence biomass and Fe(II) oxidation rates of photoferrotrophs?

b) What influence does a light/dark cycle has on Fe(III) mineral formation and mineral surface morphology?

2. Buffer concentration (Chapter 2 and 6)**:** Another aspect of laboratory-based experiments that fails to mimic environmental conditions is the buffer composition and concentration, which is maintained at a consistently high level throughout experiments. HCO_3^- is most often used for the dual purpose of providing the primary buffer as well as a carbon source for photoferrotrophs. Concentrations are kept high intentionally to avoid pH changes during Fe(II) oxidation when H^+ is released. In batch experiments we determined:

a) How does the buffer concentration and composition influence organics consumption and Fe(II) oxidation.
b) Is there an optimal buffer concentration range?

Methane (Chapter 7) is an important greenhouse gas and has been of interest due to its relevance to modern climate but also in the context of early Earth. In recent years studies have found that other bacteria produce low amounts of methane (Ernst et al., 2022). We wanted to investigate if phototrophic Fe(II)-oxidizers are also capable of producing methane when grown with Fe(II), H_2 and acetate.

a) Can photoferrotrophs produce methane?
b) Is methane production substrate- and strain-dependent?
c) What are the implications for modern and early Earth environments?

Enrichments (Chapter 8) and isolates enhance our understanding of photoferrotrophs and their role in the environment. Different enrichments of photoferrotrophs from different environments were, therefore, set up in chapter 8.

References

Akam, S. A., Chuang, P., Katsev, S., Wittkop, C., Chamberlain, M., Dale, A. W., Wallmann, K., Heathcote, A. J., & Swanner, E. D. (2024). Methane-carbon budget of a ferruginous meromictic lake and implications for marine methane dynamics on early Earth. *Geology*, *XX*(Xx), 1–6. https://doi.org/10.1130/G51713.1/6151692/g51713.pdf

Berg, J. S., Michellod, D., Pjevac, P., Martinez-Perez, C., Buckner, C. R. T., Hach, P. F., Schubert, C. J., Milucka, J., & Kuypers, M. M. M. (2016). Intensive cryptic microbial iron cycling in the low iron water column of the meromictic Lake Cadagno. *Environmental Microbiology*, *18*(12), 5288–5302. https://doi.org/10.1111/1462-2920.13587

Blankenship, R. E., Cheng, P., Causgrove, T. P., Brune, D. C., Wang, S. H., Choh, J. -U, & Wang, J. (1993). REDOX REGULATION OF ENERGY TRANSFER EFFICIENCY IN ANTENNAS OF GREEN PHOTOSYNTHETIC BACTERIA. *Photochemistry and Photobiology*, *57*(1), 103–107. https://doi.org/10.1111/J.1751-1097.1993.TB02263.X

Blankenship, R. E., & Matsuura, K. (2003). *Antenna Complexes from Green Photosynthetic Bacteria*. 195–217. https://doi.org/10.1007/978-94-017-2087-8_6/COVER

Bryce, C., Blackwell, N., Schmidt, C., Otte, J., Huang, Y. M., Kleindienst, S., Tomaszewski, E., Schad, M., Warter, V., Peng, C., Byrne, J. M., & Kappler, A. (2018). Microbial anaerobic Fe(II) oxidation – Ecology, mechanisms and environmental implications. *Environmental Microbiology*, *20*(10), 3462–3483. https://doi.org/10.1111/1462-2920.14328

Byrne, J. M., Klueglein, N., Pearce, C., Rosso, K. M., Appel, E., & Kappler, A. (2015). Redox cycling of Fe(II) and Fe(III) in magnetite by Fe-metabolizing bacteria. *Science*, *347*(6229), 1473–1476. http://www.sciencemag.org/content/347/6229/1473.full

Canfield, D., Kristensen, E., & Thamdrup, B. (2005). *Aquatic geomicrobiology*. https://books.google.de/books?hl=en&lr=&id=4m3byX7BHJEC&oi=fnd&pg=PR11&dq=Canfield,+D.+E.,+Kristensen,+E.,+and+Thamdrup,+B.+(2005).+Aquatic+geomicrobiology.+Gulf+Professional+Publishing.&ots=w_pH_2Q39X&sig=sxBOTVDi8ZoKBlclLjsQh0wCLi8

Croal, L. R., Johnson, C. M., Beard, B. L., & Newman, D. K. (2004a). Iron isotope fractionation by Fe(II)-oxidizing photoautotrophic bacteria. *Geochimica et Cosmochimica Acta*, *68*(6), 1227–1242. https://doi.org/10.1016/j.gca.2003.09.011

Croal, L. R., Johnson, C. M., Beard, B. L., & Newman, D. K. (2004b). Iron isotope fractionation by Fe(II)-oxidizing photoautotrophic bacteria. *Geochimica et Cosmochimica Acta*, *68*(6), 1227–1242. https://doi.org/10.1016/J.GCA.2003.09.011

Crowe, S. A., Hahn, A. S., Morgan-Lang, C., Thompson, K. J., Simister, R. L., Llirós, M., Hirst, M., & Hallam, S. J. (2017). Draft Genome Sequence of the Pelagic Photoferrotroph Chlorobium phaeoferrooxidans. *Genome Announcements*, *5*(13). https://doi.org/10.1128/GENOMEA.01584-16

Crowe, S. A., Jones, C. A., Katsev, S., Magen, C., O'Neill, A. H., Sturm, A., Canfield, D. E., Haffner, G. D., Mucci, A., Sundby, B., & Fowle, D. A. (2008). Photoferrotrophs thrive in an Archean Ocean analogue. *Proceedings of the National Academy of Sciences of the United States of America*, *105*(41), 15938–15943. https://doi.org/10.1073/pnas.0805313105

Ehrenreich, A., & Widdel, F. (1994). Anaerobic oxidation of ferrous iron by purple bacteria, a new type of phototrophic metabolism. *Applied and Environmental Microbiology*, *60*(12), 4517–4526. https://doi.org/10.1128/AEM.60.12.4517-4526.1994

Eickhoff, M., Obst, M., Schröder, C., Hitchcock, A. P., Tyliszczak, T., Martinez, R. E., Robbins, L. J., Konhauser, K. O., & Kappler, A. (2014). Nickel partitioning in biogenic and abiogenic ferrihydrite: The influence of silica and implications for ancient environments. *Geochimica et Cosmochimica Acta*, *140*, 65–79. https://doi.org/10.1016/j.gca.2014.05.021

Ernst, L., Steinfeld, B., Barayeu, U., Klintzsch, T., Kurth, M., Grimm, D., Dick, T. P., Rebelein, J. G., Bischofs, I. B., & Keppler, F. (2022). Methane formation driven by reactive oxygen species across all living organisms. *Nature*, *603*(7901), 482–487. https://doi.org/10.1038/s41586-022-04511-9

Han, X., Tomaszewski, E. J., Sorwat, J., Pan, Y., Kappler, A., & Byrne, J. M. (2020). Oxidation of green rust by anoxygenic phototrophic Fe(II)-oxidising bacteria. *Geochem. Persp. Let*, *12*, 52–57. https://doi.org/10.7185/geochemlet.2004

Hauruseu, D., & Koblízek, M. (2012). Influence of light on carbon utilization in aerobic anoxygenic phototrophs. *Applied and Environmental Microbiology*, *78*(20), 7414–7419. https://doi.org/10.1128/AEM.01747-12

Heising, S., Richter, L., Ludwig, W., & Schink, B. (1999). Chlorobium ferrooxidans sp. nov., a phototrophic green sulfur bacterium that oxidizes ferrous iron in coculture with a "Geospirillum" sp. strain. *Archives of Microbiology*, *172*(2), 116–124. https://doi.org/10.1007/s002030050748

Jiao, Y., Kappler, A., Croal, L. R., & Newman, D. K. (2005). Isolation and characterization of a genetically tractable photoautotrophic Fe(II)-oxidizing bacterium, Rhodopseudomonas palustris strain TIE-1. *Applied and Environmental Microbiology*. https://doi.org/10.1128/AEM.71.8.4487-4496.2005

Kappler, A., Bryce, C., Mansor, M., Lueder, U., Byrne, J. M., & Swanner, E. D. (2021). An evolving view on biogeochemical cycling of iron. *Nature Reviews Microbiology*, *19*(6), 360–374. https://doi.org/10.1038/s41579-020-00502-7

Kappler, A., & Newman, D. K. (2004). Formation of Fe(III)-minerals by Fe(II)-oxidizing photoautotrophic bacteria. *Geochimica et Cosmochimica Acta*, *68*(6), 1217–1226. https://doi.org/10.1016/J.GCA.2003.09.006

Kappler, A., Pasquero, C., Konhauser, K. O., & Newman, D. K. (2005). Deposition of banded iron formations by anoxygenic phototrophic Fe(II)-oxidizing bacteria. *Geology*, *33*(11), 865–868. https://doi.org/10.1130/G21658.1

Konhauser, K. O., Hamade, T., Raiswell, R., Morris, R. C., Ferris, F. G., Southam, G., & Canfield, D. E. (2002). Could bacteria have formed the Precambrian banded iron formations? *Geology*, *30*(12), 1079–1082. https://doi.org/10.1130/0091-7613(2002)030<1079:CBHFTP>2.0.CO;2

Kopf, S. H., Henny, C., & Newman, D. K. (2013). Ligand-enhanced abiotic iron oxidation and the effects of chemical versus biological iron cycling in anoxic environments. *Environmental Science and Technology*, *47*(6), 2602–2611. https://doi.org/10.1021/es3049459

Kucera, S., & Wolfe, R. S. (1957). a Selective Enrichment Method for Gallionella Ferruginea . *Journal of Bacteriology*, *74*(3), 344–349. https://doi.org/10.1128/jb.74.3.344-349.1957

Lalonde, K., Mucci, A., Ouellet, A., & Gélinas, Y. (2012). Preservation of organic matter in sediments promoted by iron. *Nature 2012 483:7388*, *483*(7388), 198–200. https://doi.org/10.1038/nature10855

Laufer, K., Byrne, J. M., Glombitza, C., Schmidt, C., Jørgensen, B. B., & Kappler, A. (2016). Anaerobic microbial Fe(II) oxidation and Fe(III) reduction in coastal marine sediments controlled by organic carbon content. *Environmental Microbiology*, *18*(9), 3159–3174. https://doi.org/10.1111/1462-2920.13387

Laufer, K., Niemeyer, A., Nikeleit, V., Halama, M., Byrne, J. M., & Kappler, A. (2017). Physiological characterization of a halotolerant anoxygenic phototrophic Fe(II)-oxidizing green-sulfur bacterium isolated from a marine sediment. *FEMS Microbiology Ecology*, *93*(5), 1–13. https://doi.org/10.1093/femsec/fix054

Llirós, M., Garciá-Armisen, T., Darchambeau, F., Morana, C., Triadó-Margarit, X., Inceoɔlu, Ö., Borrego, C. M., Bouillon, S., Servais, P., Borges, A. V., Descy, J. P., Canfield, D. E., & Crowe, S. A. (2015a). Pelagic photoferrotrophy and iron cycling in a modern ferruginous basin. *Scientific Reports*, *5*, 1–8. https://doi.org/10.1038/srep13803

Llirós, M., Garciá-Armisen, T., Darchambeau, F., Morana, C., Triadó-Margarit, X., Inceoɔlu, Ö., Borrego, C. M., Bouillon, S., Servais, P., Borges, A. V., Descy, J. P., Canfield, D. E., & Crowe, S. A. (2015b). Pelagic photoferrotrophy and iron cycling in a modern ferruginous basin. *Scientific Reports 2015 5:1*, *5*(1), 1–8. https://doi.org/10.1038/srep13803

McKinlay, J. B., & Harwood, C. S. (2010). Carbon dioxide fixation as a central redox cofactor recycling mechanism in bacteria. *Proceedings of the National Academy of Sciences of the United States of America*, *107*(26), 11669–11675. https://doi.org/10.1073/pnas.1006175107

Melton, E. D., Schmidt, C., Behrens, S., Schink, B., & Kappler, A. (2014). Metabolic Flexibility and Substrate Preference by the Fe(II)-Oxidizing Purple Non-Sulphur Bacterium Rhodopseudomonas palustris Strain TIE-1. *Http://Dx.Doi.Org/10.1080/01490451.2014.901439*, *31*(9), 835–843. https://doi.org/10.1080/01490451.2014.901439

Melton, E. D., Schmidt, C., & Kappler, A. (2012). Microbial iron(II) oxidation in littoral freshwater lake sediment: The potential for competition between phototrophic vs. nitrate-reducing iron(II)-oxidizers. *Frontiers in Microbiology*, *3*(MAY), 1–12. https://doi.org/10.3389/fmicb.2012.00197

Melton, E D, Schmidt, C., Behrens, S., Schink, B., & Kappler, A. (2014). *Metabolic Flexibility and Substrate Preference by the Fe (II) -Oxidizing Purple Non-Sulphur Bacterium Rhodopseudomonas palustris Strain TIE-1 Metabolic Flexibility and Substrate Preference by the Fe (II) - Oxidizing Purple Non-Sulphur Bacterium Rhodop*. *September*, 37–41. https://doi.org/10.1080/01490451.2014.901439

Melton, Emily D., Stief, P., Behrens, S., Kappler, A., & Schmidt, C. (2014). High spatial resolution of distribution and interconnections between Fe- and N-redox processes in profundal lake sediments. *Environmental Microbiology*, *16*(10), 3287–3303. https://doi.org/10.1111/1462-2920.12566

Mu, C. C., Zhang, T. J., Zhao, Q., Guo, H., Zhong, W., Su, H., & Wu, Q. B. (2016). Soil organic carbon stabilization by iron in permafrost regions of the Qinghai-Tibet Plateau. *Geophysical Research Letters*, *43*(19), 10,286-10,294. https://doi.org/10.1002/2016GL070071

Otte, J. M., Harter, J., Laufer, K., Blackwell, N., Straub, D., Kappler, A., & Kleindienst, S. (2018). The distribution of active iron-cycling bacteria in marine and freshwater sediments is decoupled from geochemical gradients. *Environmental Microbiology*, *20*(7), 2483–2499. https://doi.org/10.1111/1462-2920.14260

Patzner, M. S., Mueller, C. W., Malusova, M., Baur, M., Nikeleit, V., Scholten, T., Hoeschen, C., Byrne, J. M., Borch, T., Kappler, A., & Bryce, C. (2020). Iron mineral dissolution releases iron and associated organic carbon during permafrost thaw. *Nature Communications*, *11*(6329). https://doi.org/10.1038/s41467-020-20102-6

Pavlov, A. A., Kasting, J. F., Brown, L. L., Rages, K. A., & Freedman, R. (2000). Greenhouse warming by CH4

in the atmosphere of early Earth. *Journal of Geophysical Research: Planets*, *105*(E5), 11981–11990. https://doi.org/10.1029/1999JE001134

Peng, C., Bryce, C., Sundman, A., Borch, T., & Kappler, A. (2019). *Organic Matter Complexation Promotes Fe(II) Oxidation by the Photoautotrophic Fe(II)-Oxidizer Rhodopseudomonas palustris TIE-1*. https://doi.org/10.1021/acsearthspacechem.9b00024

Renger, G., & Wolff, C. (1977). Further evidence for dissipative energy migration via triplet states in photosynthesis. The protective mechanism of carotenoids in Rhodopseudomonas spheroides chromatophores. *Biochimica et Biophysica Acta (BBA) - Bioenergetics*, *460*(1), 47–57. https://doi.org/10.1016/0005-2728(77)90150-5

Schmidt, C., Nikeleit, V., Schaedler, F., Leider, A., Lueder, U., Bryce, C., Hallmann, C., & Kappler, A. (2021). Metabolic Responses of a Phototrophic Co-Culture Enriched from a Freshwater Sediment on Changing Substrate Availability and its Relevance for Biogeochemical Iron Cycling. *Geomicrobiology Journal*, *38*(3), 267–281. https://doi.org/10.1080/01490451.2020.1837303

Straub, K. L., Rainey, F. a, & Widdel, F. (1999). Marine Phototrophic Ferrous-Iron-Oxidizing Purple Bacteria. *International Journal of Systematic Bacteriology*, *49*(1 999), 729–735.

Stumm, W., & Morgan, J. (2012). *Aquatic chemistry: chemical equilibria and rates in natural waters*. https://books.google.de/books?hl=de&lr=&id=NLV_yfulgkQC&oi=fnd&pg=PT14&dq=morgan+and+stumm+2012&ots=cLY0aqf3IK&sig=9ncXlgU393pyLvOIhufv-1IHsFs

Thompson, K. J., Kenward, P. A., Bauer, K. W., Warchola, T., Gauger, T., Martinez, R., Simister, R. L., Michiels, C. C., Llirós, M., Reinhard, C. T., Kappler, A., Konhauser, K. O., & Crowe, S. A. (2019). Photoferrotrophy, deposition of banded iron formations, and methane production in Archean oceans. *Science Advances*, *5*(11). https://doi.org/10.1126/sciadv.aav2869

Tipping, E. (1981). The adsorption of aquatic humic substances by iron oxides. *Geochimica et Cosmochimica Acta*, *45*(2), 191–199. https://doi.org/10.1016/0016-7037(81)90162-9

Wagai, R., & Mayer, L. M. (2007). Sorptive stabilization of organic matter in soils by hydrous iron oxides. *Geochimica et Cosmochimica Acta*, *71*(1), 25–35. https://doi.org/10.1016/J.GCA.2006.08.047

Widdel, F., Schnell, S., Heising, S., Ehrenreich, A., Assmus, B., & Schink, B. (1993). Ferrous iron oxidation by anoxygenic phototrophic bacteria. *Nature*, *362*(6423), 834–836. https://doi.org/10.1038/362834a0

Winogradsky, S. (1888). *Beiträge zur Morphologie und Physiologie der Bacterien: hft. I.: Zur Morphologie und Physiologie der Schwefelbacterien.* (Vol. 1). Verlag von Arthur Felix.

Zhao, Q., Adhikari, D., Huang, R., Patel, A., Wang, X., Tang, Y., Obrist, D., Roden, E. E., & Yang, Y. (2017). Coupled dynamics of iron and iron-bound organic carbon in forest soils during anaerobic reduction. *Chemical Geology*, *464*, 118–126. https://doi.org/10.1016/j.chemgeo.2016.12.014

Zhao, Q., Poulson, S. R., Obrist, D., Sumaila, S., Dynes, J. J., McBeth, J. M., & Yang, Y. (2016). Iron-bound organic carbon in forest soils: Quantification and characterization. *Biogeosciences*, *13*(16), 4777–4788. https://doi.org/10.5194/BG-13-4777-2016

Zhi, R., Yang, A., Zhang, G., Zhu, Y., Meng, F., & Li, X. (2019). Effects of light-dark cycles on photosynthetic bacteria wastewater treatment and valuable substances production. *Bioresource Technology*, *274*, 496–501. https://doi.org/10.1016/J.BIORTECH.2018.12.021

2 Chapter: Phototrophic Fe(II) oxidation by *Rhodopseudomonas palustris* TIE-1 in organic and Fe(II)-rich condition

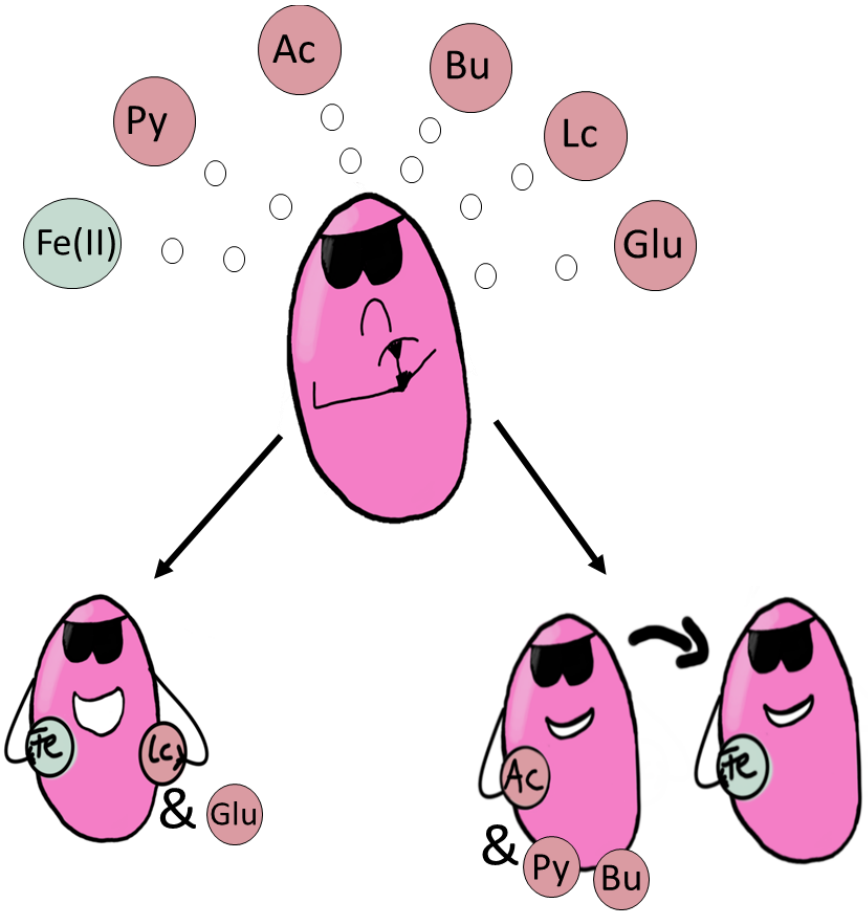

Contributions:

The original hypothesis was formulated by Dr. C. Bryce, Assoc. Prof. J.M. Byrne and Prof. Dr. A. Kappler. Resources were provided by Dr. C. Bryce, Assoc. Prof. J.M. Byrne and Prof. Dr. A. Kappler. Me and Dr. C. Bryce designed the project together with input of Assoc. Prof. Dr. J.M. Byrne, Prof. Dr. A. Kappler and Prof. C. Harwood. I conducted the analysis in the laboratory with assistance of M. Maisch. M. Maisch performed Mössbauer and SEM analysis. The manuscript was written by myself with guidance of Dr. C. Bryce and Prof. Dr. A. Kappler and revised by all co-authors.

Phototrophic Fe(II) oxidation by *Rhodopseudomonas palustris* TIE-1 in organic and Fe(II)-rich conditions

Verena Nikeleit[1], Markus Maisch[1], James M. Byrne[2], Caroline Harwood[3], Andreas Kappler[1,4] and Casey Bryce[2*]

[1]Department of Geoscience, University of Tübingen, Tübingen, Germany

[2]School of Earth Sciences, University of Bristol, Bristol, UK

[3]Department of Microbiology, University of Washington, Seattle, USA

[4]Cluster of Excellence: EXC 2124: Controlling Microbes to Fight Infections, Tübingen, Germany

*Corresponding Author: Casey Bryce

School of Earth Science, Wills Memorial Building, University of Bristol, Queens Road, Bristol, BS8 1RJ, UK.

Published in Environmental Microbiology

Abstract

Rhodopseudomonas palustris TIE-1 grows photoautotrophically with Fe(II) as an electron donor and photoheterotrophically with a variety of organic substrates. However, it is unclear whether *R. palustris* TIE-1 conducts Fe(II) oxidation in conditions where organic substrates and Fe(II) are available simultaneously. Additionally, the effect of organic co-substrates on Fe(II) oxidation rates or the identity of Fe(III) minerals formed are unknown. We incubated *R. palustris* TIE-1 with 2 mM Fe(II), amended with 0.6 mM organic co-substrate and in the presence/absence of CO_2. We found that in the absence of CO_2, only the organic co-substrates acetate, lactate and pyruvate, but not Fe(II), were consumed. When CO_2 was present, Fe(II) and all organic substrates were consumed. Acetate, butyrate and pyruvate were consumed before Fe(II) oxidation commenced, whereas lactate and glucose were consumed at the same time as Fe(II) oxidation proceeded. Lactate, pyruvate and glucose increased the Fe(II) oxidation rate significantly (by up to three-fold in the case of lactate). ^{57}Fe Mössbauer spectroscopy revealed that short-range ordered Fe(III) oxyhydroxides were formed under all conditions. This study demonstrates phototrophic Fe(II) oxidation proceeds even in the presence of organic compounds, and that the simultaneous oxidation of organic substrates can stimulate Fe(II) oxidation.

Introduction

Iron (Fe), an important redox-active element in the environment, interacts with major nutrient cycles including carbon, nitrogen and sulfur, and affects the bioavailability and fate of toxic metals, pollutants and nutrients (Eickhoff et al., 2014; Kappler et al., 2021; Mu et al., 2016; Tipping, 1981). Some anoxygenic phototrophs can oxidize Fe(II) (photoferrotrophs), and are widespread in various environments and throughout Earth's history (Ehrenreich & Widdel, 1994; Heising et al., 1999; Jiao et al., 2005; Kappler et al., 2005; Laufer et al., 2017; Llirós et al., 2015; Straub et al., 1999). The surface of Earth's ancient oceans was an ideal habitat for these bacteria, with high concentrations of dissolved Fe(II) (up to 0.5 mM), presence of light, and anoxic conditions (Poulton & Canfield, 2011). During that time, vast Fe(III)-rich deposits were formed, known as banded iron formations (BIFs), and it is thought that photoferrotrophs could have played a key role in their formation (Kappler et al., 2005; Konhauser et al., 2002; Thompson et al., 2019). Although conditions on Earth today are not as favorable for photoferrotrophs given the ubiquity of oxygen, there are still habitats where they can thrive, in sweet spots where anoxic conditions, light and dissolved Fe(II) are present simultaneously, such as stratified lakes, freshwater and marine sediments, and small iron-rich ponds (Crowe et al., 2017; Heising et al., 1999; Jiao et al., 2005; Laufer et al., 2017).

A number of strains isolated from the groups of green sulfur, purple sulfur and purple non-sulfur bacteria have given insights into the metabolism of photoferrotrophs. These include three green sulfur bacteria (GSB): *Chlorobium ferrooxidans* KoFox (freshwater co-culture, Heising et al., 1999), *Chlorobium* sp. N1 (marine co-culture, Laufer et al., 2017), *Candidatus* Chlorobium masyuteum (freshwater, co-culture, Lambrecht et al., 2021) and *Chlorobium phaeoferrooxidans* KB01 (first pure isolate, sourced from a stratified lake (Crowe et al., 2017)). For the purple non-sulfur bacteria, *Rhodobacter ferrooxidans* SW2 and *Rhodopseudomonas palustris* TIE-1 are used as models for freshwater strains and have been extensively studied

(Bird et al., 2011; Ehrenreich & Widdel, 1994; Jiao et al., 2005; Kappler & Newman, 2004; Miot et al., 2009). *R. ferrooxidans* SW2 was isolated from a freshwater sediment and *R. palustris* TIE-1 from a marsh sediment. *Rhodovulum iodosum* and *Rhodovulum robiginosum* are representatives for marine purple non-sulfur strains and from purple sulfur bacteria *Thiodictyon* sp. F4 is used as a model strain (Croal et al., 2004; Straub et al., 1999).

Although these microbes were mostly studied with regards to their ability to oxidize Fe(II), they are metabolically flexible can grow photoheterotrophically and photoautotrophically with variety of substrates as electron donors (Jiao et al., 2005; Laufer et al., 2017). When grown photoautotrophically these organisms fix CO_2 to build biomass while using different inorganic substrates (H_2, H_2S, $S_2O_3^{2-}$ or Fe(II)) as an electron source (Figure 1). For photoheterotrophic growth they can use a wide range of organic substrates like acetate, lactate and pyruvate, as well as larger molecules like glucose. These organic compounds can be used as a carbon source to build biomass or/and as an electron donor (Figure 1). McKinlay and Harwood (2010) found that 22% of acetate used by *R. palustris* was oxidized to CO_2 and used to recycle cofactors necessary for building biomass. Therefore, CO_2 plays an important role for these phototrophs as a carbon source and as a way to recycle cofactors (McKinlay & Harwood, 2010). Further studies investigated how these bacteria would behave when they have multiple substrates present, as they can grow photoautotrophically and photoheterotrophically (Figure 1).

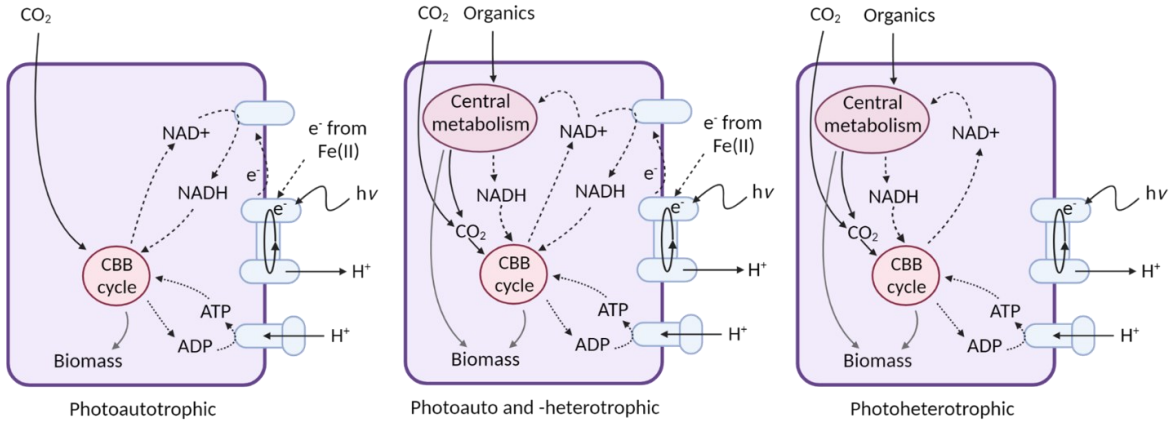

Figure 1: Schematics of photoautotrophic (left), mix of photoauto- and heterotrophic (middle), and heterotrophic growth (right) of R. palustris TIE-1. Created with Biorender.

Ehrenreich and Widdel (1994) found that organics (glucose and acetate) were used before Fe(II) was oxidized by *R. ferrooxidans* SW2, but *Chromatium* L7 used the substrates at the same time. Several years later, Melton et al. (2014) studied whether *R. palustris* TIE-1 can oxidize Fe(II) in the presence of acetate and lactate. However, in that study relatively high substrate concentrations were used (5 mM Fe(II); 20 mM acetate and lactate) and different consumption scenarios were observed. In the case of acetate and Fe(II), acetate was consumed first followed by Fe(II) oxidation, whereas with lactate and Fe(II) both substrates were used simultaneously. So far no study has explicitly investigated the effect of utilization of co-substrates on Fe(II) oxidation, especially the effect of organic co-substrates on Fe(II) oxidation rates and mineral formation at environmentally relevant substrate concentrations.

As organic compounds are ubiquitous in the environment and also play an important role for photoferrotrophs, we investigated how different organic substrates and CO_2 availability influence oxidation of Fe(II) by the photoferrotrophic strain R. *palustris* TIE-1, as well as how the presence of organics influences the identity of the minerals that is formed during Fe(II) oxidation. A wide range of organic substrates were tested including easily accessible organic compounds such as acetate, lactate and pyruvate. Butyrate was tested as an example of a more

reduced carbon substrate and glucose as a more complex organic substrate. Additionally, to assess the importance and role of CO_2 in co-substrate utilization, experiments were conducted both in the presence and absence of CO_2/HCO_3.

Material and methods

Effects of organic substrates on Fe(II) oxidation. For substrate preference experiments *R. palustris* TIE-1, a well-studied photoferrotrophic strain, was chosen (Jiao et al., 2005). *R. palustris* TIE-1 was grown for two transfers on H_2/CO_2 (80:20; v:v) prior to the experiment to avoid bias towards any of the experimental substrates. 50 mL media was added to 100 mL serum vials and inoculated with 0.5% of the pre-grown *R. palustris* TIE-1 culture. Media was prepared as stated in Jiao et al. (2005). The following salts were dissolved in one liter of ultrapure water: 0.5 g KH_2PO_4, 0.3 g NH_4Cl, 0.5 g $MgSO_4$ * $7H_2O$, 0.1 g $CaCl_2$*$2H_2O$ and autoclaved in a Widdel flask. After autoclaving, 10 mL/L filter-sterilized vitamin solution (altered from Ehrenreich & Widdel, 1994; containing 50 mg/L riboflavin), 1 mL/L SL10 trace element solution (Widdel, 1983), 1 mL/L selenite-tungstate solution (Widdel & Bak, 1992) and 0.1 mg/L vitamin B12 solution were added. The medium was prepared with a headspace of N_2/CO_2 (90:10; v:v) and buffered with 22 mM HCO_3^-. The pH of the media was adjusted to pH 7 with anoxic 1 M HCl and anoxic 0.5 mM H_2CO_3.

For the substrate preference experiments, three different setups were used. In the first setup, only $FeCl_2$ was added. In the second setup $FeCl_2$ and an organic substrate (0.6 mM) (either acetate (Ac), lactate (Lc), pyruvate (Py), butyrate (Bu) or glucose (Glu)) were added. In the third setup, only organic substrates (0.6 mM) were added. For the setups with Fe(II), 4.5 mM $FeCl_2$ was added to the medium and left for 48 h at 4°C to allow precipitation of Fe(II) minerals, before the medium was filtered (0.22 µm) in an anoxic glovebox (100% N_2). This led to a starting concentration of approximately 2 mM dissolved Fe(II) in the experimental setups. The concentrations used are the minimum required to be able to track substrate consumption by our analytical methods. Although they are on the higher side of those found in the environment they are environmentally relevant. For example, they are similar to those found in some wetlands e.g. by Patzner et al. (2020). The organic compounds were added after the filtration step. Four

replicate bottles were inoculated in the setups with Fe(II), with one used as a sacrificial bottle for mineral analysis by Fe^{57}.-.specific Mössbauer spectroscopy - this bottle was sampled only at the end of the incubation. For abiotic controls, two bottles per substrate and setup were used without adding any bacteria. Abiotic controls were set up to evaluate any adsorption of Fe(II) to the glass wall and to ensure the absence of abiotic reactions between Fe and the chosen organic substrate. In the three biotic bottles continuous sampling and analysis of Fe, cell numbers and organics was performed. The abiotic bottles were sampled and analyzed at a subset of these timepoints for concentrations of Fe and organics. Samples were taken anoxically and under sterile conditions at the bench and samples for mineral analysis were taken in an anoxic glovebox (100% N_2). During the experiments, the vials were placed in a light incubator with 25±7 µmol photons/s/m^2 at 20°C and positioned randomly on the shelf to avoid biases based on position in the incubator. The Fe(II)-only setup was repeated with four bottles and all data show average of four bottles. In the setup of Fe(II) plus butyrate only two bottles showed Fe(II) oxidation and in the glucose-only setup only two bottles showed glucose consumption.

Fe(II) oxidation experiments in PIPES buffered medium lacking CO_2. CO_2 is essential for autotrophic Fe(II) oxidation. Therefore, we tested whether Fe(II) could also be oxidized by *R. palustris* TIE-1 in the absence of CO_2/HCO_3^- when *R. palustris* TIE-1 utilizes different organic substrates in parallel to Fe(II). This experiment had the same conditions as the substrate preference experiment described above except that 20 mM PIPES (piperazine-N,N′-bis(2-ethanesulfonic acid) was chosen as a buffer and the headspace contained only N_2. For this experiment, *R. palustris* TIE-1 was also pre-grown on H_2/CO_2 (80:20; v:v) for two consecutive transfers in bicarbonate-buffered media. The pre-culture cells were washed twice before inoculation to remove any residual bicarbonate from the inoculum. For this, serum vials were

centrifuged at 5000 rpm for 5 min anoxically. The supernatant was then exchanged with a syringe to keep the serum vial anoxic and replaced with 20 mM PIPES buffer.

Fe quantification. Fe(II) and Fe(III) were quantified spectrophotometrically with a modified ferrozine assay (Hegler et al., 2008). During sampling, 0.1 mL of sample was added to 0.9 mL of 1 M HCl. Samples were stored at 4°C until analysis. The ferrozine-Fe(II) complex was quantified at 562 nm using a microtiter plate reader (Thermo Scientific Multiscan, Thermo Fisher Scientific). Ferrozine measurements were conducted in triplicates. All rates were calculated over at least three data points.

Short-chain fatty acid analysis. High Performance Liquid Chromatography (HPLC) analysis was performed with a Shimadzu Prominence HPLC with a LC-20ATsolvent delivery unit, CTO-10ASvp column oven and a RID-20a refractive index detector. After sampling, samples were centrifuged at 15,000 rpm for 10 min to remove cells and minerals, and the supernatant was transferred to a new Eppendorf tube and stored at 4°C until analysis.

Cell number quantification. 1.8 mL of samples were stored at -20°C for DNA extraction and qPCR of 16S rRNA. DNA was extracted using the UltraClean R Microbial DNA Isolation Kit (MO BIO Laboratories, Carlsbad, CS, USA) and the quantity of the DNA was measured with a Nanodrop ND-1000 Spectrometer (Nanodrop^{TM} 1000, Thermo Scientific, Waltham, MA, USA). qPCR was conducted with the iCycler iQ^{TM}Real-Time PCR Detection System and the Bio-Rad CFX Maestro 1.1 software. 16S rRNA was quantified with the 341F (CCTACGGGAGGCAGCAG) and 797R (GGACTACCAGGGTATCTAATCCTGTT) primer pair (Nadkarni et al., 2002). A mix of 5 µL SYBR green, 0.15 µL 341F primer, 0.45 µL 797R primer, 3.4 µL H_20 and 1 µL of sample was prepared for the number of samples, standards and negative control in triplicates with a reaction volume of 10 µL. For standards, plasmids with respective genes were used and quantified with Qubit 2.0 (Invitrogen, Carlsbad, CA, USA)

Statistical analysis. In order to evaluate if differences between conditions were statistically significant, we performed Welsh's t-test to account for unequal variances between each sample treatment. We chose a significance threshold of $\alpha = 0.05$.

Mineral analysis by Mössbauer spectroscopy. Within an anoxic glovebox (100% N_2), 20 mL liquid sample was collected from each microcosm, filtered through a 0.45 μm pore space syringe filter (area 1 cm^2) and covered with Kapton tape, forming a thin disc. Samples were stored under anoxic conditions at -18°C to avoid microbial activity and mineral transformation. Individual samples were transported to the Mössbauer instrument within airtight bottles which were only opened immediately prior to loading into a closed-cycle exchange gas cryostat (Janis cryogenics) under a backflow of He to minimize exposure to air. Spectra were collected at 77 K using a constant acceleration drive system (WissEL) in transmission mode with a ^{57}Co/Rh source. All spectra were calibrated against a 7 μm thick α-^{57}Fe foil that was measured at room temperature. Analysis was carried out using Recoil (University of Ottawa) and the Voigt Based Fitting (VBF) routine (Rancourt & Ping, 1991). The half width at half maximum (HWHM) was constrained to 0.134 mm/s during fitting.

Scanning electron microscopy (SEM). SEM was conducted to visualize the interactions and associations between the microbial cells and the minerals. For SEM, cultures of *R. palustris* TIE-1 were grown with Fe(II) only, Fe(II) plus acetate, Fe(II) plus lactate, and Fe(II) plus glucose. At the end of the incubation, a sample was fixed by adding glutaraldehyde (2.5%; v/v). 30 μL of fixed samples were placed on a glass slide which was coated with 50 μL of poly-L-lysine. The samples were dehydrated with increasing ethanol solutions starting from 35% to 100% (5 min per new solution; 35%, 55%, 70% 90% to 100%). The samples were then placed in HMDS two times for 30 seconds and left in the fume hood to dry. Samples were placed on aluminum stubs and sputter-coated at a working distance of 35 mm at 20 mA for 70 sec to receive a 13 nm coating (BAL-TEC SCD 005). Microscopy was done with

a ZEISS Crossbeam 550L using an electron high tension of 2 kV, working distance of 1.5 mm and a secondary electron secondary ion (SESI) detector.

Results and Discussion

R. palustris TIE-1 substrate preferences

In order to determine the effect of organic substrates on Fe(II) oxidation, *R. palustris* TIE-1 was grown in CO_2/HCO_3^- buffered media with Fe(II) only, Fe plus an organic substrate (acetate, lactate, pyruvate, butyrate or glucose) or organics alone. We found that *R. palustris* TIE-1 consumed all of the added organics completely and oxidized Fe(II). Both sequential and simultaneous consumption of organics alongside Fe(II) oxidation was observed during the experiment, depending on the identity of the organic compound. In the abiotic setup no changes in organic substrate and Fe(II) concentrations were observed (data not shown). In the setups with Fe(II) plus acetate (Ac), Fe(II) plus pyruvate (Py) and Fe(II) plus butyrate (Bu), the organics were consumed first followed by the oxidation of Fe(II) (Figure 2B, D and F). No lag phases in the consumption of these organics were observed and were consumed within 3.3 d (Ac plus Fe(II)) to 4 d (Bu and Py plus Fe(II)) (Figure 2B, D and F), respectively. Once the organics were consumed, Fe(II) was oxidized to an extent of 84±5% (with acetate), 90±2% (with pyruvate), and 84±3% (with butyrate). In the setups with Fe(II) plus lactate and Fe(II) plus glucose, Fe(II) oxidation reached 91±1% and 98±2%, respectively. In the latter two cases, simultaneous consumption of Fe(II) and organics was observed (Figure 2C and E). In the case of Fe(II) only, 89% of Fe(II) was oxidized (Figure 2A). Our data expand our understanding of different substrate preferences for *R. palustris* TIE-1 and were determined for a first time for pyruvate, butyrate and glucose. We could also show that the findings of Melton et al. (2014) regarding the substrate preference of acetate, lactate and Fe(II) hold true even at much lower, environmentally relevant, substrate concentrations.

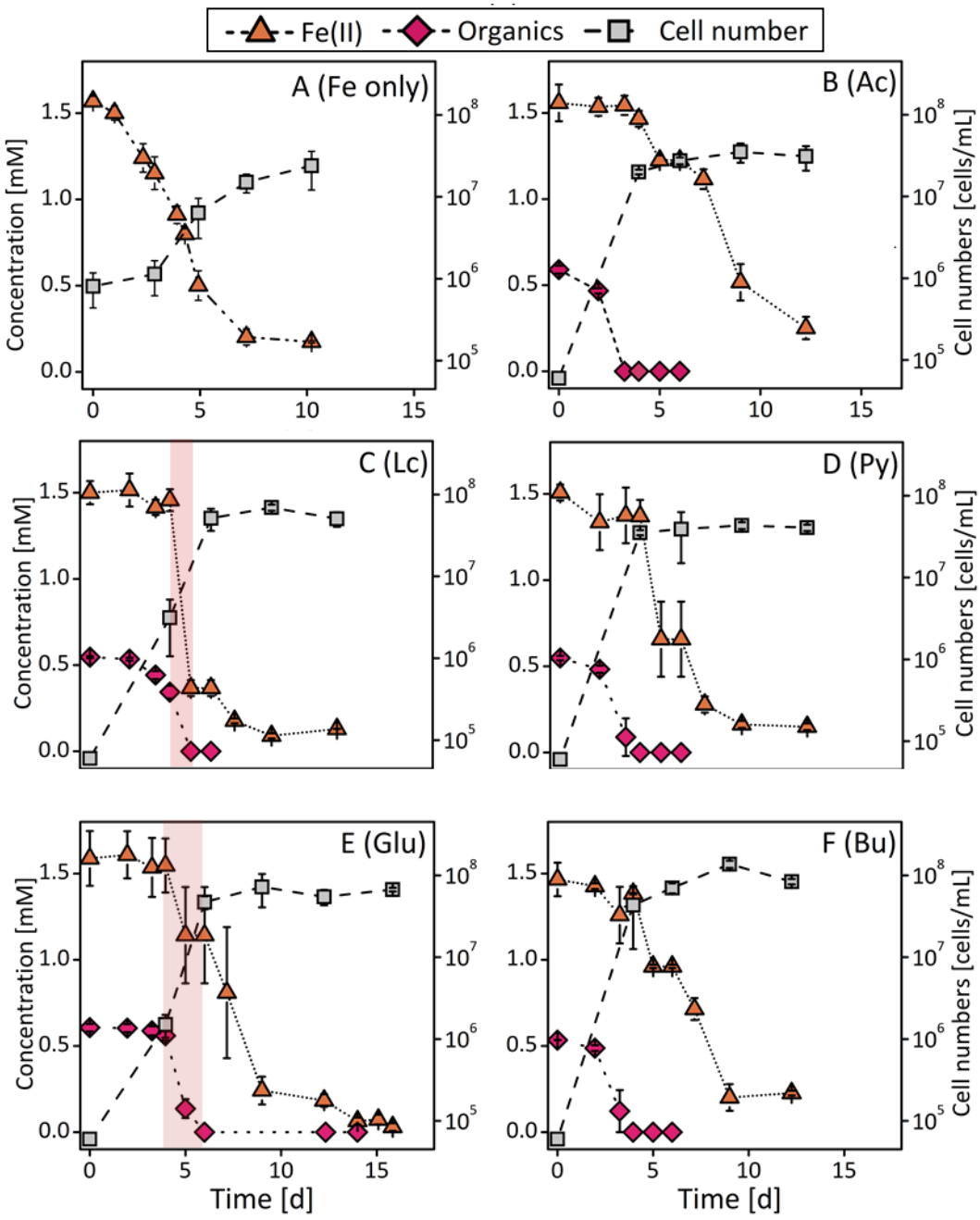

Figure 2: Figure 2: Growth of R. palustris TIE-1 *with different growth substrates. Panel A shows R. palustris* TIE-1 *grown only with Fe(II). In panel B to F R. palustris TIE-1 was grown with Fe(II) plus an organic substrate (either acetate (B-Ac), lactate (C-Lc), pyruvate (D-Py), butyrate (E-Bu) or glucose (F-Glu)). The standard deviation is based on biological triplicates, in case of A standard deviation is based on 4 bottles. The pink background shows simultaneous consumption of an organic substrate and Fe(II). All media were buffered with CO_2/HCO_3.*

However, in their study substrate concentrations were many folds higher (16 mM organic compounds and 5 mM Fe(II)). Our results in combination with theirs demonstrate that consumption order is independent of substrate concentrations. Additionally, the substrate preferences of strain *R. palustris* TIE-1 appear to differ from those of other photoferrotrophs. Ehrenreich and Widdel showed that *R. ferrooxidans* SW2 used these substrates in a sequential order (acetate and glucose before Fe(II) (Ehrenreich & Widdel, 1994). In the same study a second strain, *Chromatium* L7, was shown to consume the organics (glucose or acetate) and Fe(II) at the same time (Ehrenreich & Widdel, 1994). This contrasts with our findings where *R. palustris* TIE-1 used glucose and Fe(II) at the same time but used acetate before Fe(II). These studies suggest that substrate preferences are independent of substrate concentrations but are likely unique to individual strains of phototrophic Fe(II)-oxidizers. These results regarding the substrate preference of *R. palustris* TIE-1 help us to understand how different photoferrotrophs could actively contribute to Fe(II) oxidation under various conditions; and show that in the environment Fe(II) will still be oxidized even when these cells have the option to conduct photoheterotrophy (arguably a more favorable metabolism).

Effect of multiple substrates on consumption rates of both organics and Fe(II)

Fe(II) and organics each influenced the consumption rate of the other substrates. For the setup with Fe(II) only, in bicarbonate buffered medium, Fe(II) oxidation was completed for all four bottles after 10.2 days with an average Fe(II) oxidation rate of 0.23±0.04 mM/d (Figure 3A). This Fe(II) oxidation rate corresponds well to previously published data for the same strain (0.27±0.01 mM/d (Han et al., 2020) and 0.15±0.03 mM/d (Peng et al., 2019)) which also measured Fe(II) oxidation rates in the absence of alternative substrates. Fe(II) oxidation rates for setups with Fe(II) plus butyrate (0.24±0.01 mM/d) were in the same range as in the setup with Fe(II) only. With acetate, the Fe(II) oxidation rate was slightly lower (0.17±0.01 mM/d)

than with Fe(II) alone. For the setups with Fe(II) plus pyruvate (0.34±0.02 mM/d), Fe(II) plus glucose (0.33±0.04 mM/d) and Fe(II) plus lactate (1.05±0.02 mM/d), Fe(II) oxidation rates were significantly increased and in the case of Fe(II) plus lactate, increased more than threefold (Table S1). We also observed that Fe(II) had an effect on the consumption rates of organic compounds (Figure 3B). For lactate (with Fe(II) 0.25±0.01 mM/d and without Fe(II) 0.21±0.02 mM/d), butyrate (with Fe(II) 0.31±0.06 mM/d and without Fe(II) 0.17±0.002 mM/d) and glucose (with Fe(II) 0.27±0.01 mM/d and without Fe(II) 0.12±0.03 mM/d), the consumption of the organics was enhanced when Fe(II) was present. For lactate this increase was statistically significant (Table S1). For glucose and butyrate consumption, the addition of Fe(II) had a large beneficial impact and increased consumption rates 1.7-fold for butyrate and 2-fold for glucose. In the case of acetate and pyruvate, consumption rates with and without Fe(II) were within error range (acetate: with Fe(II) 0.18±0.01 mM/d and without Fe(II) 0.23±0.05 mM/d; pyruvate: with Fe(II) 0.24±0.01 mM/d and without Fe(II) 0.24±0.05 mM/d).

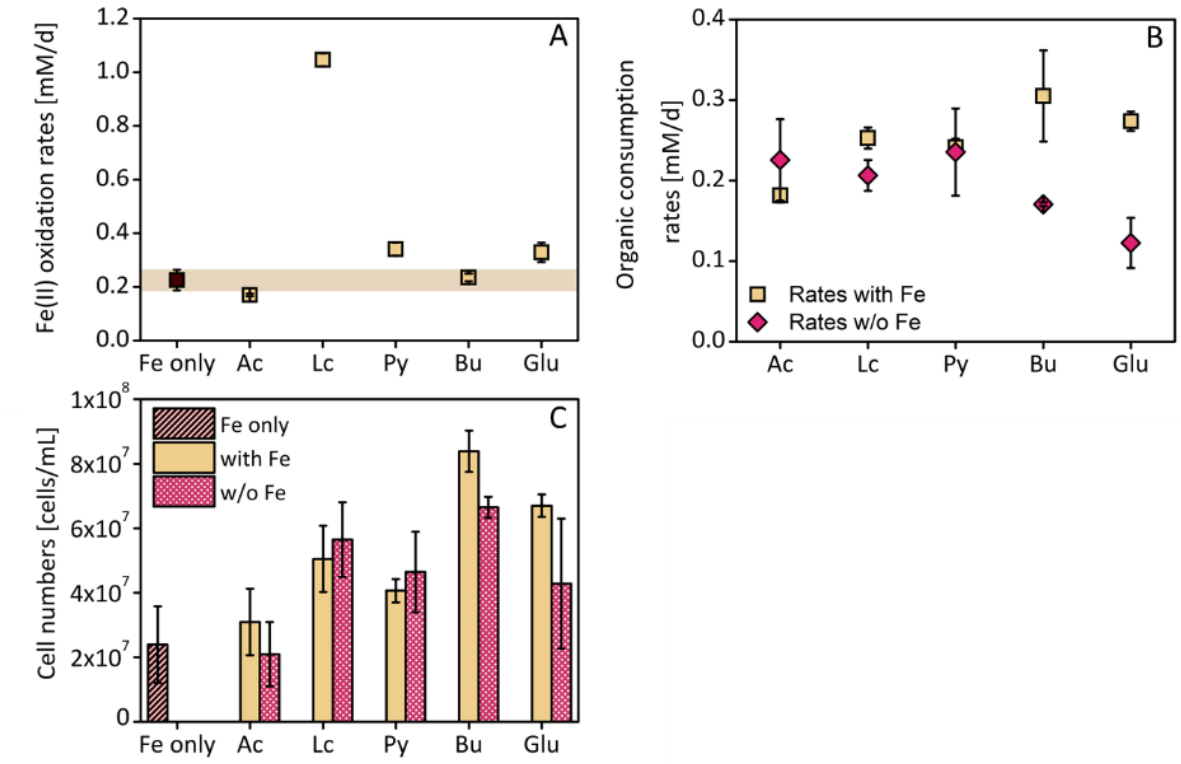

Figure 3: Panel A shows the Fe(II) oxidation rates of R. palustris TIE-1 *incubated with acetate (Ac), lactate (Lc), pyruvate (Py), butyrate (Bu) or glucose (Glu). The dark brown point shows the Fe(II) oxidation rate when only Fe(II) was added and the light brown background shows the standard deviation. Panel B shows the organic consumption rates when the organics and Fe(II) were added together (light brown square) or when only the organics were added (pink diamond). Panel C shows cell numbers of R. palustris* TIE-1 *at the end of the experiment for Fe(II) only (dark brown), organics plus Fe(II) (light brown) and only organics (pink with pattern). For Fe plus butyrate and glucose alone only duplicates are shown and the range is calculated and for Fe-only the average was calculated from 4 replicates. For all other set ups averages and rates were calculated from triplicates. All experiments were carried out in CO_2/HCO_3-buffered media.*

In general, organic compounds with more carbon atoms tended to show lower consumption rates without Fe(II) than those with fewer carbon atoms, but displayed higher consumption rates when Fe(II) was present. For Fe(II) oxidation the type of organic plays an important role in our study. Acetate and butyrate, 2 and 4-C atoms, did not influence Fe(II) oxidation whereas 3- and 6-C atom organics (lactate, pyruvate and glucose) lead to significant increase on Fe(II)

oxidation rates. We could also observe that for some substrates both consumption rates were increased (for glucose, lactate and Fe(II)), but in other cases only one consumption rate would increase (Fe(II) oxidation rate with pyruvate; butyrate consumption rate with Fe(II)). This demonstrates the complexity of these interactions and shows that co-substrate utilization can be beneficial for consumption of both substrates. With these data we expand our understanding of how turnover rates of both organic and inorganic substrates could be inter-dependent in the environment.

The observation that lactate stimulated Fe(II) oxidation by *R. palustris* TIE-1 was also made by Heising and Schink (1998) and by Melton et al. (2014); but was demonstrated at much higher substrate concentrations that apparently favored organic consumption. It has not previously been shown that these other substrates could also simulate Fe(II) oxidation. Heising and Schink showed for a different strain, *Rhodomicrobium vannielii* strain BS-1, that Fe(II) oxidation was stimulated by the addition of acetate or succinate suggesting these benefits of co-substrate utilization are likely universal across the Fe(II)-oxidizing phototrophs. Co-substrate utilization with non-organic substrates has been studied previously and, contrary to our findings with organics, found that Fe(II) oxidation rates of *R. palustris* TIE-1 and *R. ferrooxidans* SW2 decreased in the presence of H_2 and were generally higher with high (20 mM) compared to low (1 mM) $NaHCO_3$ concentrations (Croal et al., 2009). Our experiments suggest that contrary to what may be expected, the availability of organic compounds in the environment and thus the option for this strain to conduct both photoheterotrophy and photoautotrophy simultaneously, may be beneficial for both metabolisms.

Other advantages of multiple substrate use can be that bacteria can utilize substrates that were not bioavailable for them before. Our strain could use all of the tested substrates, however in a study by Govindaraju et al. (2019) *R. palustris* CGA009 could not use lactate alone, but when acetate and succinate were also added, this strain could use lactate. In another study

Rhodobacter capsulatus SB1003 could not solely grow with Fe(II) or citrate alone. When Fe(II) and citrate were used together, Fe(II) and citrate were broken down photochemically to form acetoacetic acid that supported growth (Caiazza et al., 2007). Both substrates could also bind to each other which makes it easier for the bacteria to use. For *Rhodobacter capsulatus* SB1003 it has been shown that it could oxidize Fe(II) when it was chelated with NTA (nitrilotriacetate) (Kopf & Newman, 2012). It has also been shown for this bacteria that the humic substances bind free Fe(II) and thus alleviate the toxcicity of free Fe(II) to *Rhodobacter capsulatus* SB1003 (Poulain et al., 2009).

In summary our experiments show that *R. palustris* TIE-1 consumes Fe(II) and different organic substrates simultaneously or sequentially, and that the extent and rate of Fe(II) oxidation is influenced by the identity of the organics present and vice versa. It shows that under the right conditions Fe(II) oxidation could be a more prominent reaction in the environment than previously thought .

Effects of different substrates on growth

In setups with acetate, pyruvate and butyrate plus Fe(II), rapid cell growth was observed and continued when Fe(II) was oxidized. Setups with lactate and glucose showed a slower initial rise in cell numbers. Second lowest cell numbers were measured in the setup with Fe(II) only (2.4±1.2 $*10^7$ cells/mL). In general, cell numbers in setups with Fe(II) plus organic compounds increased according to the number of carbons in the organic compound provided (i.e. butyrate > lactate > acetate) (Figure 3C). Highest cell numbers were reached with Fe(II) plus butyrate (8.4±0.6 $*10^7$ cells/mL) and Fe(II) plus glucose (6.7±0.3 $*10^7$ cells/mL). In both cases, cell numbers with Fe(II) were higher compared to cell numbers with organics alone. This was also true for Fe(II) plus acetate (with Fe(II) 3.1±1.0 $*10^7$ cells/mL and without Fe(II) 2.1±1.0 $*10^7$ cells/mL). In the cases of lactate and pyruvate, cell numbers were slightly higher without Fe(II)

(lactate: with Fe(II) 5.1±1.0 *10^7 cells/mL and without Fe(II) 5.7±1.2 *10^7 cells/mL; pyruvate: with Fe(II) 4.1±0.3 *10^7 cells/mL and without Fe(II) 4.7±1.3 *10^7 cells/mL).

We also compared these counted cell numbers to numbers predicted based on the available carbon in the organic substrates (Table S2) assuming a cell weighs 1 pg (dry weight consisting of CH_2O). For the calculations for the Fe(II) only setup, we assumed all electrons are used for fixing CO_2 into biomass (CO_2 → CH_2O; 4 electrons). Based on this calculation, the cell numbers for the setup with only Fe(II) should have been ca. 1.4 * 10^7 cells/mL which is close to our measured number of 2.4±1.2 *10^7 cells/mL For setups with organic substrates a similar approach was used. McKinlay and Harwood (2010) found that in an incubation of *R. palustris* strain CGA009 and CGA010 with 20 mM of acetate, 93% of the added acetate was converted into biomass. For simplicity, we assumed that 90% of the other organic substrates tested in our study were also converted into biomass. We would expect 1) higher cell numbers with organic compounds with more C-atoms and 2) formation of more cells when the organic compounds are used together with Fe(II) as substrates. The cell number calculations (Table S2) matched the measured cell numbers when either Fe(II) or the organic compounds were used alone. This was the case for acetate (2 C-atoms), lactate/pyruvate (3 C-atoms), and butyrate (4 C-atoms) whereas setups with glucose (6 C-atoms) showed lower cell numbers than the setups with butyrate. In the setups with lactate and pyruvate, the addition of Fe(II) did result in higher cell numbers as expected from theoretical calculations. This demonstrates that the addition of Fe(II) or substances with more C-atoms does not necessarily lead to an increase in cell number.

Influence of organics on mineral identity and morphology of cell-mineral aggregates formed during Fe(II) oxidation

A consequence of microbial Fe(II) oxidation is the formation of Fe(III) minerals. Therefore, we investigated how Fe(III) minerals and their associations with cells are affected by the presence

of organic co-substrates using Fe^{57} Mössbauer spectroscopy and Scanning Electron Microscopy (SEM). Samples from the setups containing either Fe(II) plus acetate, Fe(II) plus lactate, Fe(II) plus butyrate and Fe(II) plus glucose were collected after 12.3 days and samples from setups containing Fe(II) only and Fe(II) plus glucose were harvested after 15.8 days. Fe^{57} Mössbauer spectroscopy analyses of all samples at 77 K showed short range ordered Fe(III) oxyhydroxide minerals, likely ferrihydrite, as the dominant mineral phase (Figure S4). The only difference between the minerals collected from the different setups was the relative abundance of the remaining Fe(II) compared to the formed Fe(III) mineral . Setups with Fe(II) plus lactate showed the lowest abundance of remaining Fe(II) mineral phases (6%) whereas 94% of all iron mineral phases were present as poorly crystalline Fe(III) oxyhydroxides (Table S3). Setups with either Fe(II) only, Fe(II) plus pyruvate or Fe(II) plus butyrate showed similar abundances of remaining Fe(II) minerals of around 15% plus 85% ferrihydrite. The highest abundance of remaining Fe(II) mineral phases were detected in samples containing Fe(II) plus acetate (32%) and Fe(II) plus glucose (40%). Our results with the organics show that *R. palustris* TIE-1 consistently forms poorly crystalline Fe(III) oxyhydroxides when cultivated in this media and that the presence of external organic substrates has no influence on the minerals formed. This mineral phase is consistently found in studies of Fe(II) oxidation by *R. palustris* TIE-1 (e.g. Han et al., 2019) when no organics are present. This indicates that, despite the presence of organic compounds having an influence on the onset and rates of Fe(II) oxidation, the mineral formation is unaffected.

Although the identity of the Fe(III) minerals formed was the same for all setups (i.e. ferrihydrite), we were interested in whether there are differences in mineral surface morphology depending on the identity of the organics added as co-substrates. Therefore, SEM images were collected for the setups containing either Fe(II) only, Fe(II) plus acetate, Fe(II) plus lactate and Fe(II) plus glucose. We found that samples from setups containing Fe(II) only showed spiky

plates (Figure 4 and Figure S5). Similar mineral morphologies were also found in setups where organic substrates were present in addition to the Fe(II). We also observed cells embedded in the minerals (Figure 4). With more carbon substrates added, more cells were seen by SEM in the samples which is consistent with our data on cell numbers. Most of the cells were observed in the setup containing Fe(II) plus glucose. Here the surface of the minerals was covered with cells and web-like structures of organic matter were observed (probably EPS) (Figure 4). EPS structures in previous publications showed similar features to those we found in our SEM images (Diaz et al., 2017; Dohnalkova et al., 2011; Solmaz et al., 2018).

In summary we observed that the presence of organic substrates in addition to Fe(II) did not have an effect on the composition of the Fe(III) minerals formed by photoferrotrophs.

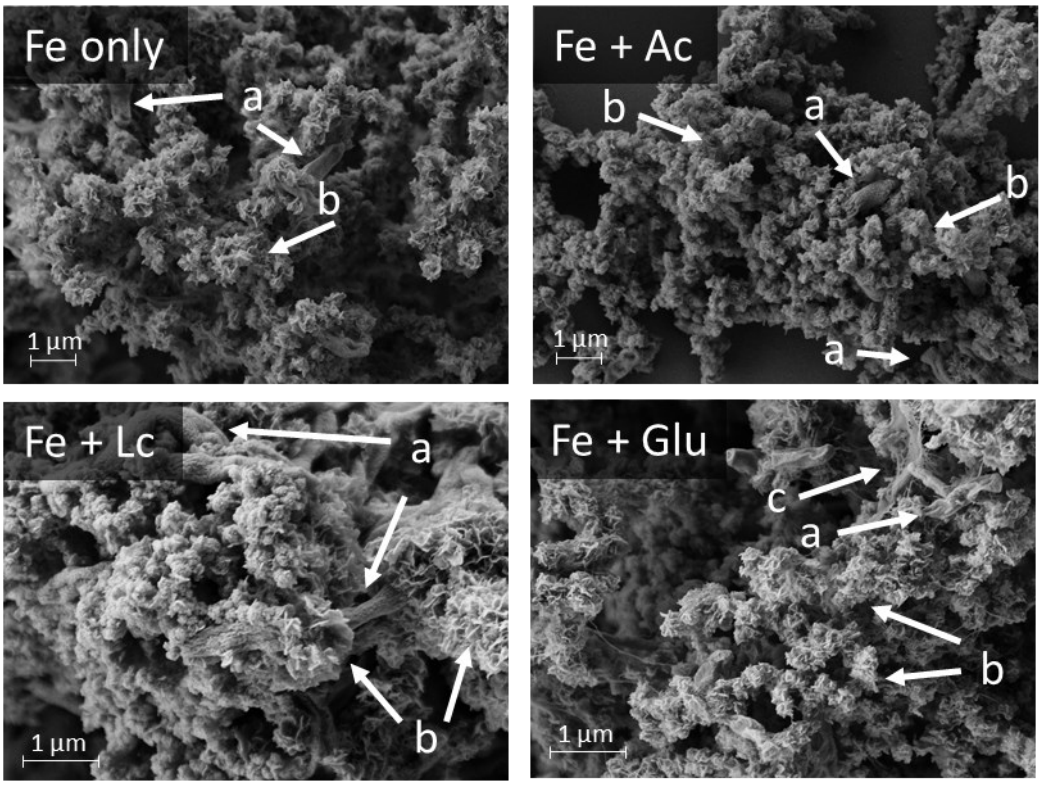

Figure 4: SEM images of R. palustris TIE-1 *grown with only Fe(II) (Fe only), with Fe(II) plus acetate (Fe + Ac), with Fe(II) plus lactate (Fe + Lc) and with Fe(II) plus glucose (Fe + Glu). Arrow a shows the cells of R. palustris* TIE-1*, arrow b shows the spiky minerals and arrow c shows web like structures.*

Effect of replacing CO_2/HCO_3 buffer with PIPES on Fe(II) oxidation and organic consumption

CO_2 is essential for autotrophic Fe(II) oxidation and for balancing internal redox potential of substrates more negative than biomass (McKinlay & Harwood, 2010). To investigate the impact of CO_2 on the patterns of substrate consumption, we exchanged the bicarbonate buffer for PIPES buffer and repeated the experiments. In the absence of CO_2/HCO_3 cells grew on acetate, lactate and pyruvate, but there was no growth with butyrate and glucose (Figure 5, Figure S1). Growth with glucose could, however, be observed in a separate experiment. (Figure S3). No Fe(II) oxidation occurred in the setup when only Fe(II) was present or when Fe(II) was present together with the organic co-substrates. However, Fe(II) did stimulate growth on lactate in PIPES-buffered medium. Cell numbers of Fe(II) plus lactate (3.0±1.6 $*10^7$ cells/mL) was three times higher than without Fe(II) (0.9±0.7$*10^7$ cells/mL; Figure 5A). For pyruvate, no beneficial effect was observed in the PIPES setups (with Fe(II) 1.7±0.5 $*10^7$ and without Fe(II) 1.7±0.1 $*10^7$ cells/mL) and in the case of acetate, cell numbers were lower (with Fe(II) 1.0±0.1 $*10^7$ and without Fe(II) 1.6±0.3 $*10^7$ cells/mL). When comparing cell numbers from PIPES-buffered medium setups to experiments with CO_2 /HCO_3^- buffered medium we found that cell numbers were higher when CO_2 was present with the exception of the setups with acetate alone (Figure 5A).

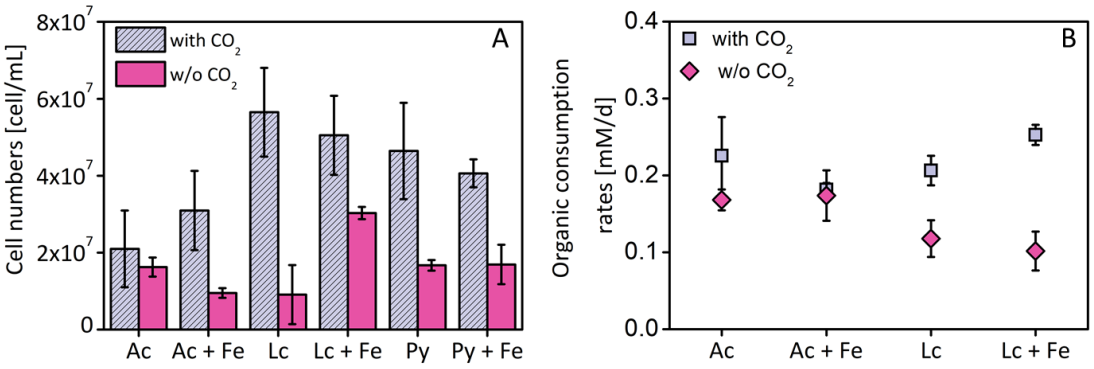

Figure 5: Panel A shows cell numbers of R. palustris TIE-1 *from experiments with CO_2/HCO_3^- (grey striped pattern, with CO_2) or with PIPES buffer (pink colored bar, w/o CO_2). For organics results are shown for acetate (Ac), lactate (lc) and pyruvate (Py). For lactate alone and Fe(II) plus pyruvate (Table S1) changes in cell numbers were significant. Panel B shows organic consumption rates with CO_2/HCO_3^- (grey striped pattern) and with PIPES buffer (pink colored, w/o CO_2). For lactate alone and Fe(II) plus lactate (Table S1) differences were significant. The standard deviation is based on triplicate measurements.*

In the next step, organic consumption rates were calculated. No difference in the consumption rates for acetate were observed; these reached 0.16±0.05 mM/d with Fe(II) and 0.14±0.01 mM/d without Fe(II) (Figure 5B, Figure S2). The same was also observed with lactate although overall consumption rates were lower compared to acetate (with Fe(II) 0.10±0.03 and without Fe(II) 0.12±0.02 mM/d). For acetate consumption rates, values were not significantly different (with/without CO_2). However, consumption rates of lactate with CO_2 were significantly higher than without CO_2. This applied to both lactate alone and with Fe(II) (Table S1). Pyruvate concentrations and consumption rates could not be measured during the experiment due to an interference of PIPES with Pyruvate peak in the HPLC but growth could be confirmed with color change and cell growth (Figure 5A, S3). Therefore, organic consumption rates could only be calculated for acetate and lactate.

This experiment confirmed, firstly, when there is no external CO_2 provided, we do not see any Fe(II) consumption even when the organics are used. We believe this demonstrates that this strain cannot conduct Fe(II) oxidation with CO_2 from respired organic matter under our

experimental conditions. Secondly, our experiment confirms that growth substrates with a more negative oxidation state than biomass need to have an additional substrate that can serve as an electron sink. In the case of butyrate, this could be CO_2 or substrates like DMSO or protons (resulting in H_2 production) (McKinlay and Harwood, 2010). Gregoire and Poulain successfully demonstrated that mercury (Hg^{II}) could also be used as electron sink in the purple non-sulfur bacteria *Rhodobacter capsulatus* SB1003, *R.palastris TIE-1* and *Rhodobacter sphaeroides* (Gregoire & Poulain, 2016). This highlights an as yet overlooked role for anoxygenic phototrophs in reducing contaminants as a core facet of their metabolism. It also demonstrates that although CO2 is the most common electron sink, these bacteria have developed a diversity of strategies to achieve this goal. The environmental importance of using alternative redox active metals as electron sinks is yet to be widely demonstrated, but would be a fruitful avenue of future research. The importance of the oxidation state of the organic compounds was also highlighted in a recent study by Haas et al., 2022. where *R.palustris* CGA010 was tested under nitrogen-fixing, CO_2 absent conditions with Fe(II) and acetate or Fe(II) and malate. Nitrogen fixation was used here as an alternative to CO_2 fixation for recycling of electron equivalents. No oxidation of Fe(II) was observed with acetate but when malate, a more oxidized compound, was added, Fe(II) was oxidized. The authors suggest that malate utilization potentially leads to a more oxidized quinone pool as less flux would go through succinate. This could mean that *R. palustris* TIE-1 could also possibly oxidize Fe(II) without external CO_2 in the presence of a more oxidized substrate like malate.

These results showed that CO_2 is crucial for Fe(II) oxidation and CO_2 produced by oxidation of organic compounds could not serve as a substitute. Fe(II) did not have a notably beneficial effect on organic consumption when PIPES was used as buffer, and the consumption of some organic compounds depend on co-utilization of CO_2.

Environmental implications

With these experiments we demonstrated that Fe(II) oxidation, organic consumption and the presence of external CO_2 are inter-dependent, revealing a complex interaction between substrates that dictates growth and Fe(II) oxidation under environmentally relevant conditions. The type of carbon present in the environment can have a marked effect on the contribution of *R. palustris* TIE-1 to Fe(II) oxidation and the contribution of photoferrotrophy to iron cycling. Since both organic compounds and Fe are present in almost all environmental systems in which photoferrotrophs exist, these interactions likely have significant influences on the rates and extent of Fe(II) oxidation, iron mineral formation and organic carbon turnover in the environment.

Acknowledgement

The study was supported by Deutsche Forschungsgemeinschaft (DFG, German Research Foundation; BR 5927/2-1 and BY 82/4-1) awarded to C. Bryce and J. Byrne. James M. Byrne is supported by a UKRI Future Leaders Fellowship, MR/V023918/1. The authors gratefully acknowledge the Tübingen Structural Microscopy Core Facility (funded by the Excellence Strategy of the German Federal and State Governments) for their support & assistance in this work. The authors would like to thank Ulf Lüder for laboratory assistance.

References

Bird, L. J., Bonnefoy, V., & Newman, D. K. (2011). Bioenergetic challenges of microbial iron metabolisms. *Trends in Microbiology*, *19*(7), 330–340. https://doi.org/10.1016/J.TIM.2011.05.001

Caiazza, N. C., Lies, D. P., & Newman, D. K. (2007). Phototrophic Fe(II) oxidation promotes organic carbon acquisition by Rhodobacter capsulatus SB1003. *Applied and Environmental Microbiology*, *73*(19), 6150–6158. https://doi.org/10.1128/AEM.02830-06

Croal, L. R., Jiao, Y., Kappler, A., & Newman, D. K. (2009). Phototrophic Fe(II) oxidation in an atmosphere of H2: Implications for Archean banded iron formations. *Geobiology*, *7*(1), 21–24. https://doi.org/10.1111/j.1472-4669.2008.00185.x

Croal, Laura R., Johnson, C. M., Beard, B. L., & Newman, D. K. (2004). Iron isotope fractionation by Fe(II)-oxidizing photoautotrophic bacteria. *Geochimica et Cosmochimica Acta*, *68*(6), 1227–1242. https://doi.org/10.1016/j.gca.2003.09.011

Crowe, S. A., Hahn, A. S., Morgan-Lang, C., Thompson, K. J., Simister, R. L., Llirós, M., Hirst, M., & Hallam, S. J. (2017). Draft Genome Sequence of the Pelagic Photoferrotroph Chlorobium phaeoferrooxidans. *Genome Announcements*, *5*(13). https://doi.org/10.1128/GENOMEA.01584-16

Diaz, M. R., Eberli, G. P., Blackwelder, P., Phillips, B., & Swart, P. K. (2017). Microbially mediated organomineralization in the formation of ooids. *Geology*, *45*(9), 771–774. https://doi.org/10.1130/G39159.1

Dohnalkova, A. C., Marshall, M. J., Arey, B. W., Williams, K. H., Buck, E. C., & Fredrickson, J. K. (2011). Imaging hydrated microbial extracellular polymers: Comparative analysis by electron microscopy. *Applied and Environmental Microbiology*, *77*(4), 1254–1262. https://doi.org/10.1128/AEM.02001-10

Ehrenreich, A., & Widdel, F. (1994). Anaerobic oxidation of ferrous iron by purple bacteria, a new type of phototrophic metabolism. *Applied and Environmental Microbiology*, *60*(12), 4517–4526. https://doi.org/10.1128/AEM.60.12.4517-4526.1994

Eickhoff, M., Obst, M., Schröder, C., Hitchcock, A. P., Tyliszczak, T., Martinez, R. E., Robbins, L. J., Konhauser, K. O., & Kappler, A. (2014). Nickel partitioning in biogenic and abiogenic ferrihydrite: The influence of silica and implications for ancient environments. *Geochimica et Cosmochimica Acta*, *140*, 65–79. https://doi.org/10.1016/j.gca.2014.05.021

Govindaraju, A., McKinlay, J. B., & LaSarre, B. (2019). Phototrophic lactate utilization by Rhodopseudomonas palustris is stimulated by coutilization with additional substrates. *Applied and Environmental Microbiology*, *85*(11). https://doi.org/10.1128/AEM.00048-19/ASSET/C81F38CC-AABF-457C-B48C-76B76673A61A/ASSETS/GRAPHIC/AEM.00048-19-F0005.JPEG

Gregoire, D. S., & Poulain, A. J. (2016). A physiological role for Hg II during phototrophic growth. *Nature Geoscience*, *9*(2), 121–125. https://doi.org/10.1038/ngeo2629

Haas, N. W., Jain, A., Hying, Z., Arif, S. J., Niehaus, T. D., Gralnick, J. A., & Fixen, K. R. (2022). PioABC-Dependent Fe(II) Oxidation during Photoheterotrophic Growth on an Oxidized Carbon Substrate Increases Growth Yield. *Applied and Environmental Microbiology*, *88*(15). https://doi.org/10.1128/aem.00974-22

Han, X., Tomaszewski, E. J., Sorwat, J., Pan, Y., Kappler, A., & Byrne, J. M. (2020). Oxidation of green rust by anoxygenic phototrophic Fe(II)-oxidising bacteria. *Geochem. Persp. Let*, *12*, 52–57. https://doi.org/10.7185/geochemlet.2004

Hegler, F., Posth, N. R., Jiang, J., & Kappler, A. (2008). *Physiology of phototrophic iron (II) -oxidizing bacteria : implications for modern and ancient environments*. *66*(Ii), 250–260. https://doi.org/10.1111/j.1574-6941.2008.00592.x

Heising, S., Richter, L., Ludwig, W., & Schink, B. (1999). Chlorobium ferrooxidans sp. nov., a phototrophic green sulfur bacterium that oxidizes ferrous iron in coculture with a "Geospirillum" sp. strain. *Archives of Microbiology*, *172*(2), 116–124. https://doi.org/10.1007/s002030050748

Heising, S., & Schink, B. (1998). Phototrophic oxidation of ferrous iron by a Rhodornicrobiurn vannielii strain. *Microbiology*, *144*, 2263–2269.

Jiao, Y., Kappler, A., Croal, L. R., & Newman, D. K. (2005). Isolation and characterization of a genetically tractable photoautotrophic Fe(II)-oxidizing bacterium, Rhodopseudomonas palustris strain TIE-1. *Applied and Environmental Microbiology*. https://doi.org/10.1128/AEM.71.8.4487-4496.2005

Kappler, A., Bryce, C., Mansor, M., Lueder, U., Byrne, J. M., & Swanner, E. D. (2021). An evolving view on biogeochemical cycling of iron. *Nature Reviews Microbiology*, *19*(6), 360–374. https://doi.org/10.1038/s41579-020-00502-7

Kappler, A., & Newman, D. K. (2004). Formation of Fe(III)-minerals by Fe(II)-oxidizing photoautotrophic bacteria. *Geochimica et Cosmochimica Acta*, *68*(6), 1217–1226. https://doi.org/10.1016/J.GCA.2003.09.006

Kappler, A., Pasquero, C., Konhauser, K. O., & Newman, D. K. (2005). Deposition of banded iron formations by anoxygenic phototrophic Fe(II)-oxidizing bacteria. *Geology*, *33*(11), 865–868. https://doi.org/10.1130/G21658.1

Konhauser, K. O., Hamade, T., Raiswell, R., Morris, R. C., Ferris, F. G., Southam, G., & Canfield, D. E. (2002). Could bacteria have formed the Precambrian banded iron formations? *Geology*, *30*(12), 1079–1082. https://doi.org/10.1130/0091-7613(2002)030<1079:CBHFTP>2.0.CO;2

Kopf, S. H., & Newman, D. K. (2012). Photomixotrophic growth of Rhodobacter capsulatus SB1003 on ferrous iron. *Geobiology*, *10*(3), 216–222. https://doi.org/10.1111/j.1472-4669.2011.00313.x

Lambrecht, N., Stevenson, Z., Sheik, C. S., Pronschinske, M. A., Tong, H., & Swanner, E. D. (2021). "Candidatus Chlorobium masyuteum," a Novel Photoferrotrophic Green Sulfur Bacterium Enriched From a Ferruginous Meromictic Lake. *Frontiers in Microbiology*, *12*(July), 1–17. https://doi.org/10.3389/fmicb.2021.695260

Laufer, K., Niemeyer, A., Nikeleit, V., Halama, M., Byrne, J. M., & Kappler, A. (2017). Physiological characterization of a halotolerant anoxygenic phototrophic Fe(II)-oxidizing green-sulfur bacterium isolated from a marine sediment. *FEMS Microbiology Ecology*, *93*(5), 1–13. https://doi.org/10.1093/femsec/fix054

Llirós, M., Garciá-Armisen, T., Darchambeau, F., Morana, C., Triadó-Margarit, X., Inceoɔlu, Ö., Borrego, C. M., Bouillon, S., Servais, P., Borges, A. V., Descy, J. P., Canfield, D. E., & Crowe, S. A. (2015). Pelagic photoferrotrophy and iron cycling in a modern ferruginous basin. *Scientific Reports*, *5*, 1–8. https://doi.org/10.1038/srep13803

McKinlay, J. B., & Harwood, C. S. (2010). Carbon dioxide fixation as a central redox cofactor recycling mechanism in bacteria. *Proceedings of the National Academy of Sciences of the United States of America*, *107*(26), 11669–11675. https://doi.org/10.1073/pnas.1006175107

Melton, E. D., Schmidt, C., Behrens, S., Schink, B., & Kappler, A. (2014). Metabolic Flexibility and Substrate Preference by the Fe(II)-Oxidizing Purple Non-Sulphur Bacterium Rhodopseudomonas palustris Strain TIE-1. *Http://Dx.Doi.Org/10.1080/01490451.2014.901439*, *31*(9), 835–843. https://doi.org/10.1080/01490451.2014.901439

Miot, J., Benzerara, K., Obst, M., Kappler, A., Hegler, F., Schädler, S., Bouchez, C., Guyot, F., & Morin, G. (2009). Extracellular iron biomineralization by photoautotrophic iron-oxidizing bacteria. *Applied and Environmental Microbiology*, *75*(17), 5586–5591.

https://doi.org/10.1128/AEM.00490-09
Mu, C. C., Zhang, T. J., Zhao, Q., Guo, H., Zhong, W., Su, H., & Wu, Q. B. (2016). Soil organic carbon stabilization by iron in permafrost regions of the Qinghai-Tibet Plateau. *Geophysical Research Letters*, *43*(19), 10,286-10,294. https://doi.org/10.1002/2016GL070071
Nadkarni, M. A., Martin, F. E., Jacques, N. A., & Hunter, N. (2002). Nadkarni MA 2002 Bacterial load by real time qPCR.pdf. *Microbiology (Reading, England)*, *148*(Pt 1), 257–266. papers3://publication/uuid/720C1476-57B5-40A2-AC1C-EA8708B08F2E
Patzner, M. S., Mueller, C. W., Malusova, M., Baur, M., Nikeleit, V., Scholten, T., Hoeschen, C., Byrne, J. M., Borch, T., Kappler, A., & Bryce, C. (2020). Iron mineral dissolution releases iron and associated organic carbon during permafrost thaw. *Nature Communications*, *11*(6329). https://doi.org/10.1038/s41467-020-20102-6
Peng, C., Bryce, C., Sundman, A., Borch, T., & Kappler, A. (2019). *Organic Matter Complexation Promotes Fe(II) Oxidation by the Photoautotrophic Fe(II)-Oxidizer Rhodopseudomonas palustris TIE-1*. https://doi.org/10.1021/acsearthspacechem.9b00024
Poulain, A. J., & Newman, D. K. (2009). Rhodobacter capsulatus catalyzes light-dependent Fe(II) oxidation under anaerobic conditions as a potential detoxification mechanism. *Applied and Environmental Microbiology*, *75*(21), 6639–6646. https://doi.org/10.1128/AEM.00054-09
Poulton, S. W., & Canfield, D. E. (2011). Ferruginous Conditions: A Dominant Feature of the Ocean through Earth's History. *Elements*, *7*(2), 107–112. https://doi.org/10.2113/gselements.7.2.107
Rancourt, D. G., & Ping, J. Y. (1991). Voigt-based methods for arbitrary-shape static hyperfine parameter distributions in Mössbauer spectroscopy. *Nuclear Inst. and Methods in Physics Research, B*, *58*(1), 85–97. https://doi.org/10.1016/0168-583X(91)95681-3
Solmaz, K. B., Ozcan, Y., Dogan, N. M., Bozkaya, O., & Ide, S. (2018). Characterization and production of extracellular polysaccharides (EPS) by bacillus pseudomycoides U10. *Environments - MDPI*, *5*(6), 1–16. https://doi.org/10.3390/environments5060063
Straub, K. L., Rainey, F. a, & Widdel, F. (1999). Marine Phototrophic Ferrous-Iron-Oxidizing Purple Bacteria. *International Journal of Systematic Bacteriology*, *49*(1 999), 729–735.
Thompson, K. J., Kenward, P. A., Bauer, K. W., Warchola, T., Gauger, T., Martinez, R., Simister, R. L., Michiels, C. C., Llirós, M., Reinhard, C. T., Kappler, A., Konhauser, K. O., & Crowe, S. A. (2019). Photoferrotrophy, deposition of banded iron formations, and methane production in Archean oceans. *Science Advances*, *5*(11), 1–10. https://doi.org/10.1126/sciadv.aav2869
Tipping, E. (1981). The adsorption of aquatic humic substances by iron oxides. *Geochimica et Cosmochimica Acta*, *45*(2), 191–199. https://doi.org/10.1016/0016-7037(81)90162-9
Widdel, F. (1983). Methods for enrichment and pure culture isolation of filamentous gliding sulfate-reducing bacteria. *Archives of Microbiology*, *134*(4), 282–285. https://doi.org/10.1007/BF00407803
Widdel, F., & Bak, F. (1992). Gram-Negative Mesophilic Sulfate-Reducing Bacteria. *The Prokaryotes*, 3352–3378. https://doi.org/10.1007/978-1-4757-2191-1_21

Supplements

Table S1: Welsh t-test results. Welsh's t-test was used to account for unequal variances between each sample treatment. We chose a significance threshold of $\alpha = 0.05$.

	Setup	t	df	p-value
Fe(II) oxidation rates with Fe(II) only and Fe(II) plus organics	Acetate	2.86	3.14	0.0613
	Lactate	-32.52	4.99	5.30E-07
	Pyruvate	-4.59	4.99	0.0059
	Butyrate	no possible	analysis	
	Glucose	-3.3	4.12	0.0287

	Setup	t	df	p-value
Organic consumption rates with Fe and without Fe	Acetate	1.24	2.08	0.34
	Lactate	2.92	3.58	0.049
	Pyruvate	0.19	2.16	0.87
	Butyrate	no possible	analysis	
	Glucose	no possible	analysis	

	Setup	t	df	p-value
Cell numbers with CO_2 and without CO_2	Acetate	0.79	2.37	0.5
	Acetate plus Fe	2.91	2.06	0.097
	Lactate	5.51	3.84	0.0059
	Lactate plus Fe	2.75	2.09	0.105
	Pyruvate	4.01	2.07	0.0518
	Pyruvate plus Fe	5.33	3.63	0.0078
	Butyrate	no possible	analysis	
	Glucose	no possible	analysis	

	Setup	t	df	p-value
Organic consumption rates with CO_2 and without CO2	Acetate	1.59	2.19	0.24
	Acetate plus Fe	0.4	2.27	0.73
	Lactate	4.61	4	0.01
	Lactate plus Fe	8.75	3.38	0.002
	Pyruvate	no possible	analysis	
	Butyrate	no possible	analysis	
	Glucose	no possible	analysis	

Table S2: Calculated and measured cell number of the substrate preference experiment with CO_2. For calculations assumptions were that 90% of electrons from Fe(II) oxidation go into biomass production and 80% of the organics go into biomass.

	Calculated cell number	Measured cell number
Fe(II)	1.2 E+07	2.39 E+07 ± 1.2E+07
Acetate	3.24 E+07	2.10 E+07 ± 8.12E06
Lactate	4.86 E+07	5.6 E+07 ± 1.02E07
Pyruvate	4.86 E+07	4.64 E07 ± 1.02E07
Butyrate	6.48 E+07	6.62 E07 ± 3.07E06
Glucose	9.72 E+07	3.01 E07 ± 2.14E07

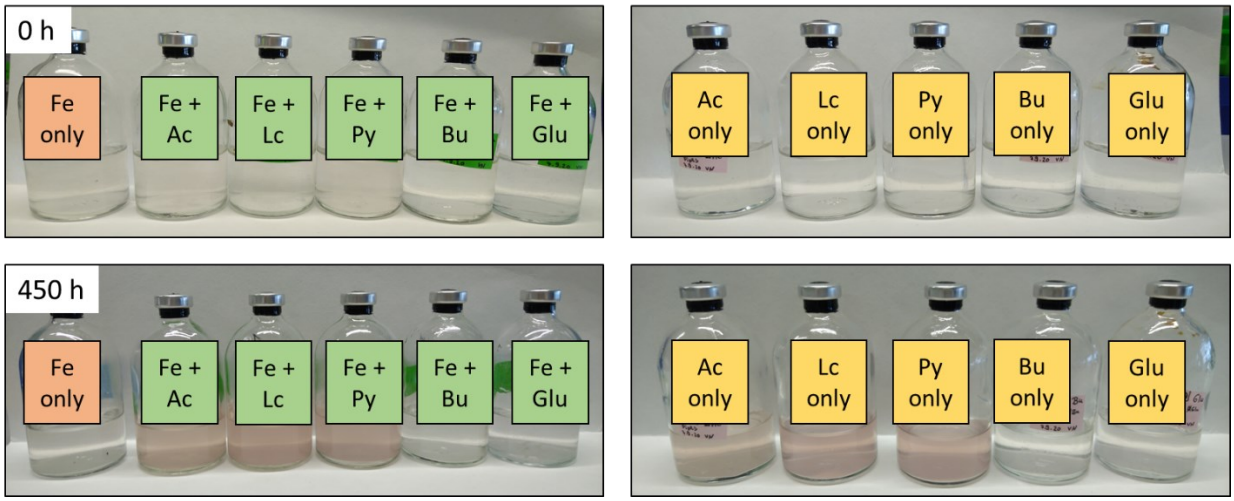

Figure S1: Removal of CO_2/HCO_3 experiment with R. palustris TIE-1*, left side with Fe(II) and organics and on the right side pictures with organics only. Growth can be seen with Fe(II) plus acetate (Ac+Fe), Fe(II) plus lactate (Lc+Fe), Fe(II) plus pyruvate (Py+Fe) and no growth with butyrate (Bu only and Bu+Fe), glucose (Glu only and Glu+Fe) and with Fe only.*

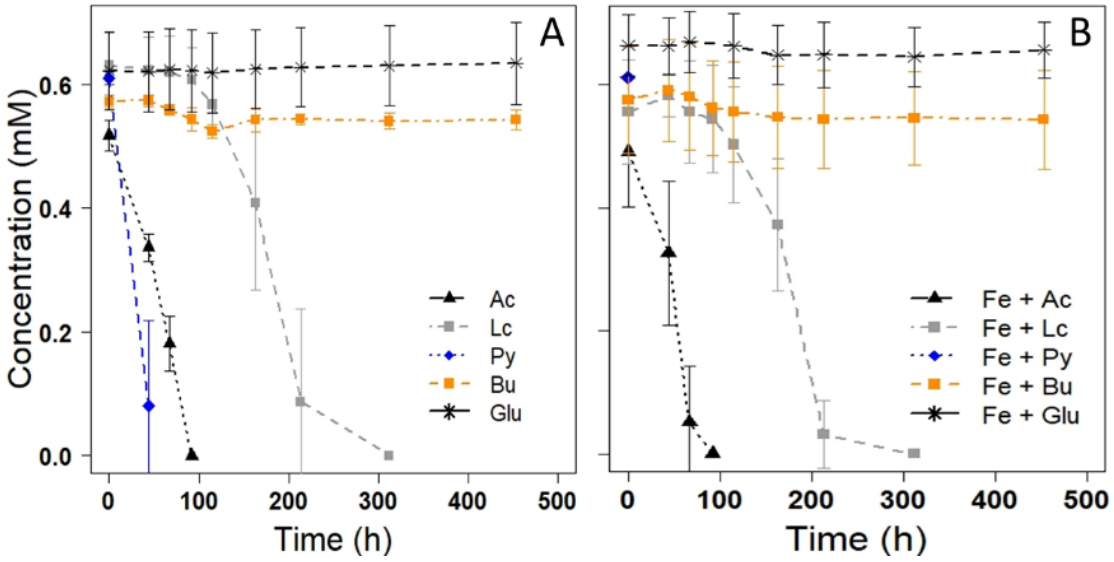

Figure S2: Organic consumption over time of R. palustris TIE-1 *with PIPES buffer. In A only organics were added and Ac, Lc and Py were consumed over time. No consumption of Bu and Glu. The same trend could also be observed when Fe(II) was added (B).*

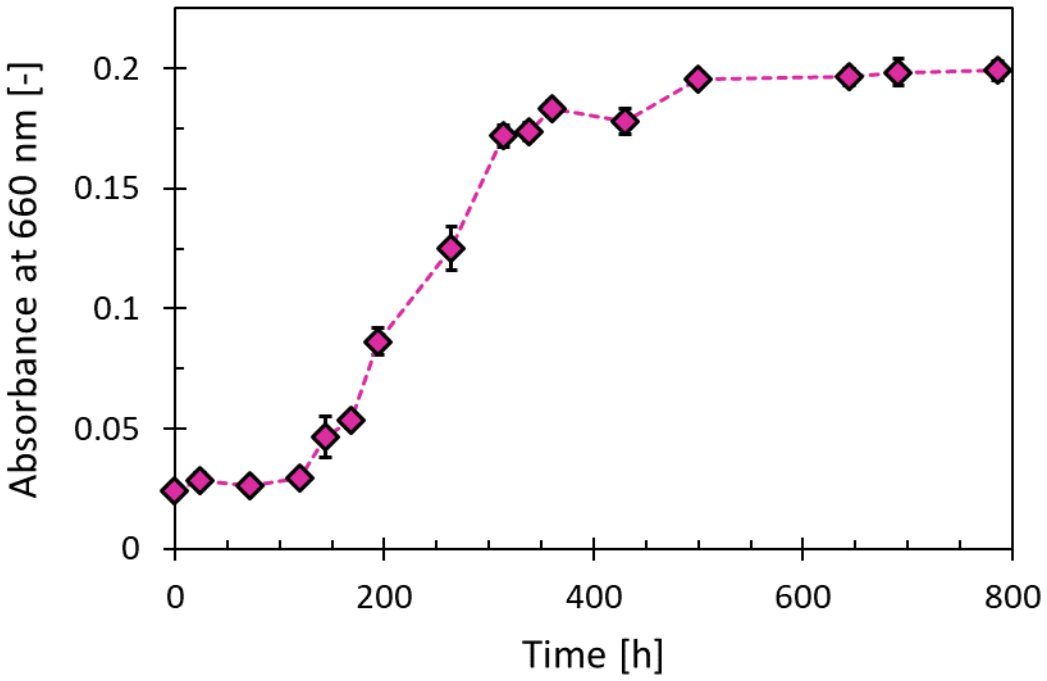

Figure S3: R. palustris TIE-1 *grown in triplicates with glucose and PIPES buffer only.*

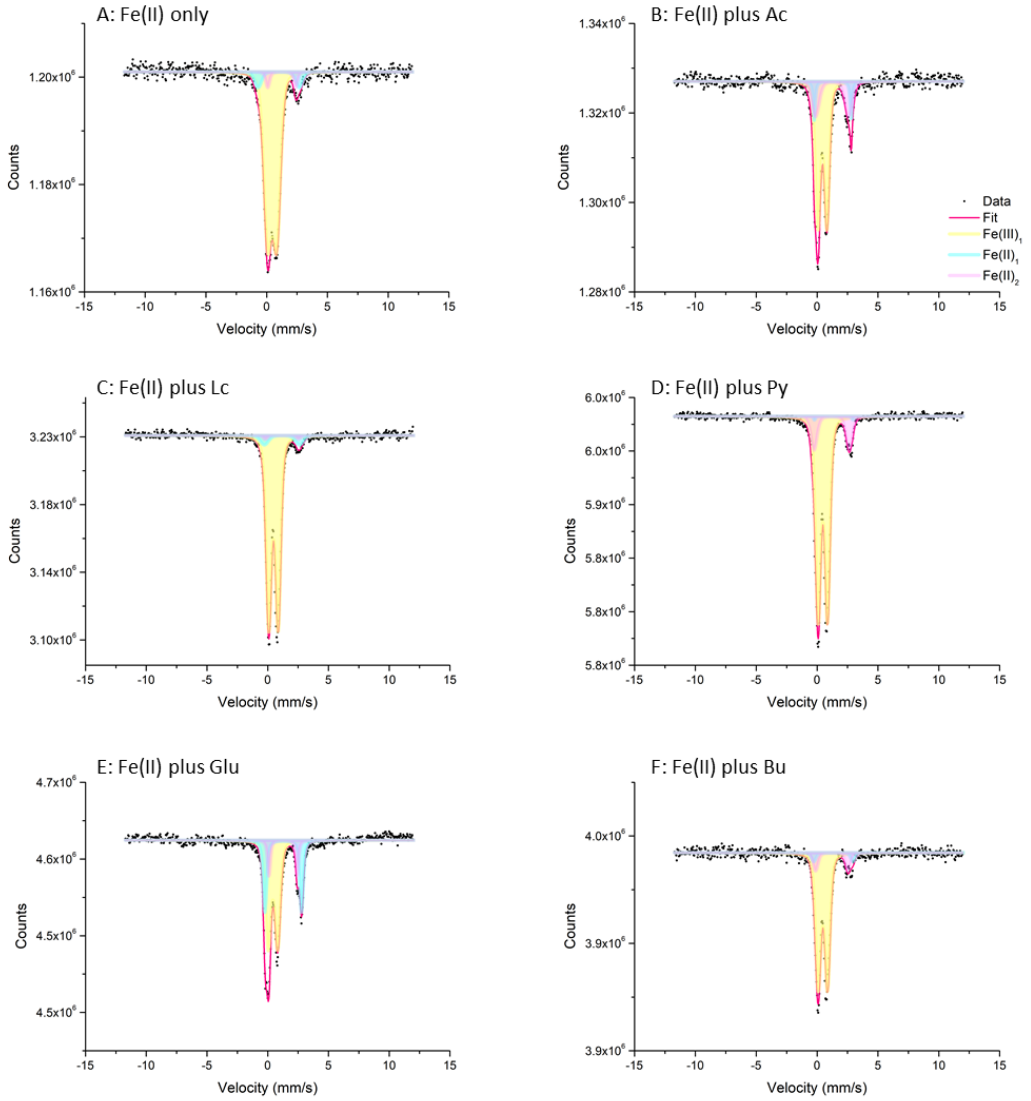

Figure S4: Mössbauer spectra collected at 77 K. All samples showed a narrow doublet (Db1; yellow) that can be attributed to the presence of a non-magnetically ordered poorly crystalline Fe(III) mineral phase similar to ferrihydrite. The wide doublet was fitted with two individual doublet features (Db2 and Db3) that can be indicative of Fe(II) mineral phases (Db2; blue) and (Db3; pink) in all samples.

The main components in all samples analyzed differ in their relative abundance. Sample Fe(II) plus lactate showed the lowest abundance of Fe(II) mineral phases with <10%. More than 90% of all iron mineral phases detected can be attributed to the presence of ferrihydrite (Table S3). Samples Fe(II) plus pyruvate and Fe(II) plus butyrate showed similar Fe(II) mineral abundances of around 15%, while ferrihydrite represented approx. 85% of the abundant iron mineral phases. The highest relative abundance of Fe(II) mineral phases was detected in samples Fe(II) only

and Fe(II) plus acetate with about 30-45% Fe(II) being present. Ferrihydrite showed a lower relative abundance in these samples compared to the previous ones, reaching a relative abundance of 50-70% only.

Table S3 – Overview on Mössbauer spectra fitting parameters. Temp. – temperature during measurement; Phase – fitted compound, Db: doublet, center shift (CS in mm/s); quadrupole splitting (ΔE_Q in mm/s); quadrupole shift (ε in mm/s); hyperfine field (B_{hf} in T), Pop – relative abundance (in %), χ^2 as goodness of fit and identified iron speciation/mineral phase: Fe(III) most likely ferrihydrite, $Fe(II)_1$ and $Fe(II)_2$ as ferrous iron mineral phases.

Sample	Temp. K	Phase	CS mm/s	ΔE_Q mm/s	Pop %	χ^2	mineral phase
TIE-1 Fe(II) only	77	Db1	0.48	0.80	87.5	0.64	Fe(III)
		Db2	1.00	3.21	7.7		$Fe(II)_1$
		Db3	1.24	2.30	4.8		$Fe(II)_2$
TIE-1 Fe(II) plus acetate	77	Db1	0.48	0.74	68.3	0.69	Fe(III)
		Db2	1.38	3.05	23.1		$Fe(II)_1$
		Db3	1.10	2.83	8.6		$Fe(II)_2$
TIE-1 Fe(II) plus lactate	77	Db1	0.48	0.77	94.4	0.69	Fe(III)
		Db2	1.18	3.16	3.5		$Fe(II)_1$
		Db3	1.13	2.72	2.1		$Fe(II)_2$
TIE-1 Fe(II) plus pyruvate	77	Db1	0.48	0.76	84.9	1.38	Fe(III)
		Db2	1.37	3.16	6.6		$Fe(II)_1$
		Db3	1.20	2.92	8.5		$Fe(II)_2$
TIE-1 Fe(II) plus butyrate	77	Db1	0.48	0.76	86.0	0.71	Fe(III)
		Db2	1.34	3.21	7.7		$Fe(II)_1$
		Db3	1.21	2.66	6.3		$Fe(II)_2$
TIE-1 Fe(II) plus glucose	77	Db1	0.43	0.78	59.3	0.73	Fe(III)
		Db2	1.28	3.01	28.9		$Fe(II)_1$
		Db3	1.27	2.32	11.8		$Fe(II)_2$

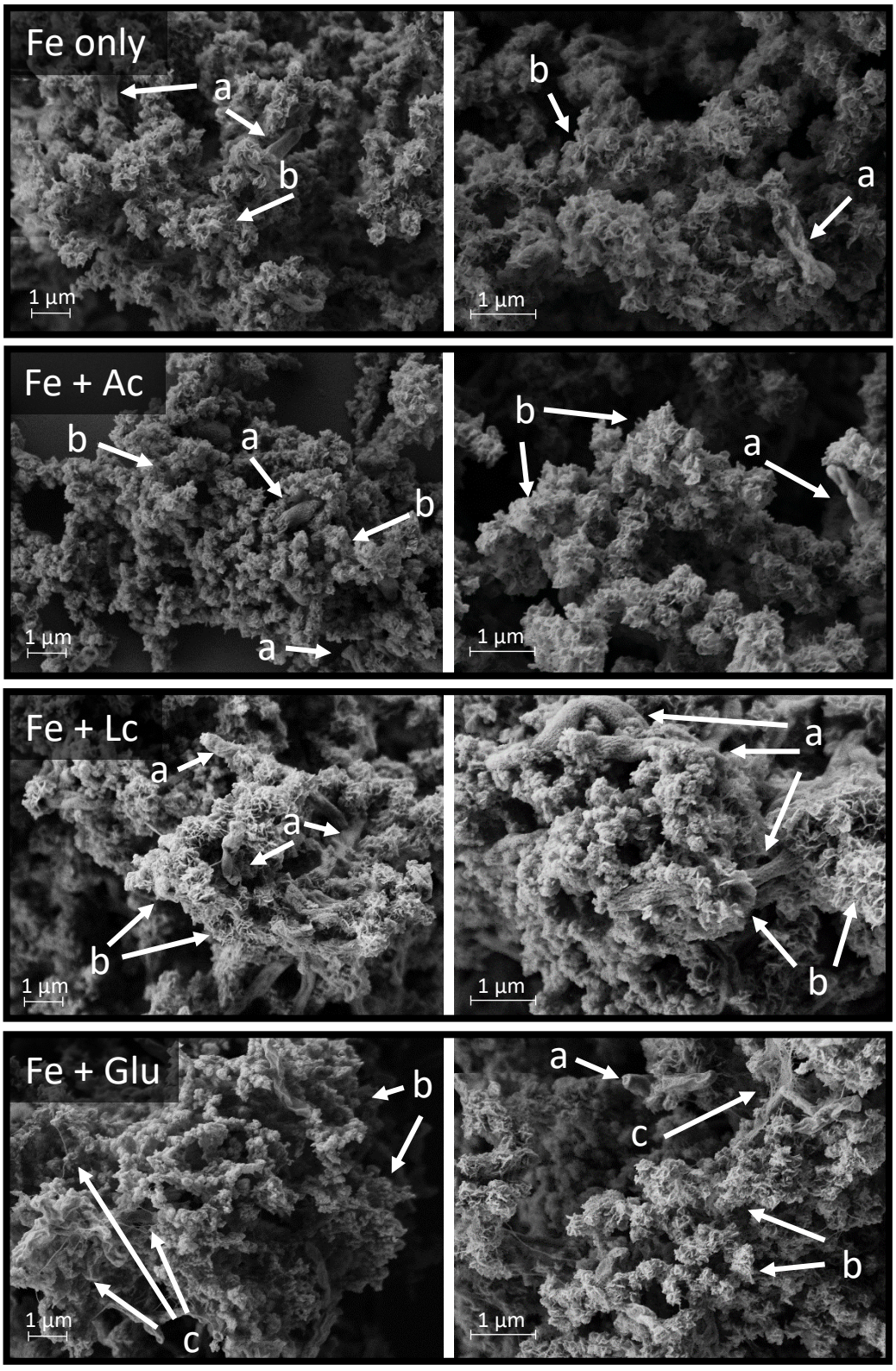

Figure S5 – SEM images of R. palustris TIE-1 *grown with only Fe(II) (Fe only), with Fe(II) plus acetate (Fe + Ac), with Fe(II) plus lactate (Fe + Lc) and with Fe(II) plus glucose (Fe + Glu). Arrow a shows the cells of R. palustris TIE-1, arrow b shows the spiky minerals and arow c shows spider-web like structures.*

3 Chapter: Advantages of multiple substrate use for phototrophic Fe(II)-oxidizer

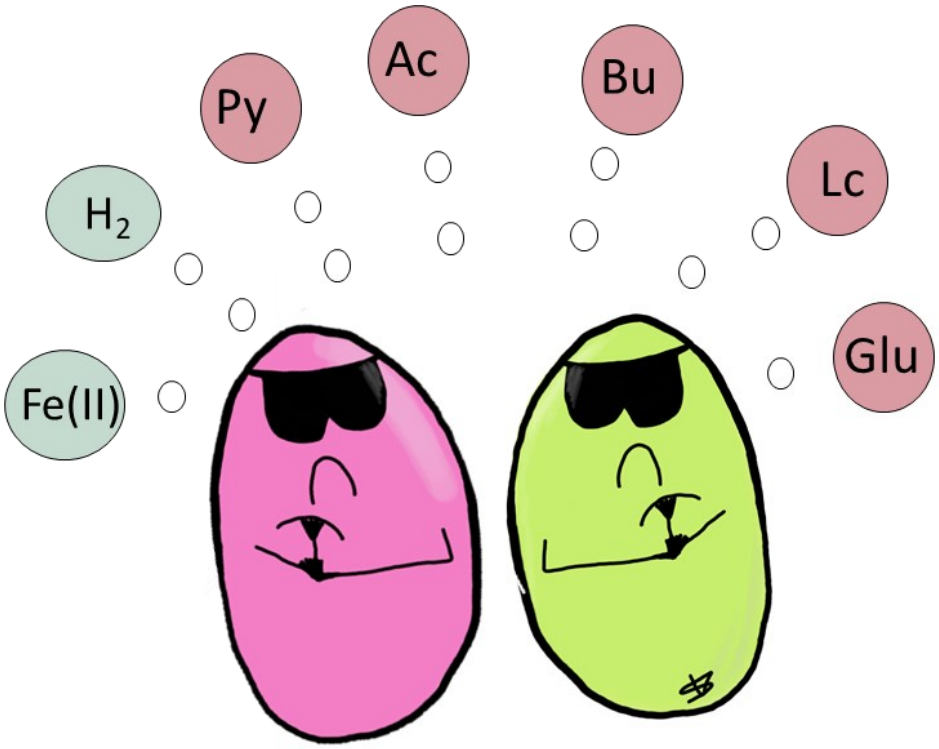

Contributions:

Resources were provided by Dr. C. Bryce, Assoc. Prof. J.M. Byrne and Prof. Dr. A. Kappler. The project was designed by me with guidance of Dr. C. Bryce. The experiments were conducted by me, J. C. Lopez-Rivoldi, M. Mergenthaler and J. Reinholdt. The manuscript was written by me with guidance of Dr. C. Bryce.

Advantages of multiple substrate use for phototrophic Fe(II)-oxidizer

Verena Nikeleit[1], Jimena C. Lopez-Rivoldi[1], Marie Mergenthaler[1], Josia Reinholdt[1], James Byrne[2], Andreas Kappler[1,3] and Casey Bryce[2*]

[1]Department of Geoscience, University of Tübingen, Tübingen, Germany

[2]School of Earth Sciences, University of Bristol, Bristol, UK

[3]Cluster of Excellence: EXC 2124: Controlling Microbes to Fight Infections, Tübingen, Germany

*Corresponding Author: Casey Bryce

School of Earth Science, Wills Memorial Building, University of Bristol, Queens Road, Bristol, BS8 1RJ, UK.

Email: casey.bryce@bristol.ac.uk

Manuscript in preparation

KEYWORDS: photoferrotroph, metabolic flexibility, Fe(II) oxidation

Abstract

Anoxygenic phototrophs are metabolically flexible and can grow photoautotrophically (with Fe(II) and H_2) and photoheterotrophically with a variety of organic substrates. However, it is unclear how Fe(II) oxidation is affected by organic and inorganic substrates. We incubated 6 different photoferrotrophs (green and purple non-sulfur bacteria) from freshwater and marine sediment origin with 2 mM Fe(II), amended with 0.6 mM organic or H_2 inorganic co-substrate. We could demonstrate that photoferrotrophs generally utilized organic and Fe(II) simultaneous and prefer Fe(II) over H_2 for two strains. Fe(II) oxidation was significantly enhance with acetate, lactate and glucose for some photoferrotrophs. On the other side H_2 slowed Fe(II) oxidation down. This study could expand the knowledge about how organic and inorganic substrates influence Fe(II) oxidation of photoferrotrophs and highlights their metabolic flexibility and its advantages.

Introduction

Anoxygenic phototrophs are widespread and play a crucial role in many environments, such as stratified lakes and sediments where they contribute to energy flow and nutrient cycling (Bryce, Blackwell, et al., 2018; Crowe et al., 2017; Laufer et al., 2017; Otte et al., 2018; Walter et al., 2014). Anoxygenic phototrophs have been historically classified into green and purple sulfur or non-sulfur bacteria based on the morphological studies of Winogradsky in 1888 that described the bacteriochlorophyll composition and ability to use and store sulfur (Winogradsky, 1888). They use photosynthesis to gain energy but, in comparison to the oxygenic phototrophs, no oxygen is produced. Instead of using water as an electron donor like in oxygenic photosynthesis, anoxygenic phototrophs use alternative substrates such as organic and inorganic compounds. By using organic substrates like acetate, lactate, glucose and butyrate they grow photoheterotrophically and can use the organics as an electron donor as well as a carbon source for biomass. However, when grown photoautotrophically inorganic substrates like H_2, H_2S, $S_2O_3^{2-}$ and Fe(II) are used to fix CO_2 to build biomass. This wide range of possible substrates makes the anoxygenic phototrophs ubiquitous as they can use, and switch between, a vast variety of substrates.

One group of anoxygenic phototrophs that has gained particular attention are photoferrotrophs which were only discovered 30 years ago but have been intensively studied, particularly due to their suggested importance for primary productivity in the Earth's ancient ferruginous oceans (Ehrenreich & Widdel, 1994a; Kappler et al., 2005; Thompson et al., 2019; Widdel et al., 1993). These phototrophs are able to use Fe(II) as an electron donor . Iron is an ubiquitous redox-active element which is linked to other crucial element cycles through both metabolism and the formation and dissolution of Fe minerals which affect the bioavailability and accessibility of other toxins, pollutants and nutrients (Eickhoff et al., 2014; Kappler et al., 2021; Mu et al., 2016; Tipping, 1981). So far only a few isolates were obtained which originated from various environments. From freshwater environments *Chlorobium ferrooxidans* KoFox, *Rhodobacter*

ferrooxidans SW2 and *Rhodopseudomonas palustris* TIE-1 (Ehrenreich & Widdel, 1994; Heising et al., 1999; Jiao et al., 2005) have been isolated. From marine environments *Chlorobium* sp. N1, *Rhodovulum iodosum* and *Rhodovulum robiginosum* (Laufer et al., 2017; Straub et al., 1999) are used as model strains. Given their ability to use multiple substrates as electron donors it is unclear whether they would contribute significantly to iron cycling in the natural environment where alternative substrates would be present. Additionally, it is unclear how the presence of multiple substrates would influence consumption rates of one or both substrates, cell numbers, or Fe(III) minerals that would be formed. Despite the significance and environmental implications of multiple substrate use by photoferrotrophs, most studies investigate growth under single substrate conditions. The few studies that have been conducted found that consumption scenarios could be strain specific (Ehrenreich & Widdel, 1994). For example, *R. ferrooxidans* SW2 sequentially consumes organics (acetate or glucose) before oxidizing Fe(II) whereas Chromatium L7 simultaneous consumed organics (acetate or glucose) with Fe(II). The nature of the organic compound also appears to be important for determining how organic and inorganic substrates are used. For example, in *R. palustris* TIE-1, simultaneous consumption was observed for Fe(II) and glucose or lactate, but sequential consumption was observed for acetate, pyruvate and butyrate over Fe(II). In this case, co-substrate utilization appeared to enhance Fe(II) oxidation rates, contrary to expectations (Melton et al., 2014; chapter 2). For inorganic substrates Croal and colleague found out that Fe(II) oxidation rates for photoferrotrophs *R. ferrooxidans* SW2 and *R. palustris* TIE-1 were decreased in the presence of H_2 (Croal et al., 2009).These previous studies typically investigated a limited range of substrates on one or two photoferrotrophic strains. However, it is unclear whether co-substrate utilization could have advantages for photoferrotrophs in general. To gain this broader perspective, we selected 6 different photoferrotrophs from marine and freshwater environments, including both purple non-sulfur and green sulfur bacteria. We investigated the

substrate preference of these strains between Fe(II) and i) 4 different organic substrates (acetate, lactate, butyrate and glucose) and ii) H_2 as an inorganic substrate.

Material and Methods

Substrate preference experiments with Fe(II) and different organics. 5 different photoferrotrophic model strains were chosen: *R. ferrooxidans* SW2, *R. iodosum, R. robiginosum, C. ferrooxidans* KoFox *and Chlorobium sp.* N1. The phototrophic bacteria were grown for two transfers on H_2/CO_2 (80:20; v:v) prior to the experiment to avoid bias towards any of the experimental substrates except *R. iodosum* which grew on $FeCl_2$. 50 mL media was added to 100 mL serum vials and inoculated with 0.5% of the pre-grown cultures. Each bacterium was cultivated with a specific media composition that can be found in Table S1. For media preparation, the salts were dissolved in 1 L ultrapure water and autoclaved at 121°C for 20 min in a Widdel flask. After autoclaving the media was cooled to room temperature under an N_2/CO_2 (90:10) atmosphere and buffered with anoxic 22 mM bicarbonate buffer. Aliquots of 1 mL/L sterile filtered 7-vitamin solution (Widdel & Pfenning, 1981), trace element solution (Widdel, 1983) and selenite-tungstate solution (Widdel & Bak, 1992) were added and the pH was adjusted to 7 with anoxic and sterile 0.5 M $NaHCO_3$ or 1 M HCl. In the first setup, only 2 mM $FeCl_2$ was added as a control. In the second setup $FeCl_2$ and an organic substrate (0.6 mM) (either acetate (Ac), lactate (Lc), pyruvate (Py), butyrate (Bu) or glucose (Glu)) were added. Biological setups were run in triplicates and abiotic controls (same setup without the addition of bacteria) were performed in duplicates. The bottles were placed randomly in a light incubator at 20°C with 25±7 µmol photons/s/m^2. Samples were taken in a glovebox with 100% N_2 atmosphere for Fe, organic and cell quantification.

Substrate preference test with Fe(II) and H_2. For this experiment the 5 photoferrotrophs listed above plus *R. palustris* TIE-1 were used and were grown for 2 transfers on acetate or lactate (except for *Chlorobium sp.* N1 which was pre-grown on $FeCl_2$). A sacrificial setup with 3 biological bottles and 1 abiotic control were set up in Hungate tubes. 9.5 mL media containing 10 mM Fe(II) were filled in sterile Hungate tubes and 0.5 mL inoculum was added.

The headspace was exchanged with H_2/CO_2 (80:20 v:v). The bottles were placed randomly in a light incubator at 20°C with 25±7 µmol photons/s/m^2. Gas samples were taken sterilely at the lab bench and samples for Fe and cells were taken in a glovebox with a 100% N_2 atmosphere.

Fe quantification. Fe(II) and total Fe were analyzed spectrophotometrically with the Ferrozine assay modified after Hegler (Hegler et al., 2008). 0.1 mL samples were diluted in 0.9 mL 1 M HCl and stored at 4°C. The ferrozine-Fe(II) complex was quantified at 562 nm using a microtiter plate reader (Thermo Scientific Multiscan, Thermo Fisher Scientific). Ferrozine measurements were conducted in triplicates.

H_2 quantification. 3 mL gas were taken and transferred into a N_2 purged headspace vial. Gas samples were analyzed on a TraceGC1300 (ThermoFisher Scientific, modified by S+HA analytics, Germany), with a 30 m long, 0.53 mm ID Molsieve column connected to a Pulse Discharge Detector.

Short-chain fatty acid quantification. Acetate, lactate, butyrate and glucose were analyzed with HPLC. Samples were centrifuged at 20,000 for 5 minutes to remove cells and minerals. A Shimadzu Prominence HPLC with a LC-20AT solvent delivery unit, CTO-10ASvp column oven and a RID-20a refractive index detector was used.

Cell quantification. Cells were counted using a flow cytometer equipped with a 488 nm laser as an excitation source (Attune Nxt flow cytometer, Thermo Fisher Scientific). 180 µL of samples were fixed with 20 µL formaldehyde solution (CH_2O). Samples were stored at 5°C until measurement. Minerals were dissolved by adding 200 µL of sterile, anoxic 100 mM Fe(II) ethylenediammonium sulfate tetrahydrate (Fe-EDAS, $FeSO_4$ *$C_2H_8N_2H_2SO_4$*4H_2O) and

600 µL oxalate solution (0.23 M $(NH_4)_2C_2O_4*H_2O$ and 0.17 M $C_2H_2O_4$, pH 7). After 10 min BacLight Green stain (Thermo Fisher Scientific, 1 µl stain/1 ml sample) was added and 200 µL of sample was distributed in triplicates in 96 well plates. The plate was incubated for 15 minutes in the dark before measuring. Cells were distinguished from noise or debris based on their properties in the side scatter and BL1 channel (with emission filter 530/30 nm). All measurements were conducted in triplicates and the results reported as an average.

Results

Substrate preference of photoferrotrophs between Fe(II) and inorganic (H_2) or organic substrates

In the substrate preference experiments, all phototrophic Fe(II)-oxidizers oxidized up to 80-100% of the Fe(II) at the end of the experiment except for *R. robiginosum* where Fe(II) oxidation only reached 52-73% (Figure 1). However, different substrate preferences (Figure 1), Fe(II) oxidation rates (Figure 2) and cell numbers (Figure 3) were observed and are discussed for each individual strain below. We also compared the measured cell numbers to the theoretical cell number using the following assumptions from chapter 2. I) one cell weighs 1 pg (dry weight consisting of CH_2O), II) for Fe(II) only we assumed all electrons are used for fixing CO_2 into biomass (CO_2 → CH_2O; 4 electrons) and III) for organic substances we assumed 90% of the other organic substrates tested in our study were also converted into biomass (McKinlay & Harwood, 2010). This calculation predicts that cells grown with Fe(II) only would have $1.2x10^7$ cells/mL , whereas we would predict: $4.4x10^7$ cells/mL for Fe(II) plus acetate, $6.0x10^7$ cells/mL for Fe(II) plus lactate, $7.7 x10^7$ cells/mL for Fe(II) plus butyrate and $1.1x10^8$ cells/mL for Fe(II) plus glucose.

Substrate preference of *R. ferrooxidans* SW2

In the substrate preference experiment with different organic substances and Fe(II) purple non-sulfur bacterium *R. ferrooxidans* SW2 could also use all 4 tested organic substances (acetate, lactate, butyrate and glucose) simultaneously with Fe(II), although in the case of butyrate only 10±3% was consumed (Figure 1). Fe(II) oxidation was between 89-95 % completed in all set ups. Fe(II) oxidation rates with Fe(II) only was 0.23±0.06 mM/d and all Fe(II) oxidation rates with organics were within the standard deviation of Fe(II) only (Figure 2). Only Fe(II) plus acetate showed a higher Fe(II) oxidation rate with 0.54±0.07 mM/d, which was significantly higher than with Fe(II) only ($p=0.005$). Cell numbers in the setup with Fe(II) only ($2.4±0.3x10^7$

cells/mL) and Fe(II) plus butyrate ($1.8\pm0.2x10^7$ cells/mL) were similar which, considering not much butyrate was used, is what would be expected (Figure 3). In the case of Fe(II) plus acetate ($6.6\pm1.0x10^7$ cells/mL) and Fe(II) plus lactate ($7.0\pm0.5x10^7$ cells/mL), cell numbers were also similar. Highest cell numbers, double what we would theoretically expect, were found in the setup with Fe(II) plus glucose ($2.4\pm0.4x10^8$ cells/mL). In the substrate preference test with Fe(II) and H_2, simultaneous consumption was observed with no lag phase for both substrates (Figure 1, S1). Fe(II) was oxidized with a rate of 0.12±0.09 mM/d to an extent of 75±18 % and 87±6 % of H_2 was used up. Both abiotic controls stayed stable over the period of the experiment. *R. ferrooxidans* SW2 could use all substrates (butyrate only partially) and consumed them simultaneously with Fe(II). Fe(II) oxidation rates were significantly increased with Fe(II) plus acetate and high cell numbers were observed with Fe(II) plus glucose.

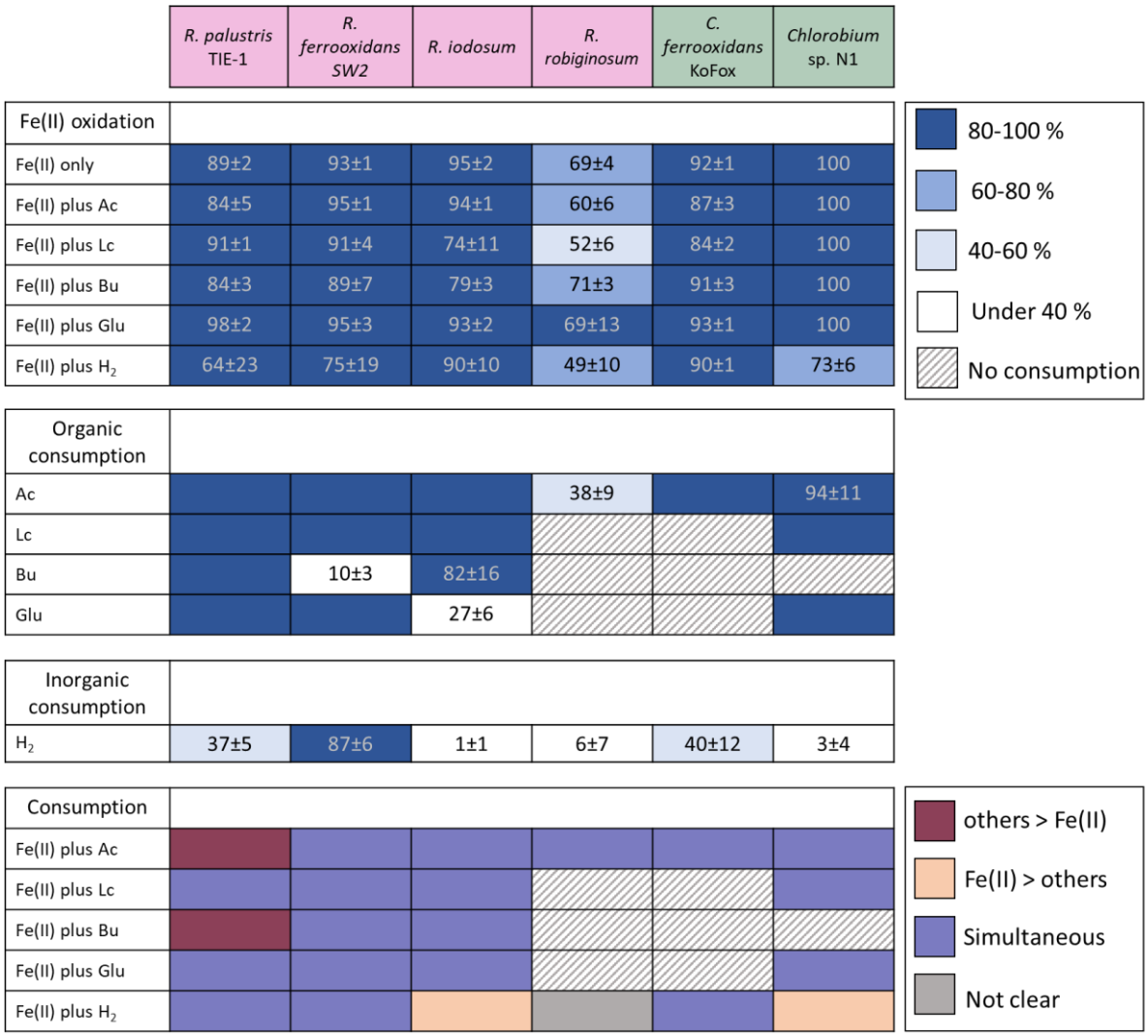

Figure 1: Schematic summary of substrate preference, Fe(II) oxidation rates, organic and H_2 consumption rates for R. palustris TIE-1*, R. ferrooxidans* SW2*, R. iodosum, R. robiginosum, C. ferrooxidans* KoFox *and Chlorobium sp.* N1.

Substrate preference of *R. iodosum*

R. iodosum, a marine purple non-sulfur bacterium, could also use all 4 organic substances, although not all completely i.e. only 82±16% of butyrate and 27±6% of glucose was used at the end of the experiment (Figure 1). Organics and Fe(II) were consumed simultaneously in all cases. Lowest Fe(II) oxidation percentage was found with Fe(II) plus lactate (74±11 %) and Fe(II) plus butyrate (79±3 %) with over 93 % oxidized in the case of Fe(II) only, Fe(II) plus acetate and Fe(II) plus glucose. For this marine strain *R. iodosum*, Fe(II) oxidation rates with

Fe(II) only was 0.14±0.03 mM/d, for Fe(II) plus lactate (0.12±0.03 mM/d) and Fe(II) plus glucose (0.12±0.02 mM/d) were within its standard deviation (Figure 2). Significantly higher Fe(II) oxidation rates were achieved with Fe(II) plus acetate (0.29±0.03 mM/d, p= 0.003) whereas a lower rate was observed with Fe(II) plus butyrate (0.08±0.03 mM/d). All measured cell numbers were higher than the theoretical calculation stated except for Fe(II) plus glucose where 7.3±2.3 $*10^7$ cells/mL were measured (Figure 3). In this case lower cell numbers could also be related to the fact that only 27±6% of glucose was used. In the case of Fe(II) plus acetate ($6.6\pm0.4x10^7$ cells/mL) and Fe(II) plus lactate ($8.2\pm0.2x10^7$ cells/mL) cell numbers were 1.5 times higher than the theoretical value. Even higher values were measured in the setup with Fe(II) plus butyrate (2 times, $1.2\pm0.2x10^8$ cells/mL) and Fe(II) only (3.5 times, $4.3\pm0.9x10^7$ cells/mL). For the setup with Fe(II) and H_2 a preferred usage of Fe(II) before H_2 could be observed. Fe(II) oxidation started after a short lag phase of 6 days and at the end 90±10 % was oxidized with a rate of 0.05±0.09 mM/d (Figure 1, S1). H_2 was only used up to 1±1 % and also did not differentiate much from the abiotic control.

R. iodosum could use all substrates except glucose partially and minimal H_2. For organics and Fe(II) simultaneous consumption occurred whereas with H_2 sequential consumption occurred with preferential Fe(II) oxidation. Higher cell numbers than predicted could be observed in all setups except Fe(II) plus glucose.

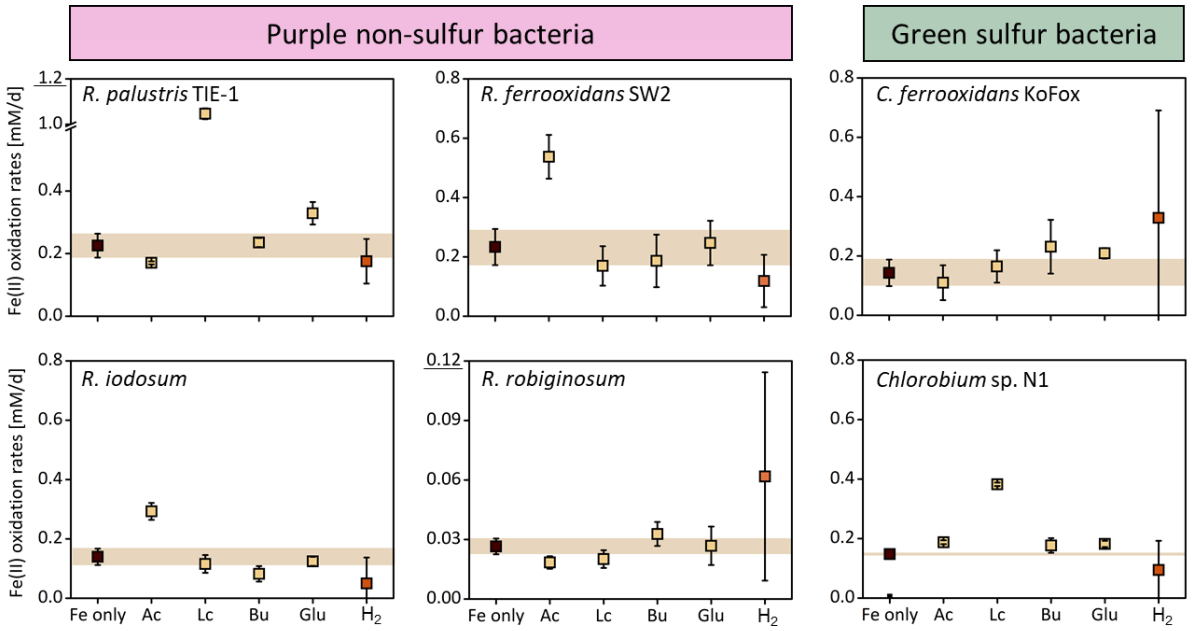

Figure 2: Panels show the Fe(II) oxidation rates of R. palustris TIE-1*, R. ferrooxidans* SW*2, R. iodosum, R. robiginosum, C. ferrooxidans* KoFox *and Chlorobium sp.* N1 *incubated with Fe(II) only, acetate (Ac), lactate (Lc), pyruvate (Py), butyrate (Bu) or glucose (Glu). The dark brown point shows the Fe(II) oxidation rate when only Fe(II) was added and the light brown background shows the standard deviation of this setup. Data from R. palustris* TIE-1 *are taken from chapter 2.*

Substrate preference of *R. robiginosum*

R. robiginosum, a marine purple non-sulfur strain, could only partially use acetate (38±9 %) from the tested organic substrates and used it simultaneously with Fe(II) (Figure 1). Fe(II) oxidation was also only partially completed (between 50-71%). Fe(II) oxidation rates were low with 0.027±0.004 mM/d and the presence of lactate, butyrate or glucose appeared to have no impact. In case of Fe(II) plus acetate, Fe(II) oxidation was a little slower (0.018±0.003 mM/d) then with Fe(II) only (Figure 2). Low cell numbers were also observed in the Fe(II) only setup with $4.9\pm1.4\times10^6$ cells/mL and all other setups were similar (Figure 3). In the experiments with Fe(II) and H_2, 49±10 % of Fe(II) was oxidized with a Fe(II) oxidation rate of 0.06±0.05 mM/d and 6±7 % of H_2 consumed (Figure 1, S1). Although abiotic and biotic H_2 data fluctuate quite a bit and no trend in the biotic setup was observed. Thus, no clear conclusion concerning the consumption scenario of these substrates could be made.

In summary, *R. robiginosum* could only partially oxidize Fe(II), acetate and H_2 and had low Fe(II) oxidation rates and cell numbers across all conditions.

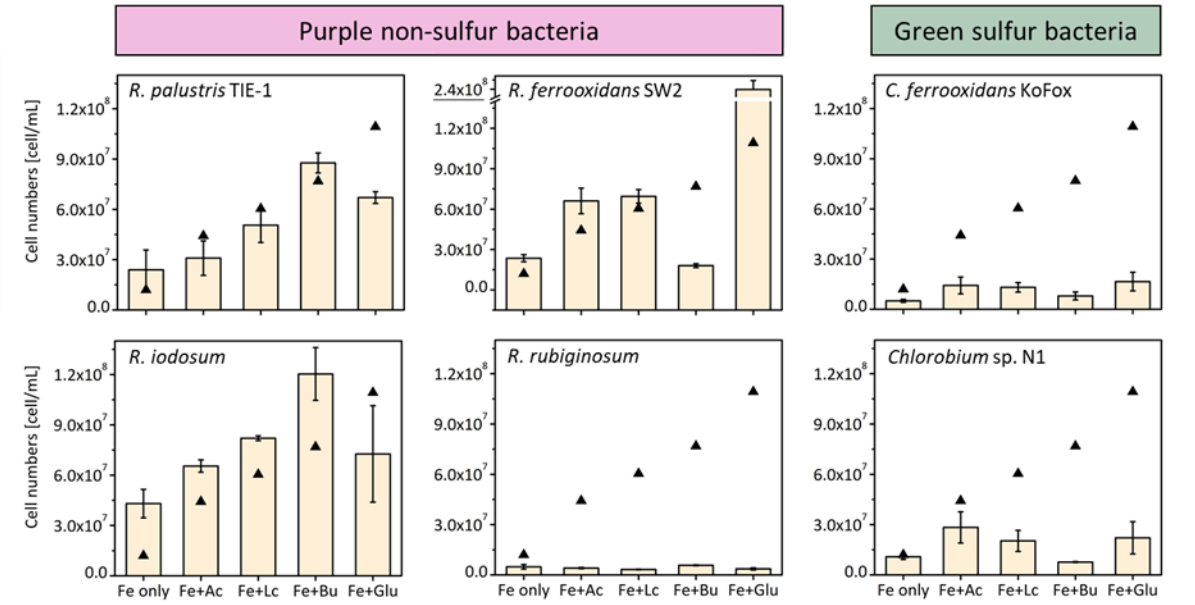

Figure 3: Panels show the cell numbers of R. palustris TIE-1*, R. ferrooxidans* SW2*, R. iodosum, R. robiginosum, C. ferrooxidans* KoFox *and Chlorobium sp.* N1 *incubated with Fe(II) only, acetate (Ac), lactate (Lc), pyruvate (Py), butyrate (Bu) or glucose (Glu). The black triangle shows the theoretical calculated cell numbers. Data were measured in triplicates and show standard deviation. Data from R. palustris* TIE-1 *are taken from chapter 2.*

Substrate preference of *C. ferrooxidans* KoFox

In the organic and Fe(II) substrate experiment *C. ferrooxidans* KoFox could only use acetate simultaneously with Fe(II). Fe(II) oxidation was between 84-93% complete (Figure 1). All Fe(II) oxidation rates were within the standard deviation of the Fe(II) only set up (0.27±0.07 mM/d) (Figure 2). The lowest Fe(II) oxidation rates were with Fe(II) plus lactate at 0.17±0.06 mM/d. For the freshwater strain *C. ferrooxidans* KoFox cell numbers were lower than the theoretical values for Fe(II) only ($5.0\pm0.9\times10^6$ cells/mL) (Figure 3). Cell numbers for Fe(II) plus acetate ($1.4\pm0.5\times10^7$ cells/mL), Fe(II) plus lactate ($1.3\pm0.3\times10^7$ cells/mL) and Fe(II) plus glucose ($1.7\pm0.6\times10^7$ cells/mL) are within the range of the theoretical cell numbers for Fe(II) only and below the theoretical cell number for conditions with Fe(II) plus organics. In the

experiment with Fe(II) and H_2 simultaneous consumption was observed and both were consumed with no lag phase (Figure 1, S1). 90±1 % of Fe(II) was oxidized with a Fe(II) oxidation rate of 0.33±0.36 mM/d and 40±12 % of H_2 was used up. Both abiotic controls were stable throughout the experiment.

C. ferrooxidans KoFox could only utilize Fe(II), acetate and H_2 and both acetate and H_2 were consumed simultaneously with Fe(II). Low cell numbers in the Fe(II) only setup were measured.

Substrate preference of *Chlorobium sp.* N1

Chlorobium sp. N1 could use acetate, lactate and glucose in the substrate preference experiment, but not butyrate. Fe(II) was 100% oxidized and all organics and Fe(II) were used simultaneously (Figure 1). All Fe(II) oxidation rates with the organics present are higher than the rate of Fe(II) only (0.15±0.01 mM/d) (Figure 2) although the rate in Fe(II) plus butyrate (0.18±0.03) was not significantly higher than Fe(II) only. Rates for Fe(II) plus acetate and Fe(II) plus glucose are very similar (0.19±0.01 and 0.18±0.01 mM/d, respectively) and Fe(II) plus lactate rates increased to 0.38±0.01 mM/d. For Fe(II) oxidation rates with Fe(II) plus acetate ($p=0.001$), Fe(II) plus lactate ($p=8*10^{-7}$) and Fe(II) plus glucose ($p=0.008$) changes were significant Although *Chlorobium sp.* N1 could use 3 organics the cell numbers are only slightly increased for Fe(II) plus acetate ($2.8±1.0x10^7$ cells/mL), Fe(II) plus lactate ($2.0±0.6x10^7$ cells/mL), and Fe(II) plus glucose ($2.2±1.0x10^7$ cells/mL) (Figure 3). Fe(II) plus butyrate ($0.9±0.3x10^6$ cells/mL) and Fe(II) only ($1.1±0.2x10^7$ cells/mL) are similar. For the substrate preference between Fe(II) and H_2, Fe(II) was oxidized before H_2 was consumed (Figure 1, S1). Fe(II) was oxidized to 73±6 % with a Fe(II) oxidation rate of 0.09±0.09 mM/d and only 3±4 % of H_2 was consumed. Although growth on H_2 was not observed during the experiment, growth

with H_2 was eventually observed later with *Chlorobium sp.* N1 after a lag phase of 30 days (Figure S2).

Chlorobium sp. N1 could use all substrates except butyrate and Fe(II) oxidation rates were significantly increased. All organics were used simultaneously with Fe(II) whereas Fe(II) was preferred in the case with H_2.

Substrate preference of *R. palustris* TIE-1

R. palustris TIE-1, a freshwater purple non-sulfur bacterium, could use all 4 organic substances (acetate, lactate, butyrate and glucose) completely. Acetate and butyrate were consumed first before Fe(II) oxidation proceeded whereas, with lactate and glucose, simultaneous consumption with Fe(II) oxidation was observed in the substrate preference experiment (Figure 1). Fe(II) was oxidized to between 84±5% (for Fe(II) plus acetate) and 98±2% (for Fe(II) plus glucose). In this case, Fe(II) oxidation significantly faster when both substrates were used simultaneously i.e. the Fe(II) oxidation rates was 0.23±0.04 mM/d with Fe(II) only and 1.1±0.01 with lactate ($p= 5.3*10^{-7}$) and 0.33±0.04 mM/d with glucose (p= 0.006) (Figure 2). Fe(II) oxidation rates were slower with acetate (0.17±0.01 mM/d) and within the standard deviation with butyrate (0.24±0.01 mM/d). Cell numbers for *R. palustris* TIE-1 were close to theoretical cell numbers except for the setup of Fe(II) plus glucose (Figure 3). Results for *R. palustris* TIE-1 have also been described in detail in chapter 2. For the substrate preference test with Fe(II) and H_2 simultaneous consumption was observed (Figure 1, S1). No lag phase in both Fe(II) and H_2 consumption was observed. The abiotic controls stayed stable except for 1 (H_2) and 2 (Fe) timepoints. By the end 37±5 % of H_2 and 64±23 % Fe(II) was oxidized with a Fe(II) oxidation rate of 0.18±0.07 mM/d.

R. palustris TIE-1 used organics, Fe(II) and H_2 showed sequential (for acetate and butyrate) and simultaneous (lactate, glucose and H_2) consumption and Fe(II) oxidation rates were significantly increased with lactate and glucose.

Discussion

Effect of multiple substrates on photoferrotrophs and Fe(II) oxidation

In these experiments we were able to determine the effects of organic and inorganic substrates on Fe(II) oxidation and how consumption, Fe(II) oxidation rates and cell numbers were affected. All photoferrotrophs oxidized Fe(II), although *R. robiginosum* showed the lowest Fe(II) oxidation extend. We could also observe that purple non-sulfur and green sulfur bacteria show different ability in metabolizing different inorganic and organic substrates. Whereas *R. palustris* TIE-1, *R. ferrooxidans* SW2 and *R. iodosum* could use all substrates, although *R. iodosum* and *R. ferrooxidans* SW2 only to some extent. *Chlorobium sp*. N1 could use all except butyrate and *R. robiginosum* and *C. ferrooxidans* KoFox could only use acetate. For consumption scenarios we could observe simultaneous consumption with the majority of substrates. The only sequential consumption where organic were preferred over Fe(II) was for *R. palustris* TIE-1 with acetate and butyrate. For *R. palustris* TIE-1 the same consumption scenario was observed before in a study by Melton et al. (2014) whereas Ehrenreich & Widdel (1994) observed sequential consumption of acetate and glucose before Fe(II) oxidation started for *R. ferrooxidans* SW2. Effect on Fe(II) oxidation rates were enhanced by the presence of specific substrates and it was also specific for each strain. Significant differences were observed with acetate (*R. ferrooxidans* SW2, *R. iodosum* and *Chlorobium sp*. N1), lactate (*R. palustris* TIE-1 and *Chlorobium sp*. N1), glucose (*R. palustris* TIE-1 and *Chlorobium sp*. N1) and pyruvate (*R. palustris* TIE-1, chapter 2). The effect on cell numbers was also strain specific. For most strains calculated cell numbers align with theoretical numbers except for *R. iodosum* more cell numbers were observed and for both green sulfur bacteria less cell were calculated. Interestingly, *R. palustris* TIE-1 and *R. iodosum* show with glucose less bacteria but the opposite was observed for *R. ferrooxidans* SW2.

For H_2 usage more than 40% were used by *R. palustris* TIE-1, *R. ferrooxidans* SW2 (87%) and *C. ferrooxidans* KoFox. In the span of the experiment only little H_2 was used by the marine

photoferrotrophs but growing them on H_2 was successful in the past and for *Chlorobium sp.* N1 at the end of the experiment (Laufer et al., 2017; Straub et al., 1999). A reason for that could also be that H_2 does not dissolve as much in water with high NaCl concentrations (Zhu et al., 2022). In case of H_2 consumption Fe(II) was oxidized first with *R. iodosum* and *Chlorobium sp.* N1. We could also observe that Fe(II) oxidation rates were lower in the presence of H_2 compared to when Fe(II) was used alone. The same trend was also observed by Croal et al. (2009) where Fe(II) oxidation rate was reduced for *R. palustris* TIE-1 (from 0.13 to 0.09 mM/h) and *R. ferrooxidans* SW2 (from 0.46 to 0.28 mM/h) in cell suspension experiments. In case of *C. ferrooxidans* KoFox and *R. robiginosum* Fe(II) oxidation was a little higher compared to Fe(II) only but the rates showed big standard deviations. Another reason for reduced Fe(II) oxidation rates could be that when grown with H_2 similar proteins are produced/used to metabolize both substrates leading to competition (Bryce et al., 2018).

Advantages of multiple substrate use

This metabolic flexibility can enhance the ecological competitiveness of photoferrotrophs against other bacteria. Many other phototrophs and heterotrophs can also use organics as an electron and carbon source and it is estimated that chemoorganotrophs grow faster than photolithotrophs (Raven et al., 2013). In this case being able to use other substrates as well is an advantage. Further, being able to oxidize Fe(II) is an exotic trait for bacteria and phototrophs and only a small percentage have been found and studied. There are only two other categorized Fe(II)-oxidizer at neutral pH which are in direct competition for Fe(II): Microaerophilic and nitrate-depended Fe(II)-oxidizer. Although they are competing for Fe(II) they have been found active in the same environments (Laufer et al., 2016; Otte et al., 2018). Additionally, iron is needed by all bacteria in small concentrations for necessary proteins but in higher

concentrations it can be a stressor, growth inhibiting and toxic for some bacteria (Ernst et al., 2022; Ratledge & Winder, 1964; Sorokina et al., 2013).

With the ability to use Fe(II) as additional electron source photoferrotrophs can also expand their ecological niche and have been found in a variety of environments like sediments (freshwater and marine), stratified lakes and soils (Ehrenreich & Widdel, 1994; Lambrecht et al., 2021; Llirós et al., 2015; Otte et al., 2018, chapter 2). They also thrive in iron-rich ponds and springs and can cope with high iron concentrations through iron homeostasis (Bryce et al., 2018; Jiao et al., 2005; chapter 8). It is quite important to respond to fluctuations in nutrient availability, enabling efficient utilization of different energy sources. This is particularly important for phototrophs in marine environments, where nutrient levels can vary widely, some daily or in dimictic stratified lakes with seasonal changes (Hojerová et al., 2011; Swanner et al., 2022). When *R. palustris* TIE-1 was grown on different Fe(II) and H_2 many proteins overlap which could help this bacteria to switch faster to a different metabolism and build resilience.

Conclusion

The ability to use multiple substrates by photoferrotrophs is an advantage for these bacteria. We could determine that Fe(II) oxidation rates are generally enhanced or not affected by other substrates and that generally substrates were used simultaneously. Fe(II) oxidation can improve the fitness of these photoferrotrophs against other phototrophs and enhance their ecological competitiveness.

Acknowledgement

The study was supported by Deutsche Forschungsgemeinschaft (DFG, German Research Foundation; BR 5927/2-1 and BY 82/4-1) awarded to C. Bryce and J. Byrne. James M. Byrne is supported by a UKRI Future Leaders Fellowship, MR/V023918/1. We would like to acknowledge Sören Drabesch for measuring H_2 samples.

References

Bryce, C., Blackwell, N., Schmidt, C., Otte, J., Huang, Y. M., Kleindienst, S., Tomaszewski, E., Schad, M., Warter, V., Peng, C., Byrne, J. M., & Kappler, A. (2018). Microbial anaerobic Fe(II) oxidation – Ecology, mechanisms and environmental implications. *Environmental Microbiology*, *20*(10), 3462–3483. https://doi.org/10.1111/1462-2920.14328

Bryce, C., Franz-Wachtel, M., Nalpas, N. C., Miot, J., Benzerara, K., Byrne, J. M., Kleindienst, S., Macek, B., & Kappler, A. (2018). Proteome response of a metabolically flexible anoxygenic phototroph to Fe(II) oxidation. *Applied and Environmental Microbiology*, *84*(16). https://doi.org/10.1128/AEM.001166-18

Croal, L. R., Jiao, Y., Kappler, A., & Newman, D. K. (2009). Phototrophic Fe(II) oxidation in an atmosphere of H2: Implications for Archean banded iron formations. *Geobiology*, *7*(1), 21–24. https://doi.org/10.1111/j.1472-4669.2008.00185.x

Crowe, S. A., Hahn, A. S., Morgan-Lang, C., Thompson, K. J., Simister, R. L., Llirós, M., Hirst, M., & Hallam, S. J. (2017). Draft Genome Sequence of the Pelagic Photoferrotroph Chlorobium phaeoferrooxidans. *Genome Announcements*, *5*(13). https://doi.org/10.1128/GENOMEA.01584-16

Ehrenreich, A., & Widdel, F. (1994). Anaerobic oxidation of ferrous iron by purple bacteria, a new type of phototrophic metabolism. *Applied and Environmental Microbiology*, *60*(12), 4517–4526. https://doi.org/10.1128/aem.60.12.4517-4526.1994

Eickhoff, M., Obst, M., Schröder, C., Hitchcock, A. P., Tyliszczak, T., Martinez, R. E., Robbins, L. J., Konhauser, K. O., & Kappler, A. (2014). Nickel partitioning in biogenic and abiogenic ferrihydrite: The influence of silica and implications for ancient environments. *Geochimica et Cosmochimica Acta*, *140*, 65–79. https://doi.org/10.1016/j.gca.2014.05.021

Ernst, L., Steinfeld, B., Barayeu, U., Klintzsch, T., Kurth, M., Grimm, D., Dick, T. P., Rebelein, J. G., Bischofs, I. B., & Keppler, F. (2022). Methane formation driven by reactive oxygen species across all living organisms. *Nature*, *603*(7901), 482–487. https://doi.org/10.1038/s41586-022-04511-9

Hegler, F., Posth, N. R., Jiang, J., & Kappler, A. (2008). *Physiology of phototrophic iron (II) -oxidizing bacteria : implications for modern and ancient environments*. *66*(Ii), 250–260. https://doi.org/10.1111/j.1574-6941.2008.00592.x

Heising, S., Richter, L., Ludwig, W., & Schink, B. (1999). Chlorobium ferrooxidans sp. nov., a phototrophic green sulfur bacterium that oxidizes ferrous iron in coculture with a "Geospirillum" sp. strain. *Archives of Microbiology*, *172*(2), 116–124. https://doi.org/10.1007/s002030050748

Hojerová, E., Mašín, M., Brunet, C., Ferrera, I., Gasol, J. M., & Koblížek, M. (2011). Distribution and growth of aerobic anoxygenic phototrophs in the Mediterranean Sea. *Environmental Microbiology*, *13*(10), 2717–2725. https://doi.org/10.1111/J.1462-2920.2011.02540.X

Jiao, Y., Kappler, A., Croal, L. R., & Newman, D. K. (2005). Isolation and characterization of a genetically tractable photoautotrophic Fe(II)-oxidizing bacterium, Rhodopseudomonas palustris strain TIE-1. *Applied and Environmental Microbiology*. https://doi.org/10.1128/AEM.71.8.4487-4496.2005

Kappler, A., Bryce, C., Mansor, M., Lueder, U., Byrne, J. M., & Swanner, E. D. (2021). An evolving view on biogeochemical cycling of iron. *Nature Reviews Microbiology*, *19*(6), 360–374. https://doi.org/10.1038/s41579-020-00502-7

Kappler, A., Pasquero, C., Konhauser, K. O., & Newman, D. K. (2005). Deposition of banded iron formations by anoxygenic phototrophic Fe(II)-oxidizing bacteria. *Geology*, *33*(11), 865–868. https://doi.org/10.1130/G21658.1

Lambrecht, N., Stevenson, Z., Sheik, C. S., Pronschinske, M. A., Tong, H., & Swanner, E. D. (2021). “Candidatus Chlorobium masyuteum,” a Novel Photoferrotrophic Green Sulfur Bacterium Enriched From a Ferruginous Meromictic Lake. *Frontiers in Microbiology*, *12*(July), 1–17. https://doi.org/10.3389/fmicb.2021.695260

Laufer, K., Niemeyer, A., Nikeleit, V., Halama, M., Byrne, J. M., & Kappler, A. (2017). Physiological characterization of a halotolerant anoxygenic phototrophic Fe(II)-oxidizing green-sulfur bacterium isolated from a marine sediment. *FEMS Microbiology Ecology*, *93*(5), 1–13. https://doi.org/10.1093/femsec/fix054

Laufer, K., Nordhoff, M., Schmidt, C., Behrens, S., Kappler, A., Røy, H., & Jørgensen, B. (2016). Coexistence of microaerophilic, nitrate-reducing, and phototrophic Fe(II) oxidizers and Fe(III) reducers in coastal marine sediment. *Applied and Environmental Microbiology*, *82*(5). https://doi.org/10.1128/AEM.03527-15

Llirós, M., Garciá-Armisen, T., Darchambeau, F., Morana, C., Triadó-Margarit, X., Inceoɨlu, Ö., Borrego, C. M., Bouillon, S., Servais, P., Borges, A. V., Descy, J. P., Canfield, D. E., & Crowe, S. A. (2015). Pelagic photoferrotrophy and iron cycling in a modern ferruginous basin. *Scientific Reports 2015 5:1*, *5*(1), 1–8. https://doi.org/10.1038/srep13803

McKinlay, J. B., & Harwood, C. S. (2010). Carbon dioxide fixation as a central redox cofactor recycling mechanism in bacteria. *Proceedings of the National Academy of Sciences of the United States of America*, *107*(26), 11669–11675. https://doi.org/10.1073/pnas.1006175107

Melton, E. D., Schmidt, C., Behrens, S., Schink, B., & Kappler, A. (2014). *Metabolic Flexibility and Substrate Preference by the Fe (II) -Oxidizing Purple Non-Sulphur Bacterium Rhodopseudomonas palustris Strain TIE-1 Metabolic Flexibility and Substrate Preference by the Fe (II) - Oxidizing Purple Non-Sulphur Bacterium Rhodop*. *September*, 37–41. https://doi.org/10.1080/01490451.2014.901439

Mu, C. C., Zhang, T. J., Zhao, Q., Guo, H., Zhong, W., Su, H., & Wu, Q. B. (2016). Soil organic carbon stabilization by iron in permafrost regions of the Qinghai-Tibet Plateau. *Geophysical Research Letters*, *43*(19), 10,286-10,294. https://doi.org/10.1002/2016GL070071

Otte, J. M., Harter, J., Laufer, K., Blackwell, N., Straub, D., Kappler, A., & Kleindienst, S. (2018). The distribution of active iron-cycling bacteria in marine and freshwater sediments is decoupled from geochemical gradients. *Environmental Microbiology*, *20*(7), 2483–2499. https://doi.org/10.1111/1462-2920.14260

Ratledge, C., & Winder, F. G. (1964). Effect of Iron and Zinc on growth patterns of Escherichia Coli in an Iron-Deficient Medium. *Journal of Bacteriology*, *87*(4), 823–827.

Raven, J. A., Beardall, J., Larkum, A. W. D., & Sánchez-Baracaldo, P. (2013). Interactions of photosynthesis with genome size and function. *Philosophical Transactions of the Royal Society B: Biological Sciences*, *368*(1622). https://doi.org/10.1098/rstb.2012.0264

Sorokina, E. V., Yudina, T. P., Bubnov, I. A., & Danilov, V. S. (2013). Assessment of iron toxicity using a luminescent bacterial test with an Escherichia coli recombinant strain. *Microbiology (Russian Federation)*, *82*(4), 439–444. https://doi.org/10.1134/S0026261713040115

Straub, K. L., Rainey, F. a, & Widdel, F. (1999). Marine Phototrophic Ferrous-Iron-Oxidizing Purple Bacteria. *International Journal of Systematic Bacteriology*, *49*(1 999), 729–735.

Swanner, E. D., Wüstner, M., Leung, T., Pust, J., Fatka, M., Lambrecht, N., Chmiel, H. E., & Strauss, H. (2022). Seasonal phytoplankton and geochemical shifts in the subsurface chlorophyll maximum layer of a dimictic ferruginous lake. *MicrobiologyOpen*, *11*(3). https://doi.org/10.1002/mbo3.1287

Thompson, K. J., Kenward, P. A., Bauer, K. W., Warchola, T., Gauger, T., Martinez, R., Simister, R. L., Michiels, C. C., Llirós, M., Reinhard, C. T., Kappler, A., Konhauser, K.

O., & Crowe, S. A. (1987). Photoferrotrophy, deposition of banded iron formations, and methane production in Archean oceans. *Nature*, *329*, 710–712. https://doi.org/10.1126/sciadv.aav2869

Tipping, E. (1981). The adsorption of aquatic humic substances by iron oxides. *Geochimica et Cosmochimica Acta*, *45*(2), 191–199. https://doi.org/10.1016/0016-7037(81)90162-9

Walter, X. A., Picazo, A., Miracle, M. R., Vicente, E., Camacho, A., Aragno, M., & Zopfi, J. (2014). Phototrophic Fe(II)-oxidation in the chemocline of a ferruginous meromictic lake. *Frontiers in Microbiology*, *5*(DEC), 1–9. https://doi.org/10.3389/fmicb.2014.00713

Widdel, F, & Bak, F. (1992). The Prokaryotes: A Handbook on the Biology of Bacteria: Ecophysiology, Isolation, Identification, and Applications. In *The Prokaryotes: A Handbook on the Biology of Bacteria*. Springer-Verlag, New York.

Widdel, F, & Pfenning, N. (1981). Studies on Dissimilatory Sulfate-Reducing Bacteria that Decompose Fatty Acids. *Archives of Microbiology*, *129*, 395–400.

Widdel, Friedrich. (1983). Methods for enrichment and pure culture isolation of filamentous gliding sulfate-reducing bacteria. *Archives of Microbiology*, *134*(4), 282–285. https://doi.org/10.1007/BF00407803

Widdel, Friedrich, Schnell, S., Heising, S., Ehrenreich, A., Assmus, B., & Schink, B. (1993). Ferrous iron oxidation by anoxygenic phototrophic bacteria. *Nature*, *362*(6423), 834–836. https://doi.org/10.1038/362834a0

Winogradsky, S. (1888). *Beiträge zur Morphologie und Physiologie der Bacterien: hft. I.: Zur Morphologie und Physiologie der Schwefelbacterien.* (Vol. 1). Verlag von Arthur Felix.

Zhu, Z., Cao, Y., Zheng, Z., & Chen, D. (2022). An Accurate Model for Estimating H2 Solubility in Pure Water and Aqueous NaCl Solutions. *Energies*, *15*(14). https://doi.org/10.3390/en15145021

Supplements

Table S1: Media composition for each photoferrotroph.

Organism	Salts	Buffer	Additives
R. iodosum and *R. robiginosum*	26.4 g/L NaCl 5.7 g/L $MgSO_4 \cdot 7 H_2O$, 5.7 g/L $MgCl_2 \cdot 6 H_2O$, 1.5 g/L $CaCl_2 \cdot 2 H_2O$, 0.66 g/L KCl, 0.09 g/L Br 0.6 g/L KH_2PO_4 and 0.3 g/L NH_4Cl were autoclaved separately	2.5 gL/ $NaHCO_3$ buffer	1 mL/L sterile filtered 7-vitamin solution (Widdel & Pfenning, 1981), 1 mL/ trace element solution (Widdel, 1983) and 1 m/L selenite-tungstate solution (Widdel & Bak, 1992) 0.5 mL/L $Na_2S_2O_3$ (1 M)
C. ferrooxidans KoFox	0.0025 g/L $MgSO_4 \cdot 7 H_2O$, 0.4 g/L $MgCl_2 \cdot 6 H_2O$, 0.1 g/L $CaCl_2 \cdot 2 H_2O$ 0.6 g/L KH_2PO_4, 0.3 g/L NH_4Cl	1.85 gL/ $NaHCO_3$ buffer	1 mL/L sterile filtered 7-vitamin solution (Widdel & Pfenning, 1981), 1 mL/ trace element solution (Widdel, 1983) and 1 m/L selenite-tungstate solution (Widdel & Bak, 1992)
R. palustris TIE-1	0.5 g KH_2PO_4, 0.3 g NH_4Cl, 0.5 g $MgSO_4 * 7H_2O$, 0.1 g $CaCl_2*2H_2O$	1.85 gL/ $NaHCO_3$ buffer	10 mL/L filter-sterilized vitamin solution (altered from Ehrenreich & Widdel, 1994; containing 50 mg/L riboflavin), 1 mL/L SL10 trace element solution (Widdel, 1983), 1 mL/L selenite-tungstate solution (Widdel & Bak, 1992) and 0.1mg/L vitamin B12 solution (c=100 mg/L) were added
Chlorobium sp. N1	17.3 g/L NaCl 0.025 g/L $MgSO_4 \cdot 7 H_2O$,	1.85 gL/ $NaHCO_3$ buffer	1 mL/L sterile filtered 7-vitamin

	8.6 g/L $MgCl_2 \cdot 6 H_2O$, 0.99 g/L $CaCl_2 \cdot 2 H_2O$, 0.39 g/L KCl, 0.059 g/L Br 0.05 g/L KH_2PO_4 and 0.25 g/L NH_4Cl were autoclaved separately		solution (Widdel & Pfenning, 1981), 1 mL/ trace element solution (Widdel, 1983) and 1 m/L selenite-tungstate solution (Widdel & Bak, 1992)
R. ferrooxidans SW2	0.6 g/L KH_2PO_4, 0.3 g/L NH_4Cl, 0.025 g/L $MgSO_4 \cdot 7 H_2O$, 0.4 g/L $MgCl_2 \cdot 6 H_2O$, 0.1 g/L $CaCl_2 \cdot 2 H_2O$	1.85 gL/ $NaHCO_3$ buffer	1 mL/L sterile filtered 7-vitamin solution (Widdel & Pfenning, 1981), 1 mL/ trace element solution (Widdel, 1983) and 1 m/L selenite-tungstate solution (Widdel & Bak, 1992)

Table S2: T-test with Fe(II) oxidation rates between Fe(II) only and Fe(II) oxidation rates with organics.

R. iodosum		**p-value**
Fe only	Fe plus Ac	0.0026
	Fe plus Lc	0.3644
	Fe plus Bu	0.0582
	Fe plus Glu	0.4509
***C.ferrooxidans* KoFox**		**p-value**
Fe only	Fe plus Ac	0.4827
	Fe plus Lc	0.6227
	Fe plus Bu	0.2057
	Fe plus Glu	0.0767
***Chlorobium* N1**		**p-value**
Fe only	Fe plus Ac	0.0012
	Fe plus Lc	8E-07
	Fe plus Bu	0.1174
	Fe plus Glu	0.008
R. robiginosum		**p-value**
Fe only	Fe plus Ac	0.0515
	Fe plus Lc	0.1398
	Fe plus Bu	0.2064
	Fe plus Glu	0.9604
***R. ferrooxidans* SW2**		**p-value**
Fe only	Fe plus Ac	0.0053
	Fe plus Lc	0.2885
	Fe plus Bu	0.4915
	Fe plus Glu	0.8195

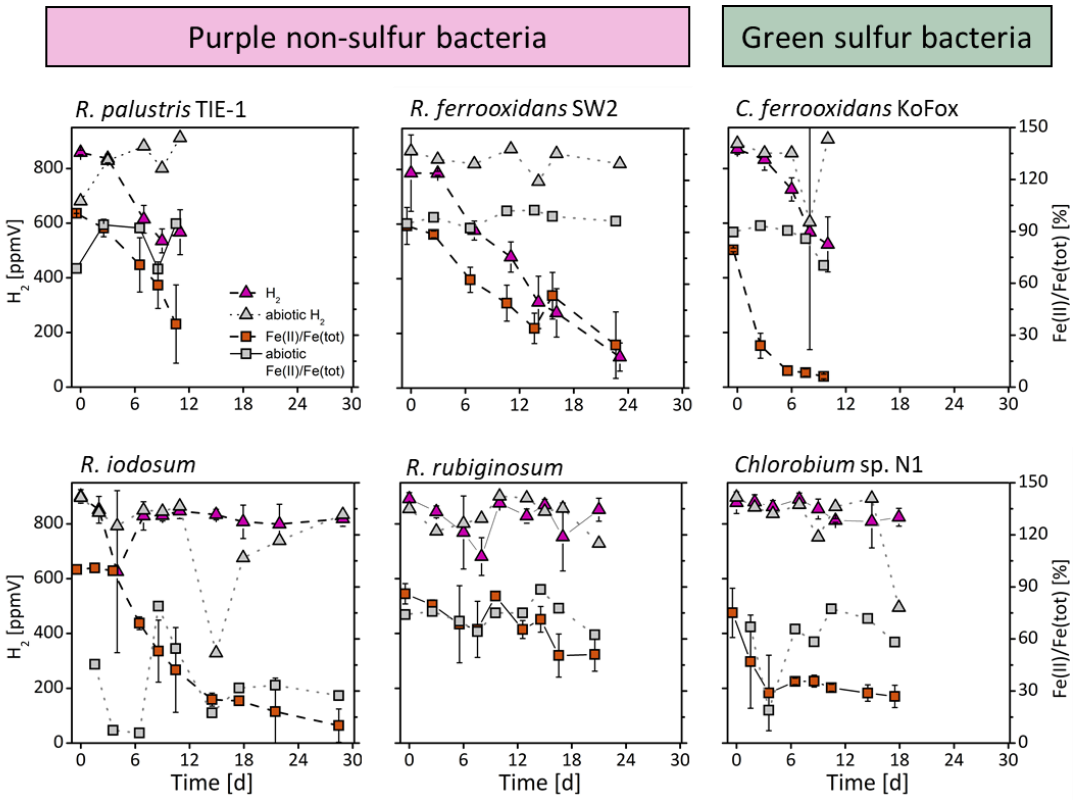

Figure S1: Panels show the substrate preference of R. palustris TIE-1*, R. ferrooxidans* SW2*, R. iodosum, R. robiginosum, C. ferrooxidans* KoFox *and Chlorobium sp.* N*1 incubated with Fe(II) and* H_2*. Biotic data are from triplicates from sacrificial setup and abiotic sample show data from one bottle.*

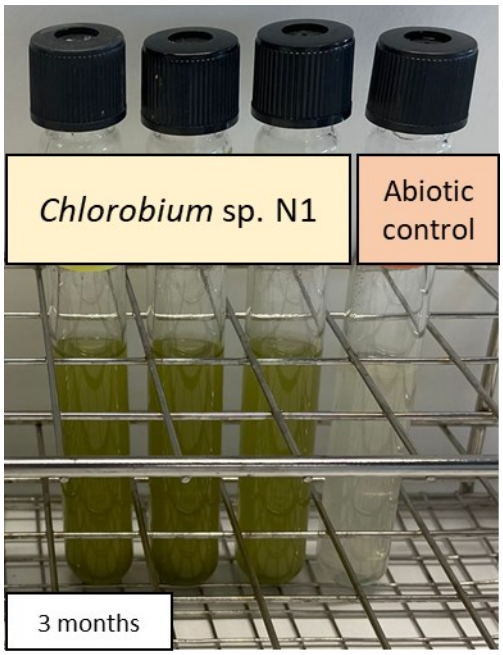

Figure S2: Growth of Chlorobium sp. N1 *on H_2 after 30 days.*

4 Chapter: Iron cycle influenced by organic carbon in a dimictic lake

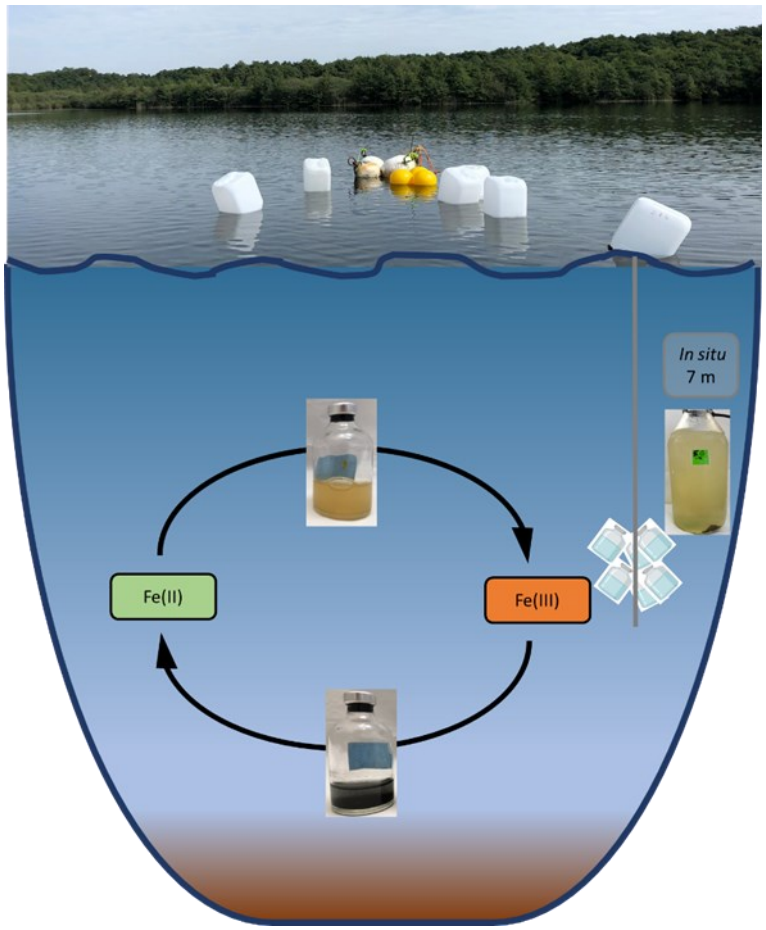

Contributions:

Resources were provided by Dr. C. Bryce, Assoc. Prof. J.M. Byrne and Prof. Dr. A. Kappler. The project was designed by me, M. Maisch, Dr. C. Bryce, Assoc. Prof. J.M. Byrne. The experiments were performed by me, J. C. Lopez-Rivoldi and M. Maisch. D. Straub conducted bioinformatic analysis and S. Eroglu and H. Strauß provided geochemical data. The manuscript was written by me with guidance of Dr. C. Bryce.

Iron cycle influenced by organic carbon in a dimictic lake

Verena Nikeleit[1], Markus Maisch[1], Daniel Straub[2], Sümeyya Eroglu[3], Jimena C. Lopez-Rivoldi[1], Harald Strauß[3], James M. Byrne[4], Andreas Kappler[1,5] and Casey Bryce[4*]

[1]Department of Geoscience, University of Tübingen, Tübingen, Germany

[2]Quantitative Biology Center (QBiC), University of Tübingen, Tübingen, Germany

[3]Institute for Geology and Paleontology, University of Münster, Münster, Germany

[4]School of Earth Sciences, University of Bristol, Bristol, UK

[4]Cluster of Excellence: EXC 2124: Controlling Microbes to Fight Infections, Tübingen, Germany

*Corresponding Author: Casey Bryce

School of Earth Science, Wills Memorial Building, University of Bristol, Queens Road, Bristol, BS8 1RJ, UK.

Email: casey.bryce@bristol.ac.uk

For submission to FEMS

KEYWORDS: phototrophic Fe(II) oxidation, photoferrotrophs, Fe(III) reduction, stratified lake

Abstract

Iron cycling and phototrophic Fe(II) oxidation has been studied before in meromictic lakes in the past, yet less attention was put on dimictic lakes. Here we investigated the potential of a dimictic lake Großes Heiliges Meer in north Germany on iron cycling with 16S rRNA amplicon sequencing, *in situ* and lab-based experiments. Bacterial community composition follows geochemical gradients is different in oxic/anoxic conditions. Potential iron metabolizing bacteria were found in 7 and 8 m depth like *Chloroboium, Thiodyction, Geobacter and Rhodoferrax*. We were able to enrich iron metabolizing bacteria and simulate Fe(II) oxidation and Fe(III) reduction and show the role of carbon in this system. Dimictic lakes expand the known habitats where iron plays an important role and highlights the ubiquity of iron cycling

Introduction

Iron cycling, consisting of Fe(II) oxidation and Fe(III) reduction, is a widespread process in stratified lakes, marine and freshwater sediments (Berg et al., 2016; Kappler et al., 2021; Otte et al., 2018). Fe(II), ferrous iron, and Fe(III), ferric iron, also interact with many relevant cycles like carbon, sulfur and nitrogen (Kappler et al., 2021). During Fe cycling and its formation and dissolution of Fe minerals nutrients like phosphor, carbon and pollutants can be bound and sequestered or released back into the environment (Eickhoff et al., 2014; Andreas Kappler et al., 2021; Mu et al., 2016; Tipping, 1981). Both reactions can be facilitated abiotically and biotically whereas microbial iron cycling plays an important part especially under microoxic and anoxic conditions (Bryce et al., 2018; Kappler et al., 2021).

Direct microbial Fe(III) reduction takes place in anoxic environments and is performed by different genera of bacteria like *Geobacter* spp.*, Shewanella* spp. and *Geothrix* spp. (Coates et al., 1999; Lovley & Phillips, 1987; Myers & Nealson, 1990). Indirect microbial Fe(III) reduction could happen in sulfur-rich environments with bacteria that can reduce sulfur-species which reacts abiotically with Fe(III) to form FeS or/and FeS_2 (D. E. Canfield, 1989). Fe(II) oxidation can happen in oxic environments either abiotically with atmospheric O_2 or microbially produced O_2 from cyanobacteria; or via microbial mediation at low pH (Kappler et al., 2021). In the interface of oxic to anoxic environments Fe(II) oxidation can be directly oxidized by microaerophilic Fe(II)-oxidizing bacteria (Kucera & Wolfe, 1957; Maisch et al., 2019). Whereas in anoxic, (sunlit) environments nitrate-reducing and phototrophic Fe(II)-oxidizers like *Chlorobium* spp., *Thiodyction* spp. and *Acidovorax* spp. can oxidize Fe(II) (Bryce et al., 2018; Croal et al., 2004; Heising et al., 1999; A. Kappler et al., 2005; Laufer et al., 2017). Both Fe(III)-reducers and Fe(II)-oxidizers have been found to be abundant and active in the same environments e.g. marine and freshwater sediments and stratified lakes (Berg et al., 2016; Otte et al., 2018). An active iron cycle with potential for rapid FeS recycling has been found seasonally meromictic Lake Cadagno which has low iron content (Berg et al., 2016). Potential

for active iron cycling has also been suggested for Lake Matano, Indonesia and Lake La Cruz, Spain which contain hundreds of micro- molar dissolved Fe(II) in the anoxic bottom waters and contained active phototropic Fe(II)-oxidizer (Crowe et al., 2008; Walter et al., 2014). In recent years the attention shifted to Boreal lakes and the potential of dimictic lakes contributing to iron cycling (Liu et al., 2022; Schiff et al., 2017; Tsuji et al., 2020).

Considering that Fe cycling is potential taking place in a lot of environments more studies should be conducted to investigate this. We chose Großes Heiliges Meer, a dimictic lake in North Germany that develops anoxic bottom layers in the summer that contain iron and sulfur as a suitable candidate. In *in sit*u and lab based experiments we investigated how the community responds to a spike of Fe(II) and/or organics (acetate, lactate) with focusing on the role of iron-metabolising bacteria in this system.

Materials and methods

Fieldsite. Großes Heiliges Meer is a dimictic lake in North Germany near Hopsten at 52°21′06.73″N and 7°38′03.22″E. It is part of a well-established field station in a protected area of the Landschaftsverband Westfalen-Lippe (LWL) Museum für Naturkunde (museum of Natural History). The lake has a maximum depth of 10.8 m and an average depth of 4.4 m. It is stratified beginning mid-April to late October (Pott, 2009; Swanner et al., 2022).

Geochemical data. Temperature and oxygen content were measured with an *in situ* electrode (ThermoScientific Orion Star) at the desired depths. Fe, SO_4^{2-} and DIC were measured in the lab. Water samples for Fe were filtered (0.45 µm) and 5 drops of 65% HNO_3^- added in the field. Total Fe was measured with ICP-OES (SpectroFlame-EOP, SPECTRO Analytical Instruments). SO_4^{2-} was measured with ion chromatography (761 compact IC, Firma Methrom AG) and DIC was determined by titration of 0.1 M HCl with 100 mL water sample to pH 4.3.

Community analysis. To get an overall view on microbial community over the depth of the lake community analysis in 4 different depth were performed. Depth selected were at 3 m, 5 m, 7 m and 8 m. Water was pumped up and directly filled in a sterile 5 L canister and filled to the top to avoid air bubbles. Samples were directly prepared for DNA extraction, 16S rRNA (gene) amplicon sequencing and analysis as described below.

***In situ* experiment.** To investigate iron cycling we incubated 1 L bottles at 7 m. Water was pumped from these depths in a sterile plastic cannister until the bottle was full and closed to avoid oxygen exposure. Water was then filled into 1L bottles and headspace was degassed with N_2 for 5-10 min. After that the substrates were to 4 different experimental setups. For each setup 2 bottles were prepared. The experimental conditions testes were: 1) no addition of substrates (as a control), 2) with the addition of 2 mM Fe(II), 3) the addition of Fe(II) and an organic

carbon mix (0.6 mM acetate and lactate) and 4) with the addition of the organic mix only. All 4 conditions were conducted both without DCMU (3-(3,4-dichlorophenyl)-1,1-dimethylurea; $C_9H_{10}Cl_2N_2O$) added, and with 10µM DCMU to inhibit cyanobacteria and thereby abiotic oxidation of Fe(II). The bottles were then placed back into the lake 7 depth, to be removed at each sacrificial sampling point. In total 3 sampling time points were chosen. For time zero water from 7 m was also collected. At each time point, the water in the bottles was analysed for Fe(II)/Fe(III) ratios, acetate and lactate concentrations, and DNA extracted for microbial community analysis.

Fe(II) oxidation and Fe(III) reduction with enrichment culture. The enrichment was obtained from the *in situ* experiment from 7 m in the setup where Fe(II) was added. Additional small bottles were set up and after the experiment these were stored in a light incubator with constant light and 20°C. After several weeks orange/brown precipitates were formed and were transferred into serum vials containing low phosphate media and 2 mM Fe(II) (Ehrenreich & Widdel, 1994). With potential Fe(II)-oxidizer and Fe(III) reducer in the enrichment different setups were performed to promote either Fe(II) oxidation or Fe(III) reduction. For Fe(II) oxidation the triplicates of the enrichment culture were randomly placed in a 20°C light incubator with 2 mM Fe(II). For Fe(III) reduction two different treatments were chosen in triplicates; I) 2 mM synthesised ferrihydrite (Fe-Red-Fh) and 1 mM lactate and acetate and II) previously oxidized Fe(II) to Fe(III)oxyhydroxides (2 mM) (Fe-Red-Bios) from the enrichment with 2mM lactate were randomly placed in a 20°C incubator wrapped in aluminium foil. Samples for Fe and HPLC were taken sterilely and anoxically and stored at 5°C for quantification.

Iron cycling experiment with *in situ* community from 8m. Incubation experiments were taken from water depth of 8 m. Water was pumped into a sterile plastic cannister and filled to the top to avoid air bubbles and, thus, oxygen exposure. In the laboratory 50 mL of the water was filled into sterile 100 mL serum vials and prepared for 3 different setups. Setup 1 had the addition of 2 mM Fe(II), for setup 2 the addition of 1 mM Fe(II) and 1 mM organic mix (respectively acetate and lactate) and setup 3 the addition of 2 mM organic mix. For every setup 3 biological bottles were prepared and one abiotic control (addition of 15 mM formaldehyde). Bottles were placed for the first part of the experiment into an incubator with 14h light and 10h at 8°C. After 33 days conditions were changed to 24h illumination to stimulate Fe(II) oxidation and after 44 days changed to 24h dark to stimulate Fe(III) reduction. Samples were taken in a glovebox with 100% N_2 atmosphere for Fe analysis and quantification.

Fe quantification. 0.1 mL Samples for Fe quantification were taken anoxically and directly aliquoted into 0.9 mL 1 M HCl. Samples were stored at 4°C until measurements and Fe(II) and total Fe were quantified with the Ferrozine assay after Hegler (Hegler et al., 2008).

Organic concentrations. After sampling, samples were centrifuged at 15,000 rpm for 10 min to remove cells and minerals, and the supernatant was transferred to a new Eppendorf tube and stored at 4°C until analysis. High Performance Liquid Chromatography (HPLC) analysis was performed with a Shimadzu Prominence HPLC with a LC-20ATsolvent delivery unit, CTO-10ASvp column oven and a RID-20a refractive index detector.

DNA extraction. Samples were filtered through SterivexTM-GP sterile filter (0.22 µm, Merck KGaA, Darmstadt, Germany) until the filter was blocked. Aterwards, the filter paper was extracted from the filter and DNA was extracted using the UltraClean R Microbial DNA

Isolation Kit (MO BIO Laboratories, Carlsbad, CS, USA) and the quantity of the DNA was measured with a Nanodrop ND-1000 Spectrometer (Nanodrop^{TM} 1000, Thermo Scientific, Waltham, MA, USA).

16S rRNA gene amplicon sequencing and analysis. DNA was amplified by using forward primer 16S-515F and reverse primer 16S-806R (Caporaso et al., 2011) targeting the V4 region of the 16S ribosomal RNA. Library preparation steps (Nextera, Illumina) and 250 bp paired-end sequencing with MiSeq (Illumina, San Diego, CA, USA) using v2 chemistry were performed by Microsynth AG (Balgach, Switzerland). Between 9,925 and 118,334 read pairs were obtained for each of the 36 samples (in total 5,124,544 read pairs). Sample *in situ* – "8m a" had the lowest number of reads (9,925), all other samples had more than 39,000. Sequencing data was analyzed with nf-core/ampliseq v2.3.1, which includes all analysis steps and software and is publicly available (Ewels et al., 2020; D. Straub et al., 2020), with Nextflow v21.10.3 (Di Tommaso et al., 2017) and singularity v3.8.7 (Kurtzer et al., n.d.). Primers were trimmed, and untrimmed sequences were discarded (<30% per sample, except 36% for QPTIJ097AB) with Cutadapt version 3.4 (Martin, 2011). Adapter and primer-free sequences were processed with DADA2 v1.22.0 (Callahan et al., 2016) to eliminate PhiX contamination, trim reads (before median quality drops below 35; forward reads were trimmed at 230 bp and reverse reads at 207 bp), correct errors, merge read pairs, and remove polymerase chain reaction (PCR) chimeras; ultimately, 5,218 amplicon sequencing variants (ASVs) were obtained across all samples. Taxonomic classification was performed with DADA2 and the SILVA v138 database (Quast et al., 2012). Intermediate results were imported into QIIME2 version 2021.8.0 (Bolyen et al., 2019). 458 ASVs classified as chloroplasts or mitochondria were removed, totaling 0% to 50.2% (average 12.7%) relative abundance per sample, and retaining 4,760 ASVs across all

samples. Alpha rarefaction curves were produced with the QIIME2 diversity alpha-rarefaction plugin, which indicated that the richness of the samples had been fully observed.

Results

Geochemical data

The temperature at the surface was 20.9°C and decreased continuously to 7.2°C at 10 m. pH was 7.1 at the surface and increased at 3-4 m to 7.6 and then decreased down to 7.0 again at 6 m (Figure 1). In Heiliges Meer oxygen content started to decrease at 3 m from 9.68 mg/L to under 0.3 mg/L at 7 m. Once oxygen was depleted Fe and Mn appear in the water column. In 7 m 7.5 mg/L (0.13 mM) Fe was detected for the first time and increased to 38 mg/L (0.7 mM) Fe at 10 m.

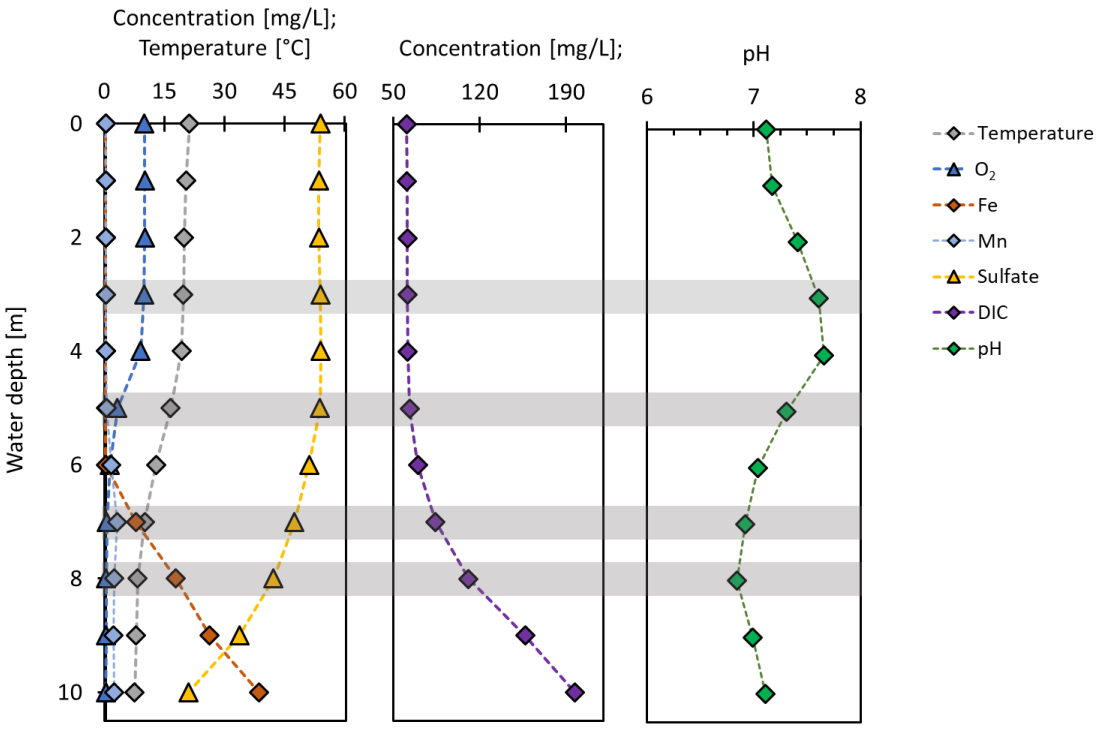

Figure 1: Geochemical data of temperature, O_2, Fe, Mn, SO_4^{2-}, DIC and pH from the water column of Heiliges Meer. Grey background indicates depth where samples for community analysis were taken.

Mn could already be quantified at 6 m (1.4 mg/L) and increased to 2.0 mg/L at 10 m. In the same depth as Mn started to increase (5 m), SO_4^{2-} concentration decreased to 40% at 10 m compared to 6 m, from 53 mg/L at 6 m to 20.6 mg/L at 10 m. Additionally, an increase in DIC was detected from 63 mg/L at 5 m to 200 mg/L at 10 m depth.

Microbial community in Großes Heiliges Meer

DNA was taken from 3, 5, 7 and 8 m and analysed in duplicates. Differences in the microbial community were observed between 3/5 and 7/8 m (Figure 2). In 3 and 5 m aerobic and facultatively anaerobic microorganisms (*hgcI clade, Flavobacterium*), and heterotrophs (*Clade III*) were found alongside cyanobacteria (*Snowella* 0TU37S04). Once oxygen is depleted the bacterial community shifts at 7 and 8 m depth to be dominated by strict anaerobes like sulfur reducers (*Desulfomonile*), sulfur oxidizers (*Sulfuricurvum*), methane oxidizers (*Methylomonadaceae, Methylotenera*), fermenters (*Terrimicrobium*), potential Fe(II)-oxidizers and Fe(III)-reducers. The potentially Fe(II)-oxidizing community members are species of *Chlorobium* and *Thiodyction* (phototrophic Fe(II)-oxidizers), and *Sideroxydans* (microaerophilic Fe(II)-oxidizer). Potential Fe(III)-reducers identified included representatives of *Rhodoferax, Geobacter* and *Geothrix*. , A clear difference in abundance was observed for potential iron metabolising bacteria between oxic and anoxic conditions in the lake. At 3 and 5 m iron metabolising bacteria were 0.4 to 0.8 % of the bacterial community whereas at 7 and 8 m 25.5 and 12% of the total bacterial community was comprised of them. In general, in anoxic conditions at Heiliges Meer, bacteria associated with iron, sulfur, methane and carbon metabolism have been found in the anoxic waters and show a diverse community linked to many environmentally relevant cycles.

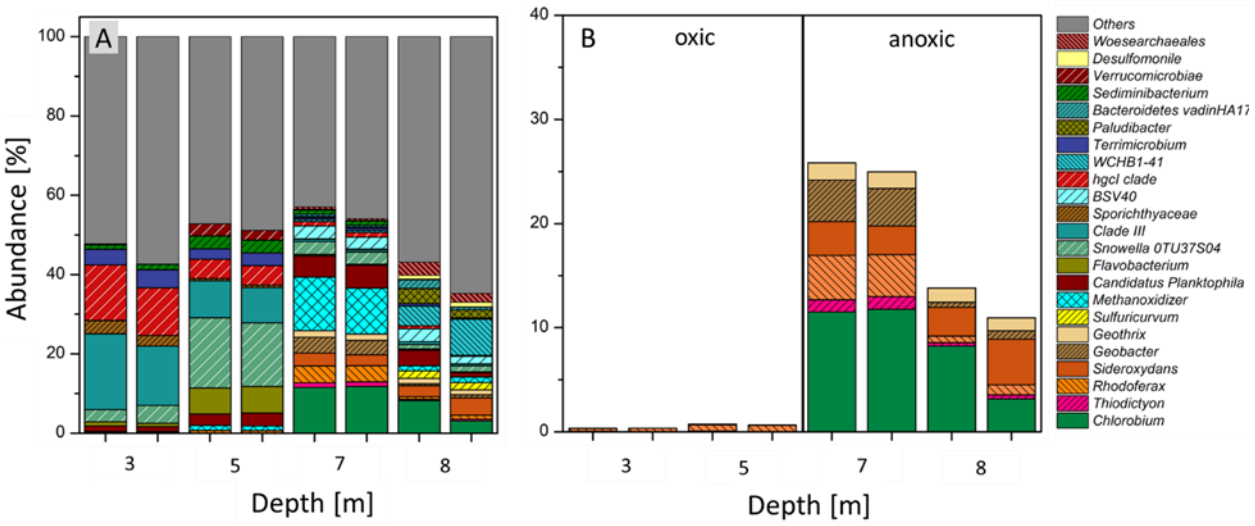

Figure 2: Panel A shows bacterial community for 3, 5, 7 and 8 m water depth in duplicates. Bacteria are shown individually if abundance was 1% or higher. Panel B shows abundances of potential iron metabolising bacteria for 3, 5, 7 and 8 m water depth.

***In situ*-experiment at 7 m**

We conducted *in situ* experiments to 1) establish whether the observed Fe(II)-oxidizing microorganisms would conduct this metabolism in the conditions present in the lake and 2) to test whether the presence of DOC inhibits Fe(II) oxidation in situ given the observed phototrophic Fe(II)-oxidizers are known to be metabolically flexible. 1 L Schott bottles of water from 7m depth were spiked with relevant substrates and placed back at 7 m depth for 3 and 23 days. After 3 days no change in Fe(II)/Fe(tot) was measured, as well as no change in acetate and lactate concentrations (Figure 3). The bacterial community was also similar to t0. Generally, a slight increase of *Chlorobium* (11% to 31%) and *Geobacter* (3% to 12%) was observed and a decrease in *Thiodyction, Rhodoferax, Geothrix* and methane oxidizers (12% to 3%). Highest abundance of potential Fe-metabolising bacteria was in the control and organic/organic+DCMU setups. For the samples collected at 23 days no control data are presented as the control bottles were, unfortunately, trapped on the buoy and could not be retrieved from the lake. No change in Fe(II)/Fe(tot) could be observed in the remaining setups. Lactate was completely used up and acetate increased to 0.7 mM. Generally, a decrease of

Chlorobium (31% to 18%), methane oxidizers (3% to 0.7-1.8%) and *Siderooxidans* (under 1%) were observed. In the setups with DCMU and/or organics an increase of *Sulfurospirillum* up to 45 % (in Fe(II)+organic+DCMU) was observed. In the setup with Fe(II)+organic+DCMU, organic and organic+DCMU also an increase in *Geothrix* (up to 3%) was observed. Additionally, in the organic setups an increase of *Thiodyction* (up to 3%) was observed.

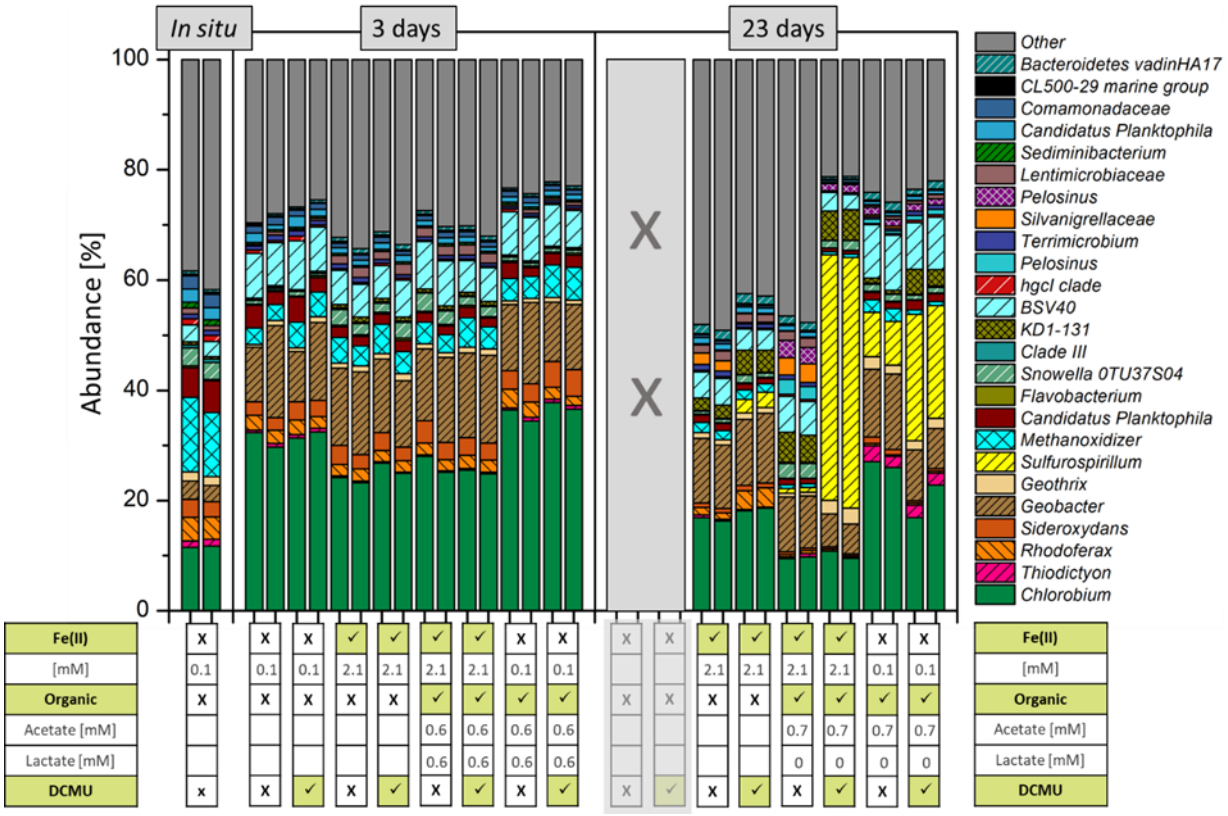

Figure 3: Bacteria community of in situ experiment from initial community (in situ), 3 and 23 days are shown in duplicates. Bacteria are shown individually if abundance was 1% or higher. Table underneath indicates different substrate addition (Fe(II), organic or/and DCMU).

Fe(II) oxidation and Fe(III) reduction with enrichment culture

From the setup Fe(II) only at 7 m we could successfully maintain an enrichment culture under autotrophic conditions with 2 mM Fe(II) as electron donor and continuous light illumination. 16S rRNA gene amplicon sequencing showed that *Thiodyction* was the dominant bacteria (32%). This was also found in the *In situ* community from 7 m. The culture also contained two

different sequences annotated as *Geobacter* that, combined, represent 9% of the community (Figure 4). Other bacteria were strictly chemotrophic anaerobes (*Anaerolineaceae, Lentimicrobiaceae* and *Williamwhitmania*). With the abundance of potential Fe(II)-oxidizer and Fe(III)-reducer we set up experiments promoting phototrophic Fe(II) oxidation and Fe(III) reduction. Phototrophic Fe(II) oxidation had a lag phase of 9 days and ended after 19 days with 90% of Fe(II) oxidized. One bottle had a longer lag phase and also its Fe(II) oxidation rate was a bit lower than the other two. Average Fe(II) oxidation rate reached 0.12±0.05 mM/d. Fe(III) reduction experiments were set up with two different initial Fe(III) minerals: I) with biotic Fe(III)oxyhydroxides and II) with synthetic ferrihydrite. Fe(III) reduction rates in both setups were similar reaching 0.33±0.07 (biotic Fe(III)oxyhydroxides) and 0.34±0.05 mM/d (synthetic ferrihydrite) and the colour changed from orange to black in both cases. Compared to the Fe(II) oxidation rates, Fe(III) reduction rates were almost 3 times higher and showed us that when organics are provided Fe(III) reduction is likely to outcompete Fe(II) oxidation when both occur simultaneously.

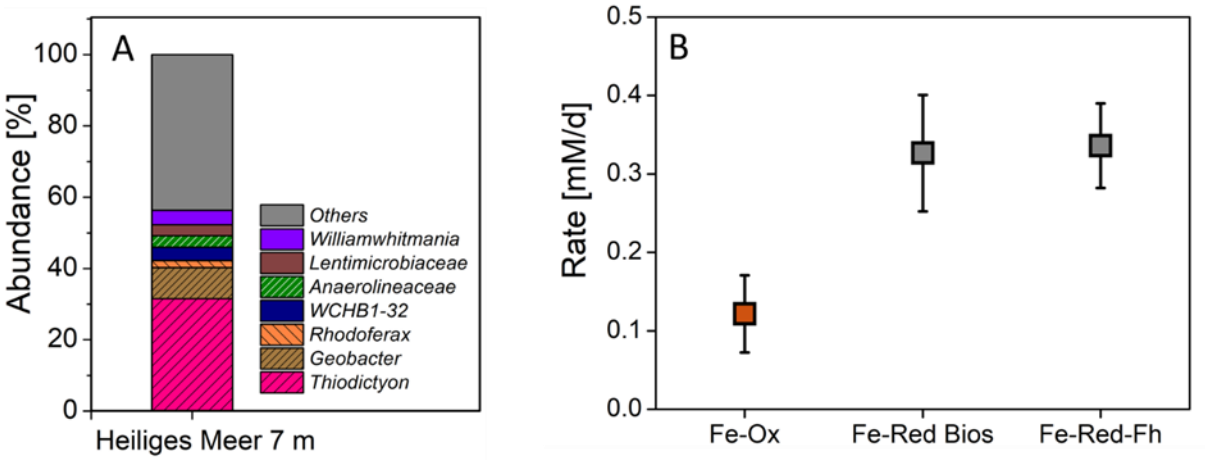

Figure 4: Panel A shows bacterial community of a phototrophic enrichment culture originated from 7 m depth of Großes Heiliges Meer. Panel B shows Fe(II) oxidation and Fe(III) reduction rates. Fe-Red Bios show Fe(III) reduction rate with biotic Fe(III)oxyhydroxides and Fe-Red-Fh shows Fe(III) reduction rates with synthesised ferrihydrite.

Cycling experiment with *in situ* community from 8 m

In this experiment we wanted to simulate iron cycling in the light and dark and the effect of organics on the system. Therefore we set up 3 different treatment where water from 8 m depth was amended with only Fe(II), Fe(II) plus organics or only organics. All three setups start with a Fe(II)/Fe(tot) ratio of around 0.83 and were exposed to a 14/10 h light/dark cycle at 8°C. Both the Fe(II) plus organics and only organics setup showed Fe(III) reduction and reached a Fe(II)/Fe(tot) ratio of 0.99± 0.03 and 0.99±0.04 respectively after 34 days (Figure 5). In the Fe(II) only setup slight Fe(II) oxidation occurred and reached a Fe(II)/Fe(tot) of 0.75±0.1 after 34 days. This could give us a first impression how organics are influencing iron cycling. When organics were added Fe(III) reduction was favoured or outcompeted Fe(II) oxidation and in the setup without organics a slight indication for Fe(II) oxidation was happening although the standard deviations were high.

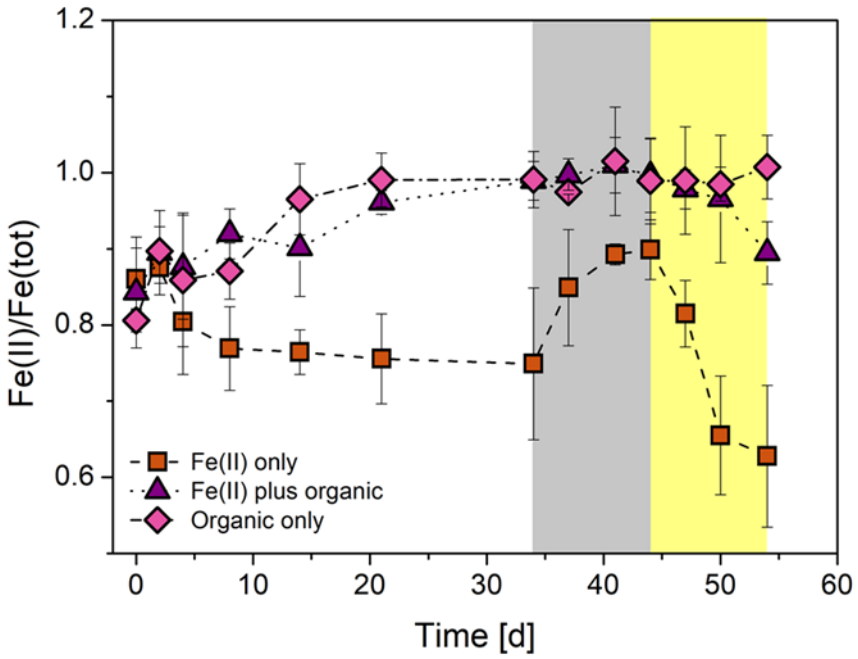

Figure 5: Iron cycling experiment from 8 m depth of Heiliges Meer with different setups. Brown square hows Fe(II) only setup, purple triangle shows Fe(II) plus organic setup and pink dimond shows organic only setup. For the first 34 days all setups were exposed to a 14/10 h light/dark cycle. Afterwards the bottles were placed for 10 days in the dark (grey backgroud) and then 10 days into the light (yellow backgroud).

To further study the individual sides of the iron cycle, namely to promote only Fe(III) reduction and Fe(II) oxidation, the setups were placed in darkness for 10 days and afterwards 10 days in the light. In the Fe(II) plus organics and organics only setup no change in Fe(II)/Fe(tot) was measured whereas Fe(III) reduction was observed in the Fe(II) only setup and Fe(II)/Fe(tot) increased to 0.90±0.04. After 44 days all three setups were placed in a light incubator with constant illumination and no change in Fe(II)/Fe(tot) was observed in the organics only setup. In the Fe(II) plus organics and Fe(II) only setup Fe(II) oxidation could be observed in both cases and reached 0.90±0.04 (Fe(II) plus organic) and 0.63±0.09 (Fe(II) only) Fe(II)/Fe(tot) after 54 days.

Discussion

Dimictic lakes as potential iron cycling habitats

So far studies on phototrophic Fe(II) oxidation, iron cycling and Archean ocean analogues has been focused on Lake Kivu (Llirós et al., 2015), Brownie Lake (Lambrecht et al., 2021), Lake Cadagno (Berg et al., 2016), Lake de la Cruz (Walter et al., 2014), Lake Pavin (Busigny et al., 2014) and Lake Matano (Crowe et al., 2008, 2017), all characterized as meromictic lakes. Meromictic lakes do not mix completely and develop (usually) anoxic bottom water body (monimolimion) that is not mixed and thus creates stable geochemical gradients (Stewart et al., 2009). Of all the lakes only a few are characterized as meromictic and most of the lakes are holomictic and mix periodically. Dimictic lakes like Großes Heiliges Meer and Lake 227 and 442 near Kenora, Canada mix twice, once in spring and once in fall. During the summer stratification anoxic bottom water can be formed. Geochemical gradient of oxygen depletion and iron rich bottom layer have been observed in Großes Heiliges Meer and Lake 227 and 442 over several years developing to similar extend, two main conditions for phototrophic Fe(II)-oxidizer (Liu et al., 2022; Schiff et al., 2017; Swanner et al., 2022). Geochemical data from Großes Heiliges Meer from 2014, 2015 and 2018 are comparable to the observations in this study with oxygen depletion at 6 to 7m (Swanner et al., 2022). In addition to favourable geochemical measurement show combined results from sequencing microbial communities and isotopic signatures potential iron cycling in Lake 227 and 442. Implying also that the microbial community adapt rapidly after geochemical conditions are favourable. In Großes Heiliges Meer 16S rRNA amplicon sequencing data showed the abundance of potential iron oxidizing and reducing bacteria with up to 25% of the microbial community. The combination of the *in situ* experiment, the iron cycling experiments with in situ community and the enrichment culture could confirm that iron cycling takes part in Großes Heiliges Meer. Although iron cycling may not play an important role during winter stratification, spring and fall mixing time, it can play

an important part during summer stratification. Thereby expanding the known habitats where iron cycling plays an important role and highlights the ubiquity of iron cycling.

Key phototrophic Fe(II) oxidizer

Although all four different types of Fe(II)-oxidizer have been found in meromictic and dimictic lakes (Acidophilic, microaerophilic, nitrate-dependent and phototrophic Fe(II)-oxidizer) the focus and dominant specie was in all field sites Chlorobium, a green sulfur bacterium, associated with Fe(II) oxidation (Berg et al., 2016; Camacho et al., 2017; Lambrecht et al., 2021; Llirós et al., 2015; Schiff et al., 2017). So far only a few isolated photoferrotrophs are in culture from all stratified lakes. From Lake de la Cruz a *Chlorobium* dominated enrichment was acquired (Walter et al., 2014), from Lake Kivu the first pelagic strain *C. phaeoferrooxidans* KB01 isolated (Crowe et al., 2017) and a co-culture dominated by *Ca.*C. *masyuteum* was enriched from Brownie lake in Minesota (Lambrecht et al., 2021). Although the *in situ* community of potential photoferrotrophs was dominated by a *Chlorobium* with 12% in Großes Heiliges Meer, the phototrophic enrichment was enriched with a *Thiodictyon* (1% *in situ* community). This is the first time that an enrichment capable of Fe(II) oxidation was successful for a dimictic lake and that the dominant Fe(II)-oxidizer is a *Thiodictyon* (31% of enrichment) and not a *Chlorobium*. *Thiodictyon* is associated with FeS recycling and acetate assimilation (Berg et al., 2016; Kappler & Newman, 2004). FeS recycling was tested in a lab incubation of an *in situ* community from Lake Cadagno. FeS was added as sole electron donor and after 6 months the enrichment was dominated by morphologically bacteria similar to sulfur bacteria to Thiodictyon (Berg et al., 2016). Acetate could be potential assimilated by *Thiodictyon* in the setups with organics in the *in situ* experiment. After day 23 an increase of *Thiodictyon* could be observed in comparison to the *in situ* community in the setup where only organics were added. In Großes Heiliges Meer we could demonstrate that phototrophic Fe(II) oxidation was

performed by an phototrophic enrichment dominated by *Thiodictyon*. Nevertheless we can't rule out the participation of Chlorobium in iron cycling or its association with other cycles like the sulfur cycle (Thompson et al., 2017).

Iron cycling in Großes Heiliges Meer

From the sequencing data we could determine potential iron oxidizer and reducer at 7 m in Großes Heiliges Meer. While photoferrotrophs (*Chlorobium* and *Thiodictyon*) may play a crucial part in the Fe(II) oxidation, microaerophilic Fe(II)-oxidizer *Sideroxydans* could contribute to Fe(II) oxidation as well especially during night times. Fe(II) could also be oxidized abiotically by O_2 which could be produced by cyanobacteria (*Snowella* OTU37S04). On the Fe(III) reduction side four different potential Fe(III)-reducer were found. *Geobacter* can couple Fe(III) reduction with the oxidation of acetate (Caccavo et al., 1994; Lovley et al., 1993), whereas *Rhodoferax* and *Geothrix* can couple reduction of Fe(III) with the oxidation of lactate and acetate (Coates et al., 1999; Finneran et al., 2003; Risso et al., 2009). Another potential Fe(III)-reducer could be *Sulfurospirillum* which couples Fe(III) reduction to oxidation of sulfur (Canfield et al., 2005; Straub & Schink, 2004). From the geochemical data alone we can't draw conlusions which Fe(III)-reducer is active and to which extend. In the enrichment however we could measure that during Fe(III)-reduction Lactate was consumed (data not shown) and that *Rhodoferax* is active there.

With the combination of all three experiments we could prove iron cycling in Großes Heiliges Meer. During the *in situ* experiment we could observe no changes in Fe speciation and all measured iron was Fe(II). This could mean 2 explanations: I) there are no active bacteria present who can oxidize iron or II) all oxidized iron is immediately reduced again, therefore no change in Fe speciation could be measured. The latter would also align with the calculated rates from the enrichments where Fe(III) reduction rates were higher than Fe(II) oxidation rates (0.33 and

0.12 mM/d, respectively). In our experiment we could also demonstrate the influence of carbon on iron cycling. We could see that Fe(II) oxidation and Fe(III) reduction are stable in a day/night cycle with no added organics (Figure 5, Fe(II) only setup). When organics are added either Fe(II) oxidation is slowed down and/or Fe(III) is stimulated and becomes the dominating process (Figure 5). Once the organics are used up Fe(II) oxidation becomes the dominating process.

Another aspect we could investigate is how vulnerable the system can be to "man-made" substrates. *Sulfurospirillum* reached up to 45% of the bacterial community and was quite abundant in all setups with DCMU. DCMU is not a natural occurring source of carbon and nitrogen and shows how a bacterial community could shift and be dominated by one strain if conditions are favourable and, in this case, "man-made" substances enter a system. This drastic shift was not observed when we added Fe(II), acetate and lactate to the system, suggesting that these are substrates that play an active role in this system.

Conclusion

In this study we could show that dimictic lakes can be habitats where iron cycling is present and plays an important role and we were able to enrich an iron metabolising culture dominated by phototrophic Fe(II)-oxidizer *Thiodictyon*. This is the first time for a dimictic lake that iron cycling could be simulated from *in situ* community and an enrichment culture could be obtained. We could also demonstrate the role of organics in the iron cycle.

Acknowledgement

The study was supported by Deutsche Forschungsgemeinschaft (DFG, German Research Foundation; BR 5927/2-1 and BY 82/4-1) awarded to C. Bryce and J. Byrne. James M. Byrne is supported by a UKRI Future Leaders Fellowship, MR/V023918/1. We would like to thank Heinrich Terlutter and Andreas Kronshage from the field station for providing field instruments and laboratory usage.

References

Berg, J. S., Michellod, D., Pjevac, P., Martinez-Perez, C., Buckner, C. R. T., Hach, P. F., Schubert, C. J., Milucka, J., & Kuypers, M. M. M. (2016). Intensive cryptic microbial iron cycling in the low iron water column of the meromictic Lake Cadagno. *Environmental Microbiology*, *18*(12), 5288–5302. https://doi.org/10.1111/1462-2920.13587

Bolyen, E., Rideout, J. R., Dillon, M. R., Bokulich, N. A., Abnet, C. C., Al-Ghalith, G. A., Alexander, H., Alm, E. J., Arumugam, M., Asnicar, F., Bai, Y., Bisanz, J. E., Bittinger, K., Brejnrod, A., Brislawn, C. J., Brown, C. T., Callahan, B. J., Caraballo-Rodríguez, A. M., Chase, J., … Caporaso, J. G. (2019). Reproducible, interactive, scalable and extensible microbiome data science using QIIME 2. *Nature Biotechnology*, *37*(8), 852–857. https://doi.org/10.1038/s41587-019-0209-9

Bryce, C., Blackwell, N., Schmidt, C., Otte, J., Huang, Y. M., Kleindienst, S., Tomaszewski, E., Schad, M., Warter, V., Peng, C., Byrne, J. M., & Kappler, A. (2018). Microbial anaerobic Fe(II) oxidation – Ecology, mechanisms and environmental implications. *Environmental Microbiology*, *20*(10), 3462–3483. https://doi.org/10.1111/1462-2920.14328

Busigny, V., Planavsky, N. J., Jézéquel, D., Crowe, S., Louvat, P., Moureau, J., Viollier, E., & Lyons, T. W. (2014). Iron isotopes in an Archean ocean analogue. *Geochimica et Cosmochimica Acta*, *133*, 443–462. https://doi.org/10.1016/j.gca.2014.03.004

Caccavo, F., Lonergan, D. J., Lovley, D. R., Davis, M., Stolz, J. F., & Mcinerneyl, M. J. (1994). Oxidizing dissimilatory metal-reducing microorganism. *Applied and Environmental Microbiology*, *60*(10), 3752–3759.

Callahan, B. J., Mcmurdie, P. J., Rosen, M. J., Han, A. W., Johnson, A. J. A., & Holmes, S. P. (2016). *dada2: high-resolution sample inference from illumina amplicon data*. *13*(7). https://doi.org/10.1038/nMeth.3869

Camacho, A., Walter, X. A., Picazo, A., & Zopfi, J. (2017). Photoferrotrophy: Remains of an ancient photosynthesis in modern environments. *Frontiers in Microbiology*, *8*(MAR). https://doi.org/10.3389/fmicb.2017.00323

Canfield, D. E. (1989). Reactive iron in marine sediments. *Geochimica et Cosmochimica Acta*, *53*(3), 619–632. https://doi.org/10.1016/0016-7037(89)90005-7

Canfield, D., Kristensen, E., & Thamdrup, B. (2005). *Aquatic geomicrobiology*. https://books.google.de/books?hl=en&lr=&id=4m3byX7BHJEC&oi=fnd&pg=PR11&dq=Canfield,+D.+E.,+Kristensen,+E.,+and+Thamdrup,+B.+(2005).+Aquatic+geomicrobiology.+Gulf+Professional+Publishing.&ots=w_pH_2Q39X&sig=sxBOTVDi8ZoKBlclLjsQh0wCLi8

Caporaso, J. G., Lauber, C. L., Walters, W. A., Berg-Lyons, D., Lozupone, C. A., Turnbaugh, P. J., Fierer, N., & Knight, R. (2011). Global patterns of 16S rRNA diversity at a depth of millions of sequences per sample. *Proceedings of the National Academy of Sciences of the United States of America*, *108*(SUPPL. 1), 4516–4522. https://doi.org/10.1073/pnas.1000080107

Coates, J. D., Ellis, D. J., Gaw, C. V., & Lovley, D. R. (1999). Geothrix fermentans gen. nov., sp. nov., a novel Fe(III)-reducing bacterium from a hydrocarbon-contaminated aquifer. *International Journal of Systematic Bacteriology*, *49*(4), 1615–1622. https://doi.org/10.1099/00207713-49-4-1615/CITE/REFWORKS

Croal, L. R., Johnson, C. M., Beard, B. L., & Newman, D. K. (2004). Iron isotope fractionation by Fe(II)-oxidizing photoautotrophic bacteria. *Geochimica et Cosmochimica Acta*, *68*(6), 1227–1242. https://doi.org/10.1016/j.gca.2003.09.011

Crowe, S. A., Hahn, A. S., Morgan-Lang, C., Thompson, K. J., Simister, R. L., Llirós, M., Hirst, M., & Hallam, S. J. (2017). Draft Genome Sequence of the Pelagic Photoferrotroph Chlorobium phaeoferrooxidans. *Genome Announcements*, *5*(13).

https://doi.org/10.1128/GENOMEA.01584-16
Crowe, S. A., Jones, C. A., Katsev, S., Magen, C., O'Neill, A. H., Sturm, A., Canfield, D. E., Haffner, G. D., Mucci, A., Sundby, B., & Fowle, D. A. (2008). Photoferrotrophs thrive in an Archean Ocean analogue. *Proceedings of the National Academy of Sciences of the United States of America*, *105*(41), 15938–15943. https://doi.org/10.1073/pnas.0805313105
Di Tommaso, P., Chatzou, M., Floden, E. W., Barja, P. P., Palumbo, E., & Notredame, C. (2017). Nextflow enables reproducible computational workflows. *Nature Biotechnology*, *35*(4), 316–319. https://doi.org/10.1038/nbt.3820
Ehrenreich, A., & Widdel, F. (1994). Anaerobic oxidation of ferrous iron by purple bacteria, a new type of phototrophic metabolism. *Applied and Environmental Microbiology*, *60*(12), 4517–4526. https://doi.org/10.1128/aem.60.12.4517-4526.1994
Eickhoff, M., Obst, M., Schröder, C., Hitchcock, A. P., Tyliszczak, T., Martinez, R. E., Robbins, L. J., Konhauser, K. O., & Kappler, A. (2014). Nickel partitioning in biogenic and abiogenic ferrihydrite: The influence of silica and implications for ancient environments. *Geochimica et Cosmochimica Acta*, *140*, 65–79. https://doi.org/10.1016/j.gca.2014.05.021
Ewels, P. A., Peltzer, A., Fillinger, S., Patel, H., Alneberg, J., Wilm, A., Garcia, M. U., Di Tommaso, P., & Nahnsen, S. (2020). The nf-core framework for community-curated bioinformatics pipelines. *Nature Biotechnology*, *38*(3), 276–278. https://doi.org/10.1038/s41587-020-0439-x
Finneran, K. T., Johnsen, C. V., & Lovley, D. R. (2003). Rhodoferax ferrireducens sp. nov., a psychrotolerant, facultatively anaerobic bacterium that oxidizes acetate with the reduction of Fe(III). *International Journal of Systematic and Evolutionary Microbiology*, *53*(3), 669–673. https://doi.org/10.1099/ijs.0.02298-0
Hegler, F., Posth, N. R., Jiang, J., & Kappler, A. (2008). *Physiology of phototrophic iron (II) -oxidizing bacteria : implications for modern and ancient environments*. *66*(Ii), 250–260. https://doi.org/10.1111/j.1574-6941.2008.00592.x
Heising, S., Richter, L., Ludwig, W., & Schink, B. (1999). Chlorobium ferrooxidans sp. nov., a phototrophic green sulfur bacterium that oxidizes ferrous iron in coculture with a "Geospirillum" sp. strain. *Archives of Microbiology*, *172*(2), 116–124. https://doi.org/10.1007/s002030050748
Kappler, A., Schink, B., & Newman, D. K. (2005). Fe(III) mineral formation and cell encrustation by the nitrate-dependent Fe(II)-oxidizer strain BoFeN1. *Geobiology*, *3*(4), 235–245. https://doi.org/10.1111/J.1472-4669.2006.00056.X
Kappler, A, & Newman, D. K. (2004). Formation of Fe(III)-minerals by Fe(II)-oxidizing photoautotrophic bacteria. *Geochimica et Cosmochimica Acta*, *68*(6), 1217–1226. https://doi.org/10.1016/J.GCA.2003.09.006
Kappler, Andreas, Bryce, C., Mansor, M., Lueder, U., Byrne, J. M., & Swanner, E. D. (2021). An evolving view on biogeochemical cycling of iron. *Nature Reviews Microbiology*, *19*(6), 360–374. https://doi.org/10.1038/s41579-020-00502-7
Kucera, S., & Wolfe, R. S. (1957). a Selective Enrichment Method for Gallionella Ferruginea . *Journal of Bacteriology*, *74*(3), 344–349. https://doi.org/10.1128/jb.74.3.344-349.1957
Kurtzer, G. M., Sochat, V., & Bauer, M. W. (n.d.). *Singularity: Scientific containers for mobility of compute*. https://doi.org/10.1371/journal.pone.0177459
Lambrecht, N., Stevenson, Z., Sheik, C. S., Pronschinske, M. A., Tong, H., & Swanner, E. D. (2021). "Candidatus Chlorobium masyuteum," a Novel Photoferrotrophic Green Sulfur Bacterium Enriched From a Ferruginous Meromictic Lake. *Frontiers in Microbiology*, *12*(July), 1–17. https://doi.org/10.3389/fmicb.2021.695260
Laufer, K., Niemeyer, A., Nikeleit, V., Halama, M., Byrne, J. M., & Kappler, A. (2017).

Physiological characterization of a halotolerant anoxygenic phototrophic Fe(II)-oxidizing green-sulfur bacterium isolated from a marine sediment. *FEMS Microbiology Ecology*, *93*(5), 1–13. https://doi.org/10.1093/femsec/fix054

Liu, K., Schiff, S. L., Wu, L., Molot, L. A., Venkiteswaran, J. J., Paterson, M. J., Elgood, R. J., Tsuji, J. M., & Neufeld, J. D. (2022). Large Fractionation in Iron Isotopes Implicates Metabolic Pathways for Iron Cycling in Boreal Shield Lakes. *Environmental Science and Technology*, *56*(20), 14840–14851. https://doi.org/10.1021/acs.est.2c04247

Llirós, M., Garciá-Armisen, T., Darchambeau, F., Morana, C., Triadó-Margarit, X., Inceoılu, Ö., Borrego, C. M., Bouillon, S., Servais, P., Borges, A. V., Descy, J. P., Canfield, D. E., & Crowe, S. A. (2015). Pelagic photoferrotrophy and iron cycling in a modern ferruginous basin. *Scientific Reports 2015 5:1*, *5*(1), 1–8. https://doi.org/10.1038/srep13803

Lovley, D. R., Giovannoni, S. J., White, D. C., Champine, J. E., Phillips, E. J. P., Gorby, Y. A., & Goodwin, S. (1993). Geobacter metallireducens gen. nov. sp. nov., a microorganism capable of coupling the complete oxidation of organic compounds to the reduction of iron and other metals. *Archives of Microbiology*, *159*(4), 336–344. https://doi.org/10.1007/BF00290916

Lovley, D. R., & Phillips, E. J. P. (1987). Competitive Mechanisms for Inhibition of Sulfate Reduction and Methane Production in the Zone of Ferric Iron Reduction in Sediments. *Applied and Environmental Microbiology*, *53*(11), 2636–2641. https://doi.org/10.1128/AEM.53.11.2636-2641.1987/FORMAT/EPUB

Maisch, M., Lueder, U., Laufer, K., Scholze, C., Kappler, A., & Schmidt, C. (2019). Contribution of Microaerophilic Iron(II)-Oxidizers to Iron(III) Mineral Formation. *Environmental Science and Technology*, *53*(14), 8197–8204. https://doi.org/10.1021/acs.est.9b01531

Martin, M. (2011). Cutadapt removes adapter sequences from high-throughput sequencing reads. *EMBnet.Journal*, *17*(1), 10–12. https://journal.embnet.org/index.php/embnetjournal/article/view/200/479

Mu, C. C., Zhang, T. J., Zhao, Q., Guo, H., Zhong, W., Su, H., & Wu, Q. B. (2016). Soil organic carbon stabilization by iron in permafrost regions of the Qinghai-Tibet Plateau. *Geophysical Research Letters*, *43*(19), 10,286-10,294. https://doi.org/10.1002/2016GL070071

Myers, C. R., & Nealson, K. H. (1990). Respiration-linked proton translocation coupled to anaerobic reduction of manganese(IV) and iron(III) in Shewanella putrefaciens MR-1. *Journal of Bacteriology*, *172*(11), 6232–6238. https://doi.org/10.1128/JB.172.11.6232-6238.1990

Otte, J. M., Harter, J., Laufer, K., Blackwell, N., Straub, D., Kappler, A., & Kleindienst, S. (2018). The distribution of active iron-cycling bacteria in marine and freshwater sediments is decoupled from geochemical gradients. *Environmental Microbiology*, *20*(7), 2483–2499. https://doi.org/10.1111/1462-2920.14260

Pott, R. (2009). Vegetationsdynamik an einem natürlichen See, dem Großen Heiligen Meer, in Nordwestdeutschland. *Drosera*, 17–44.

Quast, C., Pruesse, E., Yilmaz, P., Gerken, J., Schweer, T., Yarza, P., Rg Peplies, J., & Glö Ckner, F. O. (2012). The SILVA ribosomal RNA gene database project: improved data processing and web-based tools. *Nucleic Acids Research*. https://doi.org/10.1093/nar/gks1219

Risso, C., Sun, J., Zhuang, K., Mahadevan, R., DeBoy, R., Ismail, W., Shrivastava, S., Huot, H., Kothari, S., Daugherty, S., Bui, O., Schilling, C. H., Lovley, D. R., & Methé, B. A. (2009). Genome-scale comparison and constraint-based metabolic reconstruction of the facultative anaerobic Fe(III)-reducer Rhodoferax ferrireducens. *BMC Genomics*, *10*, 447. https://doi.org/10.1186/1471-2164-10-447

Schiff, S. L., Tsuji, J. M., Wu, L., Venkiteswaran, J. J., Molot, L. A., Elgood, R. J., Paterson, M. J., & Neufeld, J. D. (2017). Millions of boreal shield lakes can be used to probe archaean ocean biogeochemistry. *Scientific Reports*, *7*, 1–11. https://doi.org/10.1038/srep46708

Stewart, K. M., Walker, K. F., & Likens, G. E. (2009). Meromictic Lakes. *Encyclopedia of Inland Waters*, 589–602. https://doi.org/10.1016/B978-012370626-3.00027-2

Straub, D., Blackwell, N., Langarica-Fuentes, A., Peltzer, A., Nahnsen, S., & Kleindienst, S. (2020). Interpretations of Environmental Microbial Community Studies Are Biased by the Selected 16S rRNA (Gene) Amplicon Sequencing Pipeline. *Frontiers in Microbiology*, *11*. https://doi.org/10.3389/fmicb.2020.550420

Straub, K. L., & Schink, B. (2004). Ferrihydrite-dependent growth of Sulfurospirillum deleyianum through electron transfer via sulfur cycling. *Applied and Environmental Microbiology*, *70*(10), 5744–5749. https://doi.org/10.1128/AEM.70.10.5744-5749.2004

Swanner, E. D., Wüstner, M., Leung, T., Pust, J., Fatka, M., Lambrecht, N., Chmiel, H. E., & Strauss, H. (2022). Seasonal phytoplankton and geochemical shifts in the subsurface chlorophyll maximum layer of a dimictic ferruginous lake. *MicrobiologyOpen*, *11*(3). https://doi.org/10.1002/mbo3.1287

Thompson, K. J., Simister, R. L., Hahn, A. S., Sj, H., & Crowe, S. A. (2017). Nutrient Acquisition and the Metabolic Potential of Photoferrotrophic Chlorobi. *Nutrient Acquisition and the Metabolic Potential of Photoferrotrophic Chlorobi. Front. Microbiol*, *8*, 1212. https://doi.org/10.3389/fmicb.2017.01212

Tipping, E. (1981). The adsorption of aquatic humic substances by iron oxides. *Geochimica et Cosmochimica Acta*, *45*(2), 191–199. https://doi.org/10.1016/0016-7037(81)90162-9

Tsuji, J. M., Tran, N., Schiff, S. L., Venkiteswaran, J. J., Molot, L. A., Tank, M., Hanada, S., & Neufeld, J. D. (2020). Anoxygenic photosynthesis and iron–sulfur metabolic potential of Chlorobia populations from seasonally anoxic Boreal Shield lakes. *The ISME Journal 2020 14:11*, *14*(11), 2732–2747. https://doi.org/10.1038/s41396-020-0725-0

Walter, X. A., Picazo, A., Miracle, M. R., Vicente, E., Camacho, A., Aragno, M., & Zopfi, J. (2014). Phototrophic Fe(II)-oxidation in the chemocline of a ferruginous meromictic lake. *Frontiers in Microbiology*, *5*(DEC), 1–9. https://doi.org/10.3389/fmicb.2014.00713

5 Chapter: Phototrophic Fe(II) oxidation benefits from light/dark cycles

Contributions:

Resources were provided by Dr. C. Bryce, Assoc and Prof. Dr. A. Kappler. The project was designed by me with input of Dr. C. Bryce and conducted by L. Roth under my supervision. M. Maisch performed Mössbauer and SEM analysis. The manuscript was written by me with guidance of Dr. C. Bryce and input of all co-authors.

Phototrophic Fe(II) oxidation benefits from light/dark cycles

Verena Nikeleit[1], Linda Roth[1], Markus Maisch[1], Andreas Kappler[1,2] and Casey Bryce[3*]

[1]Department of Geosciences, University of Tübingen, Tübingen, Germany

[2]Cluster of Excellence: EXC 2124: Controlling Microbes to Fight Infections, Tübingen, Germany

[3]School of Earth Sciences, University of Bristol, Bristol, UK

*Corresponding Author: Casey Bryce

School of Earth Science, Wills Memorial Building, University of Bristol, Queens Road, Bristol, BS8 1RJ, UK.

Published in Environmental Microbiology Reports

Abstract

Phototrophic Fe(II)-oxidizers use Fe(II) as an electron donor for CO_2 fixation thus linking Fe(II) oxidation, ATP formation and growth directly to the availability of sunlight. We compared the effect of short (10 h light/14 h dark) and long (2-3 days light/2-3 days dark) light/dark cycles to constant light conditions for the phototrophic Fe(II)-oxidizer *Chlorobium ferrooxidans* KoFox. Fe(II) oxidation was completed first in the setup with constant light (9 mM Fe(II) oxidized within 8.9 days) compared to the light/dark cycles but both short and long light/dark cycles showed faster maximum Fe(II) oxidation rates. In the short and long light/dark cycles, Fe(II) oxidation rates reached 3.5±1.0 and 2.6±0.3 mM/d, respectively, compared to 2.1±0.3 mM/d in the constant light setup. Maximum Fe(II) oxidation were significantly faster in the short cycle compared to constant light setup. Cell growth reached roughly equivalent cell numbers across all three light conditions (from 0.2-2.0 x 10^6 cells/ml to 1.1-1.4 x 10^8 cells/ml) and took place in both the light and dark phases of incubation. SEM images showed different mineral structures independent of the light setup and ^{57}Fe Mössbauer spectroscopy confirmed the formation of poorly crystalline Fe(III) oxyhydroxides (such as ferrihydrite) in all three setups. Our results suggest that periods of darkness have a significant impact on phototrophic Fe(II)-oxidizers and significantly influence rates of Fe(II) oxidation.

Introduction

Iron is ubiquitous in the environment and influences most other major nutrient cycles: acting as a source or sink for heavy metals, carbon, nutrients and/or toxins during mineral formation and dissolution (Eickhoff et al., 2014; Kappler et al., 2021; Mu et al., 2016; Tipping, 1981). One kind of bacteria who can facilitate Fe(II) oxidation are anoxygenic phototrophic Fe(II)-oxidizers (photoferrotrophs) like *Chlorobium ferrooxidans* KoFox (Heising et al., 1999; Widdel et al., 1993). These anoxygenic phototrophs produce ATP via the light reaction with visible light and generate NADPH to be used in the dark reaction to fix CO_2 and build biomass. The latter can occur during both light and dark periods. To generate NADPH, different electron donors like organics (acetate and glucose) and other inorganic substrates like H_2, H_2S^- or thiosulfate can be used by photoferrotrophs as alternatives to Fe(II) (Croal et al., 2009; Melton et al., 2014). For Fe(II) oxidation, photoferrotrophs can use dissolved Fe(II), i.e. Fe^{2+}_{aq}, or some poorly crystalline Fe(II) minerals like siderite, FeS and Fe(II)/Fe(III) mixed minerals like green rust and magnetite (Byrne et al., 2015; Han et al., 2020; Kappler & Newman, 2004).

The process of Fe(III) mineral formation by photoferrotrophic bacteria is complex and a combination of thermodynamic, kinetic and biochemical factors control the final mineral products (Bryce et al., 2018; Kappler et al., 2021). Another important parameter that affects the activity of photoferrotrophs is light. Previous studies have investigated the importance of different light intensities and wavelengths for photoferrotrophic growth and mineral formation (Hegler et al., 2008; Schmidt et al., 2021). However, in all of these studies so far, light exposure duration was always kept constant during the incubation. Cultures were either exposed continuously to light or kept in the dark serving as a control. To represent environmentally-relevant conditions, the impact of diurnal or changing illumination conditions needs to be considered in laboratory studies. Therefore, the present study aims to understand how different light/dark cycles that simulate the natural day/night cycle influence Fe(II) oxidation, Fe(III) mineral formation and growth of photoferrotrophs.

Material and Methods

Experimental design. *C. ferrooxidans* KoFox was used as a photoferrotrophic model strain and grown anoxically in serum vials with a 90:10 N_2/CO_2 headspace according to Heising et al. (1999) and Widdel et al. (1993). Three different light/dark setups were tested: constant light (CL, permanent illumination), long light/dark cycle (LC, alternating every 2-3 days) and short light/dark cycle (SC, 10 h light and 14 h dark). Serum bottles were placed at random in an incubator and incubated at 20°C. A 46W (2700K) light bulb with a wavelength range of 400-1000 nm was used as a light source, with an intensity of 20 to 23 µmol/sm^2 photons. All setups were performed in biotic triplicates with one abiotic control. Slurry samples were taken in an anoxic glovebox for quantification of Fe and cells. Samples for mineral analyses were collected at the end of the experiment.

Ferrozine Assay. Fe(II) and Fe(total) were quantified spectrophotometrically with the ferrozine assay after Hegler et al. (2008). During sampling, 0.1 mL of slurry sample was added to 0.9 mL 1 M HCl and the samples were stored at 4°C until quantification. The ferrozine-Fe(II) complex was quantified at 562 nm using a spectrometer (Thermo Scientific Multiscan, Thermo Fisher Scientific). Measurements were conducted in triplicates.

Cell quantification via flow cytometry. For flow cytometry, 180 µL of samples were fixed with 20 µL formaldehyde solution (CH_2O). Minerals were dissolved by adding 200 µL of sterile, anoxic 100 mM Fe(II) ethylenediammonium sulfate tetrahydrate (Fe-EDAS, $FeSO_4$ $*C_2H_8N_2H_2SO_4*4H_2O$) and 600 µL oxalate solution (0.23 M $(NH_4)_2C_2O_4*H_2O$ and 0.17 M $C_2H_2O_4$, pH 7). After 10 minutes, samples were transferred in a 96 well plate for cell quantification using a flow cytometer equipped with an emission filter 585/15 nm (Attune Nxt flow cytometer, Thermo Fisher Scientific). Phototrophic cells were distinguished from noise or debris by gating based on their properties in the side scatter and YL 4 channel due the

autofluorescence from the cells (with emission filter 585/15 nm). Additionally, cells were also stained with a BacLight Green stain (Thermo Fisher Scientific, 1µl stain/1 ml sample) and measured with BL laser (with emission filter 530/30 nm). The cell numbers obtained were the same as when using autofluorescence (Figure S1). The total number of events which show yellow fluorescence in the side scatter region associated with cells was divided by the total volume of sample to give a final cell concentration in cells per millilitre. All measurements were conducted in triplicates and the results reported as an average.

Mössbauer spectroscopy. Slurry samples were passed through a filter (ø13 mm; 0.45 µm, nitrocellulose, Merck) which was then sealed between two pieces of airtight Kapton tape and kept frozen anoxically at -20°C until measurement. The sample was transferred to the instrument and only removed from the freezer prior to loading the samples inside the closed-cycle exchange gas cryostat (Janis cryogenics). Absorption spectra were collected at 77 K and at 5 K with a constant acceleration drive system (WissEL) in transmission mode with a ^{57}Co/Rh source which was calibrated against a 7 µm thick α-^{57}Fe foil measured at room temperature. All spectra were analyzed using Recoil (University of Ottawa) by applying a Voight Based Fitting (VBF) site analysis. The half width at half maximum (HWHM) was fixed to a value of 0.124 mm/s for all sample analyses.

SEM. Minerals were the main focus of this measurement and therefore cells were destroyed in the process. First, the slurry samples were washed to remove salts from the media. The sample was centrifuged at 20000 rcf for 5min, then the supernatant was removed, filled with MilliQ again and repeated a total pf three times. MilliQ was then added to suspend the minerals. Roughly 100 µL washed sample was transferred onto a carbon-coated sticker and left to dry at room temperature. Samples were placed on aluminum stubs and sputter-coated at a working

distance of 35 mm at 20 mA for 70 sec to receive a 13 nm coating (BAL-TEC SCD 005). Microscopy was conducted with a ZEISS FIB Crossbeam 550L using an electron high tension of 2 kV, working distance of 1.5 mm and a secondary electron secondary ion (SESI) detector.

Statistical analysis. Welsh t-test was performed to calculate statistically significant differences between different setups with a threshold of $\alpha=0.05$ for unequal variances.

Results and discussion

Effect of light/dark cycles on photoferrotrophic growth

The influence of light/dark cycles on Fe(II) oxidation was assessed by monitoring Fe(II) and cell numbers. All Fe(II) (9 mM) was completely (98%) oxidized and cell numbers reached a plateau at the end of the incubations in all setups. Differences in the duration of Fe(II) oxidation and Fe(II) oxidation rates were observed in the different setups. In the constant light setup, Fe(II) oxidation started immediately and was completed after 8.9 days. Cell numbers increased from 8.7±0.2 x 10^5 cells/mL to 8.2±2.8 x 10^7 cells/mL at the end of Fe(II) oxidation, and increased further even after all Fe(II) was oxidized to 1.3±0.1 x 10^8 cells/mL at 15.9 days (Figure 1). In the long light/dark cycle where light/dark conditions were switched every 2-3 days, no lag phase in Fe(II) oxidation was observed and Fe(II) was almost completely oxidized (98%) after 15.9 days. During dark cycles, no Fe(II) oxidation was observed, i.e. during the periods of 2.0-3.9 days, 6.9-8.9 days and 10.9-13.9 days. For cell numbers, no clear effect between light and dark conditions were observed and a steady cell number increase was observed until cells reached a constant number after 20.9 days (from 1.6 x 10^6±0.1 x 10^3 cells/mL to 1.1±0.04 x 10^8 cells/mL).

In the short light/dark cycle setup (10 h light/14 h dark), the timing of Fe(II) oxidation varied in the triplicates to some extent. Different Fe(II) oxidation lag phases were observed ranging from 3.9 to 7.3 days while Fe(II) oxidation in these setups was completed in 20.9 days (98%). The lag phase was also observed in cell numbers which started to increase after 3.9 days along with the start of Fe(II) oxidation and increased steadily until reaching a constant number at the end of the experiment after 20.9 days (1.4±0.5 x 10^8 cells/mL). In these setups, Fe(II) oxidation also halted during the dark phases, i.e., during the periods of 3.3-3.9 days, 8.3-8.9 days, 10.3-10.9 days and 14.3-14.9 days (Figure 1).

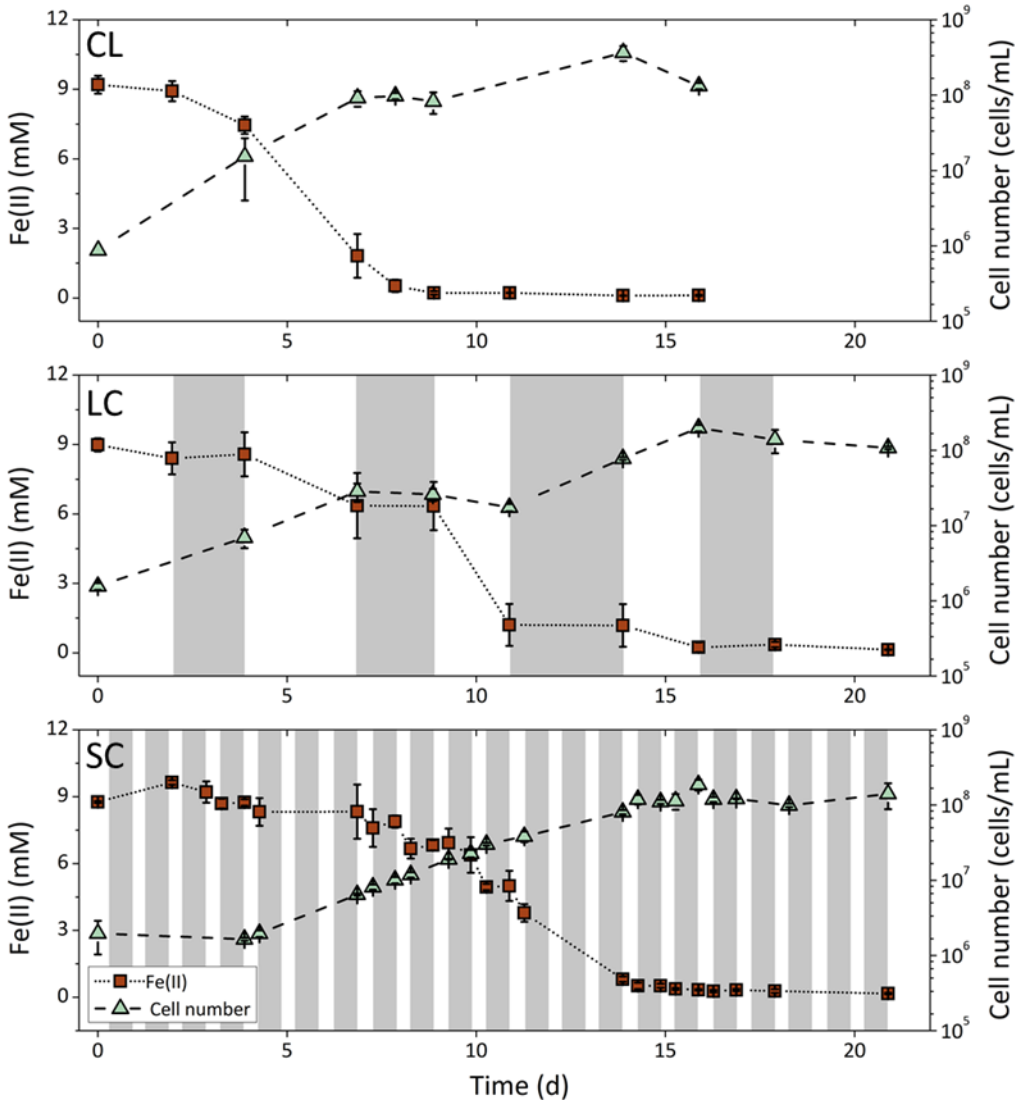

Figure 1: Figures show Fe(II) and cell numbers (averages of triplicates) of C. ferrooxidans KoFox grown in three different light conditions: Constant light (CL), long light/dark cycle (LC, alternating every 2-3 days) short light/dark cycle (SC, 10 h light and 14 h dark). Dark periods are coloured grey.

It also appears that in the beginning the duration of light exposure is responsible for the lag phase in the short light/dark cycle. In the case of the continuous and long light/dark setup no lag phase in Fe(II) oxidation and cell growth could be observed. Whereas we could see a lag phase in the short light/dark setup between 3.9 to 7.3 days. The lag phase could be attributed to the short duration of the light period for the phototrophic bacteria to produce enough ATP and oxidized Fe(II) for cell growth. This could suggest that in the beginning of cell growth it would be beneficial for the cultures to be exposed for longer time periods in the light.

Effect of light/dark cycles on Fe(II) oxidation rates

For the setup with constant light, maximum Fe(II) oxidation rates were calculated between the two fastest time points for each microcosm individually and averaged among all replicates (3.9-6.9 days)., Maximum Fe(II) oxidation rates for the long light/dark cycle were calculated from the light phases that showed the fastest Fe(II) oxidation rate for each bottle and averaged (8.9-10.9 days). In the last setup (short light/dark cycle) the maximum rates from two light phases for each bottle were selected thus, in this case, mean rates are derived from six values (values for triplicate A and B were calculated from rates between 9.9-10.3 days and 10.9-11.3 days whereas triplicate C's rates were calculated from the period 3.9-4.3 days and 10.9-11.3 days). An alternative calculation method for the short light/dark cycle resulted in similar results and can be found in Figure S2. Here Fe(II) concentrations from 9.8 d to 13.3 d were taken and divided by the time the sample was in the light. No changes in Fe(II) concentrations were observed in the abiotic bottles under all conditions (data not shown). The lowest maximum Fe(II) oxidation rates occurred in the constant light setups with a rate of 2.1±0.3 mM/d. For the long light/dark cycle the maximum Fe(II) oxidation rate in the light was 2.6±0.3 mM/d and the highest rate in the short light/dark setup was 3.5±1.0 mM/d (Figure 2). A clear trend to higher Fe(II) oxidation rates with light/dark cycles was observed and in the case of the short light/dark cycle Fe(II) rates were significantly higher than in the constant light setup (t -3.35, df 6.21, p-value 0.015). The Fe(II) oxidation rates of *C. ferrooxidans* KoFox in the constant light setup were in the range of values from previous studies conducted under similar conditions (0.6–2.4 mM/d; continuously illuminated; Gauger et al., 2016; Hegler et al., 2008).

We also calculated maximum Fe(II) oxidation rates per cell by using the Fe(II) oxidation rates and cell numbers. Cell numbers were calculated for the appropriate time interval referring to each Fe(II) oxidation rate. For Fe(II) oxidation rates per cell, similar trends were observed. The continuously illuminated setup showed lowest oxidation rates (0.06±0.03 µM/(cell*d)),

followed by the long light/dark cycle setup (0.12±0.03 µM/(cell*d)) and highest rates in the short light/dark cycle setup (3.27±3.83 µM/(cell*d)). In the setups with the short light/dark cycles, the rates per cell varied considerably. The lowest Fe(II) oxidation rates per cell measured in these set ups where comparable to the continuous and long light/dark cycle setup but at 3 periods the Fe(II) oxidation rates/cell reached values up to 8.99 µM/(cell*d) which is 150 times higher than in the continuous light setup.

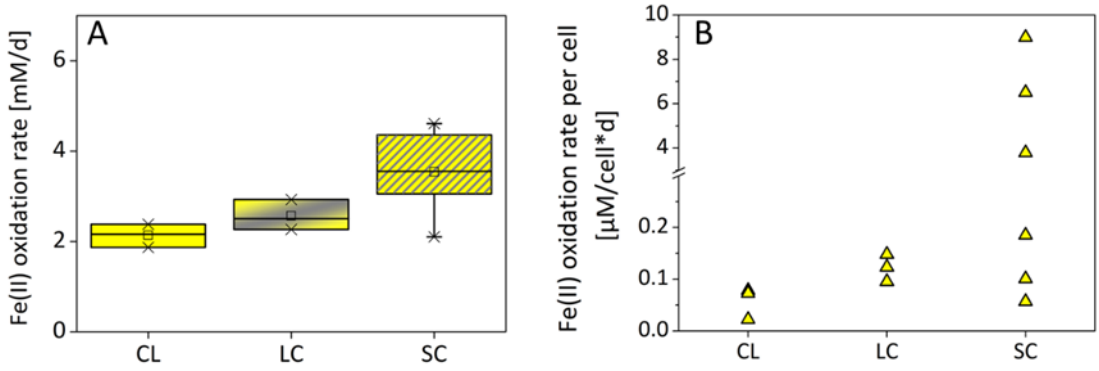

Figure 2: Panel A shows maximum Fe(II) oxidation rates of C. ferrooxidans KoFox for constant light (CL), long cycle (LC) and short cycle (SC) setup. Rates were calculated from triplicates for CL and LC, for SC 6 rates were chosen. Welsh t-test showed significant differences between the constant light and the short cycle (t -3.35, df 6.21, p-value 0.015). Panel B shows the maximum Fe(II) oxidation rate per cell. Time points chosen were the same as in Panel A.

Advantages of a light/dark lifestyle

These results indicate that a light/dark lifestyle is beneficial for phototrophic Fe(II)-oxidizer in terms of increasing the maximum Fe(II) oxidation rates. A trait that remained despite years of continuous cultivation under light conditions in the laboratory. In previous studies the effect of light/dark cycles on non-Fe(II)-oxidizing anoxygenic phototrophs were investigated and beneficial effects on biomass, protein and coenzyme Q10 production were found (Hauruseu & Koblízek, 2012; Zhi et al., 2019). For *C. ferrooxidans* KoFox, no increase for biomass production (cell growth) but increase in maximum Fe(II) oxidation rates were found with light/dark cycles.

The fact that the final cell numbers were similar in all setups can be linked to the experimental setup in the closed system. In each setup the same amount of Fe(II) was present and oxidized (~98% of 9 mM). Given that the electrons from Fe(II) oxidation are directly coupled to CO_2 fixation this has to lead to the same amount of biomass, independent of oxidation rates (of course variations in amounts of EPS, cellular proteins, carbohydrates, lipids or pigments are possible). Interestingly, cell growth not only took place during the light periods but continued in the dark, suggesting that the cells used the ATP and NADPH produced in the light during dark periods to fix CO_2.

One disadvantage of continuous light conditions could be that there is too much light which could lead to photodamage. If too much photons are absorbed and not used in the dark reaction, which is slower than the light reaction, reactive oxygen species can be created and damage bacteriochlorophylls and proteins (Wydrzynski et al., 2011). One way to reduce this is by quenching chlorosomes , FMO (Fenna–Matthews–Olson) antenna protein, quenching of carotenoids with chlorophyll and carotenoids can also scavenge singlet oxygen directly (Blankenship et al., 1993; Blankenship & Matsuura, 2003; Foote, 1968; Renger & Wolff, 1977; Tsukatani et al., 2010; Wen et al., 2010). This could have occurred here with *C. ferrooxidans* KoFox and thus more energy would have been needed to produce the additional proteins/pigments and slowed down the maximum Fe(II) oxidation rates. *C. ferrooxidans* KoFox may use dark phases to utilise excessive photons, repair photodamage and produce pigments needed for photosynthesis.

Mineral identity and surface morphology

Identification of the minerals by ^{57}Fe Mössbauer spectroscopy showed no difference between the minerals formed during Fe(II) oxidation in the different light illumination setups (Figure 3, S3, Table S1). The dominant iron mineral phase in all analysis was a short-range ordered Fe(III)

mineral, such as the Fe(III) oxyhydroxide ferrihydrite (approx. 50%), and an alternative Fe(III) phase (potentially poorly crystalline lepidocrocite) identified at 77 K (approx. 50%). Measurements at 5 K suggested very low particle size and/or low crystallinity. The formation of poorly crystalline Fe(III)-phases such as ferrihydrite has been shown in previous studies with *C. ferrooxidans* KoFox (Kappler & Newman, 2004).

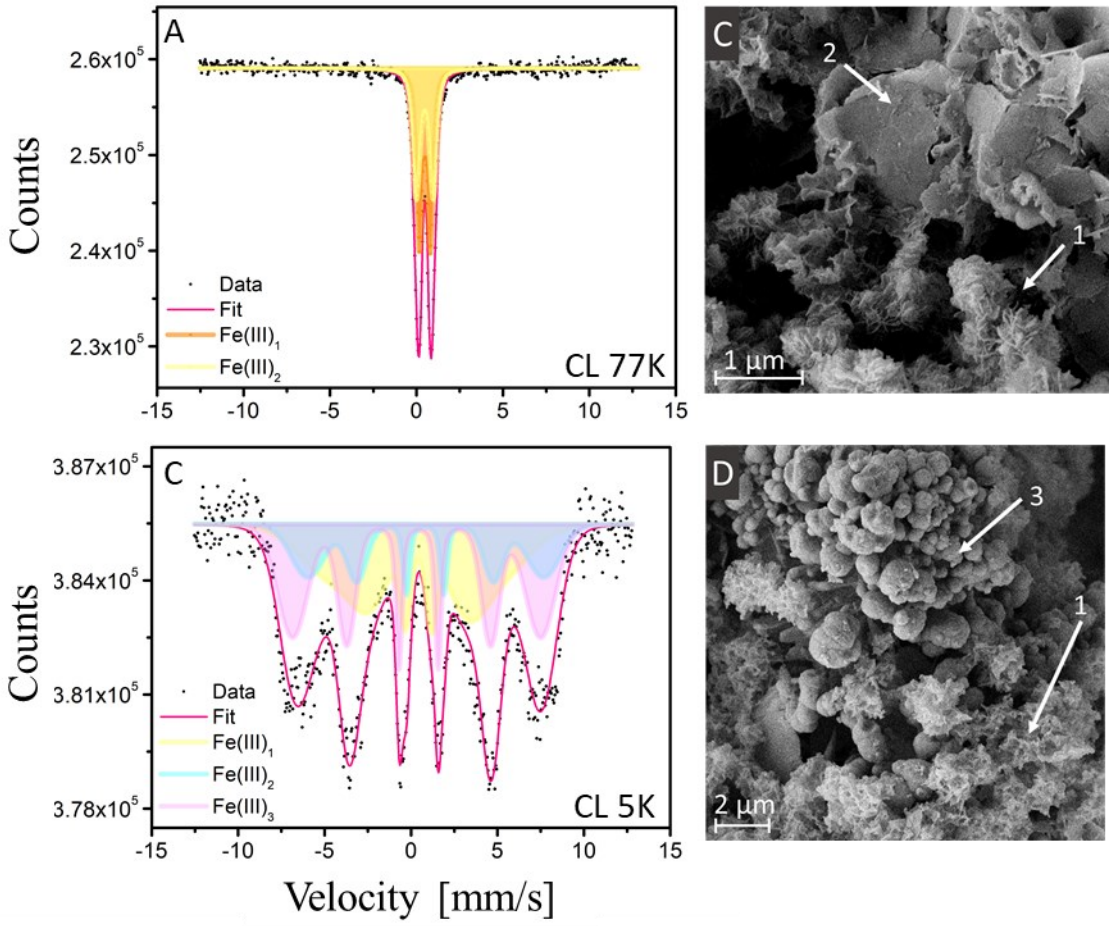

Figure 3: Mössbauer spectroscopy of C. ferroooxidans KoFox taken at 77K and 5K for constant light (A, C). SEM images of C. ferrooxidans KoFox grown under different day/night conditions. Representative images show different mineral surfaces that were present in all setup's representative for long light/dark cycle (C, D). Different mineral morphologies were detected: 1 fine flakes; 2 flaky; 3 rhombic.

We also analysed the morphology of the mineral aggregates using SEM and found that the mineral aggregates looked similar in the different light illumination setups. Three different

morphologies, resembling fine flakes, flaky and rhombic structures dominated the three setups (Figure 3). This suggests that whilst light/dark cycles influence the physiology of photoferrotrophs, they have no significant influence on the identity and the morphology of Fe(III) minerals.

Conclusions

Our results show that the metabolic activity of phototrophic Fe(II)-oxidizers varies with different diurnal cycles. This results in higher maximum Fe(II) oxidation rates during short light/dark cycles (10 h/14 h). The influence of diurnal cycles is rarely investigated in laboratory studies but should be considered when phototrophic Fe(II) oxidation rates are derived from experiments performed under continuous illumination and further extrapolated to quantify their impact on iron cycling in the environment. Overlooking the impact of diurnal cycling may result in the contribution of anoxygenic phototrophic Fe(II) oxidation being underestimated. We suggest further that cultivating phototrophic Fe(II)-oxidizers (and phototrophs in general) in light/dark cycles is essential to better understand their physiology and environmental behaviour.

Acknowledgements

This study was funded by the German Research Foundation (DFG, BR 5927/3-1). The authors gratefully acknowledge the Tübingen Structural Microscopy Core Facility (funded by the Excellence Strategy of the German Federal and State Governments) for their support & assistance in this work. AK acknowledges infrastructural support by the DFG under Germany's Excellence Strategy, cluster of Excellence EXC2124, project ID 390838134.

References:

Blankenship, R. E., Cheng, P., Causgrove, T. P., Brune, D. C., Wang, S. H., Choh, J. -U, & Wang, J. (1993). REDOX REGULATION OF ENERGY TRANSFER EFFICIENCY IN ANTENNAS OF GREEN PHOTOSYNTHETIC BACTERIA. *Photochemistry and Photobiology*, *57*(1), 103–107. https://doi.org/10.1111/J.1751-1097.1993.TB02263.X

Blankenship, R. E., & Matsuura, K. (2003). *Antenna Complexes from Green Photosynthetic Bacteria*. 195–217. https://doi.org/10.1007/978-94-017-2087-8_6/COVER

Bryce, C., Blackwell, N., Schmidt, C., Otte, J., Huang, Y. M., Kleindienst, S., Tomaszewski, E., Schad, M., Warter, V., Peng, C., Byrne, J. M., & Kappler, A. (2018). Microbial anaerobic Fe(II) oxidation – Ecology, mechanisms and environmental implications. *Environmental Microbiology*, *20*(10), 3462–3483. https://doi.org/10.1111/1462-2920.14328

Byrne, J. M., Klueglein, N., Pearce, C., Rosso, K. M., Appel, E., & Kappler, A. (2015). Redox cycling of Fe(II) and Fe(III) in magnetite by Fe-metabolizing bacteria. *Science*, *347*(6229), 1473–1476. http://www.sciencemag.org/content/347/6229/1473.full

Croal, L. R., Jiao, Y., Kappler, A., & Newman, D. K. (2009). Phototrophic Fe(II) oxidation in an atmosphere of H2: Implications for Archean banded iron formations. *Geobiology*, *7*(1), 21–24. https://doi.org/10.1111/j.1472-4669.2008.00185.x

Eickhoff, M., Obst, M., Schröder, C., Hitchcock, A. P., Tyliszczak, T., Martinez, R. E., Robbins, L. J., Konhauser, K. O., & Kappler, A. (2014). Nickel partitioning in biogenic and abiogenic ferrihydrite: The influence of silica and implications for ancient environments. *Geochimica et Cosmochimica Acta*, *140*, 65–79. https://doi.org/10.1016/j.gca.2014.05.021

Foote, C. S. (1968). Mechanisms of photosensitized oxidation. *Science*, *162*(3857), 963–970. https://doi.org/10.1126/science.162.3857.963

Gauger, T., Byrne, J. M., Konhauser, K. O., Obst, M., Crowe, S., & Kappler, A. (2016). Influence of organics and silica on Fe(II) oxidation rates and cell–mineral aggregate formation by the green-sulfur Fe(II)-oxidizing bacterium Chlorobium ferrooxidans KoFox – Implications for Fe(II) oxidation in ancient oceans. *Earth and Planetary Science Letters*, *443*, 81–89. https://doi.org/10.1016/j.epsl.2016.03.022

Han, X., Tomaszewski, E. J., Sorwat, J., Pan, Y., Kappler, A., & Byrne, J. M. (2020). Oxidation of green rust by anoxygenic phototrophic Fe(II)-oxidising bacteria. *Geochem. Persp. Let*, *12*, 52–57. https://doi.org/10.7185/geochemlet.2004

Hauruseu, D., & Koblízek, M. (2012). Influence of light on carbon utilization in aerobic anoxygenic phototrophs. *Applied and Environmental Microbiology*, *78*(20), 7414–7419. https://doi.org/10.1128/AEM.01747-12

Hegler, F., Posth, N. R., Jiang, J., & Kappler, A. (2008). *Physiology of phototrophic iron (II) -oxidizing bacteria : implications for modern and ancient environments*. *66*(Ii), 250–260. https://doi.org/10.1111/j.1574-6941.2008.00592.x

Heising, S., Richter, L., Ludwig, W., & Schink, B. (1999). Chlorobium ferrooxidans sp. nov., a phototrophic green sulfur bacterium that oxidizes ferrous iron in coculture with a "Geospirillum" sp. strain. *Archives of Microbiology*, *172*(2), 116–124. https://doi.org/10.1007/s002030050748

Kappler, A., Bryce, C., Mansor, M., Lueder, U., Byrne, J. M., & Swanner, E. D. (2021). An evolving view on biogeochemical cycling of iron. *Nature Reviews Microbiology*, *19*(6), 360–374. https://doi.org/10.1038/s41579-020-00502-7

Kappler, A., & Newman, D. K. (2004). Formation of Fe(III)-minerals by Fe(II)-oxidizing photoautotrophic bacteria. *Geochimica et Cosmochimica Acta*, *68*(6), 1217–1226. https://doi.org/10.1016/J.GCA.2003.09.006

Melton, E. D., Schmidt, C., Behrens, S., Schink, B., & Kappler, A. (2014). Metabolic Flexibility

and Substrate Preference by the Fe(II)-Oxidizing Purple Non-Sulphur Bacterium Rhodopseudomonas palustris Strain TIE-1. *Http://Dx.Doi.Org/10.1080/01490451.2014.901439*, *31*(9), 835–843. https://doi.org/10.1080/01490451.2014.901439

Mu, C. C., Zhang, T. J., Zhao, Q., Guo, H., Zhong, W., Su, H., & Wu, Q. B. (2016). Soil organic carbon stabilization by iron in permafrost regions of the Qinghai-Tibet Plateau. *Geophysical Research Letters*, *43*(19), 10,286-10,294. https://doi.org/10.1002/2016GL070071

Renger, G., & Wolff, C. (1977). Further evidence for dissipative energy migration via triplet states in photosynthesis. The protective mechanism of carotenoids in Rhodopseudomonas spheroides chromatophores. *Biochimica et Biophysica Acta (BBA) - Bioenergetics*, *460*(1), 47–57. https://doi.org/10.1016/0005-2728(77)90150-5

Schmidt, C., Nikeleit, V., Schaedler, F., Leider, A., Lueder, U., Bryce, C., Hallmann, C., & Kappler, A. (2021). Metabolic Responses of a Phototrophic Co-Culture Enriched from a Freshwater Sediment on Changing Substrate Availability and its Relevance for Biogeochemical Iron Cycling. *Geomicrobiology Journal*, *38*(3), 267–281. https://doi.org/10.1080/01490451.2020.1837303

Tipping, E. (1981). The adsorption of aquatic humic substances by iron oxides. *Geochimica et Cosmochimica Acta*, *45*(2), 191–199. https://doi.org/10.1016/0016-7037(81)90162-9

Tsukatani, Y., Jianzhong, •, Robert, W. •, Blankenship, E., & Bryant, D. A. (2010). Characterization of the FMO protein from the aerobic chlorophototroph, Candidatus Chloracidobacterium thermophilum. *Photosynthesis Research*, *104*, 201–209. https://doi.org/10.1007/s11120-009-9517-0

Wen, J., Tsukatani, Y., Cui, W., Zhang, H., Gross, M. L., Bryant, D. A., & Blankenship, R. E. (2010). *Structural model and spectroscopic characteristics of the FMO antenna protein from the aerobic chlorophototroph, Candidatus Chloracidobacterium thermophilum*. https://doi.org/10.1016/j.bbabio.2010.09.008

Widdel, F., Schnell, S., Heising, S., Ehrenreich, A., Assmus, B., & Schink, B. (1993). Ferrous iron oxidation by anoxygenic phototrophic bacteria. *Nature*, *362*(6423), 834–836. https://doi.org/10.1038/362834a0

Wydrzynski, T. J., Hillier, W., & Royal Society of Chemistry (Great Britain). (2011). *Molecular solar fuels*. 553. https://books.google.com/books/about/Molecular_Solar_Fuels.html?id=WHMoDwAAQBAJ

Zhi, R., Yang, A., Zhang, G., Zhu, Y., Meng, F., & Li, X. (2019). Effects of light-dark cycles on photosynthetic bacteria wastewater treatment and valuable substances production. *Bioresource Technology*, *274*(December 2018), 496–501. https://doi.org/10.1016/j.biortech.2018.12.021

Supplements

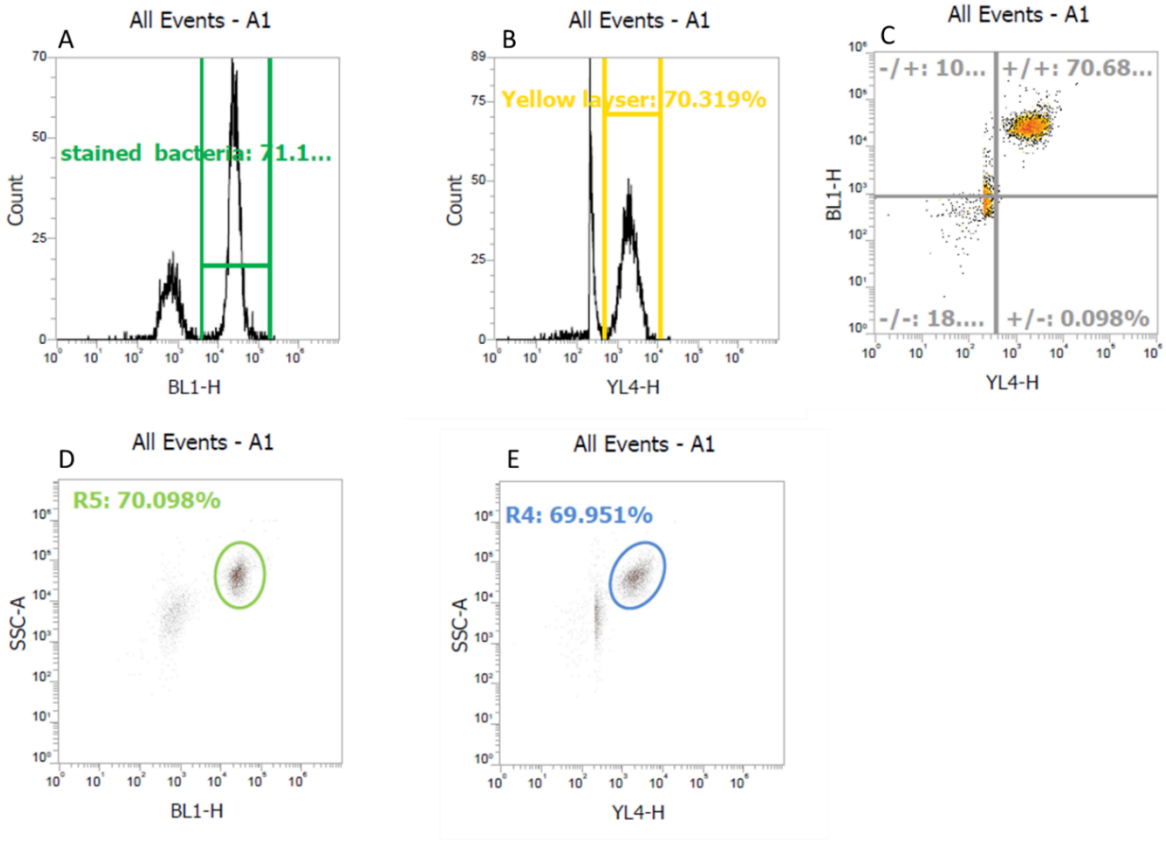

Figure S1: Flow cytometry plots. Panel A and B show counts and laser (BL1- blue laser; YL4- yellow laser), Panel C combines blue and yellow laser. In the panels D and E side scatter is plotted with one laser (BL or YL).

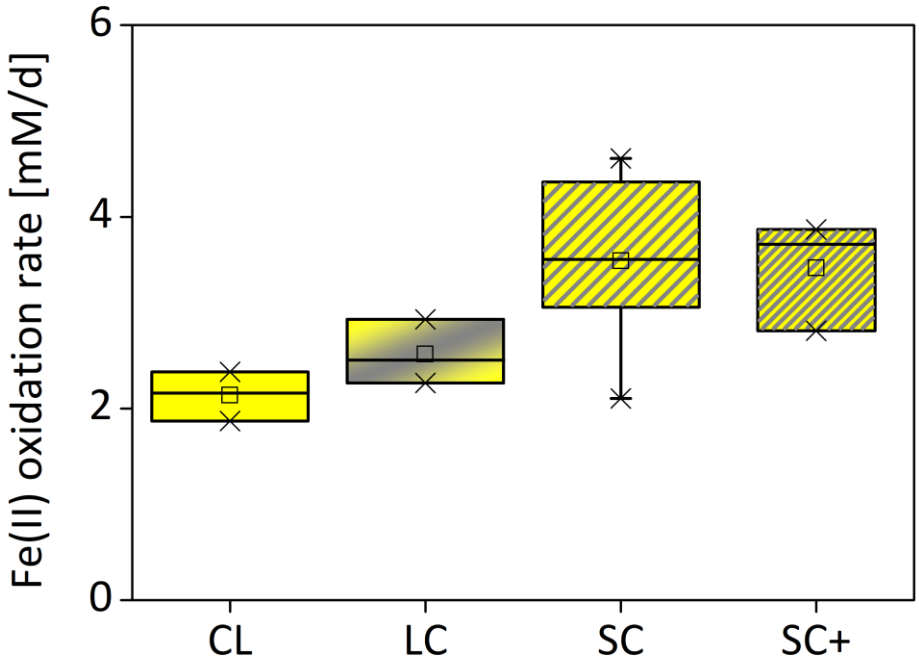

Figure S2: Panel A shows maximum Fe(II) oxidation rates of C. ferroooxidans KoFox for constant light (CL), long cycle (LC) and short cycle (SC) setup. Rates were calculated from triplicates for CL and LC, for SC 6 rates were chosen. SC+ was calculated from 9.8-13.8 days and divided by the light days.

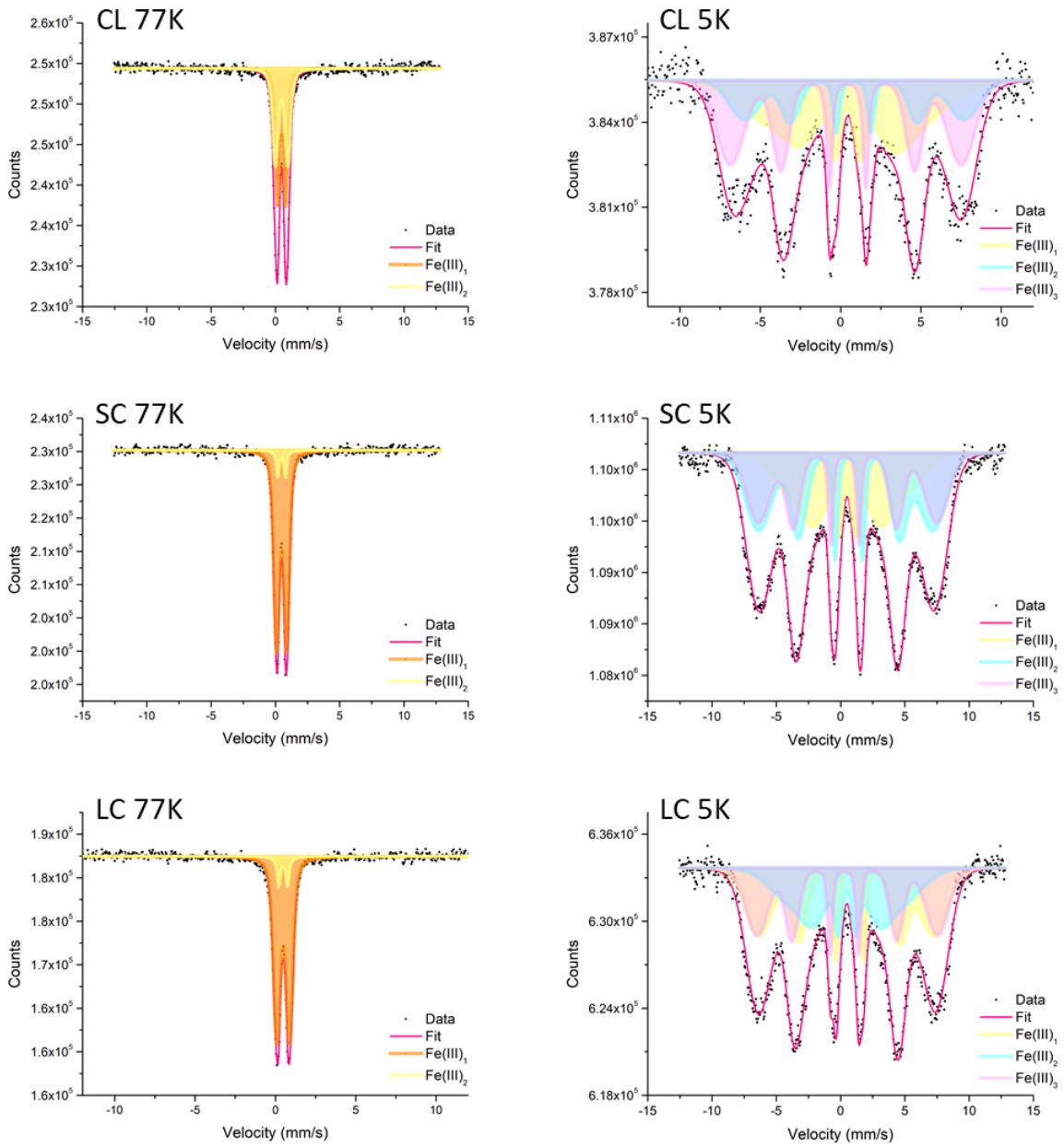

Figure S3: Mössbauer spectroscopy of C. ferrooxidans KoFox taken at 77K and 5K for constant light (CL), short light/dark cycle (SC) and long light/dark cycle (LC).

Table S1: Summary of the Mössbauer parameters obtained by fitting. CS - center shift; QS - quadrupole splitting; ε - quadrupole shift; H – hyperfine field; sigma – standard deviation of H; Pop – site population, i.e. relative spectral area. Db – doublet; S (Coll) – collapsed sextet; S (Wide) – widened sextet; S (Def) – defined narrow sextet; χ^2 – goodness of the fit; Fe phase – identified iron phase. Samples were analyzed for constant light (CL), short light/dark cycle (SC) and long light/dark cycle (LC).

Sample	Temp.	Phase	CS	ΔE_Q	ε	H	sigma	Pop (±)	χ^2	Fe
	K		mm/s	mm/s	mm/s	T	mm/s	%		phase
CL	77	Db1	0.48	0.74				52.1	0.69	Fe(III)
		Db2	0.48	0.69				47.9		Fe(III)
	5	S1 coll	0.31		-0.12	29.1	11.0	39.3	0.76	Fe(III)
		S2 wide	0.63		0.01	42.3	5.6	20.7		Fe(III)
		S3 def	0.48		-0.05	44.5	3.1	40.0		Fe(III)
SC	77	Db1	0.48	0.76				50.0	0.56	Fe(III)
		Db2	0.48	0.69				50.0		Fe(III)
	5	S1 coll	0.51		-0.12	25.2	9.73	31.3	1.02	Fe(III)
		S2 wide	0.52		0.01	41.9	6.25	38.2		Fe(III)
		S3 def	0.45		0.10	43.01	3.45	30.5		Fe(III)
LC	77	Db1	0.48	0.78				48.2	0.59	Fe(III)
		Db2	0.49	0.67				51.8		Fe(III)
	5	S1 coll	0.47		-0.01	26.2	9.99	29.8	0.78	Fe(III)
		S2 wide	0.57		-0.13	42.1	6.26	37.8		Fe(III)
		S3 def	0.41		0.11	43.55	5.2	32.4		Fe(III)

6 Chapter: Buffer concentration influences substrate consumption and growth of *Rhodopseudomonas palustris* TIE-1

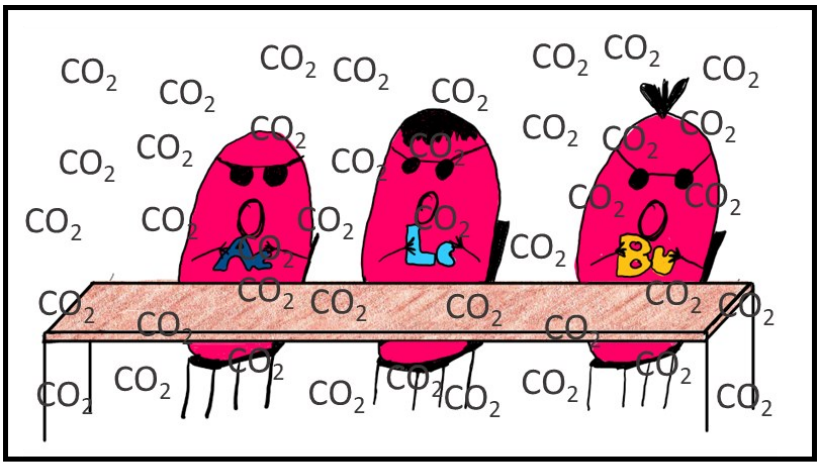

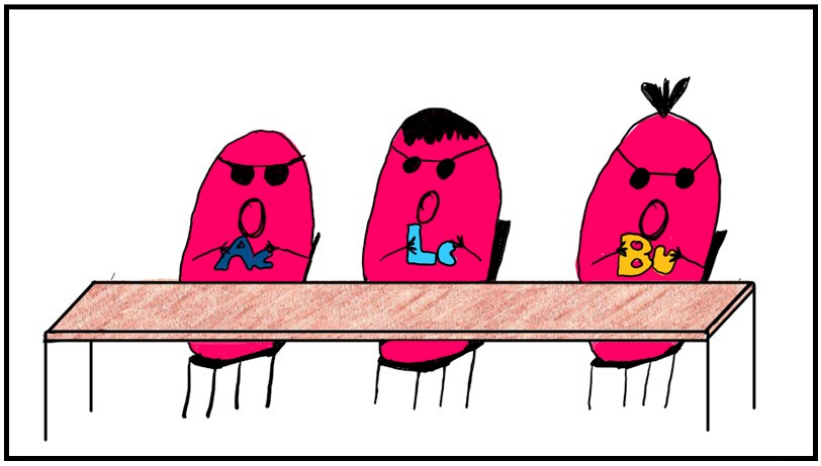

Contributions:

Resources were provided by Dr. C. Bryce and Prof. Dr. A. Kappler. The project was designed by me with guidance of Dr. C. Bryce and the chapter was written by me. The experiment was conducted by me. M. Maisch performed SEM analysis.

Buffer concentration influences substrate consumption and growth of *Rhodopseudomonas palustris* TIE-1

Verena Nikeleit[1], Markus Maisch[1], Andreas Kappler[1,2] and Casey Bryce[3]

[1]Department of Geoscience, University of Tübingen, Tübingen, Germany
[2]Cluster of Excellence: EXC 2124: Controlling Microbes to Fight Infections, Tübingen, Germany
[3]School of Earth Sciences, University of Bristol, Bristol, UK

Introduction

Phototrophic Fe(II)-oxidizer are metabolically flexible and can grow photoautotrophically with Fe(II) and H_2 as electron donor and fix CO_2 to build biomass. They also can grow photoheterotrophically with a variety of carbon substrates (i.e. acetate, lactate and glucose) that they can use as electron donors and source for biomass. McKinlay and Harwood (2010) found that 22% of acetate used by *Rhodopseudomonas palustris* was oxidized to CO_2 and used to recycle cofactors necessary for building biomass. Therefore, CO_2 plays an important role for these phototrophs as a carbon source and as a way to recycle cofactors (McKinlay & Harwood, 2010). This is particularly true for carbon substrates that are more reduced than biomass like butyrate. In addition to having a crucial role in bacterial metabolism, it plays an important role in maintaining stable pH conditions in the organism's growth environment. In the environment dissolved inorganic carbon DIC (CO_2, HCO_3^- and CO_3^{2-}) plays an essential role in buffering environmental systems and neutralize pH. In freshwater systems the DIC can range from 0.15-3.27 mM (Howard et al., 1984; Neubauer & Anderson, 2003; Stumm & Morgan, 2012). This is quite low compared to the high concentrations used in laboratory experiments (up to 22 mM HCO_3^-) studying these bacteria (Croal et al., 2009; Ehrenreich & Widdel, 1994). These high HCO_3^- concentrations are necessary as high substrate concentrations are used which could influence the pH. This difference in DIC concentration could have an impact on autotrophic phototrophs. Indeed in a study by Croal they found out that the concentration of CO_2 had an effect on the Fe(II) oxidation rates. For both *R. palustris* TIE-1 and *Rhodobacter ferrooxidans* SW2 Fe(II) oxidation rates were 0.07 and 0.15 mM/h with 1 mM $NaHCO_3$ respectively and increased to 0.13 and 0.46 mM/h with 20 mM $NaHCO_3^-$ respectively (Croal et al., 2009).

In this study we wanted to expand on these first findings and investigate the impact of buffer concentration and composition on Fe(II) oxidation. Furthermore, we would like to explore the consumption of organic substrates like acetate or butyrate.

Material and Methods

Buffer depended growth experiment with organics. *R. palustris TIE-1* was grown in Hungate tubes with 9.5 mL media and 0.5 mL of *R. palustris TIE-1* grown on H_2/CO_2 (80:20; v:v) for 2 transfers. The inoculum in the 20 mM PIPES set up was washed 2 times and end concentration of HCO_3^- was less than 0.1 mM. 6 different buffer compositions were chosen: 22 mM HCO_3^- buffer, 3 mM HCO_3^- buffer, 1 mM HCO_3^- buffer plus 20 mM PIPES buffer, 3 mM HCO_3^- buffer plus 20 mM PIPES, 22 mM HCO_3^- buffer plus 20 mM PIPES buffer and 20 mM PIPES buffer. For media preparation the following salts were dissolved in one Liter of ultrapure water: 0.5 g KH_2PO_4, 0.3 g NH_4Cl, 0.5 g $MgSO_4$ * $7H_2O$, 0.1 g $CaCl_2$*$2H_2O$ and autoclaved in a Widdel flask (Jiao et al., 2005). After autoclaving, 10 mL/L filter-sterilized vitamin solution (altered from Ehrenreich & Widdel, 1994; containing additional 50 mg/L riboflavin), 1 mL/L SL10 trace element solution (Widdel, 1983), 1 mL/L selenite-tungstate solution (Widdel & Bak, 1992) and 0.1 mg/L vitamin B12 solution were added. The medium was prepared with a headspace of N_2/CO_2 (90:10; v:v) and buffered with the appropriate buffer. In the setups containing PIPES buffer 100% N_2 headspace was used. The pH of the media was adjusted to pH 6.9 with anoxic 1 M HCl and anoxic 1 mM NaOH. 6 different organics were chosen: Either acetate (Ac), lactate (Lc), pyruvate (Py), butyrate (Bu), glucose (Glu)) or a mix of 0.2 mM acetate, lactate and butyrate (Mix) were added. The Hungate tubes were placed randomly in a light incubator at 20°C with 25±7 µmol photons/s/m^2. Growth was monitored by measuring optical density at 660 nm.

Buffer depended growth experiment with Fe(II). 50 mL media was added to 100 mL serum vials and inoculated with 0.5% of the pre-grown *R. palustris* TIE-1 culture. Media was prepared as stated above. In this experiment 5 different buffer setups were chosen: 22 mM HCO_3^-, 3 mM HCO_3^-, 1 mM HCO_3^- buffer plus 20 mM PIPES and 3 mM HCO_3^- buffer plus 20 mM PIPES.

In all setups 2 mM $FeCL_2$ was added after media preparation. The pH was adjusted to 7.1 in all setups. The bottles were placed randomly in a light incubator at 20°C with 25±7 µmol photons/s/m^2. In a glovebox (100% N_2 atmosphere) samples for Fe quantification were taken.

Fe quantification. Fe(II) and Fe total was quantified with the Ferrozine assay modified by (Hegler et al., 2008). 0.1 mL of sample was added to 0.9 mL 1 M HCl and stored at 5°C until analysis.

Cell growth. Cell growth was determined by measuring optical density at 660 nm with Specord®50 plus, Analytikjena, Jena, Germany. Thereby, measurements were taken with the Hungate Tubes which ensured that the system and the buffer concentrations was undisturbed over the experiment. Cell numbers were calculated with a regression curve from Schmidt et al. (2021).

Scanning electron microscopy (SEM). SEM was conducted to visualize the interactions and associations between the microbial cells and between the cells and the minerals. For SEM, cultures of *R. palustris* TIE-1 grown with 1 and 3 mM HCO_3^-+PIPES were chosen. At the end of incubation, a sample was fixed by adding glutaraldehyde (2.5%; v/v). 30 µL of fixed samples were placed on a glass slide which was coated with 50 µL of poly-L-lysine. The samples were dehydrated with increasing ethanol solutions starting from 35% to 100% (5 min per new solution; 35%, 55%, 70% 90% to 100%). The samples were then placed in HMDS two times for 30 sec and left in the fume hood to dry. Samples were placed on aluminium stubs and sputter-coated at a working distance of 35 mm at 20 mA for 70 sec to receive a 13 nm coating (BAL-TEC SCD 005). Microscopy was done with a ZEISS Crossbeam 550L using an electron

high tension of 2 kV, working distance of 1.5 mm and a secondary electron secondary ion (SESI) detector.

Results and discussion

Buffer depended growth experiment with organics

R. palustris TIE-1 was grown with acetate, lactate, pyruvate, butyrate, glucose or mix (acetate, lactate and butyrate) in 6 different buffer compositions and bicarbonate (HCO_3^-) concentrations. Indeed, different cell growth dependent on the buffer could be observed for all substrates (Figure 1). Highest cell numbers were quantified with the 1 mM HCO_3^-+PIPES buffer with all the substrates and ranged from $1.5\pm0.2*10^7$ with acetate to $4.0\pm0.1*10^7$ cells/mL in the mix setup (acetate, lactate and butyrate). Lowest cell numbers were always measured with 3 mM HCO_3^- and 22 mM HCO_3^- (for acetate and pyruvate). Second lowest cell numbers were quantified with 3 mM HCO_3^-+PIPES and 22 mM HCO_3^-+PIPES and second highest with PIPES only in the acetate setup. The same trend was also observed in the setup with pyruvate and lactate.

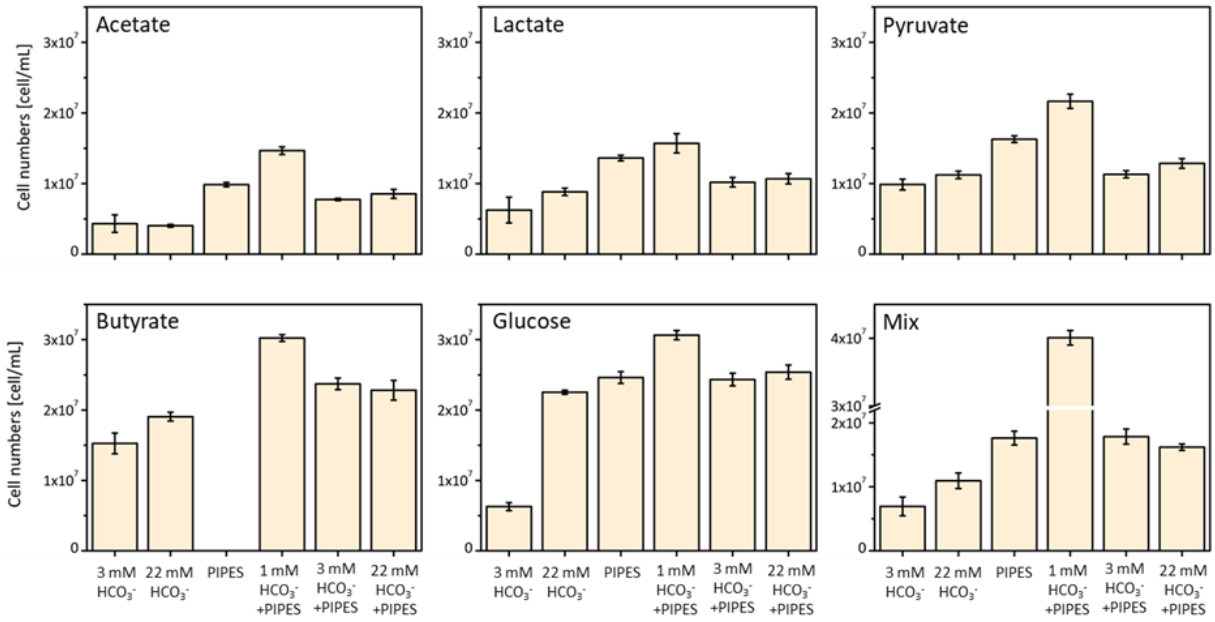

Figure 1: Cell growth of R. palustris TIE-1 *with acetate, lactate, pyruvate, butyrate, glucose and mix (mix of acetate, lactate and butyrate) in media with different buffer concentration (1-22 mM) and composition (HCO_3^- and PIPES).*

For butyrate no cell growth could be observed with PIPES buffer only and highest cell number were reached with 1 mM HCO_3^-+PIPES with $3.0\pm0.1*10^7$ cells/mL. Highest cell numbers were

reached with glucose reaching between 2.0-2.5*10^7 cells/mL with 22 mM HCO_3, PIPES and 3/22 mM HCO_3^-+PIPES with highest in 1 mM HCO_3^-+PIPES (3.0±0.1*10^7 cells/mL).

Generally, *R. palustris* TIE-1 grew best when the system was well buffered and low HCO_3^- concentration. Cell numbers were lower as expected if cell numbers are calculated like in chapter 2 and 3. Reasons for that could be that 1) bacteria in this experiment were grown in different tubes which could change the surface due to a smaller diameter which could limited gas exchange and 2) OD values from Schmidt et al. (2021) were measured in different vials (96 well plates). Nonetheless it could show us a first indication of cell growth and preference growth of different buffer concentration and composition.

Buffer depended growth experiment with Fe(II)

The phototrophic Fe(II) oxidation of *R. palustris* TIE-1 was impacted by both the buffer composition and HCO_3^- concentration (Figure 2). In the 1 and 3 mM HCO_3^-+PIPES setup most of the Fe(II) was oxidized at the end of the experiment after 49 days (85±2 and 80±2%, respectively). Whereas, Fe(II) oxidation extend in the setup with 3 mM HCO_3^- was lower with 68±1% and 22 mM HCO_3^- with 66±15%. Small differences were also observed in the Fe(II) oxidation rates. Fe(II) oxidation rate in the 1 and 3 mM HCO_3^-+PIPES setup (0.09±0.2 and 0.09±0.04 mM/d, respectively) and 22 mM HCO_3^- setup (0.1±0.09 mM/d) showed similar Fe(II) oxidation rates although in the 22 mM HCO_3^- setup big standard deviation was measured. Lowest Fe(II) oxidation was observed in the 3 mM HCO_3^- setup with 0.05±0.03 mM/d.

Fe(II) oxidation rates are a little bit lower than previously published data from the same strain with 0.23±0.04 mM/d (chapter 2), 0.27±0.01 mM/d (Han et al., 2020) and 0.15±0.03 mM/d (Peng et al., 2019). Although Fe(II) oxidation rates in chapter 2 were quantified with 0.22 µm sterile filtered media which removed Fe-carbonates and Fe-phosphates resulting in very small Fe(II) minerals and dissolved Fe(II). Our results affirm the results by Croal et al. (2009) that

Fe(II) oxidation are slower with lower HCO_3^- concentration although not to the same extend. With our experiment we could also show that HCO_3^- concentration is not the only indicator responsible for Fe(II) oxidation extend. A well buffered system with low HCO_3^- concentrations will not affect the Fe(II) oxidation and slightly increased the extend of Fe(II) oxidation.

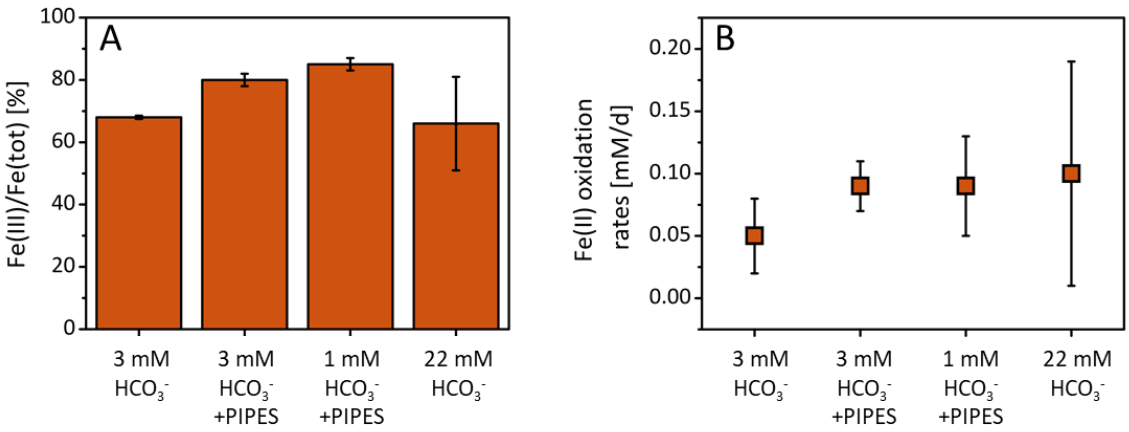

Figure 2: Panel A shows Fe(III)/Fe(total) of R. palustris TIE-1 *when grown with Fe(II) and different buffer concentrations and compositions after 49 days. Panel B shows the Fe(II) oxidation rates. Standard deviation results from triplicates.*

Optical differences between the different setups were also observed (Figure 3). The precipitates in the set up with 22 mM HCO_3^- appeared between green/grey and brown. In the setup with 3 mM HCO_3^- the colour turned grey/green after 49 days. In the setup with 1 and 3 mM HCO_3^- +PIPES the colour was green/grey with a little bit of pink when the bottle was shaken. Upon settling, two distinct layers appeared: a pink layer at the bottom, potential indicative for *R. palustris* TIE-1, a purple non-sulfur bacterium, and a green/grey layer above, suggesting the presence of Fe(III) minerals.

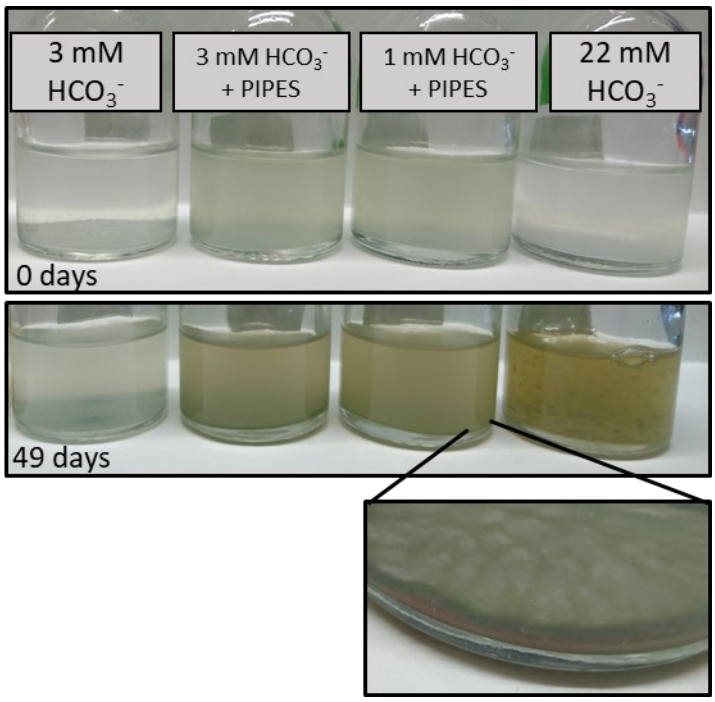

Figure 3: Pictures of serum bottles with R. palustris TIE-1 *grown with Fe(II) and different buffer concentration and composition.* for filtered media.*

What interested us in the next step was to see if we could possible see any differences in mineral structures and also cell-mineral associations. Therefore, samples with 1 and 3 mM HCO_3^- +PIPES were chosen and prepared. Between the 1 and 3 mM HCO_3^-+PIPES setup no morphological differences were observed. Microbes were imbedded in the minerals but not encrusted (Figure 4, arrow a). Mineral structures in the 1 and 3 mM HCO_3^-+PIPES setup showed the same morphology and two main structure were identified as flakes and branched minerals (Figure 4, arrow b and c).

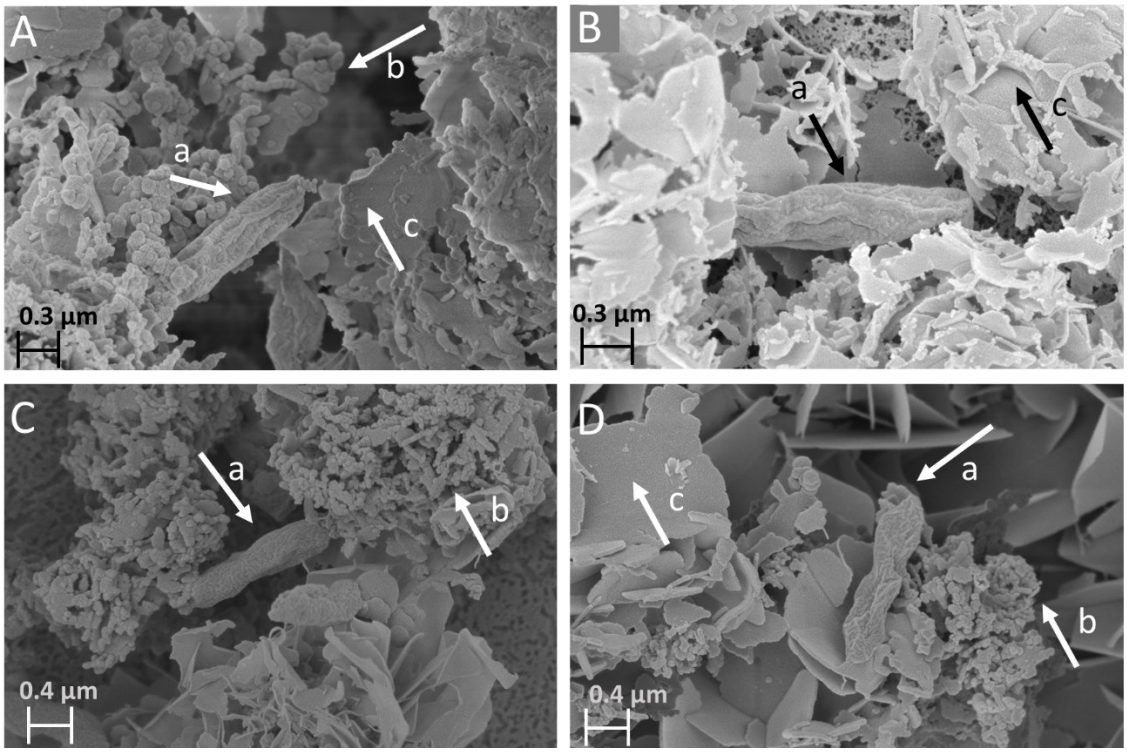

Figure 4: SEM images of R. palustris TIE-1 *grown with Fe(II) in media with different buffer concentration and composition. Panel A and B show R. palustris* TIE-1 *and minerals from 3 mM HCO_3^-+PIPES and Panel C and D from 1 mM HCO_3^-+PIPES. Arrow a show microbe, arrow b show branch-like minerals and arrow c flake minerals.*

Similar morphology as the flakes (arrow c) were also observed for a different phototrophic Fe(II)-oxidizer *C. ferrooxidans* KoFox (chapter 5). In chapter 2 SEM images of *R. palustris* TIE-1 grown on 2 mM filtered media showed only one morphology described as spiky flakes. In this case the setup with 22 mM HCO_3^- media was filtered through a 0.22 µm sterile filter and thereby removing most of the Fe-carbonates and Fe-phosphates.

Additionally the pH has a big effect on how much of the CO_2 is dissolved in the solution and can be taken up by organisms (Beer et al., 2021). During Fe(II) oxidation H^+ are produced decreasing the pH (Widdel et al., 1993). We could also see slight shifts in the pH of the different setups. Stable pH value was only found in the 22 mM HCO_3^- setup with pH 7.1. Second highest pH was with 3 mM HCO_3^-+PIPES with 6.8, followed by 1 mM HCO_3^-+PIPES with 6.6 and 3 mM $HCO_3^-$with 6.5.

Conclusion

In our experiments we saw that Fe(II) oxidation and organic consumption are favoured in a well buffered system. While for organic consumption low HCO_3^- are beneficial, the opposite was observed for Fe(II) oxidation. This could be intertwined that during Fe(II) oxidation H^+ are produced and pH remained stable with high HCO_3^- concentrations. In this study we could show that depending on the consumed substrates different buffer concentrations and compositions are more beneficial for phototrophic Fe(II)-oxidizer.

Acknowledgement

The authors gratefully acknowledge the Tübingen Structural Microscopy Core Facility (funded by the Excellence Strategy of the German Federal and State Governments) for their support & assistance in this work.

References

Beer, S., Björk, M., & Beardall, J. (2021). *Carbon Dioxide vs. Bicarbonate Utilisation BT - Research Methods of Environmental Physiology in Aquatic Sciences* (K. Gao, D. A. Hutchins, & J. Beardall (eds.); pp. 153–164). Springer Singapore. https://doi.org/10.1007/978-981-15-5354-7_18

Croal, L. R., Jiao, Y., Kappler, A., & Newman, D. K. (2009). Phototrophic Fe(II) oxidation in an atmosphere of H2: Implications for Archean banded iron formations. *Geobiology*, *7*(1), 21–24. https://doi.org/10.1111/j.1472-4669.2008.00185.x

Ehrenreich, A., & Widdel, F. (1994). Anaerobic oxidation of ferrous iron by purple bacteria, a new type of phototrophic metabolism. *Applied and Environmental Microbiology*, *60*(12), 4517–4526. https://doi.org/10.1128/AEM.60.12.4517-4526.1994

Han, X., Tomaszewski, E. J., Sorwat, J., Pan, Y., Kappler, A., & Byrne, J. M. (2020). Oxidation of green rust by anoxygenic phototrophic Fe(II)-oxidising bacteria. *Geochem. Persp. Let*, *12*, 52–57. https://doi.org/10.7185/geochemlet.2004

Hegler, F., Posth, N. R., Jiang, J., & Kappler, A. (2008). *Physiology of phototrophic iron (II) -oxidizing bacteria : implications for modern and ancient environments*. *66*(Ii), 250–260. https://doi.org/10.1111/j.1574-6941.2008.00592.x

HOWARD, J. R., SKIRROW, G., & HOUSE, W. A. (1984). Major ion and carbonate system chemistry of a navigable freshwater canal. *Freshwater Biology*, *14*(5), 515–532. https://doi.org/10.1111/j.1365-2427.1984.tb00172.x

Jiao, Y., Kappler, A., Croal, L. R., & Newman, D. K. (2005). Isolation and characterization of a genetically tractable photoautotrophic Fe(II)-oxidizing bacterium, Rhodopseudomonas palustris strain TIE-1. *Applied and Environmental Microbiology*. https://doi.org/10.1128/AEM.71.8.4487-4496.2005

McKinlay, J. B., & Harwood, C. S. (2010). Carbon dioxide fixation as a central redox cofactor recycling mechanism in bacteria. *Proceedings of the National Academy of Sciences of the United States of America*, *107*(26), 11669–11675. https://doi.org/10.1073/pnas.1006175107

Neubauer, S. C., & Anderson, I. C. (2003). Transport of dissolved inorganic carbon from a tidal freshwater marsh to the York River estuary. *Limnology and Oceanography*, *48*(1 I), 299–307. https://doi.org/10.4319/lo.2003.48.1.0299

Peng, C., Bryce, C., Sundman, A., Borch, T., & Kappler, A. (2019). *Organic Matter Complexation Promotes Fe(II) Oxidation by the Photoautotrophic Fe(II)-Oxidizer Rhodopseudomonas palustris TIE-1*. https://doi.org/10.1021/acsearthspacechem.9b00024

Schmidt, C., Nikeleit, V., Schaedler, F., Leider, A., Lueder, U., Bryce, C., Hallmann, C., & Kappler, A. (2021). Metabolic Responses of a Phototrophic Co-Culture Enriched from a Freshwater Sediment on Changing Substrate Availability and its Relevance for Biogeochemical Iron Cycling. *Geomicrobiology Journal*, *38*(3), 267–281. https://doi.org/10.1080/01490451.2020.1837303

Stumm, W., & Morgan, J. (2012). *Aquatic chemistry: chemical equilibria and rates in natural waters*. https://books.google.de/books?hl=de&lr=&id=NLV_yfulgkQC&oi=fnd&pg=PT14&dq=morgan+and+stumm+2012&ots=cLY0aqf3IK&sig=9ncXlgU393pyLvOIhufv-1IHsFs

Widdel, F. (1983). Methods for enrichment and pure culture isolation of filamentous gliding sulfate-reducing bacteria. *Archives of Microbiology*, *134*(4), 282–285. https://doi.org/10.1007/BF00407803

Widdel, F., & Bak, F. (1992). Gram-Negative Mesophilic Sulfate-Reducing Bacteria. *The Prokaryotes*, 3352–3378. https://doi.org/10.1007/978-1-4757-2191-1_21

Widdel, F., Schnell, S., Heising, S., Ehrenreich, A., Assmus, B., & Schink, B. (1993). Ferrous iron oxidation by anoxygenic phototrophic bacteria. *Nature*, *362*(6423), 834–836.

https://doi.org/10.1038/362834a0

7 Chapter: Methane production by anoxygenic phototrophic Fe(II)-oxidizing bacteria

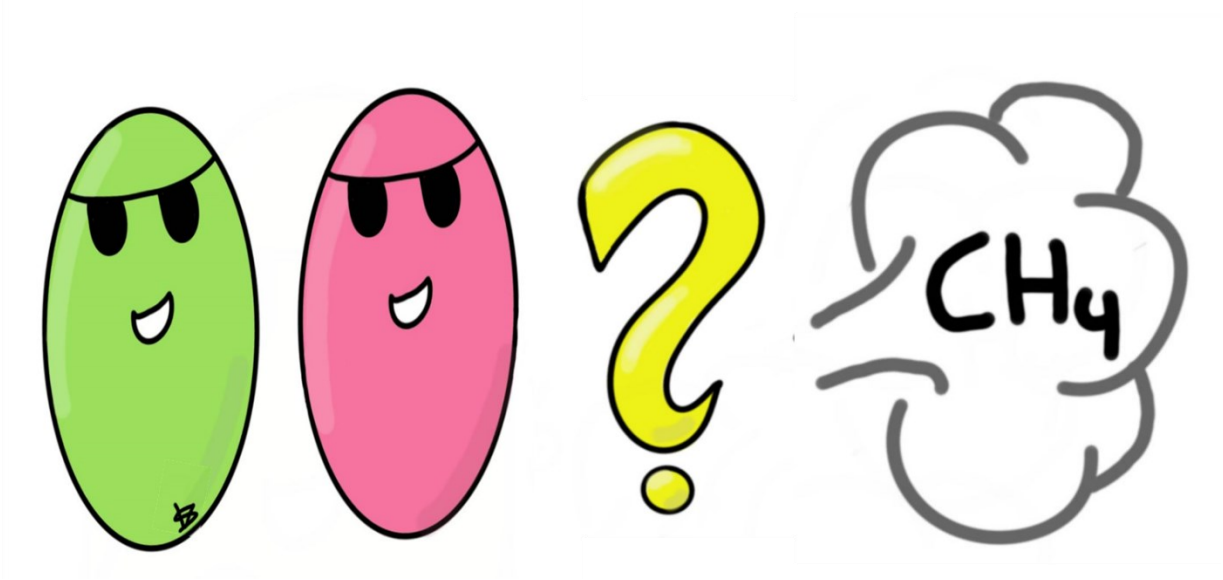

Contributions:

Resources were provided by Prof. Dr. A. Kappler, Dr. C. Bryce and Prof. Dr. Frank Keppler. The original hypothesis was formulated by Prof. Dr. A. Kappler and Prof. F. Keppler. The project was designed by me, Prof. Dr. A. Kappler and Prof. F. Keppler. Me and S. Gruss conducted the experiments and I did DNA extractions and qPCR. M. Schneider and S. Gruss conducted gas and isotope measurements. The manuscript was written by me and Prof. Dr. A. Kappler with input of all co-authors.

Methane production by anoxygenic phototrophic Fe(II)-oxidizing bacteria

Verena Nikeleit[1], Marcus Schneider[2], Savinja Gruss[2], Kurt O. Konhauser[3], Casey Bryce[4], Frank Keppler[2,5*] and Andreas Kappler[1,6*]

[1]Department of Geosciences, University of Tübingen, Tübingen, Germany

[2]Institute of Earth Science, Heidelberg University, Heidelberg, ‘Germany

[3]Department of Earth and Atmospheric Sciences, University of Alberta, Edmonton, Canada

[4]School of Earth Sciences, University of Bristol, Bristol, UK

[5]Heidelberg Center for the Environment (HCE), Heidelberg University, 69120 Heidelberg, Germany

[6]Cluster of Excellence EXC 2124: Controlling Microbes to Fight Infections, Tübingen, Germany

* Corresponding Authors: Andreas Kappler and Frank Keppler

Andreas Kappler

Department of Geosciences, University of Tübingen, Tübingen, Germany

Email: andreas.kappler@uni-tuebingen.de

Frank Keppler

Institute of Earth Science, Heidelberg University, Heidelberg, ‘Germany

Email: frank.keppler@geow.uni-heidelberg.de

Manuscript in preparation for submission to Geochemical Perspective Letters

KEYWORDS: greenhouse gas, methane, photoferrotrophs,

Abstract

Methane (CH_4) is a potent greenhouse gas that is primarily produced by methanogenic archaea. In recent years, methane production has also been detected in a diverse array of organisms, such as plants, fungi, and bacteria, including phototrophic microorganisms. Among the latter are photoautotrophic bacteria that can use Fe(II) (photoferrotrophs) and/or H_2 as electron donors for anoxygenic photosynthesis while others can additionally use acetate to grow as photoheterotrophs. However, the capacity of photoferrotrophs to produce CH_4 remains unexplored. Using ^{13}C-labelled HCO_3^- we demonstrated the biotic production of CH_4 by various photoferrotrophic bacteria. The highest CH_4 formation rate of up to 0.4±0.2 amol CH_4/(cell*d) was found in the purple non-sulfur bacterium *Rhodopseudomonas palustris* TIE-1 when it grew on H_2. When grown with acetate and Fe(II), the CH_4 rates reached 0.16±0.1 amol CH_4/(cell*d) and 0.04±0.04 amol CH_4/(cell*d), respectively. We also observed biotic CH_4 production by the green-sulfur Fe(II)-oxidizer *Chlorobium ferrooxidans* KoFox (0.03±0.01 amol CH_4/(cell*d)) and *Chlorobium phaeoferrooxidans* KB01 (0.11±0.004 amol CH_4/(cell*d)) when grown with Fe(II) as electron donor. Considering the pivotal role that photoferrotrophs had as primary producers during the Archean era we estimated up to 2% of the biological produced CH_4 could have been produced by photoferrotrophs.

Keywords: photoferrotrophs, early earth, anoxic environments, Fe(II) oxidation;

Introduction

Methane, an important greenhouse gas, has garnered increasing attention in recent years due to its critical role in changing Earth`s current climate. It can originate from both abiotic and biogenic sources, with around 70% of all CH_4 arising from microbial processes (Conrad, 2009). Primary methane-producing microbes – the methanogens – belong exclusively to the domain Archaea and they generate methane under anoxic conditions using a unique suite of enzymes, e.g. the methyl-coenzyme M reductase. Methane can also be produced by sulfate-reducing bacteria with the carbon monoxide dehydrogenase and by bacteria and archaea using nitrogenases or nitrogenase-like reductases (Vorholt et al., 1995) . In recent years the formation of methane under oxic conditions has also been observed by many organisms from unicellular to multicellular organisms including algae (Lenhart et al., 2016), cyanobacteria (Bižić et al., 2020), plants (Keppler et al., 2006) and fungi (Lenhart et al., 2012). In oxic environments CH_4 might be produced via the formation of reactive oxygen species (ROS). This mechanism involves the reaction of ROS with free iron (II) ions (Fenton-type chemistry) and methylated precursor compounds in living cells, potentially occurring in all three domains of life (Ernst et al., 2022). In a recent study CH_4 was produced abiotically via the formation of ROS with Fe^{2+} and H_2O_2 under anoxic conditions (Ernst et al., 2023). Anoxygenic phototrophic bacteria, such as *Rhodobacter capsulatus* and *Rhodopseudomonas palustris* strains, produce methane under nitrogen-fixing conditions via the nitrogenase (Ernst et al., 2022; Fixen et al., 2016; Zheng et al., 2018).

A subgroup of anoxygenic phototrophs are capable of using Fe(II) as electron donor (photoferrotrophs) and can be found across diverse environmental habitats today (Bryce et al., 2018). Iron is ubiquitous in the environment and photoferrotrophs facilitate Fe(II) oxidation under anoxic conditions. Photoferrotrophs have also been suggested as the primary producers during the Archean era when oceans were abundant in Fe(II) (Camacho et al., 2017). However, it is unknown i) whether methane is produced during Fe(II) oxidation by phototrophs and ii)

whether methane production by photoferrotrophs is substrate-dependent. Methane formation by phototrophic Fe(II) oxidation on early Earth is of particular interest because methane has the potential to retain energy from the Earth, thereby prolonging the period during which heat is retained on our planet.. Its importance extends back into Earth early history, where it has been proposed playing an important role in heating up the planet when the sun`s radiance was less intense than today (Pavlov et al., 2000). Investigating whether photoferrotrophs can also produce methane provides valuable insights not only into modern ecosystems but also into the potential contribution of these microorganisms to early Earth`s atmospheric composition. Therefore, we incubated three model strains of photoferrotrophs, i.e. *Rhodopseudomonas palustris* TIE-1, *Chlorobium ferrooxidans* KoFox and *Chlorobium pheaoferrooxidans* KB01 with both Fe(II), acetate and H_2 quantified methane formation. Isotopic labelled ^{13}C-labelled bicarbonate was applied to track and verify the origin of produced methane.

Material and Methods

Experimental setup. Three different model strains of phototrophic Fe(II)-oxidizers were cultivated from our lab culture collection at constant light at 20°C: Purple non-sulfur bacteria *R. palustris* TIE-1 and the two green sulfur bacteria *C. ferrooxidans* KoFox and *C. phaeoferrooxidans* KB01. They were grown with three different substrates: 10 mM Fe(II) (*R. palustris* TIE-1, *C. ferrooxidans* KoFox and *C. phaeoferrooxidans* KB01), H_2/CO_2 (80/20 v/v) (*R. palustris* TIE-1) or 5 mM acetate (*R. palustris* TIE-1). *C. phaeoferrooxidans* KB01 was provided by S. Crowe. A sacrificial setup was chosen and at each sampling point three biotic bottles and one abiotic bottle were analyzed. Serum vials were filled with 25 mL of a 22 mM bicarbonate-buffered medium (media composition for each strain can be found in Table S1). For isotope labelling, 5% of the 22 mM bicarbonate contained ^{13}C-labelled bicarbonate. Headspace contained N_2/CO_2 (90:10 v:v). All bottles were inoculated with 1% of a bacterial culture pre-grown on the same substrate. Abiotic samples were prepared the same way but inactivated by the addition of 160 mM sodium azide. Bottles were incubated in light at 20°C. Gas samples, samples for OD measurements and HPLC analysis were taken from acetate- and H_2-grown bottles at the lab bench. Setups containing Fe(II) were sampled in a glovebox (100% N_2 atmosphere) for Fe(II) quantification and cell counts.

Fe quantification. Fe(II) and Fe total was quantified with the Ferrozine assay modified by Hegler et al. (2008). 0.1 mL of sample was added to 0.9 mL 1 M HCl and stored at 5°C until analysis.

Acetate analysis. Samples were centrifuged at 15,000 rpm for 10 min. Supernatant was transferred into a new Eppendorf tube and stored at 5°C until measurement. Acetate was quantified with a High-Performance Liquid Chromatography (HPLC) from Shimadzu Prominence HPLC with a CTO-10ASvp

column oven, LC-20ATsolvent delivery unit, CTO-10ASvp column oven and a RID-20a refractive index detector.

Cell quantification. For the setups containing Fe(II) cell quantification was done via DNA extraction and qPCR of 16S rRNA. 1.8 mL of samples were stored at -20°C for DNA extraction and qPCR of 16S rRNA. DNA was extracted using the UltraClean R Microbial DNA Isolation Kit (MO BIO Laboratories, Carlsbad, CS, USA) and the quantity of the DNA was measured with a Nanodrop ND-1000 Spectrometer (Nanodrop^{TM} 1000, Thermo Scientific, Waltham, MA, USA). qPCR was conducted with the iCycler iQ^{TM}Real-Time PCR Detection System and the Bio-Rad CFX Maestro 1.1 software. 16S rRNA was quantified with the 341F (CCTACGGGAGGCAGCAG) and 797R (GGACTACCAGGGTATCTAATCCTGTT) primer pair (Nadkarni et al., 2002). A mix of 5 µL SYBR green, 0.15 µL 341F primer, 0.45 µL 797R primer, 3.4 µL H_20 and 1 µL of sample was prepared for the number of samples, standards and negative control in triplicates with a reaction volume of 10 µL. For standards plasmids with respective genes were used and quantified with Qubit 2.0 (Invitrogen, Carlsbad, CA, USA). Growth in the setups with acetate and H_2 were monitored with OD measurements at 660 nm and cell numbers were calculated based on a calibration curve from Schmidt et al. (2021).

Gas measurement. 15 mL of gas were transferred from the headspace into an exetainer (12 ml) and stored until samples were measured at Heidelberg University. An aliquot of headspace gas (5 mL) was taken from the exetainer vials using a gastight syringe. The gas sample was passed through a chemical trap filled with Drierite® to remove water before entering the analytical system, Methane gas was separated via gas chromatography using a GC-14B (Shimadzu, Japan) equipped with a 2 m column (Ø = 3.175 mm inner diameter) packed with a Molecular Sieve 5A 60/80 mesh from Supelco. Methane was recorded using an FID, and its

concentration was quantified by using two reference gases containing 2.192 parts per million by volume (ppmv) and 9.837 ppmv. Main gases of total headspace composition (H_2, O_2, Ar, N_2, CO) were measured with a GC-2010 Plus (Shimadzu) with a BID-2010- Plus detector and a ST 80/100 mesh, shin carbon column (data not shown).

Stable carbon isotope measurements of CH_4. The $\delta^{13}C$ stable isotope value of CH_4 was analyzed using a continuous flow isotope mass spectrometry system (CF-IRMS) with an inhouse build preconcentration unit and a HP 6890N GC (Agilent, Santa Clara, USA). The samples were transferred to the pre-concentration unit using an evacuated 40 ml sample loop. Methane was pre-concentrated on Hayesep D in a cryo trap and separated from other hydrocarbons by the GC equipped with PoraPLOT Q (Agilent Technologies) (25 m x 0.25 mm i.d., film thickness 8 µm) and a GS-CarbonPLOT capillary column (Agilent Technologies) (30 m x 0.32 mm i.d., film thickness 1.50 µm). The injection temperature was 200°C and the GC is operating with an isothermal oven temperature of 30°C and methane-free helium as carrier gas with a flow of 1.8 $ml*min^{-1}$.

The GC is coupled (open split) to a DeltaPLUSXL isotope ratio mass spectrometer (ThermoQuest Finnigan, 130 Bremen, Germany) with an oxidation reactor (ceramic tube (Al_2O_3), length 320 mm, 1.0 mm i.d., with Ni/Pt wires inside activated by oxygen, reactor temperature 960 °C) and a GC Combustion III Interface (ThermoQuest Finnigan, Bremen, Germany). The working reference gas was CO_2 of high purity (carbon dioxide 4.5, Messer Griesheim, Frankfurt, Germany) with a $\delta^{13}C$ value of -23.6 (VPDB) per mil (calibrated at MPI for Biogeochemistry in Jena, Germany). All $\delta^{13}C$ values were corrected using two daily analyzed reference gases with $\delta^{13}C_{(CH4)}$ value of -42,3 ± 0,2 ‰ and -66,4 ± 0,2 ‰ (VPDB). All samples were normalized with a two-point correction after Paul et al., 2007. The isotopic data are expressed in the δ notation in per mil (‰) versus Vienna Pee Dee Belemnite (VPDB).

Results and discussion

Methane production by anoxygenic photoferrotrophs

Methane was produced during oxidation of Fe(II) by *C. phaeoferrooxidans* KB01, *C. ferroooxidans* KoFox, and *R. palustris* TIE-1. *C. phaeoferrooxidans* KB01 oxidized all initial Fe(II) within 14 days (from 7.2±0.9 mM to 0.2±0.2 mM) and cell numbers rose from initial $1.6x10^3$±$2.7x10^3$ to $7.1x10^6$±$1.0x10^6$ cells/mL (Figure 1 A). As a result, CH_4 production of *C. phaeoferrooxidans* KB01 increased during the experiment reaching the highest value of 0.52±0.03 ppmv (0.28±0.04 nmol CH_4) after 14 days (Figure 1 C). Abiotic CH_4 concentrations did not change over the whole incubation time with a mean concentration of 0.32±0.05 ppmv (average of all individual abiotic controls) and were subtracted from all concentrations measured in the biotic setups. Abiotic CH_4 concentrations resulted from the background air in the vials. δ^{13}C-CH_4 values in the abiotic setup remained stable with an average value of -48.2±1.7 ‰ (reflecting the initial background value), whereas in the biotic setup an enrichment of ^{13}C in the CH_4 could be observed with δ^{13}C-CH_4values starting at -49.1±1.4 ‰ and successively increasing up to 156 ±41 ‰ at the end of the experiment (Figure 1 E). Since in these experiments the initially added CO_2/HCO_3^- was enriched in ^{13}C (5% added, see methods), this unambiguously confirms that the produced CH_4 was formed during the growth of the cells. For the second green-sulfur bacterium tested, i.e. *C. ferrooxidans* KoFox, we observed the same time-trend for CH_4 formation as for *C. phaeoferrooxidans* strain KB01 (Figure S1 A, B). Fe(II) was oxidized from 7.2±0.7 mM to 0.4±0.02 mM after 10 days with $1.3x10^8$±$1.7x10^8$ cells/mL and CH_4 concentrations reached 0.43±0.01 ppmv (0.21±0.02 nmol CH_4; please note: only 2 out of 3 bottles showed CH_4 and δ^{13}C isotopic enrichment) (Figure S1). δ^{13}C-CH_4 values were slightly enriched from -50.9±1.1 ‰ to -43.3±1.2 ‰ δ^{13}C-CH_4 after (abiotic δ^{13}C-CH_4 was -49.1±0.3 ‰).

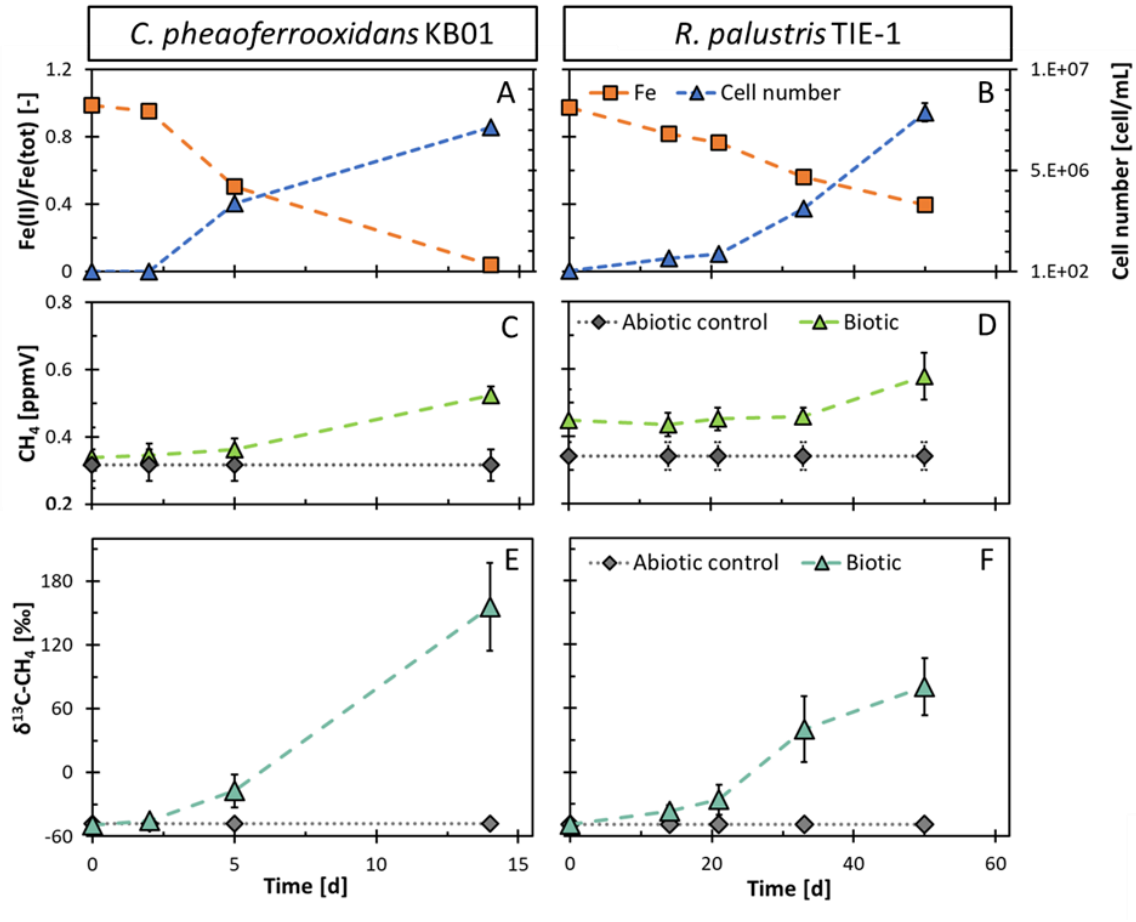

Figure 1: C. phaeoferrooxidans KB01 *(A, C and E) and R. palustris* TIE-1 *(B, D and F) grown with Fe(II). Panels A and B shown Fe(II)/Fe total ratio and cell numbers. Panels C and D show CH_4 concentrations and panels E and F $\delta^{13}C$-CH_4 values produced in the serum vial. In panel C and D t0 CH_4 concentrations are from the background air. Error bars result from biological triplicates.*

In case of *R. palustris* TIE-1, in addition to Fe(II), also two other substrates, i.e. acetate and H_2, were tested. When growing on Fe(II), *R. palustris* TIE-1 oxidized 60.4±0.3% of Fe(II), starting from 9.6±0.3 mM to 3.9±0.2 mM after 50 days and cell number reached $7.9x10^6$±$3.8x10^6$ cells/mL from initial $3.7x10^4$±$1.0x10^4$ cells/mL (Figure 1 B). Concurrently, an increase in CH_4 concentration up to 0.58±0.07 ppmv (0.32±0.09 nmol CH_4) accompanied by an enrichment of ^{13}C leading to a $\delta^{13}C$-CH_4 value of up to 80.4±26.9 ‰ was observed (the abiotic control value was -49±1.4 ‰) (Figure 1 D, F). When oxidizing acetate and H_2, CH_4 concentrations also rose in *R. palustris* TIE-1 cultures (Figure S1). With acetate, the CH_4 concentration rose to 0.76±0.02 ppmv (0.77±0.04 nmol CH_4) with an isotopic value of $\delta^{13}C$-CH_4 up to -39±3 after 6

days (Figure S1 C, D). With H_2, the CH_4 concentration rose to 1.9±0.9 ppmv (2.0±1.0 nmol CH_4) after 14 days with isotopic value of $\delta^{13}C$-CH_4 up to 195±145 ‰ (Figure S1 E, F). Again, since in these H_2-experiments the initially added CO_2/HCO_3^- was enriched in ^{13}C (by 5%), this again verifies that the produced CH_4 was formed during cell growth of the biotic experiments. In summary, we found that photoferrotrophs can produce CH_4 as a by-product during growth on H_2, acetate and Fe(II) – this is the first report stating CH_4 production during microbial Fe(II) oxidation.

CH_4 production by photoferrotrophs compared to CH_4 production by other microorganisms

To compare CH_4 production by these three different photoferrotrophs, we calculated the CH_4 production rate per cell (Figure 2A). The production of CH_4 production per cell was highest with H_2, followed by Fe(II) and acetate. Highest values were obtained for *R. palustris* TIE-1 growing on H_2 with 3.6±1.8 amol CH_4/cell, followed with Fe(II) (1.7±1.1 amol CH_4/cell) and lowest production were produced with acetate 0.95±0.07 amol CH_4/cell. CH_4 formation for *C. phaeoferrooxidans* KB01 was 1.6±0.05 amol CH_4/cell and lowest formation in all setups were found in *C. ferrooooxidans* KoFox with 0.3±0.17 amol CH_4/cell on Fe(II).

Additionally, we calculated the rates of CH_4 per cell and day as the experiments ran over different periods of time (Figure 2B). We observed that most CH_4 was produced by *R. palustris* TIE-1 growing on H_2 and acetate (0.4±0.2 amol CH_4/(cell*d) and 0.16±0.01 amol CH_4/(cell*d), respectively). The third highest rate of CH_4 formation was observed during Fe(II) oxidation by *C. phaeoferrooxidans* KB01 with 0.11±0.004 amol CH_4/(cell*d) and was almost three times higher than values from *R. palustris* TIE-1 and *C. ferrooooxidans* KoFox grown on Fe(II) (0.04±0.04 amol CH_4/(cell*d) and 0.03±0.01 amol CH_4/(cell*d), respectively). To further compare setups with Fe(II) we calculated the CH_4 production rates per 1 mol oxidized Fe(II)

and found that *R. palustris* TIE-1 produced 0.3±0.2 amol CH_4/cell similar as *C. phaeoferrooxidans* KB01 with 0.23±0.02 amol CH_4/cell, whereas *C. ferrooooxidans* KoFox produced the least amount with 0.05±0.02 amol CH_4/cell (Figure 2C). We next compared the observed rates by anoxygenic phototrophic bacteria with non-methanogenic bacteria/organisms such purple non-sulfur phototrophs but also with aerobic microorganisms.

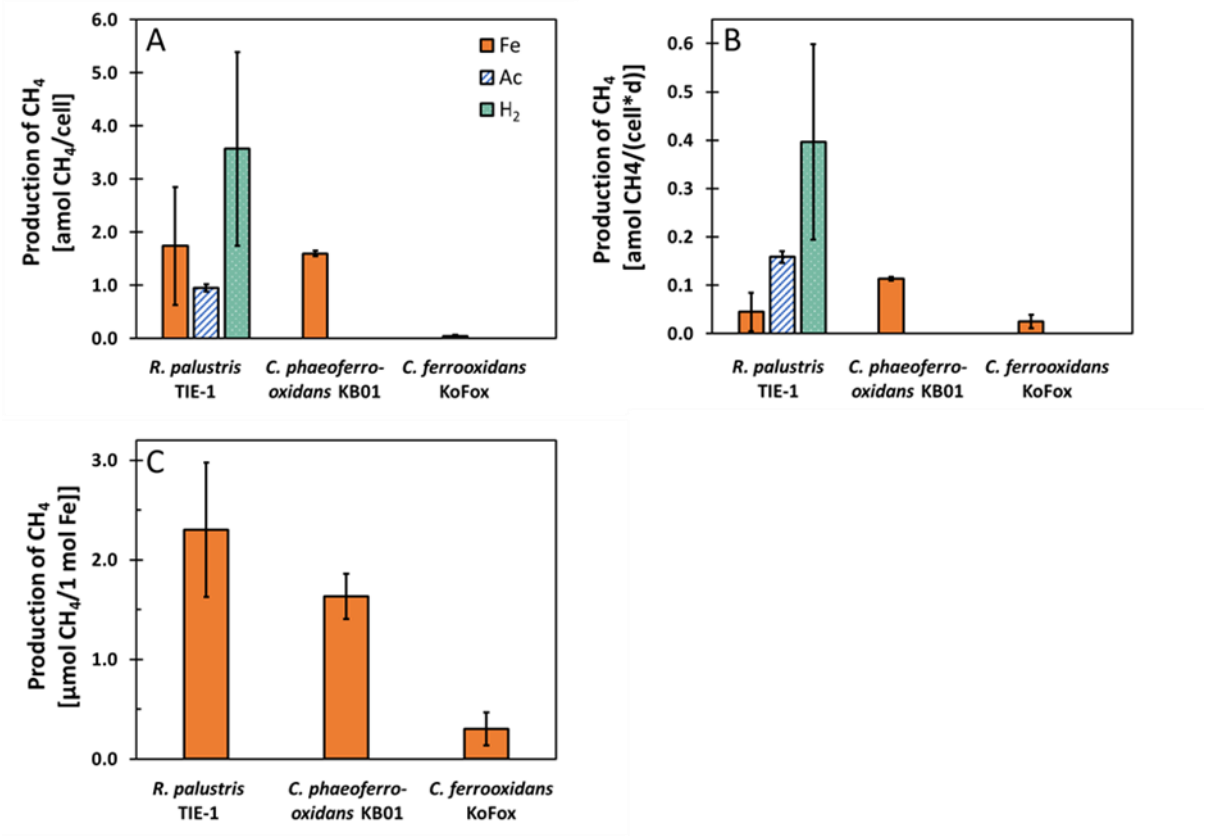

Figure 2: Panel A shows production of CH_4 per cell for R. palustris TIE-1*, C. phaeoferrooxidans* KB01 *and C. ferrooxidans* KoFo*x grown with acetate, H_2 and Fe(II). Panel B shows production of CH_4 per cell and per day for R. palustris* TIE-1*, C. phaeoferrooxidans* KB01 *and C. ferrooxidans* KoFox*. Panel C shows production of CH_4 per 1 mol Fe(II) oxidized for R. palustris TIE-1, C. phaeoferrooxidans KB01 and C. ferrooxidans* KoFox*. Error bars result from biological triplicates, values from C. ferrooxidans* KoFo*x resulted from biological duplicates.*

Previous studies have shown that purple non-sulfur phototrophs can produce CH_4 when growing with different organic compounds in the absence of ammonia to enhance the activity of their nitrogenase (Fixen et al., 2016; Zheng et al., 2018). Fixen et al. (2016) found that *R.*

palustris strain CGA009 produced 30 nmol CH_4 per mg total protein with an engineered nitrogen fixation (*Nif*) gene and 20 mM acetate at the end of the experiment. If we assume 50% of the cell dry weight is protein (Nasseri et al., 2011; Simon & Azam, 1989) and a cell weighs 1 pg, the CH_4 production by strain CGA009 would be 15 amol/cell . As shown in Zheng et al. (2018), *R. palustris* strain CGA010 produced 150 nmol CH_4 per mg total protein (75 amol/cell if 50% protein per cell is assumed; 20 mM acetate) and could even facilitate growth in a methanotrophic co-culture. These values are 1 order of magnitude higher than the production we measured with *R. palustris* TIE-1 with acetate as growth substrate. One reason for that could be that in our case we added ammonia as N-source to the media and therefore did not specifically activate the nitrogenase. Genomic data shows that both *R. palustris* TIE-1 and the green sulfur bacteria *C. phaeoferrooxidans* KB01 and *C. ferroooxidans* KoFox have nitrogen-fixing genes (Thompson et al., 2017) which could be an additional way to produce CH_4. Nevertheless, we observed biogenic production of CH_4 in our experiments, even in the presence of added ammonium.

Another non-enzymatic way of CH_4 production via ROS was studied by Ernst and colleagues (Ernst et al., 2022) proposing that all aerobic organisms produce CH_4 *per se*. They found that *E. coli* produced 0.04 amol CH_4/ (cell*d) under oxic conditions. This methane production rate is in the same range as observed for our photoferrotrophs which showed CH_4 production from 0.03 to 0.4 amol CH_4/(cell*d) under anoxic conditions. However, *E. coli* responded strongly to stressors like HOCl and Fe(II) (50 µM) increasing methane production rate by two to three orders of magnitude. In contrast to their observation, our tested photoferrotrophs did not respond in such a significant way when Fe(II) was added. This shows how well adapted photoferrotrophs are too high levels of Fe (in our experiment up to 8 mM). Our findings reinforce and extend previous results that various microorganisms and higher life forms release

some methane. Additionally, we could also show that anoxygenic photoferrotrophs generate methane in comparable levels, thereby contributing in environments where they thrive.

Implications for early earth

Due to the high abundance of photoferrotrophs in the Archean oceans, we calculated the potential contribution of phototrophic Fe(II)-oxidizer to the overall CH_4 production during early earth from 4 to 2.5 Ga ago. If we assume a coastal zone of $3.6*10^{12}$ m^2 (Martin et al., 1987) with a water column of 20 m depth and a bacterial density of 10^6 cells/mL (F. Azam et al., 1983). This would result in a total of $7.2*10^{25}$ cells in the coastal area. If we further assume a methane formation rate of 0.04 to $0.4*10^{-18}$ mol per cell per day (see figure 2B), this yields methane formation of 0.29 to 2.9 $*10^7$ mol CH_4 per day; multiplied by 365 (days) resulting in $1*10^9$ mol to $1*10^{10}$ mol CH_4 per year. This would account for a contribution of 0.0004-0.004% by the photoferrotrophs to the total CH_4 formation of $250*10^{12}$ mol CH_4 per year (Pavlov et al., 2000)). This indicates that CH_4 production by photoferrotrophs might only had a minor impact on CH_4 formation in ancient oceans. Nevertheless, it could be that the contribution still is substantial if we look only at the biologically produced CH_4. Laasko and Schrag (2019) proposed two scenarios and respective biological production rates. In the first scenario biological production would be 0.5-3 Tmol CH_4 per year assuming limited hydrogen recycling and a productive community dominating by oxygenic phototrophs (Laakso & Schrag, 2019). In this case photoferrotrophs could have contributed up to 0.3-2 % of the biological CH4 production. In the second scenarios oxygen levels are low enough for efficient hydrogen recycling allowing oxygenic or anoxygenic photosynthesis and would result in 50 Tmol CH_4 per year. If phosphorous would be limited production could decrease to 20 Tmol CH_4 per year and anoxygenic photoferrotrophs could have contributed 0.2-0.05 % of biologically produced CH_4. In total, the contribution of CH_4 production by photoferrotrophs is relatively modest.

However, this should not diminish the potential significance of CH_4 for the bacterial community.

References

Azam F., T. Fenchel, J. G. Field, J. S. Gray, L. A. M.-R. and F. T. (1983). *The Ecological Role of Water-Column Microbes in the Sea*. MARINE ECOLOGY - PROGRESS SERIES. https://www.degruyter.com/document/doi/10.7208/chicago/9780226125534-024/pdf

Bižić, M., Klintzsch, T., Ionescu, D., Hindiyeh, M. Y., Günthel, M., Muro-Pastor, A. M., Eckert, W., Urich, T., Keppler, F., & Grossart, H. P. (2020). Aquatic and terrestrial cyanobacteria produce methane. *Science Advances*, *6*(3). https://doi.org/10.1126/SCIADV.AAX5343/SUPPL_FILE/AAX5343_SM.PDF

Bryce, C., Blackwell, N., Schmidt, C., Otte, J., Huang, Y. M., Kleindienst, S., Tomaszewski, E., Schad, M., Warter, V., Peng, C., Byrne, J. M., & Kappler, A. (2018). Microbial anaerobic Fe(II) oxidation – Ecology, mechanisms and environmental implications. *Environmental Microbiology*, *20*(10), 3462–3483. https://doi.org/10.1111/1462-2920.14328

Camacho, A., Walter, X. A., Picazo, A., & Zopfi, J. (2017). Photoferrotrophy: Remains of an ancient photosynthesis in modern environments. *Frontiers in Microbiology*, *8*(MAR). https://doi.org/10.3389/fmicb.2017.00323

Conrad, R. (2009). The global methane cycle: Recent advances in understanding the microbial processes involved. *Environmental Microbiology Reports*, *1*(5), 285–292. https://doi.org/10.1111/J.1758-2229.2009.00038.X

Ernst, L., Barayeu, U., Hädeler, J., Dick, T. P., Klatt, J. M., Keppler, F., & Rebelein, J. G. (2023). Methane formation driven by light and heat prior to the origin of life and beyond. *Nature Communications*, *14*(1), 0–9. https://doi.org/10.1038/s41467-023-39917-0

Ernst, L., Steinfeld, B., Barayeu, U., Klintzsch, T., Kurth, M., Grimm, D., Dick, T. P., Rebelein, J. G., Bischofs, I. B., & Keppler, F. (2022). Methane formation driven by reactive oxygen species across all living organisms. *Nature*, *603*(7901), 482–487. https://doi.org/10.1038/s41586-022-04511-9

Fixen, K. R., Zheng, Y., Harris, D. F., Shaw, S., Yang, Z. Y., Dean, D. R., Seefeldt, L. C., & Harwood, C. S. (2016). Light-driven carbon dioxide reduction to methane by nitrogenase in a photosynthetic bacterium. *Proceedings of the National Academy of Sciences of the United States of America*, *113*(36), 10163–10167. https://doi.org/10.1073/pnas.1611043113

Hegler, F., Posth, N. R., Jiang, J., & Kappler, A. (2008). *Physiology of phototrophic iron (II) -oxidizing bacteria : implications for modern and ancient environments*. *66*(Ii), 250–260. https://doi.org/10.1111/j.1574-6941.2008.00592.x

Holland, H. D. (1973). The Oceans; A Possible Source of Iron in Iron-Formations. *Economic Geology*, *68*(7), 1169–1172. https://doi.org/10.2113/gsecongeo.68.7.1169

Keppler, F., Hamilton, J. T. G., Braß, M., & Röckmann, T. (2006). *Methane emissions from terrestrial plants under aerobic conditions*. https://doi.org/10.1038/nature04420

Laakso, T. A., & Schrag, D. P. (2019). Methane in the Precambrian atmosphere. *Earth and Planetary Science Letters*, *522*, 48–54. https://doi.org/10.1016/j.epsl.2019.06.022

Lenhart, K., Bunge, M., Ratering, S., Neu, T. R., Schüttmann, I., Greule, M., Kammann, C., Schnell, S., Müller, C., Zorn, H., & Keppler, F. (2012). Evidence for methane production by saprotrophic fungi. *Nature Communications*. https://doi.org/10.1038/ncomms2049

Lenhart, K., Klintzsch, T., Langer, G., Nehrke, G., Bunge, M., Schnell, S., & Keppler, F. (2016). Evidence for methane production by the marine algae Emiliania huxleyi. *Biogeosciences*, *13*, 3163–3174. https://doi.org/10.5194/bg-13-3163-2016

Martin, J. H., Knauer, G. A., Karl, D. M., & Broenkow, W. W. (1987). VERTEX: carbon cycling in the northeast Pacific. *Deep Sea Research Part A, Oceanographic Research Papers*, *34*(2), 267–285. https://doi.org/10.1016/0198-0149(87)90086-0

Morris, R. C. (1993). Genetic modelling for banded iron-formation of the Hamersley Group,

Pilbara Craton, Western Australia. *Precambrian Research*, *60*, 243–286.
Nadkarni, M. A., Martin, F. E., Jacques, N. A., & Hunter, N. (2002). Nadkarni MA 2002 Bacterial load by real time qPCR.pdf. *Microbiology (Reading, England)*, *148*(Pt 1), 257–266. papers3://publication/uuid/720C1476-57B5-40A2-AC1C-EA8708B08F2E
Nasseri, A. T., Rasoul-Amini, S., Morowvat, M. H., & Ghasemi, Y. (2011). Single cell protein: Production and process. *American Journal of Food Technology*, *6*(2), 103–116. https://doi.org/10.3923/ajft.2011.103.116
Pavlov, A. A., Kasting, J. F., Brown, L. L., Rages, K. A., & Freedman, R. (2000). Greenhouse warming by CH4 in the atmosphere of early Earth. *Journal of Geophysical Research: Planets*, *105*(E5), 11981–11990. https://doi.org/10.1029/1999JE001134
Schmidt, C., Nikeleit, V., Schaedler, F., Leider, A., Lueder, U., Bryce, C., Hallmann, C., & Kappler, A. (2021). Metabolic Responses of a Phototrophic Co-Culture Enriched from a Freshwater Sediment on Changing Substrate Availability and its Relevance for Biogeochemical Iron Cycling. *Geomicrobiology Journal*, *38*(3), 267–281. https://doi.org/10.1080/01490451.2020.1837303
Simon, M., & Azam, F. (1989). Protein content and protein synthesis rates of planktonic marine bacteria. *Marine Ecology Progress Series*, *51*(3), 201–213. https://doi.org/10.3354/meps051201
Thompson, K. J., Simister, R. L., Hahn, A. S., Sj, H., & Crowe, S. A. (2017). Nutrient Acquisition and the Metabolic Potential of Photoferrotrophic Chlorobi. *Nutrient Acquisition and the Metabolic Potential of Photoferrotrophic Chlorobi. Front. Microbiol*, *8*, 1212. https://doi.org/10.3389/fmicb.2017.01212
Vorholt, J., Kunow, J., Stetter, K. O., Thauer, R. K., Vorholt, J., Kunow K Thauer, J. R., & Stetter, K. O. (1995). Enzymes and coenzymes of the carbon monoxide dehydrogenase pathway for autotrophic C02 fixation in Archaeoglobus lithotrophicus and the lack of carbon monoxide dehydrogenase in the heterotrophic A. profundus. *Arch Microbiol*, *163*, 112–118.
Zheng, Y., Harris, D. F., Yu, Z., Fu, Y., Poudel, S., Ledbetter, R. N., Fixen, K. R., Yang, Z. Y., Boyd, E. S., Lidstrom, M. E., Seefeldt, L. C., & Harwood, C. S. (2018). A pathway for biological methane production using bacterial iron-only nitrogenase. *Nature Microbiology*, *3*(3), 281–286. https://doi.org/10.1038/s41564-017-0091-5

Supplements

Table S1: Media composition of C. ferrooxidans KoFox*, R. palustris* TIE-1 *and C. phaeoferrooxidans* KB01

Organism	Salts	Buffer	Additives
C. ferrooxidans KoFox	0.0025 g/L $MgSO_4 \cdot 7\ H_2O$, 0.4 g/L $MgCl_2 \cdot 6\ H_2O$, 0.1 g/L $CaCl_2 \cdot 2\ H_2O$ 0.6 g/L KH_2PO_4, 0.3 g/L NH_4Cl	1.85 gL/ $NaHCO_3$ buffer	1 mL/L sterile filtered 7-vitamin solution (Widdel & Pfenning, 1981), 1 mL/ trace element solution (Widdel, 1983) and 1 m/L selenite-tungstate solution (Widdel & Bak, 1992)
R. palustris TIE-1	0.5 g KH_2PO_4, 0.3 g NH_4Cl, 0.5 g $MgSO_4 * 7H_2O$, 0.1 g $CaCl_2*2H_2O$	1.85 gL/ $NaHCO_3$ buffer	10 mL/L filter-sterilized vitamin solution (altered from Ehrenreich & Widdel, 1994; containing 50 mg/L riboflavin), 1 mL/L SL10 trace element solution (Widdel, 1983), 1 mL/L selenite-tungstate solution (Widdel & Bak, 1992) and 0.1mg/L vitamin B12 solution (c=100 mg/L) were added
C. phaeoferrooxidans KB01	0.6 g/L KH_2PO_4, 0.3 g/L NH_4Cl, 0.025 g/L $MgSO_4 \cdot 7\ H_2O$, 0.4 g/L $MgCl_2 \cdot 6\ H_2O$, 0.1 g/L $CaCl_2 \cdot 2\ H_2O$	1.85 gL/ $NaHCO_3$ buffer	1 mL/L sterile filtered 7-vitamin solution (Widdel & Pfenning, 1981), 1 mL/ trace element solution (Widdel, 1983) and 1 m/L selenite-tungstate solution (Widdel & Bak, 1992)

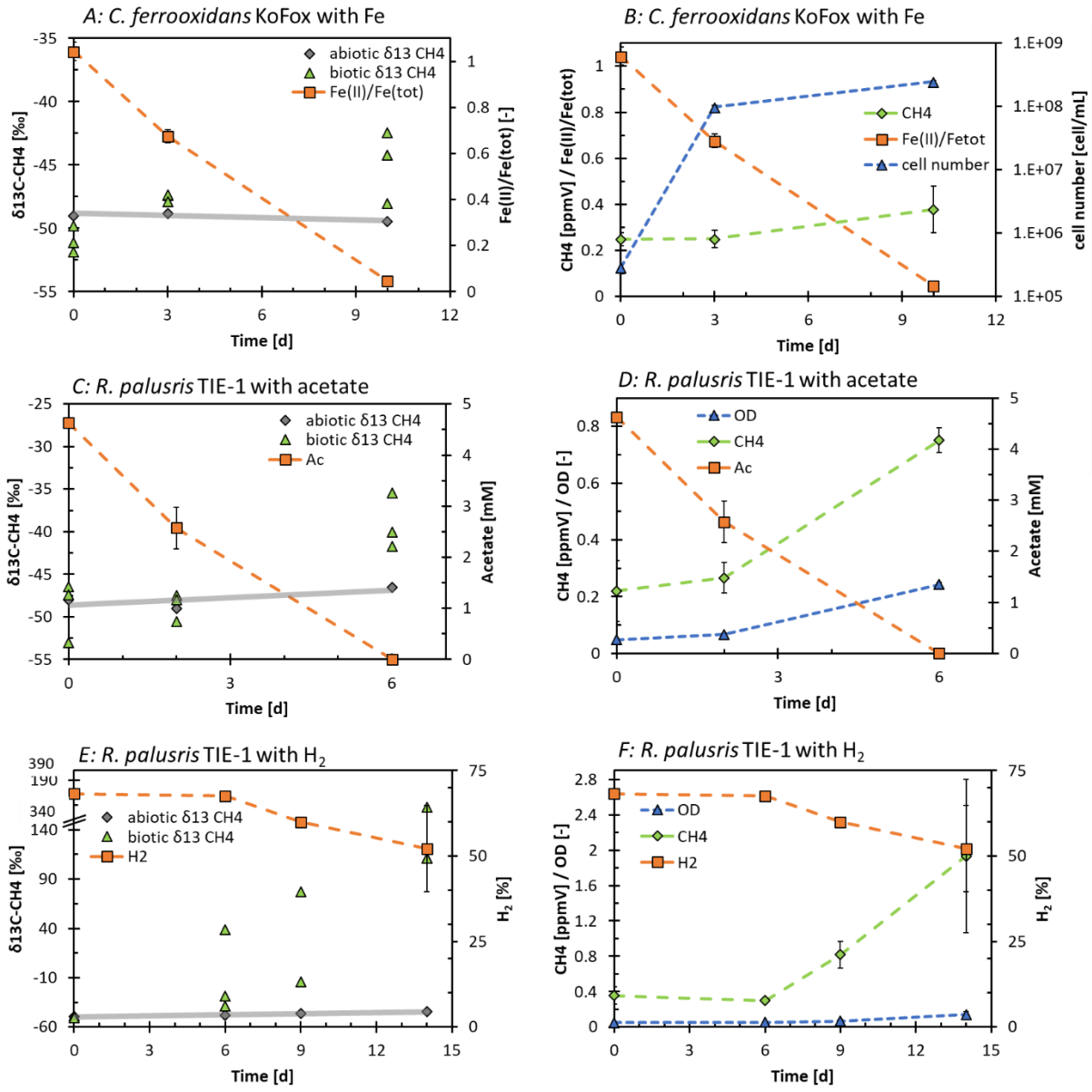

Figure 1S: Figure shows growth of C. ferrooxidans KoFox *on Fe (A, B) and R. palustris* TIE-1 *on acetate (C, D) and H_2 (E, F) while producing CH_4. In panel B, D and F t0 CH_4 concentrations are from the background air. Error bars result from biological triplicates.*

8 Chapter: Enrichment of phototrophic and microaerophilic Fe(II)-oxidizers

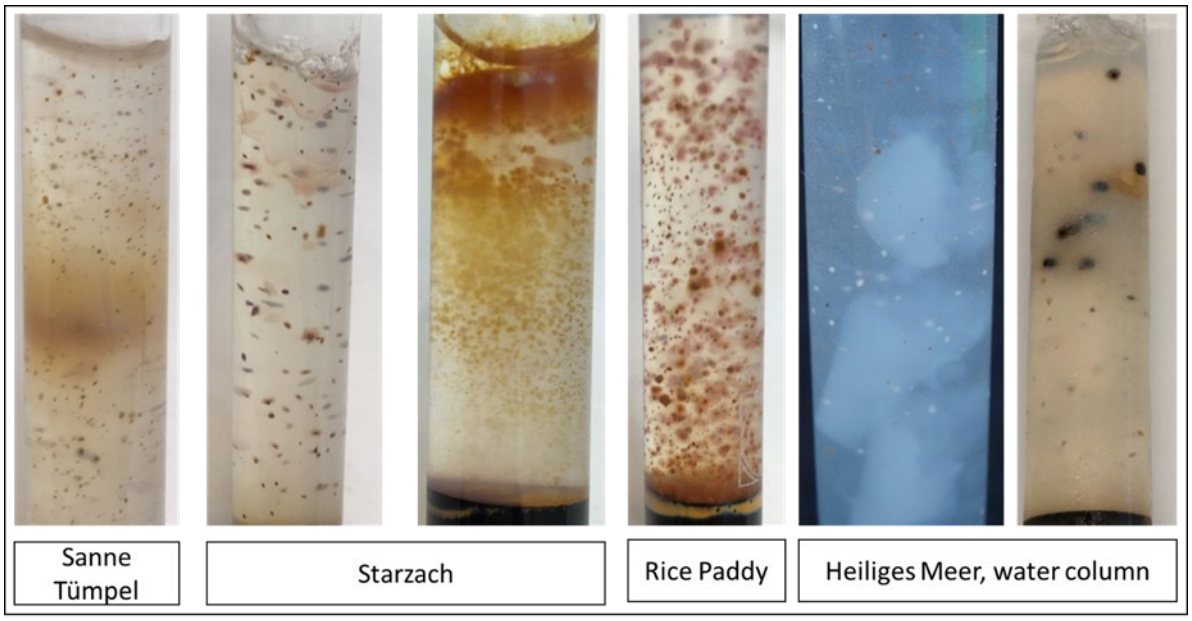

Contributions:

Resources were provided by Dr. C. Bryce and Prof. Dr. A. Kappler. The project was designed by me and conducted by me, P. Liebrecht and J. C. Lopez-Rivoldi. D. Straub performed bioinformatic analyses. The chapter was written by me.

Enrichment of phototrophic and microaerophilic Fe(II)-oxidizers

Verena Nikeleit[1], Philip Liebrecht[1], Jimena C. Lopez-Rivoldi[1], Daniel Straub[2], Andreas Kappler[1,3] and Casey Bryce[4]

[1]Department of Geoscience, University of Tübingen, Tübingen, Germany

[2]Quantitative Biology Center (QBiC), University of Tübingen, Tübingen, Germany

[3]Cluster of Excellence: EXC 2124: Controlling Microbes to Fight Infections, Tübingen, Germany

[4]School of Earth Sciences, University of Bristol, Bristol, UK

Introduction

Iron metabolizing bacteria are ubiquitous in the environment and facilitate Fe(II) oxidation and Fe(III) reduction especially in microoxic and anoxic environments (Bryce et al., 2018; Kappler et al., 2021). During Fe(II) oxidation and subsequent Fe(III) mineral formation many other elemental cycles (carbon, sulfur and nitrogen) are affected and nutrients, contaminants and organic matter can be sequestered and become inaccessible to microbes (Eickhoff et al., 2014; Kappler et al., 2021; Lalonde et al., 2012; Mu et al., 2016; Tipping, 1981; Zhao et al., 2017). However, currently our knowledge on the physiology, metabolism and role of various Fe(II)-oxidizers in the environment is incomplete. Therefore, it is imperative to try to enrich and isolate new strains of these microbes.

One kind of Fe(II)-oxidizer are microaerophilic Fe(II)-oxidizers. Prominent representatives are found in the freshwater genera *Gallionella, Sideroxydans, Lepthothrix* and the marine genera *Mariprofundus* (Fleming et al., 2011; Kucera & Wolfe, 1957; Singer et al., 2011; Weiss et al., 2007). In microoxic environments with up to 20 µM O_2 these bacteria are able to compete with the abiotic Fe(II) oxidation as they need small amounts of oxygen for them to oxidize Fe(II) and fix CO_2 (Maisch et al., 2019). They have been found in various environments such as freshwater and marine sediments, biological mats at black smokers and in paddy soils (Emerson & Moyer, 2002; Nakagawa et al., 2020; Otte et al., 2018). In this study we tried to isolate microaerophilic bacteria from a high alpine iron rich spring and from a mofette which is high in iron and carbonate.

Additionally, enrichments were performed for phototrophic Fe(II)-oxidizers. Since the discovery of this microbial metabolism in the early 1990s only a handful of isolates were isolated and characterised (Bryce et al., 2018; Ehrenreich & Widdel, 1994; Friedrich Widdel et al., 1993). These isolates come from freshwater and marine sediments, iron rich ditches and stratified lakes (Crowe et al. 2017; Heising et al. 1999; Jiao et al. 2005; Straub et al. 1999). Although the importance of phototrophic Fe(II)-oxidizers in stratified lakes has been identified

only one isolated strain is in culture (Berg et al., 2016; Crowe et al., 2017; Llirós et al., 2015). Therefore, adding new isolates, especially from different environments would add to our understanding of their importance in these systems. Another main objective was to isolate anoxygenic photoferrotrophs from soils. So far, no study was able to successfully isolate these bacteria from this habitat which leaves open questions to their importance and abundance there. Consequently, we took samples from different soils with the aim of isolating anoxygenic photoautotrophic Fe(II) oxidizers as well as microaerophilic Fe(II) oxidizers.

Material and methods

Field sites. For the enrichments following sites were chosen and are shown in Table 1:

Table 1: List of field site of phototrophic and microaerophilic Fe(II)-oxidizer with coordinates.

Enrichment name	Field site	Coordinates	Origin of sample	Type of enrichment
Rice paddy	Rice paddy soil, Italy	45.323889, 8.373611	soil, upper 20 cm	Phototrophic Fe(II)-oxidizer
Sanne Tümpel, Brocken	Brocken, Germany	51.802945, 10.552079	Iron-rich pond	Phototrophic Fe(II)-oxidizer
Heiliges Meer stream	Großes Heiliges Meer, Germany,	52.350738, 7.634967	stream next to Großes Heiliges Meer, Sediment	Phototrophic Fe(II)-oxidizer
Starzach	Mofette, Starzach, Germany	48.44304, 8.819249	Iron and carbonate-rich spring, sediment	Phototrophic and microaerophilic Fe(II)-oxidizer
Heiliges Meer water column	Großes heiliges Meer, Germany	52.350738, 7.634967	Water column 7 m	Phototrophic Fe(II)-oxidizer
Engadin	Engadin, Switzerland	46.805326, 10.321643	Iron-rich spring, sediment	Phototrophic and microaerophilic Fe(II)-oxidizer

Sampling. Sediment/soil samples were taken with a spatula into a sterile falcon tube or plastic bag and stored in the dark at 4°C. For the Heiliges Meer water column enrichment a sample from a promising bottle from the *in situ* experiment in chapter 2 (set up with Fe(II) only) was taken and transferred to new media.

Phototrophic Fe(II)-oxidizer enrichment. For phototrophic Fe(II)-oxidizers enrichments 0.5-1.0 g of sediment was put into a 58 mL serum vial filled with 25 mL media. Media consisted of 0.14 g/L KH_2PO_4, 0.3 g/L NH_4Cl, 0.025 g/L $MgSO_4 \cdot 7\ H_2O$, 0.4 g/L $MgCl_2 \cdot 6\ H_2O$, 0.1 g/L $CaCl_2 \cdot 2\ H_2O$ and 0.2 g/L NaCl per 1 L ultrapure water and autoclaved at 121°C for 20 min in a Widdel flask. After autoclaving the media was cooled to room temperature under an N_2/CO_2 atmosphere (90:10 v:v) and buffered with anoxic 22 mM bicarbonate buffer. Aliquots of 1 mL/L sterile filtered 7-vitamin solution (F Widdel & Pfenning, 1981), trace element solution

(Widdel, 1983) and selenite-tungstate solution (F Widdel & Bak, 1992) were added and the pH was adjusted to 7 with anoxic and sterile 0.5 M $NaHCO_3$ or 1 M HCl. For the enrichment "Sanne Tümpel" 0.6 g/L KH_2PO_4 and no NaCl was used. Approximately 0.5 to 1 g of sample were put into the serum vial under sterile conditions and the headspace was flushed with N_2/CO_2. Afterwards 5 mM $FeCl_2$ and 10 µM DCMU (3-(3,4-dichlorophenyl)-1,1-dimethylurea) were added, in case of Heiliges Meer water column 2 mM $FeCl_2$. Serum vials were placed into a light incubator at 20°C with 40 W light bulb. Once Fe(II) oxidation and an increase of living cells under the microscope were observed 10% were transferred into a new vial.

Isolation approach for photoferrotrophs. Agar Shakes were chosen for isolation method for photoferrotrophs (Schmidt et al., 2021). In a 60°C water bath a sterile agar solution (15 g "Agar Agar Kobe 1" in 1 L MQ water) was maintained. The second water bath (~38°C) contained the media, the enrichment, and a rack holding 6 15 mL test tubes for each enrichment. Throughout the entire process, the tubes were purged with N_2/CO_2 (90:10, v:v), and precautions were taken to ensure anoxic conditions, including purging the media bottle and using an anoxic syringe for transferring the enrichment. Initially, 3 mL of the agar solution were pipetted into each tube, followed by the addition of 6 mL of media. Subsequently, 1 mL of the enrichment was transferred to the first tube and thoroughly mixed through pipetting in the agar-media mixture. After that 1 mL was extracted and transferred into the next tube, repeating this process until the 6^{th} tube was reached and sealed with a sterile butyl stopper. The test tubes were then placed inside a light incubator with 40 W light bulb at a constant temperature of 20°C. After single colonies were formed, they were picked under sterile and anoxic conditions and transferred into liquid culture with 5/2 mM $FeCl_2$. If Fe(II) oxidation was observed in the liquid culture, the Agar Shakes were repeated 2 times.

Microaerophilic Fe(II)-oxidizer enrichment. Initial enrichment of microaerophilic Fe(II)-oxidizers were performed on zero valent iron (ZVI). 0.5 g of sediment was incubated with approximately 0.25 g sterile Fe^0 and 8 mL modified Wolfs media (MWMM) (Laufer et al., 2016). After successful growth was confirmed under the microscope the enrichment was then transferred to gradient tubes.

Gradient tubes were prepared after Emerson and Floyd and FeS was prepared after a modified version of Kucera and Wolfe (Emerson & Floyd, 2005; Kucera & Wolfe, 1957; Lueder et al., 2018). Headspace vials for the bottom FeS layer consisted of 0.1 g high melt agar, 5 mL MWMM and 5 mL FeS solution. The Top layer was prepared with 0.15 g low melt agar, 0.084 g $NaHCO_3$ and 100 mL MWMM (pH 6.5). Both solutions were prepared anoxically and autoclaved at 121°C for 20 minutes. First 760 µL of bottom layer were filled in sterile vials, followed by 3.875 mL of top layer (100 µL of 7 vitamin solution and 100 µL trace element solution was added after autoclaving to the top layer). The headspace was flushed with N_2/CO_2 (90/10, v/v) and closed with a sterile butyl stopper. By opening of the sterile vials the next day oxygen entered the system thus creating a gradient of oxygen through the top whilst a gradient of iron from the bottom was formed. 100 µL of inoculum was added in the top layer. Growth was determined via visual changes, such as biofilm development and colour changes, in combination with Dead/Live stain (Live/Dead^{TM} BacLight^{TM}, Invitrogen, Thermo Fisher Scientific, USA) under the microscope (Leica DM5500 B).

Fe quantification. Fe(II) and Fe total was quantified with the Ferrozine assay modified by (Hegler et al., 2008). 0.1 mL of sample was added to 0.9 mL 1 M HCl and stored at 5°C until analysis.

16S rRNA gene amplicon sequencing and analysis. For DNA extraction 1.8 mL of samples were taken from the enrichment cultures. DNA was extracted using the UltraClean R Microbial DNA Isolation Kit (MO BIO Laboratories, Carlsbad, CS, USA) and the quantity of the DNA was measured with a Nanodrop ND-1000 Spectrometer (Nanodrop^{TM} 1000, Thermo Scientific, Waltham, MA, USA). DNA was amplified by using forward primer 16S-515F and reverse primer 16S-806R (Caporaso et al., 2011) targeting the V4 region of the 16S ribosomal RNA. Library preparation steps (Nextera, Illumina) and 250 bp paired-end sequencing with MiSeq (Illumina, San Diego, CA, USA) using v2 chemistry were performed by Microsynth AG (Balgach, Switzerland). Between 45,414 and 76,173 read pairs were obtained for each of the 8 samples (in total 451,913 read pairs). Sequencing data was analyzed with nf-core/ampliseq v2.3.1, which includes all analysis steps and software and is publicly available(Ewels et al., 2020; D. Straub et al., 2020), with Nextflow v21.10.3 (Di Tommaso et al., 2017) and singularity v3.8.7 (Kurtzer et al., n.d.). Primers were trimmed, and untrimmed sequences were discarded (<32% per sample) with Cutadapt version 3.4 (Martin, 2011). Adapter and primer-free sequences were processed with DADA2 v1.22.0 (Callahan et al., 2016) to eliminate PhiX contamination, trim reads (before median quality drops below 35; forward reads were trimmed at 194 bp and reverse reads at 207 bp), correct errors, merge read pairs, and remove polymerase chain reaction (PCR) chimeras; ultimately, 160 amplicon sequencing variants (ASVs) were obtained across all samples. Taxonomic classification was performed with DADA2 and the SILVA v138 database(Quast et al., 2012). Intermediate results were imported into QIIME2 version 2021.8.0 (Bolyen et al., 2019). 3 ASVs classified as chloroplasts or mitochondria were removed, totaling <0.1% relative abundance per sample, and retaining 157 ASVs across all samples. Alpha rarefaction curves were produced with the QIIME2 diversity alpha-rarefaction plugin, which indicated that the richness of the samples had been fully observed.

Result and discussion

Successful enrichment of phototrophic Fe(II)-oxidizers was achieved from a stratified lake (Großes Heiliges Meer, Germany), an iron-rich stream (next to Großes Heiliges Meer, Germany), an iron-rich pond (Sanne Tümpel, Brocken im Hartz, Germany), an iron and carbonate-rich spring (mofette, Starzach, Germany) and from a rice paddy soil (0-20 cm, Vercelli, Italy) (Figure 1). Starzach and Rablönch have been characterized in detail by Liebrecht (Liebrecht, 2022). Iron extractions, XRD and Mössbauer revealed the iron content ranges between 10-20% and consist of Fe carbonates, ferrihydrite and (nanoscale) goethite (Liebrecht, 2022). In Großes Heiliges Meer, water column Fe(II) concentration were 0.1 mM and more geochemical data can be found in chapter 4 and Swanner et al. (2022).

Figure 1: Map of phototrophic and microaerophilic Fe(II)-oxidizers (A). Panel B (Heiliges Meer), C (Starzach) and D(Rablönch) show more detailed picture of these sampling sites.

All phototrophic Fe(II)-oxidizers completely oxidized all Fe(II) (2 or 5 mM) in 3 to 6 weeks. Fe(III) minerals looked bright orange-brown for Heiliges Meer stream, Rice Paddy and Starzch whereas Fe(III) minerals appeared light beige-brown for Heiliges Meer 7 m water column and Sanne Tümpel (Figure 2). Microaerophilic Fe(II)-oxidizer enrichments were successful for the two sites Starzach and Rablönch. After growth on ZVI plates the enrichments were transferred to gradient tubes (Figure 2). We could detect sharp lines (indicated by arrow in Figure 2) and cloudy formations that are associated by microaerophilic Fe(II)-oxidizer (Lueder et al., 2018).

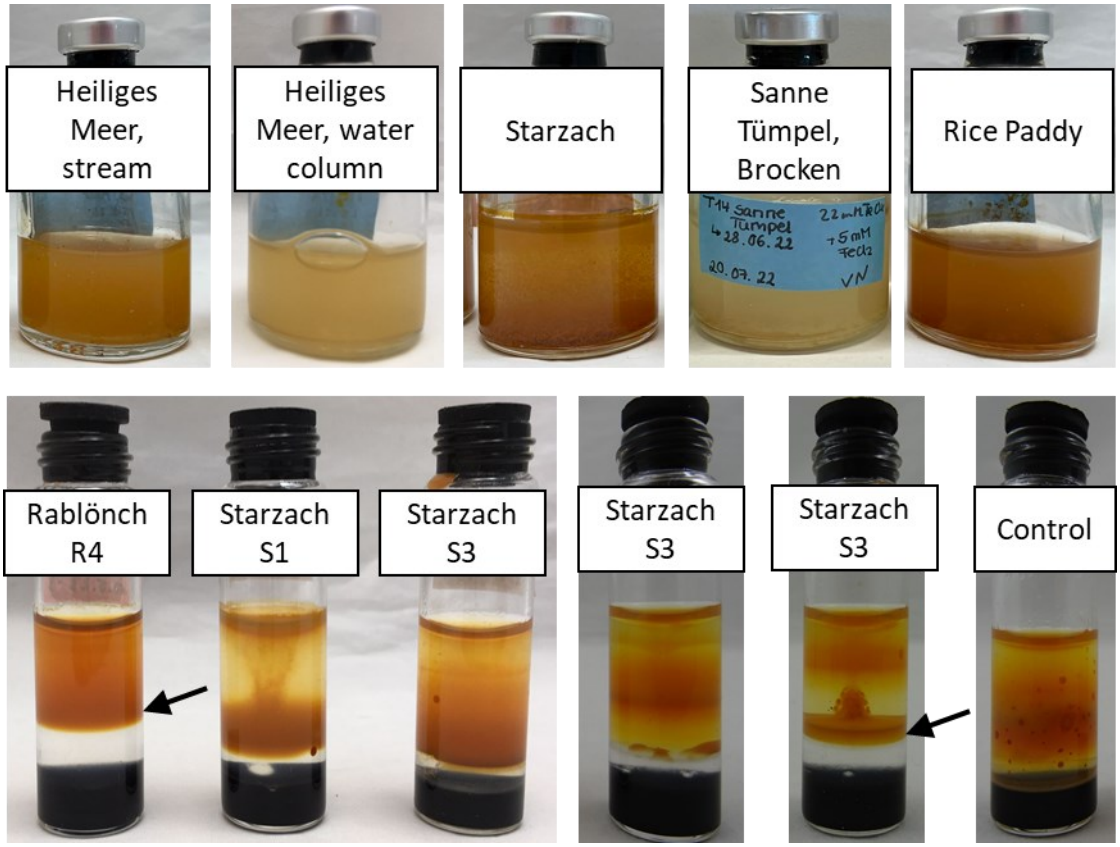

Figure 2: Pictures of enrichments of phototrophic Fe(II)-oxidizer (top line) and microaerophilic Fe(II)-oxidizer (bottom line). Arrow indicate sharp band where microaerophile grow. On the bottom right, a picture of a control tube (no microbe) is shown.

Enrichments for both phototrophic and microaerophilic Fe(II)-oxidizers were successfully transferred over several transfers. In the next step the enrichments were sequenced to get a better overview of the enriched cultures.

Sequencing data

For the three sequenced microaerophilic Fe(II)-oxidizer enrichments "Starzach 3" and "Starzach 1" showed similar results. Dominant genera were annotated as *Sulfuricurvum*, a sulfur oxidizer, *Gallionella*, and *Pseudomonas* whereas most dominated genera was *Sulfuricurvum* (37 and 42%) and *Gallionella* (24 and 17%) (Figure 3). *Gallionella* is a well known microaerophilic Fe(II)-oxidizer and has been extensively studied and found in various environments (De Vet et al., 2011; Emerson, 2012; Hallberg & Ferris, 2004). The abundance of *Sulfuricurvum* is also rational as FeS used in the gradient tubes could be used by the microbes as a sulfur source.

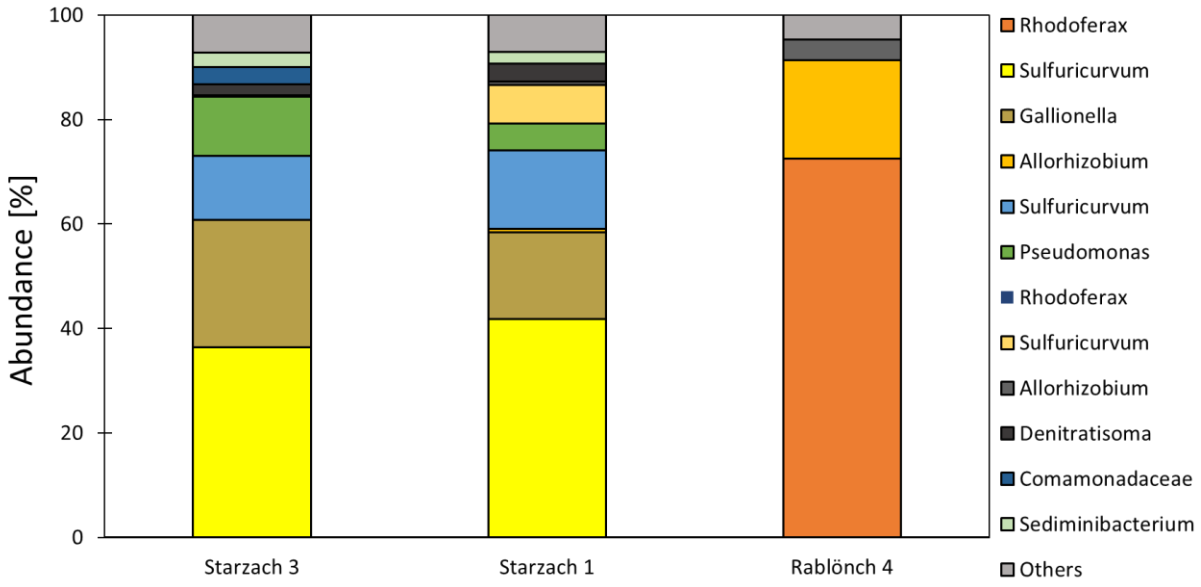

Figure 3: Amplicon sequencing data for microaerophilic Fe(II)-oxidizer enrichments from Starzach and Rablönch.

In case of the alpine, iron rich spring Rablönch dominating genera are *Rhodoferax* with 72% abundance and an *Allorhizobium* (19%), a nitrogen-fixing heterotroph. *Rhodoferax* has been known as Fe(III)-reducer but recently it has been studied for its potential to perform Fe(II) oxidation (Finneran et al. 2003; Kato and Ohkuma 2021). In the gradient tubes we saw the distinctive sharp lines usually formed by microaerophilic Fe(II)-oxidizer. If *Rhodoferax* would

perform Fe(III) reduction then we would see the formation of Fe(III) minerals with a black colour. This could be further investigated via inoculation of the enrichment from Rablönch with ferrihydrite to see if *Rhodoferax* would perform Fe(III) reduction.

In the next step all three microaerophilic enrichments could be transferred back to ZVI plates. This would help reduce the abundance of *Sulfuricurvum* and *Allorhizobium* as there is no source of organic carbon and sulfur.

For all phototrophic Fe(II)-oxidizers the dominant ASVs were annotated as *Thiodictyon* with a different sequence, however, further taxonomic distinction (i.e. species) of the *Thiodictyon* ASVs was not obtainable (Figure 4). So far only one *Thiodictyon* strain F4 was isolated that was also able to oxidize Fe(II) (Croal et al., 2004). For the enrichment "Heiliges Meer, stream" the dominant bacterial genus was a *Thiodictyon* with 55% abundance. Additionally, *Sulfurospirilum* (7%), an sulfur oxidizer, a *Rhodoferax* (11%), a genus associated with Fe(III)-reducer and Fe(II)-oxidizer, and another *Thiodyction* (6%) were sequenced (Figure 4A). In the enrichment "Heiliges Meer, water column 7 m" *Thiodyction* reached 32% and two different *Geobacter* ASVs (6 and 3%), potential Fe(III)-reducers, were found. This enrichment is still highly diverse with many other bacteria (Figure 4B). Another diverse enrichment sample was "Rice Paddy" with dominating potential Fe(II)-oxidizer *Thiodyction* (32%), two *Rhodopseudomona*s ASVs (17 and 9%), *Geobacter* (9%) and *Rhodoferax* (6%) present in the enrichment (Figure 4C). Sequencing data from "Sanne Tümpel" showed a dominant sequence annotated to *Thiodyction* with 65%, 10% of *Pauudibater*, 6% *Rhodoferax* and 5% *Rhodopseudomonas*. In the last phototrophic enrichment "Starzach 2" *Thiodyction* reached 60% with 9 % *Rhodoferax* and 3% *Rhodopseudomonas* (Figure 4C). Although the enrichments are not isolated strains yet, bacterial interactions in a selective community can be monitored and investigated. As all phototrophic enrichments have the potential for iron cycling is possible as

they are both enriched in Fe(II)-oxidizer and Fe(III)-reducer. It would be interesting to further investigate iron cycling from those enrichments to further study the importance of iron cycling in their respective environments. And indeed, in chapter 4 we could demonstrate phototrophic Fe(II) oxidation and Fe(III) reduction from the "Heiliges Meer, stream" enrichment and could show that carbon input had an effect on the iron cycle.

In the next step we wanted to try to isolate the phototrophic Fe(II)-oxidizers and performed agar shakes.

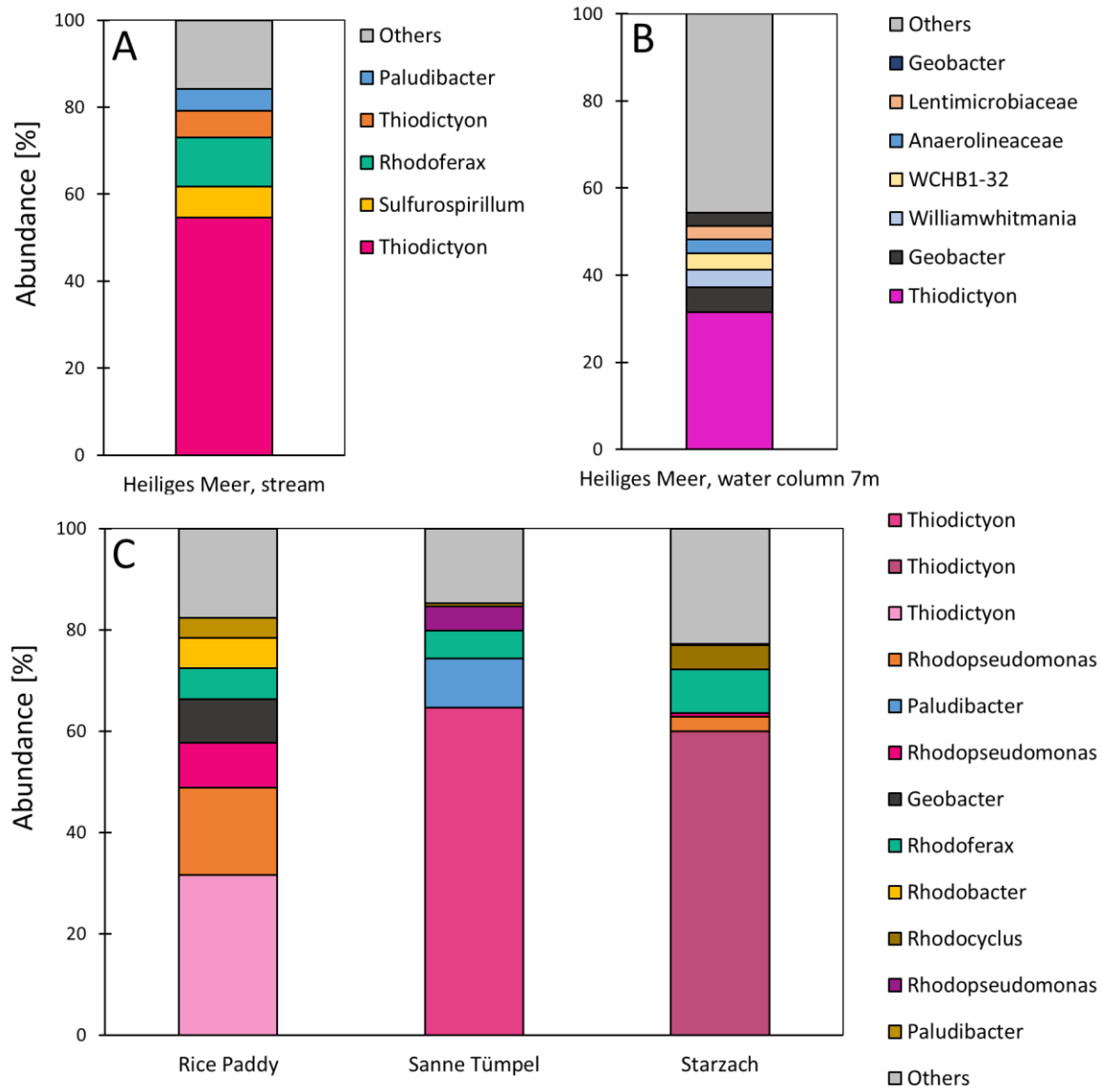

Figure 4: Illumina sequencing data for phototrophic Fe(II)-oxidizer enrichments from Heiliges Meer, stream (A), Heiliges Meer, water column 7m (B), Rice Paddy (C), Sanne Tümpel (C) and Starzach (C).

Isolation approach for phototrophic Fe(II)-oxidizer enrichments

Agar shakes results will be highlighted in this section but additional isolation methods (dilution to extinction and LB plates) have been tried as well (Lopez Rivoldi, 2022). Successful growth of single colonies was observed for all enrichments and the colonies differed in colors and shapes (Figure 5). In case of "Heiliges Meer, water column" small brown and pink and bigger black colonies were observed. The black colonies appeared in places where previously a brown colony was observed. This could possibly indicate the abundance of a succession of Fe(II)-oxidizers and Fe(III)-reducers. Additionally, white colonies that could indicate of the presence of heterotrophic bacteria were detected. For "Rice Paddy" agar shakes brown cloudy colonies were spotted at the bottom, small pink colonies throughout the tube and at the top bigger pink colonies with a whitish layer around them. For transfers brownish colonies were picked and transferred into liquid media with Fe(II). After successful growth and observation of Fe(II) oxidation another set of agar shakes was performed. After the second transfer into liquid media only successful growth for "Rice Paddy" was observed. Fe(II) oxidation proceeded but after 2 subsequent transfers in liquid media Fe(II) oxidation slowed down and other bacteria grew and the liquid in the tube turned purple. Currently two different single colonies in liquid culture remain being able to oxidize Fe(II) partially from the "Rice Paddy" enrichment. All other isolation approaches with the other enrichments were unsuccessful.

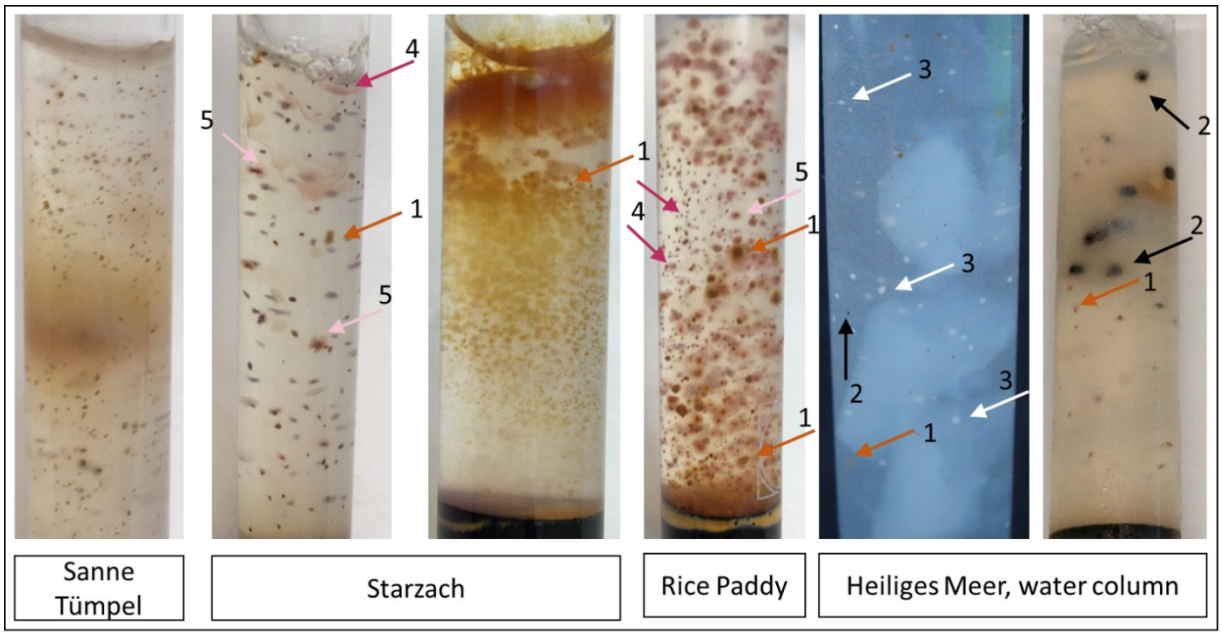

Figure 5: Pictures of agar shakes from 4 different phototrophic Fe(II)-oxidizing enrichments. Different arrows show different colored colonies: Orange arrows (1, orange/brown colonies), black arrows (2, black colonies), white arrow (3, white colonies), pink arrows (4, pink colonies) and rose arrows (5, pink cloudy colonies).

As growth in the agar shakes were partially successful and showed the formation of brownish colonies, the question arises why the transfer into liquid media was unsuccessful. It could be that during the picking of the colonies the bacteria were exposed to oxygen. Therefore, colony picking should be done in a nearly completely anoxic environment like a glovebox. In another case it could be that some bacteria need to be in a co-culture as it have been shown for other anoxygenic phototrophic Fe(II)-oxidizer (Heising et al., 1999; Schmidt et al., 2021).

Conclusion and next steps

After initial successful growth of the bacteria in agar shakes the transfer into liquid media were not successful. Although partially successful the agar shakes are a nice optical tool to display different bacteria making it easy to identify and pick different community members based on different colony colour, shape and size. Two picked colonies of the "Rice Paddy" enrichment are still in continuous culture but the degree of purity was not determined. In the next step the

purity of the two picked colonies could be further determined by sequencing, microscopy and growing them on different substrates. For the other enrichments either agar shakes should be repeated or other isolation methods should be pursued like dilutions and striking on LB plates (Lopez Rivoldi, 2022). Although no isolate was obtained at the end the successful enrichment of both phototrophic and microaerophilic Fe(II)-oxidizers showed us that Fe(II)-oxidizer are widespread and can be found in environments not previously studied. Therefore, their role and importance in these environments remains enigmatic and where isolates would provide us with a crucial tool to resolve their environmental role.

References

Berg, J. S., Michellod, D., Pjevac, P., Martinez-Perez, C., Buckner, C. R. T., Hach, P. F., Schubert, C. J., Milucka, J., & Kuypers, M. M. M. (2016). Intensive cryptic microbial iron cycling in the low iron water column of the meromictic Lake Cadagno. *Environmental Microbiology*, *18*(12), 5288–5302. https://doi.org/10.1111/1462-2920.13587

Bolyen, E., Rideout, J. R., Dillon, M. R., Bokulich, N. A., Abnet, C. C., Al-Ghalith, G. A., Alexander, H., Alm, E. J., Arumugam, M., Asnicar, F., Bai, Y., Bisanz, J. E., Bittinger, K., Brejnrod, A., Brislawn, C. J., Brown, C. T., Callahan, B. J., Caraballo-Rodríguez, A. M., Chase, J., … Caporaso, J. G. (2019). Reproducible, interactive, scalable and extensible microbiome data science using QIIME 2. *Nature Biotechnology*, *37*(8), 852–857. https://doi.org/10.1038/s41587-019-0209-9

Bryce, C., Blackwell, N., Schmidt, C., Otte, J., Huang, Y. M., Kleindienst, S., Tomaszewski, E., Schad, M., Warter, V., Peng, C., Byrne, J. M., & Kappler, A. (2018). Microbial anaerobic Fe(II) oxidation – Ecology, mechanisms and environmental implications. *Environmental Microbiology*, *20*(10), 3462–3483. https://doi.org/10.1111/1462-2920.14328

Callahan, B. J., Mcmurdie, P. J., Rosen, M. J., Han, A. W., Johnson, A. J. A., & Holmes, S. P. (2016). *dada2: high-resolution sample inference from illumina amplicon data*. *13*(7). https://doi.org/10.1038/nMeth.3869

Caporaso, J. G., Lauber, C. L., Walters, W. A., Berg-Lyons, D., Lozupone, C. A., Turnbaugh, P. J., Fierer, N., & Knight, R. (2011). Global patterns of 16S rRNA diversity at a depth of millions of sequences per sample. *Proceedings of the National Academy of Sciences of the United States of America*, *108*(SUPPL. 1), 4516–4522. https://doi.org/10.1073/pnas.1000080107

Croal, L. R., Johnson, C. M., Beard, B. L., & Newman, D. K. (2004). Iron isotope fractionation by Fe(II)-oxidizing photoautotrophic bacteria. *Geochimica et Cosmochimica Acta*, *68*(6), 1227–1242. https://doi.org/10.1016/j.gca.2003.09.011

Crowe, S. A., Hahn, A. S., Morgan-Lang, C., Thompson, K. J., Simister, R. L., Llirós, M., Hirst, M., & Hallam, S. J. (2017). Draft Genome Sequence of the Pelagic Photoferrotroph Chlorobium phaeoferrooxidans. *Genome Announcements*, *5*(13). https://doi.org/10.1128/GENOMEA.01584-16

De Vet, W. W. J. M., Dinkla, I. J. T., Rietveld, L. C., & Van Loosdrecht, M. C. M. (2011). *Biological iron oxidation by Gallionella spp. in drinking water production under fully aerated conditions*. https://doi.org/10.1016/j.watres.2011.07.028

Di Tommaso, P., Chatzou, M., Floden, E. W., Barja, P. P., Palumbo, E., & Notredame, C. (2017). Nextflow enables reproducible computational workflows. *Nature Biotechnology*, *35*(4), 316–319. https://doi.org/10.1038/nbt.3820

Ehrenreich, A., & Widdel, F. (1994). Anaerobic oxidation of ferrous iron by purple bacteria, a new type of phototrophic metabolism. *Applied and Environmental Microbiology*, *60*(12), 4517–4526. https://doi.org/10.1128/AEM.60.12.4517-4526.1994

Eickhoff, M., Obst, M., Schröder, C., Hitchcock, A. P., Tyliszczak, T., Martinez, R. E., Robbins, L. J., Konhauser, K. O., & Kappler, A. (2014). Nickel partitioning in biogenic and abiogenic ferrihydrite: The influence of silica and implications for ancient environments. *Geochimica et Cosmochimica Acta*, *140*, 65–79. https://doi.org/10.1016/j.gca.2014.05.021

Emerson, D. (2012). Biogeochemistry and microbiology of microaerobic Fe(II) oxidation. *Biochemical Society Transactions*, *40*(6), 1211–1216. https://doi.org/10.1042/BST20120154

Emerson, D., & Floyd, M. M. (2005). Enrichment and Isolation of Iron-Oxidizing Bacteria at Neutral pH. *Methods in Enzymology*, *397*, 112–123. https://doi.org/10.1016/S0076-

6879(05)97006-7
Emerson, D., & Moyer, C. L. (2002). Neutrophilic Fe-oxidizing bacteria are abundant at the Loihi Seamount hydrothermal vents and play a major role in Fe oxide deposition. *Applied and Environmental Microbiology*, *68*(6), 3085–3093. https://doi.org/10.1128/AEM.68.6.3085-3093.2002
Ewels, P. A., Peltzer, A., Fillinger, S., Patel, H., Alneberg, J., Wilm, A., Garcia, M. U., Di Tommaso, P., & Nahnsen, S. (2020). The nf-core framework for community-curated bioinformatics pipelines. *Nature Biotechnology*, *38*(3), 276–278. https://doi.org/10.1038/s41587-020-0439-x
Finneran, K. T., Johnsen, C. V., & Lovley, D. R. (2003). Rhodoferax ferrireducens sp. nov., a psychrotolerant, facultatively anaerobic bacterium that oxidizes acetate with the reduction of Fe(III). *International Journal of Systematic and Evolutionary Microbiology*, *53*(3), 669–673. https://doi.org/10.1099/IJS.0.02298-0/CITE/REFWORKS
Fleming, E. J., Langdon, A. E., Martinez-Garcia, M., Stepanauskas, R., & Poulton, N. J. (2011). What's New Is Old: Resolving the Identity of Leptothrix ochracea Using Single Cell Genomics, Pyrosequencing and FISH. *PLoS ONE*, *6*(3), 17769. https://doi.org/10.1371/journal.pone.0017769
Hallberg, R., & Ferris, F. G. (2004). Biomineralization by Gallionella. *Geomicrobiology Journal*, *21*(5), 325–330. https://doi.org/10.1080/01490450490454001
Hegler, F., Posth, N. R., Jiang, J., & Kappler, A. (2008). *Physiology of phototrophic iron (II) -oxidizing bacteria : implications for modern and ancient environments*. *66*(Ii), 250–260. https://doi.org/10.1111/j.1574-6941.2008.00592.x
Heising, S., Richter, L., Ludwig, W., & Schink, B. (1999). Chlorobium ferrooxidans sp. nov., a phototrophic green sulfur bacterium that oxidizes ferrous iron in coculture with a "Geospirillum" sp. strain. *Archives of Microbiology*, *172*(2), 116–124. https://doi.org/10.1007/s002030050748
Jiao, Y., Kappler, A., Croal, L. R., & Newman, D. K. (2005). Isolation and characterization of a genetically tractable photoautotrophic Fe(II)-oxidizing bacterium, Rhodopseudomonas palustris strain TIE-1. *Applied and Environmental Microbiology*. https://doi.org/10.1128/AEM.71.8.4487-4496.2005
Kappler, A., Bryce, C., Mansor, M., Lueder, U., Byrne, J. M., & Swanner, E. D. (2021). An evolving view on biogeochemical cycling of iron. *Nature Reviews Microbiology*, *19*(6), 360–374. https://doi.org/10.1038/s41579-020-00502-7
Kato, S., & Ohkuma, M. (2021). A Single Bacterium Capable of Oxidation and Reduction of Iron at Circumneutral pH. *Microbiology Spectrum*, *9*(1). https://doi.org/10.1128/spectrum.00161-21
Kucera, S., & Wolfe, R. S. (1957). a Selective Enrichment Method for Gallionella Ferruginea . *Journal of Bacteriology*, *74*(3), 344–349. https://doi.org/10.1128/jb.74.3.344-349.1957
Kurtzer, G. M., Sochat, V., & Bauer, M. W. (n.d.). *Singularity: Scientific containers for mobility of compute*. https://doi.org/10.1371/journal.pone.0177459
Lalonde, K., Mucci, A., Ouellet, A., & Gélinas, Y. (2012). Preservation of organic matter in sediments promoted by iron. *Nature 2012 483:7388*, *483*(7388), 198–200. https://doi.org/10.1038/nature10855
Laufer, K., Nordhoff, M., Schmidt, C., Behrens, S., Kappler, A., Røy, H., & Jørgensen, B. (2016). Coexistence of microaerophilic, nitrate-reducing, and phototrophic Fe(II) oxidizers and Fe(III) reducers in coastal marine sediment. *Applied and Environmental Microbiology*, *82*(5). https://doi.org/10.1128/AEM.03527-15
Liebrecht, P. (2022). *Characterization of two iron-rich mineral springs*. Bachelor thesis. University of Tuebingen, Germany.
Llirós, M., Garciá-Armisen, T., Darchambeau, F., Morana, C., Triadó-Margarit, X., Inceoɨlu,

Ö., Borrego, C. M., Bouillon, S., Servais, P., Borges, A. V., Descy, J. P., Canfield, D. E., & Crowe, S. A. (2015). Pelagic photoferrotrophy and iron cycling in a modern ferruginous basin. *Scientific Reports*, *5*, 1–8. https://doi.org/10.1038/srep13803

Lopez Rivoldi, J. C. (2022). *Iron cycling and isolation of iron metabolizing bacteria from Heiliges Meer and other lakes*. Bachelor thesis. University of Tuebingen, Germany.

Lueder, U., Druschel, G., Emerson, D., Kappler, A., & Schmidt, C. (2018). Quantitative analysis of O2and Fe2+profiles in gradient tubes for cultivation of microaerophilic Iron(II)-oxidizing bacteria. *FEMS Microbiology Ecology*, *94*(2), 1–15. https://doi.org/10.1093/femsec/fix177

Maisch, M., Lueder, U., Laufer, K., Scholze, C., Kappler, A., & Schmidt, C. (2019). Contribution of Microaerophilic Iron(II)-Oxidizers to Iron(III) Mineral Formation. *Environmental Science and Technology*, *53*(14), 8197–8204. https://doi.org/10.1021/acs.est.9b01531

Martin, M. (2011). Cutadapt removes adapter sequences from high-throughput sequencing reads. *EMBnet.Journal*, *17*(1), 10–12. https://journal.embnet.org/index.php/embnetjournal/article/view/200/479

Mu, C. C., Zhang, T. J., Zhao, Q., Guo, H., Zhong, W., Su, H., & Wu, Q. B. (2016). Soil organic carbon stabilization by iron in permafrost regions of the Qinghai-Tibet Plateau. *Geophysical Research Letters*, *43*(19), 10,286-10,294. https://doi.org/10.1002/2016GL070071

Nakagawa, K., Murase, J., Asakawa, S., & Watanabe, T. (2020). Involvement of microaerophilic iron-oxidizing bacteria in the iron-oxidizing process at the surface layer of flooded paddy field soil. *Journal of Soils and Sediments*, *20*(11), 4034–4041. https://doi.org/10.1007/s11368-020-02717-w

Otte, J. M., Harter, J., Laufer, K., Blackwell, N., Straub, D., Kappler, A., & Kleindienst, S. (2018). The distribution of active iron-cycling bacteria in marine and freshwater sediments is decoupled from geochemical gradients. *Environmental Microbiology*, *20*(7), 2483–2499. https://doi.org/10.1111/1462-2920.14260

Quast, C., Pruesse, E., Yilmaz, P., Gerken, J., Schweer, T., Yarza, P., Rg Peplies, J., & Glö Ckner, F. O. (2012). The SILVA ribosomal RNA gene database project: improved data processing and web-based tools. *Nucleic Acids Research*. https://doi.org/10.1093/nar/gks1219

Schmidt, C., Nikeleit, V., Schaedler, F., Leider, A., Lueder, U., Bryce, C., Hallmann, C., & Kappler, A. (2021). Metabolic Responses of a Phototrophic Co-Culture Enriched from a Freshwater Sediment on Changing Substrate Availability and its Relevance for Biogeochemical Iron Cycling. *Geomicrobiology Journal*, *38*(3), 267–281. https://doi.org/10.1080/01490451.2020.1837303

Singer, E., Emerson, D., Webb, E. A., Barco, R. A., Kuenen, J. G., Nelson, W. C., Chan, C. S., Comolli, L. R., Ferriera, S., Johnson, J., Heidelberg, J. F., & Edwards, K. J. (2011). Mariprofundus ferrooxydans PV-1 the First Genome of a Marine Fe(II) Oxidizing Zetaproteobacterium. *PLOS ONE*, *6*(9), e25386. https://doi.org/10.1371/JOURNAL.PONE.0025386

Straub, D., Blackwell, N., Langarica-Fuentes, A., Peltzer, A., Nahnsen, S., & Kleindienst, S. (2020). Interpretations of Environmental Microbial Community Studies Are Biased by the Selected 16S rRNA (Gene) Amplicon Sequencing Pipeline. *Frontiers in Microbiology*, *11*. https://doi.org/10.3389/fmicb.2020.550420

Straub, K. L., Rainey, F. a, & Widdel, F. (1999). Marine Phototrophic Ferrous-Iron-Oxidizing Purple Bacteria. *International Journal of Systematic Bacteriology*, *49*(1 999), 729–735.

Swanner, E. D., Wüstner, M., Leung, T., Pust, J., Fatka, M., Lambrecht, N., Chmiel, H. E., & Strauss, H. (2022). Seasonal phytoplankton and geochemical shifts in the subsurface

chlorophyll maximum layer of a dimictic ferruginous lake. *MicrobiologyOpen*, *11*(3). https://doi.org/10.1002/mbo3.1287

Tipping, E. (1981). The adsorption of aquatic humic substances by iron oxides. *Geochimica et Cosmochimica Acta*, *45*(2), 191–199. https://doi.org/10.1016/0016-7037(81)90162-9

Weiss, J. V., Rentz, J. A., Plaia, T., Neubauer, S. C., Merrill-Floyd, M., Lilburn, T., Bradburne, C., Megonigal, J. P., & Emerson, D. (2007). Characterization of neutrophilic Fe(II)-oxidizing bacteria isolated from the rhizosphere of wetland plants and description of Ferritrophicum radicicola gen. nov. sp. nov., and Sideroxydans paludicola sp. nov. *Geomicrobiology Journal*, *24*(7–8), 559–570. https://doi.org/10.1080/01490450701670152

Widdel, F, & Bak, F. (1992). The Prokaryotes: A Handbook on the Biology of Bacteria: Ecophysiology, Isolation, Identification, and Applications. In *The Prokaryotes: A Handbook on the Biology of Bacteria*. Springer-Verlag, New York.

Widdel, F, & Pfenning, N. (1981). Studies on Dissimilatory Sulfate-Reducing Bacteria that Decompose Fatty Acids. *Archives of Microbiology*, *129*, 395–400.

Widdel, Friedrich. (1983). Methods for enrichment and pure culture isolation of filamentous gliding sulfate-reducing bacteria. *Archives of Microbiology*, *134*(4), 282–285. https://doi.org/10.1007/BF00407803

Widdel, Friedrich, Schnell, S., Heising, S., Ehrenreich, A., Assmus, B., & Schink, B. (1993). Ferrous iron oxidation by anoxygenic phototrophic bacteria. *Nature*, *362*(6423), 834–836. https://doi.org/10.1038/362834a0

Zhao, Q., Adhikari, D., Huang, R., Patel, A., Wang, X., Tang, Y., Obrist, D., Roden, E. E., & Yang, Y. (2017). Coupled dynamics of iron and iron-bound organic carbon in forest soils during anaerobic reduction. *Chemical Geology*, *464*, 118–126. https://doi.org/10.1016/j.chemgeo.2016.12.014

9. Chapter: General conclusion and outlook

Substrate preference (batch experiments) (Chapters 2 and 3)

Key findings

In chapters 2 and 3, we investigated the substrate preference of 6 different photoferrotrophs and *R. palustris* TIE-1 in detail. We found that substrate preference is strain- and substrate-specific and we also observed simultaneous and sequential consumption of the substrates. Our results showed that photoferrotrophs use Fe(II) even if organics and H_2 are available. Fe(II) oxidation rates were unaffected or enhanced for some photoferrotrophs with the presence of acetate, lactate, pyruvate and glucose. The dominant minerals formed by the Fe(II) oxidation were poorly crystalline Fe(III) oxyhydroxides and were not impacted by the presence or absence of organics. The flexible metabolism and utilization of multiple substrates enhance the competitiveness and environmental resilience of phototrophic Fe(II)-oxidizer.

Open questions and further experiments

1. One additional photoferrotroph that was left out in our experiments is *Thiodictyon* strain F4. It would be interesting and would complete the study to investigate the substrate preference of this purple sulfur bacteria.
2. Since we observed an effect of buffer (HCO_3^- and PIPES) on the extend and rate Fe(II) oxidation and organic consumption, it would be interesting to investigate the optimal buffer concentration and composition for an ideal growth of *R. palustris* TIE-1 with organic and inorganic substrates. This question was further addressed in Chapter 6.
3. All the experiments so far were conducted in the setting of bath experiments. However, batch experiments are closed systems that provide a very limited representation of environmental dynamics. Therefore, it would be really interesting to conduct our experiments in a bioreactor simulating constant inflow of both Fe(II) and organic

substrates. With bioreactors, we would be able to simulate constant substrate supply and can identify if substrates will be consumed the same way as in the batch experiments. We already conducted some preliminary test experiments in serum vials to simulate spike events in the environment (Mergenthaler, 2023). Two specific scenarios were examined in the serum vials. In the first scenario, Fe(II) and acetate were simultaneously introduced at the beginning of the experiment, with acetate continuously spiked until the end of the experiment. Notably, in this case, *R. palustris* TIE-1 exclusively utilized acetate, and no Fe(II) oxidation occurred over time. In the second scenario, Fe(II) was initially provided, followed by subsequent acetate addition. Here, it was observed that Fe(II) oxidation occurred, but its rate slowed down upon the acetate addition, indicating the preferential utilization of acetate by *R. palustris* TIE-1 over Fe(II).

4. Different strains of photoferrotrophs have been found to coexist in the environment. This raises the question if there are competitive interactions among different photoferrotrophs for the same substrates? In a preliminary experiment, we incubated *R. palustris* TIE-1 (prefers acetate over Fe(II)) and *C. ferrooxidans* KoFox (uses both at the same time) and monitored the rate and extent of substrate consumption and individual cell growth using qPCR with specific primers (Mergenthaler, 2023). Our results indicate that most of the acetate was consumed by *R. palustris* TIE-1 while Fe(II) was oxidized by *C. ferrooxidans* KoFox at the same time.
5. It would be interesting to know how much CO_2 is fixed when *R. palustris* TIE-1 grows photoautotrophically with Fe(II) and photoheterotrophically with different organics (acetate, lactate, pyruvate, butyrate and glucose), respectively. So far, CO_2 fixation with different substrates was only studied for one strain of *R. palustris* (McKinlay & Harwood, 2010). Such investigation should also be conducted for the other substrates for *R. palustris* TIE-1 with labelled HCO_3^- following methods from Pjevac et al. (2019).

Substrate preference in Großes Heiliges Meer and iron cycling (Chapter 4)

Key findings

The dimictic lake Großes Heiliges Meer develops over the summer stagnation into an anoxic and iron-rich water body that provides an ideal condition for the growth of Fe(II)-oxidizers and Fe(III)-reducers. Bacterial community sequencing also confirmed the potential presence of Fe(II)-oxidizers and Fe(III)-reducers in this lake. In this study, we further demonstrated that dimictic lakes were perfect habitats for microbial iron cycling. We were able to enrich a phototrophic culture dominated by a phototrophic Fe(II)-oxidizer *Thiodictyon*. With the *in-situ* microbial community analyses and batch experiments, we could demonstrate the influence of organic substrates on iron cycling in lake Großes Heiliges Meer. The iron cycling in this lake is dominated by Fe(II) oxidation when there is adequate sunlight but limited organics, however, with the presence of organics, Fe(III) reduction will be stimulated. Overall, in this study, we concluded that dimictic lakes are a possible habitat for iron cycling and these processes could be more widespread than we thought.

Open questions and further experiments

1. The main focus of these experiments was on the iron cycling in lake Großes Heiliges Meer. However, our sequence data indicated that sulfur and methane cycles might also play an important role in this lake. Therefore, future studies should also consider sulfur- and methane-metabolizing bacteria and how they affect the iron cycle and interact with iron-metabolizing bacteria.
2. We should further investigate iron cycling. For example, what other factor are influencing the iron cycle in this lake? What minerals are formed and are they impacted by the type of substrates and climate conditions? This could be carried out in a

bioreactor or a column where *in-situ* conditions could be simulated and we could further study the settling of the produced minerals.

3. In a study by Liu et al. (2022) they showed through iron isotopes iron cycling in two Boreal Shield Lakes. With the addition of analysing iron isotopes in the lake, sediment, iron precipitates and the enrichment culture further could help complete analyse the processes that influence the iron cycling in this system.
4. Given the established occurrence of iron cycling in this lake, it is a perfect field site to explore potential environmental markers indicative of Fe(II) oxidation and/or Fe(III) reduction. This could include identifying specific metabolomic footprints or proteomic signatures that emerge when particular substrates and mechanisms predominate. Such investigative efforts could significantly enhance our understanding of the environmental conditions favouring iron cycling, facilitating the prediction and monitoring of these biogeochemical dynamics also in other environments.

Day/night cycle (Chapter 5)

Key findings

We could demonstrate that a day/night cycle increased the maximum Fe(II) oxidation rate of anoxygenic Fe(II)-oxidizer *Chlorobium ferrooxidans* KoFox. Maximum Fe(II) oxidation was significantly faster in the day/night cycle setup compared to the setup with a constant light supply. Cell growth reached roughly equivalent cell numbers across all three light conditions. SEM images showed different mineral structures independent of the light setup and ^{57}Fe Mössbauer spectroscopy confirmed the formation of poorly crystalline Fe(III) oxyhydroxides (such as ferrihydrite) in all three setups. With this experiment, we clearly demonstrated that a light/dark cycle benefits phototrophic Fe(II)-oxidizer.

Open questions and further experiments

1. Although it was possible to determine the effect of light/dark cycles on Fe(II) oxidation, other factors like different proteins and pigment contents were overlooked. Additionally, the effects of light/dark cycles on cell numbers could not be observed in a closed system. Therefore, it would be beneficial to set up the experiment in an open system or bioreactor to answer this question.
2. It is also worth looking at whether light/dark cycles also benefit other photoferrotrophs. In a preliminary experiment we could observe that light/dark cycles are also beneficial for *R. palustris* TIE-1 and that the organic uptake are affected by light/dark cycles (Roth, 2021).

Buffer (Chapter 6)

Key findings

Our experiments showed that buffer concentration and composition affected the rate and extent of Fe(II) oxidation and consumption of organic substrates by photoferrotrophs. The highest cell numbers were measured in the setup of 1 mM HCO_3^-+PIPES for all tested organic substrates (acetate, lactate, pyruvate, butyrate, glucose and mix). The extent of Fe(II) oxidation was the highest in the setup with 1 and 3 mM HCO_3^-+PIPES. Fe(II) oxidation rates were highest with 22 mM HCO_3^-, 1 and 3 mM HCO_3^-+PIPES. For organic and inorganic substrate consumption a well buffered system is important and for organic consumption low HCO_3^- concentrations are favourable.

Open questions and further experiments

1. It would be interesting to investigate whether other buffers except HCO_3^- and PIPES also affect the Fe(II) oxidation and consumption of organics by photoferrotrophs.

Methane (Chapter 7)

Key findings:

We could quantify that methane (CH_4) was produced while anoxygenic Fe(II)-oxidizer *Rhodopseudomonas palustris* TIE-1, *Chlorobium ferrooxidans* KoFox and *Chlorobium phaeoferrooxidans* KB01 were using Fe(II), acetate and hydrogen (H_2) as substrates. The amount of methane produced was strain- and substrate-specific and it ranged from 0.03±0.01 amol CH_4 $cell^{-1}$ d^{-1} to 0.4±0.2 amol CH_4 $cell^{-1}$ d^{-1}. Due to the high abundance of photoferrotrophs in early Earth (4.4 to 2.5 Ga ago) they could have contributed up to 2 % of biologically produced CH_4.

Open questions and further experiments

1. The mechanism of CH_4 production by photoferrotrophs is still unclear. Although a recent study revealed a potential pathway (Ernst et al. (2022)), it is worth studying if the CH_4 production mechanism is the same for different photoferrotrophs.
2. Could there also be stressors that could enhance CH_4 production of photoferrotrophs as was studied by Ernst et al. (2022)?
3. In the setup with acetate, it is unclear if the carbon in the produced CH_4 originates from HCO_3^- or acetate or from both of them. To answer this question, future experiments should be conducted with isotopically labelled acetate.

Enrichment (Chapter 8)

Key findings

In this study, we were able to enrich several microaerophilic and phototrophic Fe(II)-oxidizers from diverse habitats like iron-rich ponds, high-carbonate springs, stratified lakes and rice paddy soil, which further demonstrated that microaerophilic and phototrophic Fe(II)-oxidizers are able adapted to certain extreme conditions, therefore are widespread in the environment. In these enrichments, the dominant bacteria genus was annotated as a *Thiodictyon,* which is a purple sulfur bacteria that is closely associated with phototrophic Fe(II) oxidation. Some enrichments have potential iron reducer present which could be used to study iron cycling in those environments.

Open questions and further experiments

1. Is it possible to isolate *Thiodictyon* from the enrichment? For this purpose, different methods could be modified and combined:
    a. Agar Shake was a successful method in regards to observing cell growth. Therefore, it could be used for the isolation of *Thiodictyon* with a few modifications. Firstly, a dilution to almost extinction should be done to out-dilute less abundant microbes before the Agar Shakes. Moreover, the colony-picking process should be considered to be done under anoxic conditions such as in an anoxic glovebox.
    b. Modified anoxic “LB plates” could be tested for isolation. Instead of a normal plate, sterile serum vials could be used. Media- and substrates-containing agar will be poured into the serum vials, and then the vials will be sealed anoxically and placed horizontally to create a large enough area for microbe streaking. The phototrophic Fe(II)-oxidizer enrichment could then be streaked on the “plate” and if growth is observed, picking colonies would be simplified.

2. As all enrichments originated from different habitats demonstrated the presence of *Thiodyction* as a potential Fe(II)-oxidizer, it would be interesting to sequence and characterize the *Thiodyction* from these different enrichments to see how similar their genomes are. It would also be interesting to investigate if *Thiodictyon* from different enrichments have unique genes that are generated in response to the stressors that are unique in the specific environment where they are isolated from. For example, if the enrichment from a rice paddy soil can tolerate higher concentrations of arsenic?

References

Ernst, L., Steinfeld, B., Barayeu, U., Klintzsch, T., Kurth, M., Grimm, D., Dick, T. P., Rebelein, J. G., Bischofs, I. B., & Keppler, F. (2022). Methane formation driven by reactive oxygen species across all living organisms. *Nature*, *603*(7901), 482–487. https://doi.org/10.1038/s41586-022-04511-9

Liu, K., Schiff, S. L., Wu, L., Molot, L. A., Venkiteswaran, J. J., Paterson, M. J., Elgood, R. J., Tsuji, J. M., & Neufeld, J. D. (2022). Large Fractionation in Iron Isotopes Implicates Metabolic Pathways for Iron Cycling in Boreal Shield Lakes. *Environmental Science and Technology*, *56*(20), 14840–14851. https://doi.org/10.1021/acs.est.2c04247

McKinlay, J. B., & Harwood, C. S. (2010). Carbon dioxide fixation as a central redox cofactor recycling mechanism in bacteria. *Proceedings of the National Academy of Sciences of the United States of America*, *107*(26), 11669–11675. https://doi.org/10.1073/pnas.1006175107

Mergenthaler, M. (2023). *Influence of nutrient input and competition with other phototrophic Fe(II)-oxidizer on the Fe(II) oxidation of Rhodopseudomonas palustris TIE-1*. Bachelor thesis. University of Tuebingen, Germany.

Pjevac, P., Dyksma, S., Goldhammer, T., Mujakić, I., Koblížek, M., Mußmann, M., Amann, R., & Orlić, S. (2019). In situ abundance and carbon fixation activity of distinct anoxygenic phototrophs in the stratified seawater lake Rogoznica. *Environmental Microbiology*, *21*(10), 3896–3908. https://doi.org/10.1111/1462-2920.14739

Roth, L. (2021). *Influence of day/night cycle on Fe(II) oxidation of phototrophic Fe(II)-oxidizer*. Bachelor thesis, University of Tuebingen, Germany.

Acknowledgements

Through this journey I got to know inspiring and supporting people that I am especially thankful for. Biggest thanks go to Casey Bryce. I first worked with you just after my masters and then during the research project. During that time, I already got a feeling that we can work well together and we would complement each other. You always gave me the feeling that it is ok to asked and you are always there. That motivated me highly and gave me also the necessary freedom to grow in my ways. I am still very happy that we worked together in this project and will never forget this time. Another big thank you goes to Andreas Kappler for being so positive and creating such a supportive and wholesome group. I always felt very welcome and I consider it part of my home. You are always open and never shy of new ideas. I want to thank you both for supporting me during this time and for leaving me 100% freedom to do and try things out in the lab.

Next, I want to thank the rest of the Metaflex team Markus, James and Carrie. It was a pleasure to work with you, getting your insights and advice.

I want to also include all the collaboration partners where I had a pleasure working with them and expanding my knowledge: I) Methane project with Frank and Marcus, II) substrate preference with Patricia and Giorgio and III) Heiliges Meer Team Sümeyya, Harald and the research station.

I also want to thank all my students Caro, Bianca, Savinja, Linda, Marie, Jimena, Josia and Philip. You helped my grow and fuel my passion for teaching.

I also want to thank Caroline and Franzi who supported me during my Hiwi and master work and laid the foundation for me to continue this journey. You encouraged me to work independently in my early days which helped me grow in regards as to do lab work and plan accordingly.

Big, big thank you and best wishes goes to all former and current member of the Kappler group. It is really nice to work with you and also be a part of the Kappler family. This companionship and helpfulness are really welcoming and supportive. All the memories I made will have a special place in my heart. Thanks to all my former/current lab and office mates, all the technicians and all of the group. I got to know some awesome people here that I will never want to miss and hope we can keep seeing us for a while to come.

Big thanks to Manu, Yuge, Akanksha and Kate for reading part of my thesis.

And at last I want to thank my friends and family who supported me during through this journey. Ganz speziellen Dank an meine Familie, die mich immer unterstützt hat während dieser langen Zeit. Danke.